Crystallographic Order and Disorder in Quasi-One-Dimensional Conductors

Thesis by

Roger Macauley Williams

In Partial Fulfillment of the Requirements

for the Degree of

Doctor of Philosophy

California Institute of Technology

Pasadena, California

1979

(Submitted December 18, 1978)

Acknowledgements

I would most like to thank the friends I have met at Caltech and in Southern California in the past four years. The time I have spent with them has made these years enjoyable.

My advisor, Dr. Sten Samson, has provided me with guidance and encouragement, and has shown great patience with my assorted wild theories.

Dr. Joseph Gordon has continued his interest in my work. The success of the work reported in Chapter 2 of this thesis was very much dependent on his advice and encouragement.

Most of this research has been performed in collaboration with the organic metals group at JPL. They performed the electrical measurements (Appendix 2) and the photoaccoustic spectroscopic measurements (Chapter 2). I would like to thank Dr. Robert Somoano for many interesting discussions.

Dr. Richard Marsh provided much assistance at several stages of crystal structure determination and refinement. Jean Westphal aided me in the use of the crystallographic computing system. CRYM does pay.

Discussions with Charlotte Ma were extremely useful in understanding the unusual structural features of crystals I've worked on. Her careful analysis of diffraction experiments and her computing skills helped immeasurably.

Hamil Ma prepared some of the more complicated figures.

The shops and other support facilities at Caltech are excellent. I would especially like to thank Erich Segal in the glass shop and Jan Mitchell in the analytical lab.

I would like to thank Beth Cooper for typing this thesis. Pat Anderson and Allison Kimball have also helped me many times over the past four years.

The organic donors, TTF and TSF, were provided by the JPL organic metals group. TMTSF and HMTSF were kindly provided by Dr. D. Cowan and Dr. P. Shu at John Hopkins.

Funding for this research came from a variety of sources, including NSF (Grant No. DMR 74-19029A1), NASA-JPL, and the President's Fund (Caltech). I would especially like to thank Eastman Kodak for support under an Eastman Fellowship.

Finally, I would like to thank my parents for their support and understanding.

Abstract

Stacked, conducting isocyanide complexes of rhodium(I) were synthesized and characterized by x-ray diffraction and electrical measurements. Good crystals of orthorhombic $[Rh(CNCHCH_2)_4]ClO_4$, with a_o = 8.81 Å, b_o = 22.85 Å, c_o = 12.70 Å, were obtained and a structural refinement was carried out in space group Immm. The rhodium chain is nearly uniform (Rh-Rh = 2.94 Å) and ligands and anions show considerable disorder. The room temperature conductivity is ~2 Ω^{-1} cm^{-1} and conductivity is activated. The moderately high conductivity of $[Rh(CNCHCH_2)_4]ClO_4$ is due to the presence of a low-lying conduction band rather than a non-integral rhodium oxidation state.

The disorder, tetragonal phase of $(TTF)Cl_x$, a_o = 11.19 Å, c_o = 3.60 Å, was studied for compositions x = 0.67, x = 0.70. A room temperature structural refinement in space group $P4_2/mnm$ revealed eclipsed stacking of TTF cations and extremely high disorder of chlorides in channels. Low temperature studies revealed ordering of chloride ions for both compositions. $(TTF)Cl_{0.67}$ undergoes an incomplete structural transition to a monoclinic symmetry phase at ~250° K. Ordering of chloride ions occurs at the same temperature. Fast cooling (>1° K/hr) results in peak broadening which is apparently due to the very small size of diffracting domains within the crystal. Both small domain size and the inequivalent environments of TTF

cations following chloride ordering may contribute to the drop in conductivity observed at the phase transition.

Structural refinements of both the subcell (space group Cmca, a_o = 18.47 Å, b_o = 4.95 Å, c_o = 18.30 Å) and full cell (space group $Pmc2_1$, a_o = 18.47 Å, b_o = 9.90 Å, c_o = 18.30 Å) of a low disorder cyrstal of TTT_2I_3 were carried out. The iodine chain is highly disordered and all sites have less than full occupancy. The presence of I_3^- and I_2 species in the chain is likely. The resulting aperiodic potential due to the iodide chain may be expected to be retained at low temperature and inhibit a metal-to-insulator transition.

Electrochemical crystal-growth experiments involving TTF, TMTSF, and HMTSF gave successful results with the first two donors. Crystals of $(TMTSF)Br_{0.8}$ and $(TMTSF)(SCN)_{0.5}$ are isostructural, although the latter exhibits satellite reflections (period = 4.6 x c_o) in diffraction patterns. Both structures were refined in space group Cmcm, and the satellite data of $(TMTSF)(SCN)_{0.5}$ was modeled in space group $Cmc2_1$. Unit cell parameters are a_o = 9.798 Å, b_o = 23.837 Å, c_o = 7.095 Å, for the bromide and a_o = 9.919 Å, b_o = 24.124 Å, c_o = 7.220 Å, for the thiocyanate. The planes of these cations are perpendicular to the z-axis and consecutive cations slip back and forth by ~1.3 Å to reduce methyl group steric repulsion.

All of the systems studied are single carrier conductors with conduction along the cation stack and high disorder of anions. The nature of the disorder and its relationsihp to phase transitions, as well as interchain coupling and stacking in the cation chain, were evaluated in these compounds. Comparison of $(TTF)Cl_{0.67}$ and $(TTT)_2I_3$ were especially useful, as both exhibit comparably very short range order of halide ions at room temperature, but different cation stacking arrangements (eclipsed and slipped, respectively) and hence different interchain coupling and electronic bandwidth. Structural studies at room temperature and low temperature provided an opportunity to understand the important differences in the electrical properties of these two materials.

Table of Contents

CHAPTER 1

Introduction

During the past few years there has been considerable interest in highly anisotropic conductors (1-2). From a theoretical viewpoint, one-dimensional metals are much simpler than two- or three-dimensional metal, and they are predicted to have interesting properties such as a Peierl's distortion -- an instability with respect to a metal-to-insulator transition (3-4). Also, a great deal of controversy has originated from theories predicting high temperature superconductivity in highly anisotropic conductors (5-7).

Quasi-one-dimensional conductors, which have high conductivity along one crystal axis and much lower conductivity along the other two axes (8), may approach the behavior of a true one-dimensional metal in some respects, but consideration of the three-dimensional structure and electronic properties of these real materials is necessary for more complete understanding of their properties.

There are two major classes of quasi-one-dimensional conductors. Organic charge-transfer (Figure 1) salts may have two kinds of conducting chains, as in tetrathiafulvalene-tetracyanoquinodimethane (TTF-TCNQ) (9), or only one conducting chain, as in the partially oxidized halide salts of TTF (10-13). These materials generally exhibit metallic conductivity down to a temperature, T_{MI} ~50-200° K,

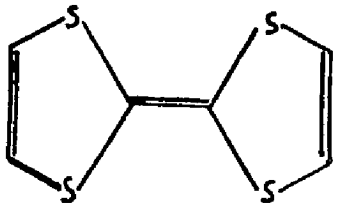

tetrathiafulvalene
TTF

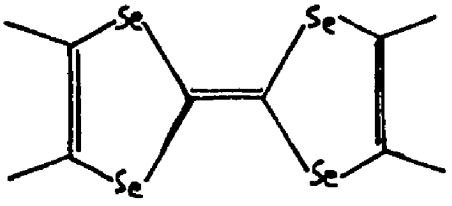

tetramethyltetraselenofulvalene
TMTSF

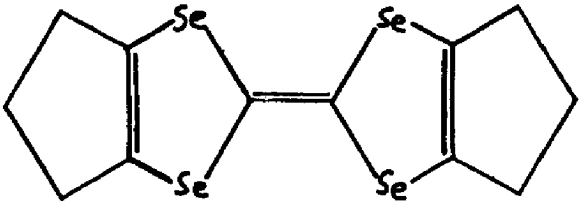

hexamethylenetetraselenofulvalene
HMTSF

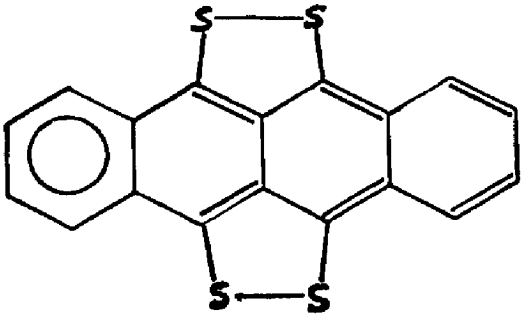

tetrathiatetracene
TTT

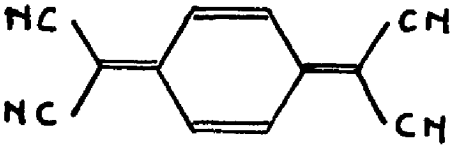

tetracyanoquinodimethane
TCNQ

Figure 1. Donors, and the acceptor, TCNQ, in organic conductors.

where a metal-to-insulator transition takes place. The nature of this transition is affected by the presence of disorder, the degree of interchain coupling, and the nature of the molecular stacking along the chain (i.e., eclipsed vs. slipped stacking).

The second major class of quasi-one-dimensional conductors, stacked square planar d^8 transition metal complexes, include various iridium carbonyl halides and partially oxidized platinum cyanide and oxalate salts (14-18). Disorder and interchain coupling are very important in understanding these compounds; stacking may be quite complicated in these materials. The electronic description of the stacked d^8 complexes is somewhat simpler, since metal-metal bonds are the only strong interactions between adjacent monomer units (19-21).

The materials which will be described here include members of both classes. Rhodium(I) isocyanide complexes are electronically similar to the other d^8 metal complexes mentioned above. Since a variety of isocyanide ligands may be employed, systematic alteration of the electrical properties within the series of complexes may be achieved. Conducting salts of organic donors with simple anions were also studied. The donors include TTF, tetramethyltetraseleno-fulvalene (TMTSF), and tetrathiatetracene (TTT) (see Figure 1). Disorder, especially that associated with the anions, is an important structural feature of all of the compounds. The results of detailed structure determinations of tetrakis(vinylisocyanide)rhodium(I)

perchlorate, TTF $Cl_{.67}$, TTT_2I_3, TMTSF$(Br)_{.8}$, and TMTSF$(SCN)_{.5}$ are reported. Less detailed crystallographic studies of other materials are described.

This work has three specific goals. First, the synthesis and crystallization of new quasi-one-dimensional conductors is important, since the few materials which have received intense study are not sufficient for a good understanding of nearly one-dimensional conductivity. The newer materials have often had more exciting properties, such as retention of high conductivity at very low temperature (22,23).

Second, structural investigations, chemical analysis, and physical measurements carried out concurrently on crystals of the same origin allow extremely useful correlation of subtle structural features with physical properties.

Finally, these materials are of significant crystallographic and chemical interest because of their unique structural characteristics. TTT_2I_3 and TTF $Cl_{.67}$ have disordered halide lattices with periods two and three times the stacking axis length of the organic sublattice. Tetrakis(vinylisocyanide)rhodium(I) perchlorate has a rhodium atom sublattice with $a_{rh} = a_{o/3}$; the ligands and perchlorate anion have extremely high disorder. TMTSF$(Br)_{\sim .8}$ and TMTSF$(SCN)_{\sim .5}$ are nearly isostructural. In the latter, however, the thiocyanate positions are modulated with a period $C' \simeq 4.5\ c_o$. Important parts of the structural work on TTF $Cl_{.67}$ and tetrakis(vinylisocyanide)rhodium(I) perchlorate are the low temperature investigations. A structural

phase transition of TTF $Cl_{.67}$ at ~250° K was studied in detail, and the symmetry of the low temperature phase was determined. A partial structure refinement was carried out on diffraction data of tetrakis (vinylisocyanide)rhodium(I) perchlorate at 22° K.

The structural and electrical characterization of $[Rh(CNCHCH_2)_4]ClO_4$ provides an example of a second way of obtaining high conductivity in d^8 metal complexes, and provides evidence for the importance of interchain coupling in quasi-one-dimensional materials. The importance of disorder in allowing retention of conductivity in single-carrier quasi-one-dimensional materials was revealed in $(TTT)_2I_3$ and $(TTF)Cl_x$, which exhibit comparable halide chain disorder at room temperature. Ordering of chloride was in $(TTF)Cl_x$ occurs with a simultaneous drop in conductivity at ~250° K. In contrast, disorder and moderate conductivity are retained at low temperature in $(TTT)_2I_3$. It appears that the Peierls' transition is incomplete because of the aperiodic potential due to the iodine chain, which produces states within the energy gap. The metal-to-insulator transition is complete in $(TTF)Cl_x$, although the effect of chloride ordering on the transition is not thoroughly understood. Since the superperiod of the chloride lattice has reciprocal lattice period $\frac{1}{3}c^* = 2k_F$, a favorable interaction between chloride ordering and commensurate charge density formation is expected.

The effect of disorder on conductivity of single-carrier systems was further explored in $(TMTSF)(SCN)_{0.5}$ and $(TMTSF)Br_{0.8}$. Moderate

disorder associated with the anion lattice is seen in both cases, and an incommensurate superperiod which may result from a $2k_F$ distortion is seen in the thiocyanate.

Structure factor lists are collected in Appendix 1. Electrical properties are described briefly in the text, and plots of the temperature dependence of electrical conductivity and thermoelectric power are collected in Appendix 2. A few remarks concerning structure and refinement for these crystals are given in Appendix 3.

References

1. Annals of the New York Academy of Sciences, 313, Ed., J. S. Miller and A. J. Epstein, The New York Academy of Sciences, New York, New York (1978).
2. J. S. Miller and A. J. Epstein, Chapter in Progress in Inorganic Chemistry, Vol. 20. Ed. S. J. Lippard, John Wiley and Sons, Inc., New York (1976).
3. R. L. Peierls, Quantum Theory of Solids, Ch. IV, Oxford University Press, London (1955).
4. G. Beni, Solid State Communications, 15, 269 (1974).
5. David Allender, James Brag, and John Bardeen, Phys. Rev., B17, 1020 (1973).
6. W. A. Little, Phys. Rev., A13, 1416 (1964).
7. V. L. Ginzburg, Soviet Physics Uspekki, 13, 335 (1970).
8. Conductivities for $K_2Pt(CN)_4Br_{0.30}\cdot 3H_2O$ are ~300 and ~0.001 Ω^{-1} cm^{-1} in the directions parallel and perpendicular to the stacking axis, respectively. H. R. Zeller and H. Beck, J. Phys. Chem. Solids, 35, 77 (1974). Conductivities for (TTF)(TCNQ) are ~500 and ~5 Ω^{-1} cm^{-1} in directions parallel and perpendicular to the stacking axis, respectively (9).
9. M. J. Cohen, L. B. Coleman, A. F. Garito, and A. J. Heeger, Phys. Rev., B10, 1298 (1974).

10. R. B. Somoano, A. Gupta, V. Hadek, M. Novotny, M. Jones, T. Datta, R. Deck, and A. M. Hermann, J. Chem. Phys., 63, 4970 (1973); R. B. Somoano, A. Gupta, V. Hadek, M. Novotny, M. Jones, T. Datta, R. Deck, and A. M. Hermann, Phys. Rev., B15, 595 (1977).

11. F. Wudl, D. E. Schafer, W. M. Walsh, Jr., L. W. Rupp, Jr., F. J. DiSalvo, J. V. Waszczak, M. L. Kaplan, and G. A. Thomas, J. Chem. Phys., 66, 377 (1977).

12. R. J. Warmack, T. A. Callcott, and C. R. Watson, Phys. Rev. B12, 3336 (1975).

13. B. A. Scott, S. J. LaPlaca, J. B. Torrance, B. D. Silverman, and B. Welber, J. Am. Chem. Soc., 99, 6631 (1977).

14. K. Krogmann, Angew. Chem. Int. Ed., 8, 35 (1969).

15. H. R. Zeller, Adv. Solid State Phys., 13, 31 (1973).

16. T. W. Thomas and A. E. Underhill, Chem. Soc. Rev., 1, 99 (1972).

17. H. J. Keller in Low Dimensional Cooperative Phenomena, Ed. H. J. Keller. Nato Advanced Studies Institute Series, 7B, Plenum Press, p. 315.

18. A. P. Ginsberg, J. W. Koepke, J. J. Hansen, K. W. West, F. J. DiSalvo, C. R. Sprinkle, and R. L. Cohen, J. Inorg. Chem., 15, 514 (1976).

19. K. R. Mann, N. S. Lewis, R. M. Williams, H. B. Gray, and J. G. Gordon II, Inorg. Chem., 17, 829 (1978).

20. K. R. Mann, J. G. Gordon II, and H. B. Gray, J. Am. Chem. Soc., 97, 3553 (1975).

21. J. G. Gordon II, R. Williams, C. -H Hsu, E. Cuellar, S. Samson, K. Mann, H. B. Gray, V. Hadek, and R. Somoano, Annals of the New York Academy of Sciences, 313, 580 (1978).

22. L. C. Isett and E. A. Perez-Albuerne, Solid State Comm., 21, 433 (1977); L. C. Isett, to be published in Phys. Rev., B.

23. A. N. Black, D. O. Cowan, K. Bechgaard, R. P. Pyle, R. H. Banks, and T. O. Poehler, Phys. Rev. Lett., 34, 1561 (1975).

CHAPTER 2

Conducting Rhodium(I) Isocyanide Complexes

The unusual properties of quasi-one-dimensional conductors have stimulated much interest in the synthesis of new examples of these compounds. While a great variety of organic conductors have been prepared, fewer examples of conducting stacked square planar d^8 metal complexes are known. All of the highly conducting members of the latter group are either iridium carbonyl halides or partially oxidized platinum cyanide and oxalate salts (1-6). The rhodium isocyanide complexes (7-9) reported here are electronically similar to the iridium and platinum compounds.

The intense colors of crystalline rhodium isocyanide complexes indicate that there are significant interactions between monomeric units in the solid state. In addition, the electronic spectra of solutions of these complexes have intense bands in the visible region which show a non-Beers law dependence on concentration (8,10). These bands indicate the presence of oligomers of the tetrakis(isocyanide)rhodium(I) cations. The presence of a mixture of oxidation states is not necessary for oligomerization in solution.

An investigation of several rhodium isocyanide complexes was undertaken in order to determine if highly conducting solids could be prepared. High conductivity could result in these compounds in

two ways. The essential feature of these d^8 compounds is that square-planar complex ions stack along an axis perpendicular to the coordination plane to form linear chains of metal atoms (Figure 1). Electrons are delocalized along this chain in a band formed by overlapping dz^2 metal orbitals, as shown in Figure 2. Since this is a filled band, partial oxidation is required to generate the free carriers needed for metallic conductivity. A simple molecular orbital approach predicts that there will be a low-lying unoccupied band derived from metal Pz and ligand π^* orbitals. If the gap between this band and the filled dz^2 band is sufficiently small, thermally activated conduction will result without partial oxidation (11). The shorter the metal-metal bond, the greater the interaction between monomeric units which give rise to both the dz^2 and Pz-π^* bands will be. The gap will consequently be smaller (Figure 2). Crystalline disorder may also be expected to increase conductivity in this type of material, due to band broadening or creation of states within the gap. In order to understand the electrical behavior of conducting d^8 complexes, it is necessary to evaluate such parameters as the metal-metal bond length, the degree and nature of crystalline disorder, and the oxidation state of the metal.

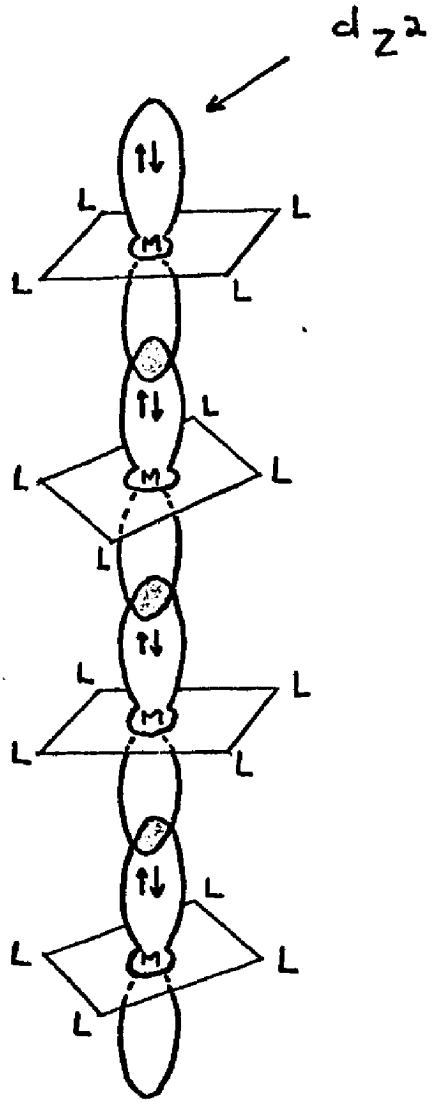

Figure 1. Stacking in square planar d^8 complexes.

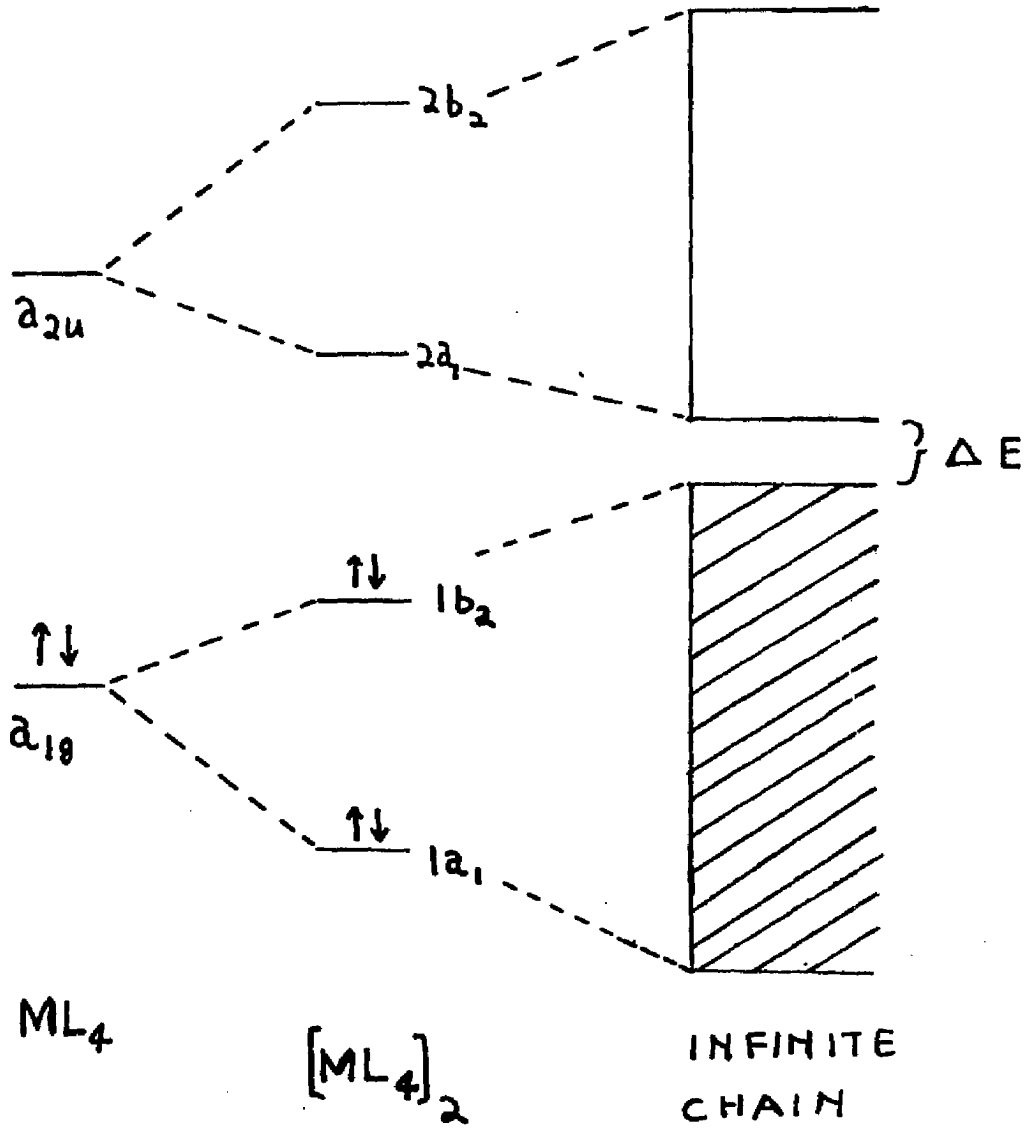

Figure 2. Molecular Orbital diagram of monomer, dimer, and infinite chain of $Rh(CN\text{-}R)_4^+$.

Experimental

Synthesis

Bis(1,5-cyclooctadiene)-μ-dichlororhodium, $[Rh(1,5\text{-}C_8H_{12})Cl]_2$, was prepared by the method of Chatt and Venanzi (12), except that recrystallization from acetic acid was omitted.

Bis(1,5-cyclooctadiene)-bis(acetonitrile)rhodium perchlorate and tetrafluoroborate, $[Rh(1,5\text{-}C_8H_{12})(CH_3CN)_2]^+ClO_4^-$ and $[Rh(1,5\text{-}C_8H_{12})(CH_3CN)_2]^+BF_4^-$, were prepared by reacting $[Rh(1,5\text{-}C_8H_{12})Cl]$ with $AgClO_4$ and $AgBF_4$ respectively, in 1:2 molar ratio in acetonitrile. AgCl was removed by filtration. Addition of diethyl ether yielded the yellow crystalline products. Both $[Rh(1,5\text{-}C_8H_{12})(CH_3CN)_2]^+ClO_4^-$ and $[Rh(1,5\text{-}C_8H_{12})(CH_3CN)_2]^+BF_4$ were extremely soluble in acetonitrile and other highly polar solvents, and quite insoluble in diethyl ether and hydrocarbons. If not stored in sealed vials, discoloration of the solids occurred, presumably due to loss of acetonitrile. (Caution: All organometallic perchlorates are potentially explosive.)

All isocyanides were prepared by standard methods described in the literature (13-17). Vinylisocyanide was synthesized and used as 30 to 60 mole percent solution in ethanol, rather than in pure form, and was identified by NMR. (Caution: Some isocyanides are explosive. An intermediate in the preparation of vinylisocyanide is reported to be explosive.)

Rhodium(I) isocyanide complexes were obtained by reacting each isocyanide with $[Rh(1,5\text{-}C_8H_{12})Cl]_2$, $[Rh(1,5\text{-}C_8H_{12})(CH_3CN)_2]^+ClO_4^-$, or $[Rh(1,5\text{-}C_8H_{12})(CH_3CN)_2]^+BF_4^-$. Since the chloride salts were invariably the most soluble, anion exchange reactions in acetonitrile were also useful in the preparation of the other salts. Growth of crystals was inhibited by the presence of water or cyclooctadiene, among other impurities. Multiple recrystallization of the complexes from acetonitrile solutions containing excess isocyanide was necessary if good single crystals were desired. Acetonitrile was degassed on the vacuum line and distilled from molecular sieves; diethyl ether was distilled from sodium benzophenone ketal. Single crystals of several complexes could be obtained by layering diethyl ether onto an acetonitrile solution of the purified complex; or by slow cooling an acetonitrile-diethyl ether solution of the complex. All syntheses were carried out on the vacuum line. Analytical data are reported in Table 1.

<u>$Rh(CNCH_3)_{3.38}BF_4$</u>: 0.33 g $[Rh(1,5\text{-}C_8H_{12})(CH_3CN)_2]^+BF_4^-$ was dissolved in about 5 ml acetonitrile in a flask with attached Schlenk fritted filters. About 0.5 ml methyl isocyanide was distilled into the reaction flask. The solution became brown, and addition of 10 ml diethyl ether precipitated the complex. The solid was collected on the frit and then recrystallized twice by addition of 1) 5 ml acetonitrile and 0.5 ml methylisocyanide followed by 2) 10 ml diethyl

Table 1. Analytical Data for Rhodium Isocyanide Complexes

		%C	%N	%H	%Cl	%Rh	%O
$Rh(CNC_6H_5)_4ClO_4$	calc	54.70	9.11	3.27	5.77	16.74	10.41
614.85	found	54.52	9.01	3.54	5.6	15.7	(11.63)
		C, H, N average of six analyses					
$Rh(CNC_6H_5)_{3.67}(ClO_4)_{1.33}$	calc	50.28	8.38	3.01	7.68	16.77	13.87
						%(Rh+O)=30.64	
613.65	found	50.76	7.77	3.85	7.14	Δ=30.58	
		C, H, N, Cl average of two analyses					
$Rh(CNC_6H_5)_4Cl$	calc	61.05	10.17	3.66	6.44	18.68	
550.86	found	60.83	10.61	4.11	6.17	(18.28)	
		Cl average of two analyses					
$Rh(CNC_6H_5)BF_4$	calc	55.85	9.30	3.35	%F=12.62;%R=17.09;%B=1.7		
602.20	found	56.69	9.58	3.80			
		C, H, N average of two analyses					
$Rh(CNCHCH_2)_4Cl$	calc	41.11	15.98	3.45	10.11	29.35	
350.4	found	41.06	16.04	3.74	10.14	29.12	
		C, H, N average of two analyses					
$Rh(CNCHCH_2)_4ClO_4$	calc	34.76	13.51	2.92	8.55	24.82	15.44
414.6	found	34.96	13.70	3.08	8.80	24.60	(14.86)
		C, H, N average of four analyses					
$Rh(CNCH_3)_{3.38}ClO_4$	calc	23.82	13.95	3.00	10.39	30.16	18.75
341.24	found	24.41	13.37	2.92	--	--	--
$Rh(CNCHCH_2)_{2.7}Cl$	calc	34.54	13.42	2.90	12.59	36.54	
281.5	found	35.16	12.48	3.18	--	--	

ether. Crystals suitable for x-ray photographic work were obtained by layering 15 ml diethyl ether onto a solution of the complex in 20 ml acetonitrile and 1.0 ml methylisocyanide.

<u>$Rh(CNCHCH_2)_4Cl$</u>: 2.0 g $[Rh(1,5\text{-}C_8H_{12})Cl]_2$ was reacted with ~3.0 g vinyl isocyanide in 8 ml diethyl ether. The black precipitate was collected on a fritted filter and washed several times with additional ether. Yield after drying was 2.7 g. The infrared C≡M stretching frequency was 2170 cm^{-1} (KCl pellet).

<u>$Rh(CNCHCH_2)_{2.7}Cl$</u>: 2.0 g (.008 mole) $[Rh(1,5\text{-}C_8H_{12})Cl]_2$ was reacted with 1.26 g (.024 mole) vinylisocyanide in diethyl ether. The solid product was extracted with acetonitrile and dried.

<u>$Rh(CNCHCH_2)_4ClO_4$</u>: 0.77 g $[Rh(1,5\text{-}C_8H_{12})(CH_3CN)_2]^+ClO_4^-$ was dissolved in 40 ml acetonitrile. About 1 g of vinylisocyanide was added. Solution was warmed to dissolve all of the complex, then cooled to -15° C and filtered. The red-brown microcrystalline residue was redissolved in 30 ml acetonitrile and ~.5 g vinyl isocyanide. 40 ml diethyl ether was added and product was again collected on the frit. The red-brown mat of hair-like microcrystals was dried by pumping. Failure to recrystallize the initial product apparently results in incorporation of 1,5-cyclooctadiene, which, if present, seems to inhibit formation of good single crystals in later experiments.

Microcrystalline tetrakis(vinylisocyanide)rhodium(I) could also be obtained by Soxhlet extraction of 1.0 g of $Rh(CNCHCH_2)_4 \cdot Cl$ with 100 ml dry, degassed acetonitrile containing 10.0 g tetraethylammonium perchlorate under a pressure of ~100 torr dry, oxygen-free nitrogen. After completion of the extraction, the flask was allowed to cool slowly and was left undisturbed for about a day. The yield after filtration was 0.5 g. (Caution: The dry complex will detonate on heating to about 270° C.)

$\underline{Rh(CNCHCH_2)_4BF_4}$ could be prepared in an analogous manner, but was very hygroscopic.

$\underline{Rh(CNC_6H_5)_4Cl}$: 4.0 g $[Rh(1,5\text{-}C_8H_{12})Cl]_2$ was dissolved in a 1:1 mixture of acetonitrile and diethyl ether. 12 ml (~9.6 g) phenyl isocyanide was added to the reaction flask. Solid $Rh(CNC_6H_5)_4Cl$ was collected in two fractions totalling 8.25 g. The first fraction consisted of brown microcrystals.

$\underline{Rh(CNC_6H_5)_4BF_4}$: 3.0 g $[Rh(1,5\text{-}C_8H_{12})Cl]_2$ and 1.5 g $NaBF_4$ were dissolved in 40 ml acetonitrile. After filtration to remove NaCl, 8.0 g phenylisocyanide was added. Addition of ether gave 6.15 g coppery-brown microcrystals. The infrared C≡N stretching frequency of a sample in dichloromethane was 2160 cm^{-1}.

<u>$Rh(CNC_6H_5)_4ClO_4$</u>: 0.5 g $[Rh(1,5\text{-}C_8H_{12})(CH_3CN)_2]^+ClO_4^-$ was dissolved in 13 ml acetonitrile. About 1 ml phenylisocyanide was distilled into the reaction flask, giving a blue solution. About 20 ml diethyl ether was added to precipitate product, which was collected on a fritted filter and washed with an additional 10 ml of ether. Layering of the additional ether over the filtrate in the receiving flask resulted in crystals up to 0.05 x 0.05 x 0.5 ml.

<u>$Rh(CNC_6H_5)_{3.67}(ClO_4)_{1.33}$</u>: 0.5 g $Rh(CNC_6H_5)_4Cl$, somewhat oxidized by several months exposure to air, was extracted with about 10 ml acetonitrile. 0.11 g $NaClO_4$ was added and after stirring, the solution was filtered to remove the fine precipitate of NaCl. Addition of diethyl ether gave the complex as fine hair-like crystals.

<u>$Rh(CNC_6H_5)_{3.67}(ClO_4)_{1.33}$ crystals</u>: 0.05 g $Rh(CNC_6H_5)_{3.67}(ClO_4)_{1.33}$ was placed in a solvent diffusion cell (Figure 3). About 3 ml acetonitrile were distilled onto the complex and about 5 ml diethyl ether were distilled into the other leg of the cell. After sealing and allowing the solvent to reach room temperature, the diethyl ether was slowly distilled onto the acetonitrile solution of the complex. Crystals ~1 mm long appeared after about 5 days.

<u>$Rh(CNCHCH_2)_4ClO_4$ single crystals</u>: 0.40 g $Rh(CNCHCH_2)_4ClO_4$ was placed in a solvent diffusion cell and degassed. 4 ml acetonitrile

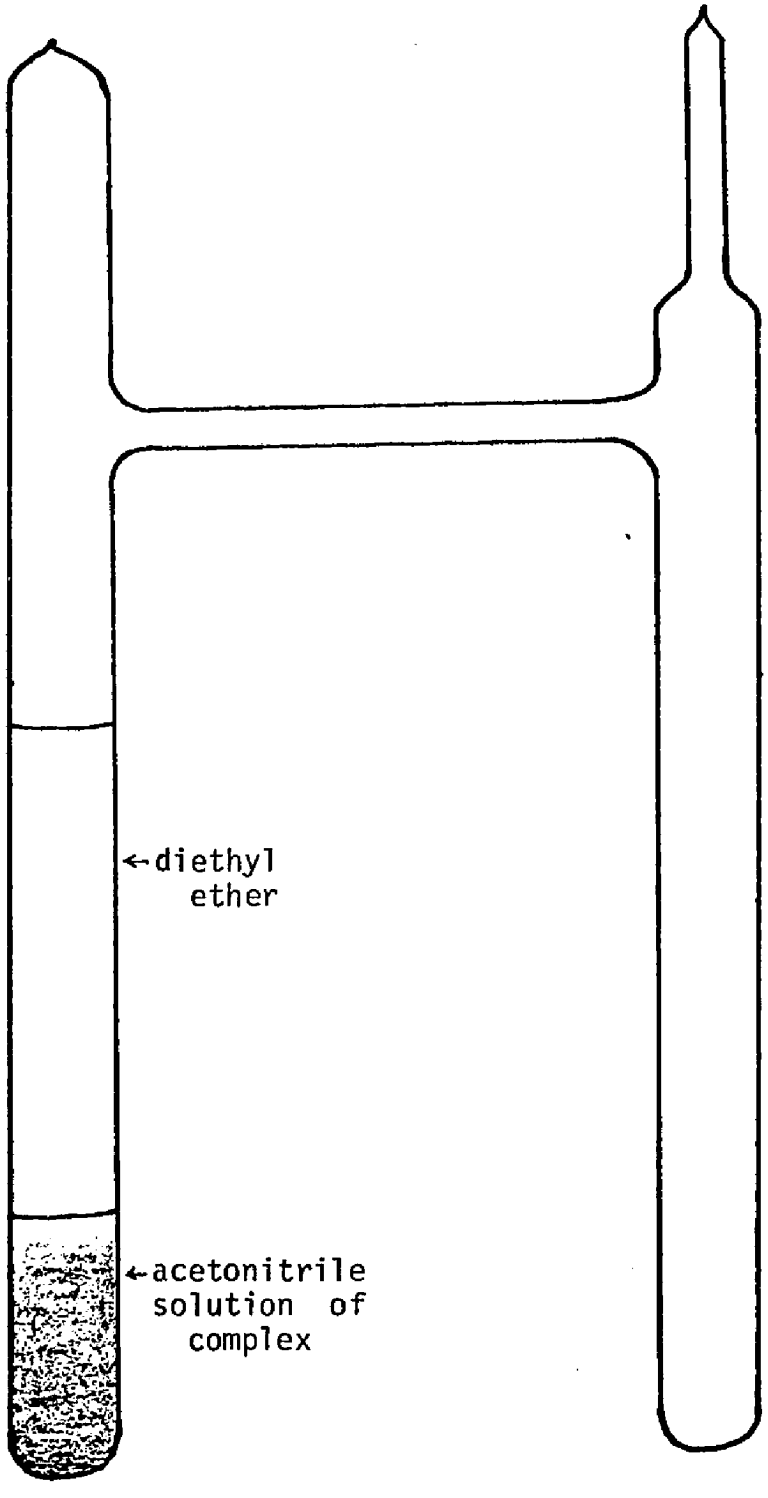

Figure 3. Solvent diffusion crystallization apparatus.

and 15 ml diethyl ether were distilled onto the complex and into the second leg of the cell, respectively. After warming to room temperature, the ether was distilled onto the acetonitrile solution. Coppery crystals, ~10 mm x 0.08 mm x 0.04 mm, were harvested after four days.

Electrical measurements

The electrical conductivity was measured on each complex with the use of two probes applied to a pressed powder of thickness 0.25-0.6 mm. Single crystals of tetrakis(vinylisocyanide)rhodium(I) perchlorate were large enough for four probe conductivity measurements with silver paint contacts. Both kinds of conductivity data obtained at room temperature are given in Table 2. The temperature dependence of the conductivity of tetrakis(vinylisocyanide)rhodium(I) perchlorate is given in Appendix 2.

X-ray and density measurements

The sharp extinction of transmitted polarized light was used as the criterion for selecting crystals for x-ray diffraction work. Most crystals were fibrous and twinned; however, this resulted in misalignment of the diffracting domains (within the crystal) only in the directions perpendicular to the stacking axis. Axis lengths and strong repeats along the stacking (needle) axis could be identified, although the other unit cell parameters could not be determined for most crystals. Tetrakis(vinylisocyanide)rhodium(I) perchlorate formed good single crystals and oscillation and Weissenberg

Table 2. Room Temperature Conductivities of Stacked Rhodium Isocyanide Complexes

Complex	Source	Conductivity Ω^{-1} cm^{-1}
$Rh(CNCHCH_2)_4ClO_4$	single crystal	2
	powder	5.6×10^{-3}
$Rh(CNCHCH_2)_4Cl$	powder	2.9×10^{-4}
$Rh(CNCHCH_2)_{2.7}Cl$	powder	2×10^{-4}
$Rh(CNC_6H_5)_4Cl$	powder	6×10^{-7}
$Rh(CNC_6H_5)_4BF_4$	powder	2×10^{-5}
$Rh(CNC_6H_5)_{3.67}(ClO_4)_{1.33}$	powder	1.7×10^{-4}
$Rh(CNCH_3)_{4-x}BF_4$	powder	2.2×10^{-2}

photographs were used to determine its space group and unit cell dimensions. Table 3 gives stacking axis lengths and strong repeats for the complexes studied. The axis length of tetrakis(phenyl isocyanide)rhodium(I) chloride was determined from a tentative indexing of a Guinier-Hägg powder photograph.

More accurate unit cell parameters (Table 3) were determined for tetrakis(vinylisocyanide)rhodium(I) perchlorate by least-squares refinement based on 2θ, ϕ, and χ of 12 accurately centered reflections, measured on the quarter circle General Electric diffractometer. The crystal used measured 0.05 x 0.1 x 0.5 mm. The intensities of 1199 unique reflections were measured using 2θ-θ at rates of 1°/min or 2°/min. Intensities were corrected for Lorentz, polarization, background, absorption and decay; atomic scattering factors of rhodium and chloride were corrected for anomalous dispersion (real part) (18). Initial atom positions were assigned on the basis of Patterson maps. Oxygen atoms and vinyl carbon atoms (as well as hydrogen atoms) could not be seen on Pattersons and were added at calculated 2- or 4-fold disordered positions. After refinement reached $R \simeq 0.09$, the vinyl carbon atoms were removed from the model and their positions were reassigned on the basis of difference Fourier maps. Refinement in space group Immm proceeded to $R = 0.084$, $wR = 0.02567$ for 1199 reflections; $R = 0.058$, $wR = 0.02462$ for 676 reflections with $F^2 > 3\sigma$. The real goodness-of-fit reached 4.37 for 1199 reflections. Difference maps were essentially flat after

Table 3. Unit Cell Parameters of Rhodium Isocyanide Complexes

a) Stacking Repeats

Complex	$\bar{a}_o$ (Å)	n	$\bar{a}_o/n$ (Å)	Source
$[Rh(CNCHCH_2)_4]ClO_4$	8.78	3	2.93	oscillation
$[Rh(CNCH_3)_{3.38}]BF_4$	5.87	2	2.93	oscillation
$[Rh(CNC_6H_5)_4]BF_4$			3.03	oscillation
$[Rh(CNC_6H_5)_4]Cl$	23.54	8	2.94	powder
$[Rh(CNC_6H_5)_{3.67}](ClO_4)_{1.33}$	23.79	8	2.98	oscillation
$[Rh(CNC_6H_5)_4]\ ClO_4$			3.20	oscillation

b) Unit Cell Parameters of $[Rh(CNCHCH_2)_4]ClO_4$

	a (Å)	b (Å)	c (Å)	v (Å^3)
Room Temperature	8.810	22.851	12.696	2556
22° K	8.671	22.114	12.391	2376

Space Group, Immm
Absorbtion Coefficient 99.6 cm^{-1} $CuK\bar{\alpha}$; 11.56 cm^{-1} $MoK\bar{\alpha}$
Density, calc. 1.623 g/cm^3 (6 Formula Units/cell)
Major Crystal Faces [010], [011], [001]

c) Indexing of $[Rh(CNC_6H_5)_4]Cl$ Powder Patterns

θ(obs)	hKℓ
5.63	003
7.25	222
8.625	400
11.33	006
11.685	520
13.61	620
16.96	650
17.39	652
18.67	654
19.10	0010
31.36	0016

$\bar{a}_o = \bar{b}_o = 20.64$ Å

$\bar{c}_o = 23.54$ Å

refinement, except for small residual peaks ($\sim 1e^-/\mathring{A}^3$) at rhodium and chloride positions.

The intensities of 1506 unique reflections were measured at 21.4 - 22.4° K using 2θ-ω scans on the locally designed low temperature diffractometer (19). Graphite monochromatized $MoK\bar{\alpha}$ radiation was used. The crystal used measured 0.036 x 0.081 x 0.36 mm^3. The scan rate used was 1°(2θ)/minute, and backgrounds were measured at both ends of the scan range for a total of 1 minute. The same kind of corrections applied to room temperature data were applied (18). Because of the small size of the crystal, and the low intensity of diffraction with $MoK\bar{\alpha}$, only 1032 reflections had observed intensities greater than zero after correction for background. Only 282 reflections had $F^2 > 3\sigma$. Moreover, the rapid drop-off in intensity with increasing 2θ is nearly unchanged between 300° K and 22° K.

The low temperature structure of $[Rh(CNCHCH_2)_4]ClO_4$ was partially refined by least-squares. Only the coordinates and temperature factors of the rhodium atoms and the atoms of one of the three independent vinylisocyanide ligands could be refined, due to the poor quality of the data. The coordinates of the atoms of the other two ligands were determined from Fourier maps. Spurious (noise) peaks on the Fourier map had a magnitude of up to $\pm 3e^-/\mathring{A}^3$, while the isocyanide carbon and nitrogen peaks had a magnitude about twice as great. Vinyl carbon peaks were of about the same intensity as the larger noise peaks, and were assigned on the basis of both

Fourier maps and geometrical considerations. The partly refined model gave R = 0.342 for 1032 reflections with F > 0, and R = 0.132 for 282 reflections with $F^2 > 3\sigma$. Weighted residuals, wR were 0.0729 and 0.0613 for all 1506 reflections, and 282 reflections having $F^2 > 3\sigma$, respectively. The weighted goodness-of-fit was 2.58 for the full data set.

Electronic Spectra

Electronic absorption spectra of tetrakis(vinylisocyanide) rhodium(I) chloride and tetrafluoroborate in a variety of polar solvents were obtained from 10,000 to 50,000 cm^{-1}. The observed bands and intensities are tabulated in Table 4. The absorption spectra of the chloride salt at different concentrations are shown in Figure 4. Photoaccoustic spectra of $[Rh(CNCHCH_2)_4]ClO_4$ and the partially oxidized $[Rh(CNC_6H_5)_{3.67}](ClO_4)_{1.33}$ were obtained using powder samples, and are shown in Figure 5 (9).

Results

Characterization and composition

The complexes are black or coppery-brown, hygroscopic (especially with smaller ligands and anions), and difficult to crystallize. The chloride salts are soluble in water and polar organic solvents, while salts of larger anions are nearly insoluble in water. Complexes

Table 4. Solution Spectroscopic Data - $[Rh(CNCHCH_2)_4]Cl$ and $[Rh(CHCHCH_2)_4]\ BF_4$

Monomer Spectra

Absorbtion band	$Rh(CNCHCH_2)_4BF^{+}$		$Rh(CNCHCH_2)_4Cl^{\ddagger}$	
	λ	ε	λ	ε
intraligand absorbtion	233	(34,000)	not measured	
$^1A_{1g} \rightarrow {}^1E_u$	329	(19,000)	324	(17,000)
$^1A_{1g} \rightarrow {}^1A_{2u}$	409	(5,000)	395	(3,000)
$^1A_{1g} \rightarrow {}^3A_{2u}$	457	(700)	450	(550)

$^{+}$in CH_3CN
5×10^{-5} and 3×10^{-4} M

‡in H_2O
9×10^{-5} M

Positions of lowest intense band in the spectra of $[Rh_n(CNCHCH_2)_{4n}]^{n+}$

	$BF_4^{-\ddagger}$	$Cl^{-\ddagger}$
n = 1	403	395
n = 2	555	550
n = 3	715	715
n = 4		962

‡in H_2O
9×10^{-4} M

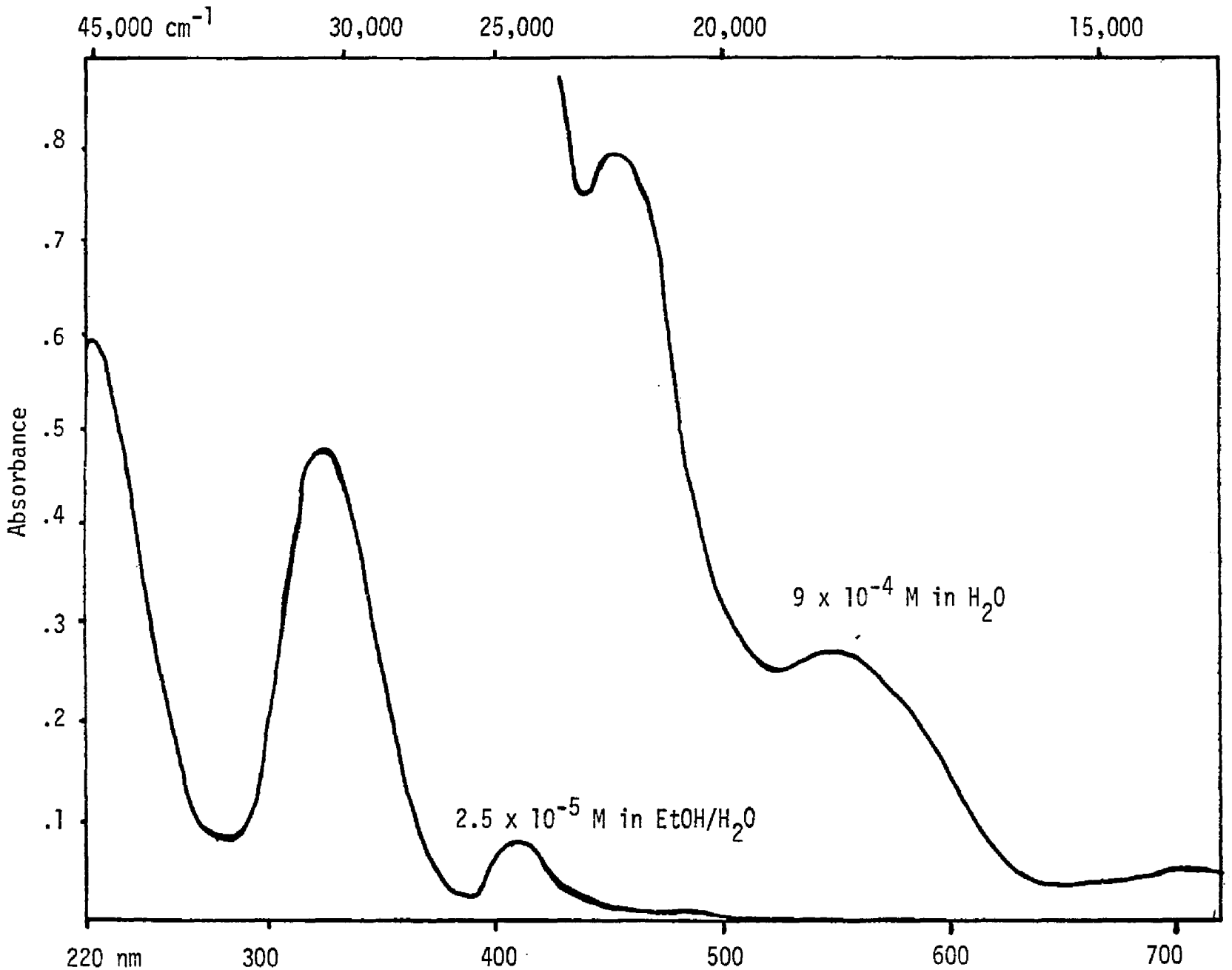

Figure 4. Absorbtion spectra of $Rh(CNCHCH_2)_4Cl$

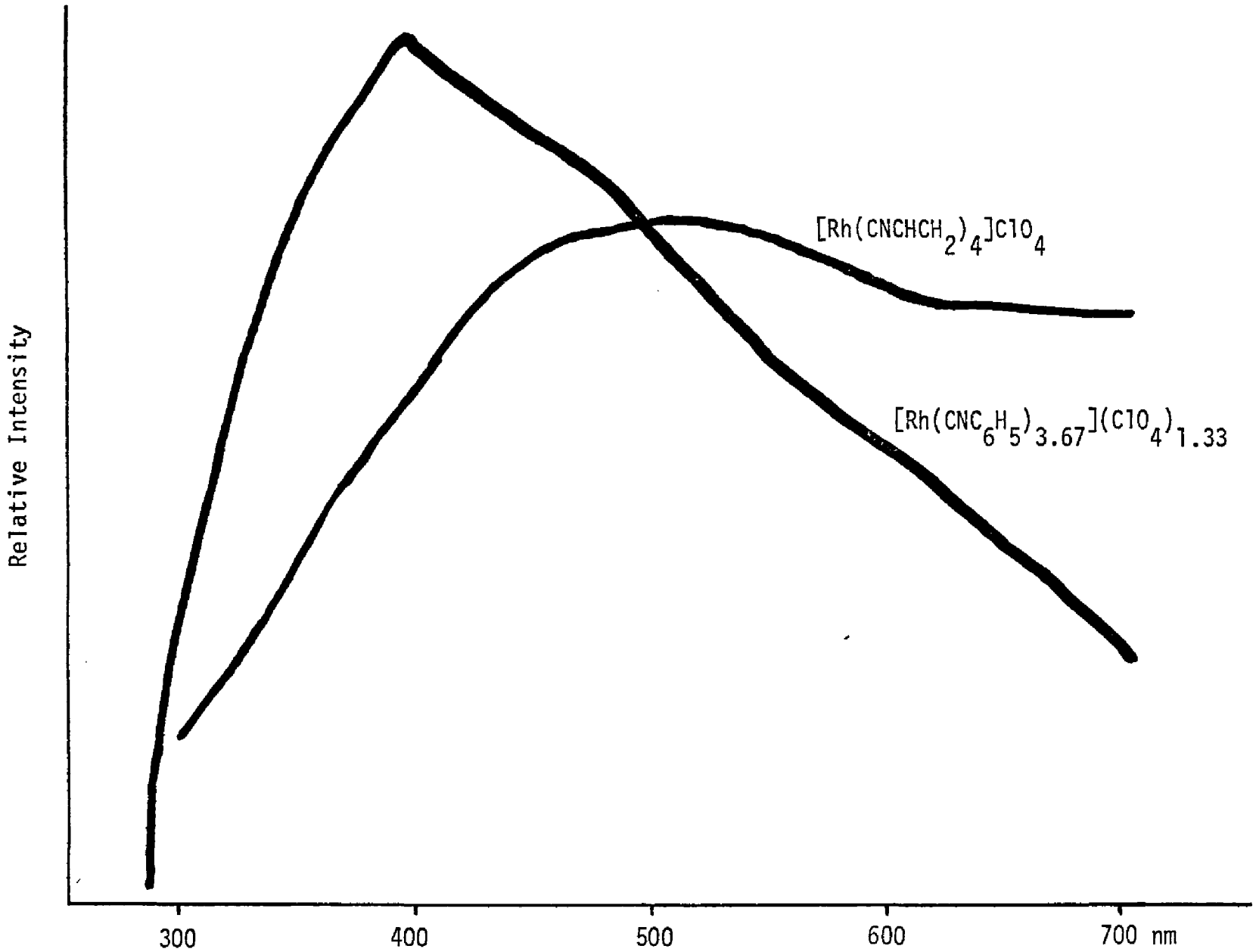

Figure 5. Photoaccoustic spectra of solid $[Rh(CNCHCH_2)_4]ClO_4$ and $Rh(CNC_6H_5)_{3.67}](ClO_4)_{1.33}$

decrease in solubility with decrease in size of ligand, reflecting stronger crystal-binding forces.

The analytical data in Table 1 indicate that deviations from the expected stoichiometry of tetrakis(isocyanide)rhodium(I) salts may occur. $Rh(CNC_6H_5)_{3.67}(ClO_4)_{1.33}$ clearly demonstrates both non-integral ligand-to-rhodium and anion-to-rhodium ratios, although the C, H, N analyses of "$Rh(CNCH_3)_{3.38}BF_4$" and "$Rh(CNCHCH_2)_{2.7}Cl$" suggest similar non-integral stoichiometry. Careful preparation of tetrakis(phenylisocyanide)rhodium(I) perchlorate in the absence of oxygen results in a material without partial oxidation. Tetrakis(phenylisocyanide)rhodium(I) chloride, tetrakis(vinylisocyanide)rhodium(I) chloride and perchlorate all appear to have little or no partial oxidation. Deliberate attempts to produce high degrees of partial oxidation by addition of Rh(III) complexes to the rhodium(I) vinylisocyanide complexes have not been successful.

The stoichiometry of $Rh(CNC_6H_5)_{3.67}(ClO_4)_{1.33}$ may reflect its structural details. Extra perchlorate anions may occupy ligand positions within the structure. Partial oxidation may account for the increase in conductivity of this complex with respect to tetrakis(phenylisocyanide)rhodium(I) chloride (Table 2).

Optical properties and crystal structures

Well formed needle-shaped crystals of $[Rh(CNCHCH_2)_4]ClO_4$, $[Rh(CNC_6H_5)_{3.67}(ClO_4)_{1.33}$, $[Rh(CNC_6H_5)_4]ClO_4$, $[Rh(CNC_6H_5)_4]BF_4$, and $[Rh(CNCH_3)_{3.38}]BF_4$ exhibit strong optical dichroism in plane

polarized light. Maximum extinction occurs when the electric vector is parallel to the needle axis, which in all cases coincides with a unique crystallographic direction ($\bar{a}_o$). All crystals transmit when the electric vector is perpendicular to $\bar{a}_o$, if the crystal is not extremely thick. Crystals of $[Rh(CNCHCH_2)_4]ClO_4$ transmit red light in the b_o direction.

The rotation photographs of each of the crystals (rotation axis = $\bar{a}_o$) showed the same typical set of intense layer lines corresponding to a d spacing of about 2.95 Å, except that the extremely fibrous crystal of $[Rh(CNC_6H_5)_4]ClO_4$ showed a significantly larger "strong repeat" of 3.20 Å. In contrast, the partially oxidized $[Rh(CNC_6H_5)_{3.67}](ClO_4)_{1.33}$ showed a well defined pattern of seven pairs of weak layer lines and one pair of strong layer lines corresponding to $d = a_o/8 =$ 2.98 Å.

Gunier powder photographs of $[Rh(CNC_6H_5)_4]Cl$ showed a simple pattern of 11 lines which could be indexed to a tetragonal cell having $c_o/8 = d(Rh\text{-}Rh)$ as in $[Rh(CNC_6H_5)_{3.67}](ClO_4)_{1.33}$. All of the lines could be indexed to a tetragonal cell with $\bar{a}_o = 20.64$; $c_o = 23.54$ Å (Table 3c). Since the cell is large, the indexing is questionable, but the four strong 00ℓ reflections (especially, very strong, broad $00^{1}6$ at $2\theta = 62.72$) lend strong support to a Rh-Rh repeat of 2.94 Å.

The Rh-Rh bond lengths in these crystals are considerably shorter than in dimeric rhodium isocyanide complexes (3.19 Å); longer than in rhodium metal (2.69 Å) (20) or in rhodium(0) complexes such as

$[Rh(CO)(PPh_3)_2]_2$ (2.63 Å) (21); and similar to the bond lengths in rhdoium(II) complexes as $Rh_2(DMG)_2(PPh_3)_2 \cdot H_2O \cdot C_3H_7OH$ (2.936 Å) (22). Only $[Rh(CNCHCH_2)_4]ClO_4$ crystals showed the diffraction patterns, on oscillation and Weissenberg photographs, of non-fibrous single crystals. The strong layer lines of this crystal were interspaced with two additional, very weak layer lines, indicating that $\bar{a}_0$ = 3 x 2.93 Å for this compound.

Weissenberg photographs indicate that $[Rh(CNCHCH_2)_4]ClO_4$ forms body centered orthorhombic crystals. All reflections are of the kind $h + k + \ell = 2n$, and there are no other systematic absences. Thus, the probable space group was determined to be Immm, Imm2 $I2_12_12_1$, or I222.

Crystal structure of $[Rh(CNCHCH_2)_4]ClO_4$

A three-dimensional Patterson map, calculated with all of the available room temperature diffractometer data, revealed that six rhodium atoms occupy two point sets: 2 Rh in (000, ½½½) and 4 Rh in (000,½½½) + (x00,$\bar{x}$00), where x = 0.33272(27). Six perchlorate chlorines also occupy two point sets: 2 Cl in (0½0,½0½) and 4 Cl in (00½,½½0) + (0x0,0$\bar{x}$0), where x = ¼. There are twenty-four ligands of three independent kinds, four of each of two kinds bonded to Rh at (000,½½½) and sixteen of one kind bonded to the other set of Rh atoms. The former two ligands have vinyl carbons exhibiting high thermal motion and disorder. Ligand 1 lies along the (0,y,0)

axis and both vinyl carbons have very high thermal motion, indicating that the electron density maximum along the (0y0) axis is the result of an average of multi-fold disorder of atoms about this axis. Since the root-mean-squared amplitude of vibration of these atoms is so high, ~0.4 Å, the required geometry of the ligand (a C = C-N bond angle of ~120°) is not contradicted. Ligand 2 lies along the (00z) axis. Its end vinyl carbon atom is disordered across the mirror plane at y = 0, and has extremely high thermal motion in the x direction, perhaps reflecting torsional motion of the ligand. This atom was revealed in Fourier maps (Figure 6) and its position was not refined due to proximity to the z = 0 mirror plane. Ligand 3 is not disordered, but has fairly high thermal motion. It is bent significantly out of the x = 1/3 plane, allowing mirror related ligands on Rh atoms at (±0.33272, 0.0, 0.0) to minimize their steric interactions. The only close ligand-ligand interatomic distances involve isocyanide carbon atoms. Atom positions and temperature factors are collected in Table 5. Bond lengths and angles, as well as some non-bonding contact distances, are shown in Table 6. An ORTEP diagram of the structure is shown in Figure 7. Note that all light atom bond lengths have fairly high standard deviations, due to the dominance of rhodium scattering. Bond lengths and angles associated with the vinyl carbon atoms have especially high standard deviations.

The low intensity of the low temperature data set impeded refinement of the structure. A rapid drop-off in intensity with

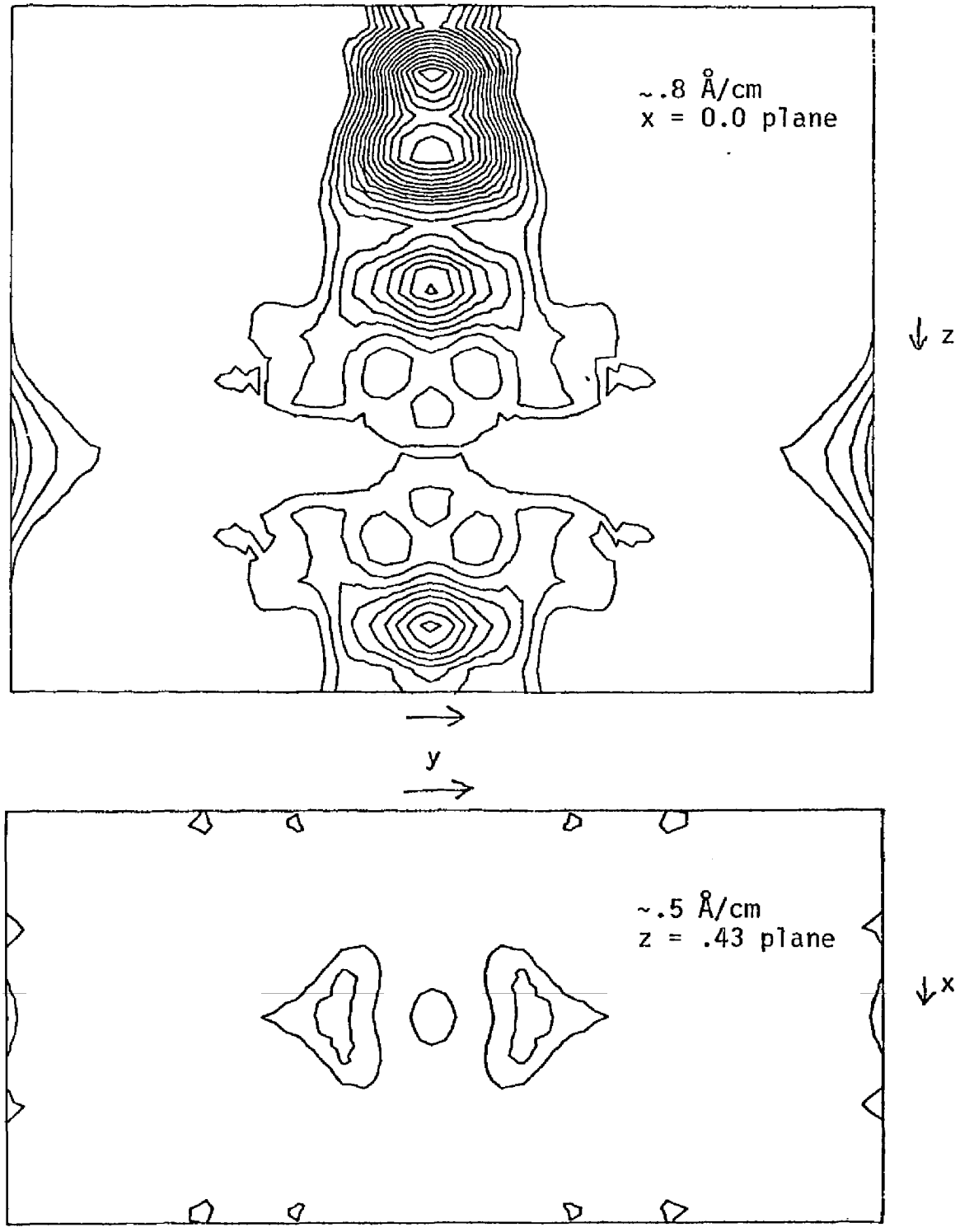

Figure 6. Fourier map of ligand 2, $[Rh(CNCHCH_2)_4]ClO_4$. Contours at $.2e^-/Å^3$ intervals.

Table 5a. Refined Atomic Coordinates for $Rh(CNCHCH_2)_4ClO_4$ at Room Temperature

	x	y	z
Rh 1	0	0	0
Rh 2	33272 (27)	0	0
Cl 1	0	50000	0
Cl 2	0	25000	50000
C 1	0	8954 (134)	0
N 1	0	13490 (113)	0
C 2	0	20425 (286)	0
C 3	0	25026 (354)	0
C 4	0	0	16582 (373)
N 2	0	0	25189 (326)
C 5	0	0	36326 (282)
C 6	0	5000	41651 (635)
C 7	32687 (199)	5936 (67)	11363 (107)
N 3	31173 (176)	9442 (60)	18026 (110)
C 8	28888 (360)	13990 (160)	25897 (242)
C 9	27718 (537)	13591 (267)	34075 (413)

	x	y	z
O1	0	5639	0
O2	0	4787	1084
O3	1348	4788	-539
O4	0	3139	5000
O5	0	2287	6084
O6	1348	2288	4460
O7	0	1861	5000
O8	0	2713	3916
O9	-1347	2712	5540

Oxygen coordinates have been multiplied by 10^4. All others have been multiplied by 10^5.

Table 5b. Refined Temperature Factors for $Rh(CNCHCH_2)_4ClO_4$ at Room Temperature.

	U11	U22	U33	U12	U13	U23
Rh 1	592 (22)	962 (33)	974 (40)	0	0	0
Rh 2	568 (11)	798 (14)	859 (18)	0	0	0
Cl 1	2590 (298)	4070 (363)	4126 (394)	0	0	0
Cl 2	1480 (102)	1736 (103)	4853 (246)	0	0	0
C 1	943 (215)	899 (190)	1767 (349)	0	0	0
N 1	1105 (217)	837 (163)	2865 (434)	0	0	0
C 2	4082	1738 (539)	4203	0	0	0
C 3	3063 (938)	4837	1901 (563)	0	0	0
C 4	312 (118)	1175 (241)	2456 (500)	0	0	0
N 2	1468 (314)	3076 (529)	1886 (427)	0	0	0
C 5	3814 (879)	4256 (937)	508 (188)	0	0	0
C 6	6184	3085 (960)	3048	0	0	-1887 (751)
C 7	653 (68)	1530 (114)	1196 (95)	238 (132)	-48 (134)	-49 (90)
N 3	844 (98)	1795 (117)	1705 (115)	-57 (93)	-35 (95)	-770 (103)
C 8	1726 (270)	3598 (355)	2630 (296)	-273 (237)	-184 (230)	-2235 (290)
C 9	4301 (554)	5815 (780)	5313 (783)	-599 (457)	1714 (533)	-4321 (746)

	B
O1	16.00
O2	16.00
O3	16.00
O4	16.00
O5	16.00
O6	16.00
O7	16.00
O8	16.00
O9	16.00

All Uij's have been multiplied by 10^4.

Table 6

$Rh(CNCHCH_2)_4ClO_4$ Room Temperature Structure, Bond Lengths, Angles, and Contact Distances

Rh 1 - Rh 2	2.9314 (24) Å
Rh 2 - Rh 2′	2.9475 (48) Å
Rh 1 - C 1	2.05 (3) Å
Rh 1 - C 4	2.11 (4) Å
Rh 2 - C 7	1.93 (2) Å
C 1 - N 1	1.04 (4) Å
C 4 - N 2	1.09 (5) Å
C 7 - N 3	1.17 (3) Å
N 1 - C 2	1.58 (6) Å
N 2 - C 5	1.41 (4) Å
N 3 - C 8	1.46 (6) Å
C 2 - C 3	1.05 (12) Å
C 5 - C 6	1.33 (10) Å
C 8 - C 9	1.05 (12) Å
< N 2 - C 5 - C 6	120 (7)°
< Rh2 - C 7 - N 3	175 (2)°
< C 7 - N 3 - C 8	177 (4)°
< N 3 - C 8 - C 9	129 (8)°
C 7 ---- C 7′	3.05 (4) Å
C 7 ---- C 7′′	2.71 (2) Å
C 1 ---- C 4	2.94 (3) Å

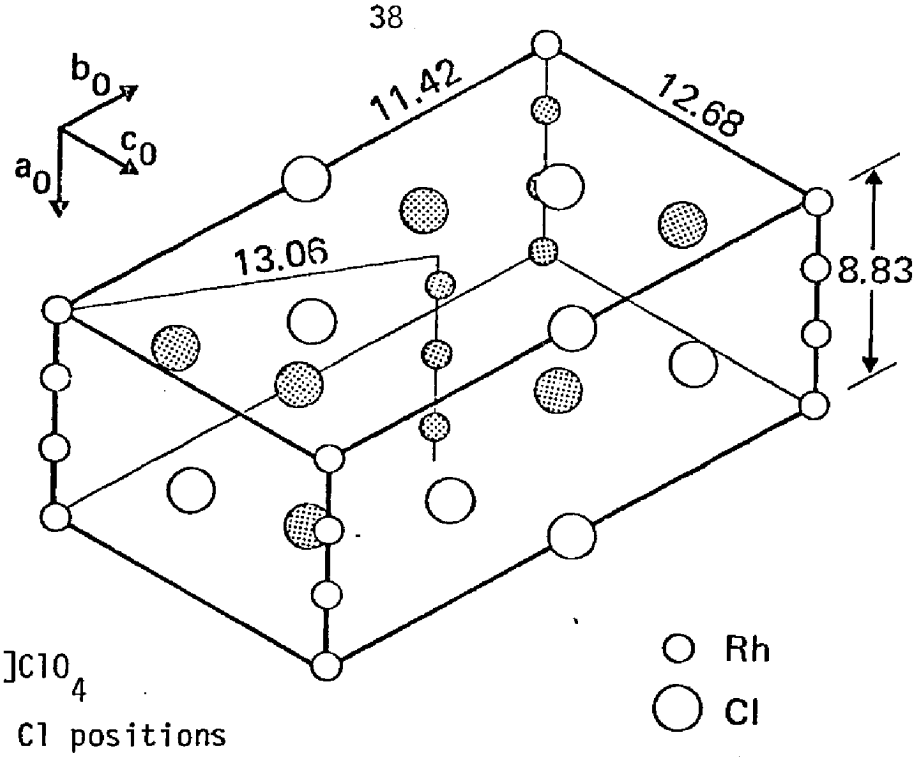

Unit cell of $[Rh(CNCHCH_2)_4]ClO_4$ having Rh and Cl positions

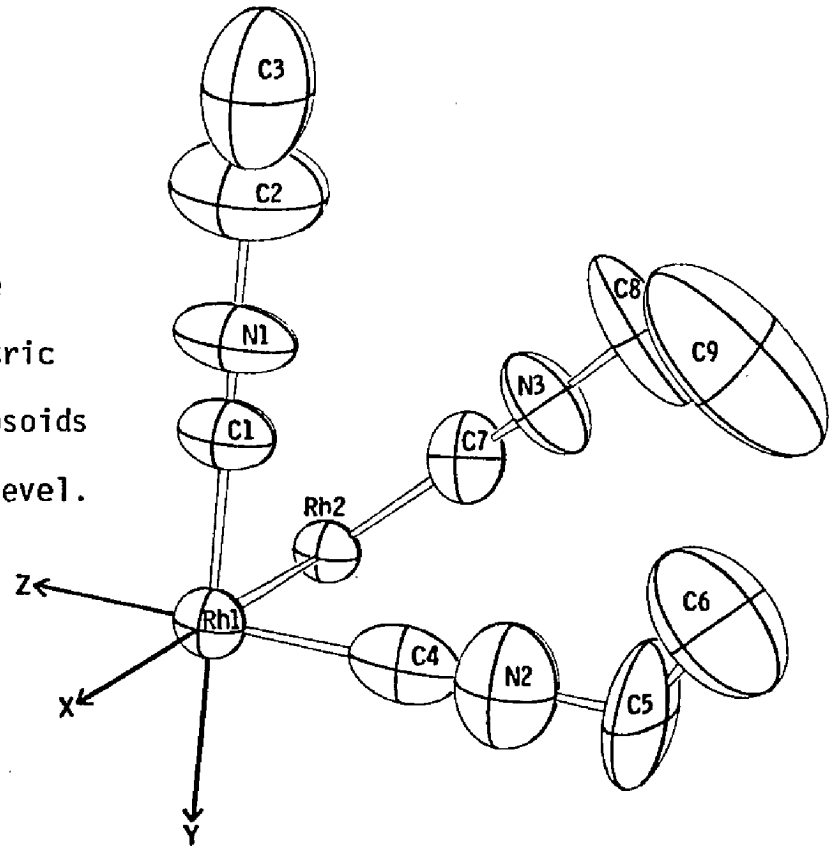

ORTEP diagram of the carbon chain asymmetric unit. Thermal ellipsoids at 30% probability level.

Figure 7. $[Rh(CNCHCH_2)_4]ClO_4$ structure.

increasing k and ℓ remained at low temperature, indicating retention of disorder in y and z parameters. However, h = 9 and 12 reflections were observed, reflecting a precisely defined Rh-Rh distance in the x direction. The "high thermal motion" of several atoms at room temperature is resolved into two-fold disorder at 22° K. However, only the rhodium atom coordinates, anisotropic temperature factors, and coordinates of the atoms of ligand 3, may be refined by least-squares. Other atom positions were obtained from Fourier maps. Atom positions and temperature factors are shown in Table 7; bond lengths, and bond angles are collected in Table 8.
There is no structural phase transition between 22° K and 300° K in $[Rh(CNCHCH_2)_4]ClO_4$. There is some reduction in thermal motion, but disorder is retained. There is no crystallographic evidence for partial oxidation in $Rh(CNCHCH_2)_4ClO_4$.

Electronic Structure

The electronic properties of crystalline $[Rh(CNR)_4]^+X^-$ may be rationalized from simple molecular orbital arguments and a knowledge of the properties of oligomeric species in the solid state and solution (1,2,10). Figure 2 shows a molecular orbital diagram for $[Rh(CNR)_4]_n^{n+}$ where n = 1,2, and 3, as well as a simple band diagram for the polymeric solid. The dimer and trimer are assumed to have staggered configurations, resulting in D_{4d} and D_{4h} symmetry, respectively. The highest occupied orbital of the monomer is $a_{1g}(dz^2)$; the lowest empty orbital is an a_{2u} orbital with Rh Pz and ligand π* character.

Table 7a. Atomic coordinates of $Rh(CNCHCH_2)_4ClO_4$ at 22° K.

	x	y	z
Rh 1	0	0	0
Rh 2	33333	0	0
C 1	0	9700	0
C 2	4000	21000	2000
C 3	0	24000	9000
C 4	0	1000	14300
C 5	0	1000	33000
C 6	6000	5000	37000
C 7	32761	6109	12042
C 8	29552	14164	25196
C 9	25326	12772	34295
N 1	0	15700	0
N 2	0	1000	22500
N 3	31422	9248	18062
Cl 1	0	50000	0
Cl 2	0	25000	46000
O1	0	56390	0
O2	0	47870	10840
O3	13480	47880	5400
O4	0	31790	46000
O5	0	23270	56840
O6	13480	23280	40600

All coordinates have been multipled by 10^5.

Table 7b. Temperature Factors of $Rh(CNCHCH_2)_4ClO_4$ at 22° K.

	U11	U22	U33	U12	U13	U23
Rh 1	743	1179	746	0	0	0
Rh 2	632	616	1189	0	0	0
C 1	464	791	3047	0	0	0
C 2	B = 10.0					
C 3	B = 10.0					
C 4	1063	1090	1786	0	0	0
C 5	B = 10.0					
C 6	B = 10.0					
C 7	793	2005	1620	584	564	136
C 8	1266	5911	3337	-423	61	-3084
C 9	4468	4744	4748	-801	2386	-3794
N 1	746	1409	3202	0	0	0
N 2	712	3126	1638	0	0	0
N 3	563	2294	1920	-225	-14	-685
Cl 1	1746	8654	8334	0	0	0
Cl 2	1287	1666	6200	0	0	0
O1	B = 16.0					
O2	B = 16.0					
O3	B = 16.0					
O4	B = 16.0					
O5	B = 16.0					
O6	B = 16.0					

All Uij's have been multiplied by 10^4.

Table 8

$[Rh(CNCHCH_2)_4]ClO_4$ Low Temperature Structure, Bond Lengths, and Angles

Rh 1 - C 1	2.14*	Rh 1 - Rh 2	2.890 (10)
Rh 1 - C 4	1.78*	Rh 2 - Rh 2′	2.890 (10)
Rh 2 _ C 7	2.01 (3)		
C 1 - N 1	1.26*		
C 4 - N 2	1.02*		
C 7 - N 3	1.03 (4)		
N 1 - C 2	1.29*		
N 2 - C 5	1.30*		
N 3 - C 8	1.41 (5)		
C 2 - C 3	1.05*		
C 5 - C 6	1.14*		
C 8 - C 9	1.22 (6)		
< C 1 - N 1 - C 2	164° *		
< N 1 - C 2 - C 3	145° *		
< N 2 - C 5 - C 6	116° *		
< Rh2 - C 7 - N 3	175 (3)°		
< C 7 - N 3 - C 8	172 (4)°		
< N 3 - C 8 - C 9	115 (5)°		

*At least one atom position estimated from Fourier map, and not refined by least-squares.

On dimerization, in symmetry D_{4d}, two sets of a and b_2 orbitals result, each of which is primarily associated with either the $a_{1g}(dz^2)$ or $a_{2u}(Pz\pi^*)$ orbitals of the monomer. The low energy transition at 550 nm in water or acetonitrile solutions of $[Rh(CNCHCH_2)_4]ClO_4$ is assigned to the $1b_2 \rightarrow 2a_1$ transition of $[Rh(CNCHCH_2)_4]_2^{2+}$. Likewise, the 715 nm band is assigned to the $2a_{1g} \rightarrow 2a_{2u}$ transition of $[Rh(CNCHCH_2)_4]_3^{3+}$. Oligomerization is allowed because of significant mixing of the $a_{1g}(dz^2)$ and $a_{2u}(P_2\pi^*)$ derived levels of the monomer, stabilizing the lower, filled orbitals of the oligomer, and destabilizing the higher, empty orbitals. If the Rh-Rh interaction in the stacked crystalline modifications is similar in strength to that in the oligomers, a band gap between the dz^2 and Pz-π^* bands might be expected to be significantly smaller than lowest energy band of the tetramer at 962 nm (10,400 cm^{-1} = 1.3 eV). Furthermore, the Rh-Rh bond length in the polymer is apparently significantly shorter than in the oligomers. Photoaccoustic spectroscopy of $[Rh_2(CNC_6H_5)_8][B(C_6H_5)_4]_2$ in the solid state reveals absorbtion at about the same wavelength as the $1b_2 \rightarrow 2a_1$ band in solution. The Rh-Rh bond length in $[Rh_2(CNC_6H_5)_8][B(C_6H_5)_4]_2$, from refinement of the crystal structure, is 3.19 Å. The significant shortening of the Rh-Rh bond in $[Rh(CNCHCH_2)_4]ClO_4$ must lead to a much stronger overlap of dz^2 and $Pz\pi^*$ orbitals in the adjacent monomeric units, and a much lower band gap than would be predicted from the oligomer spectra.

The photoaccoustic spectra of $[Rh(CNC_6H_5)_{3.67}](ClO_4)_{1.33}$ and $[Rh(CNCHCH_2)_4]ClO_4$ have strong absorbtion throughout the visible

region. This is consistent with strong interactions resulting in a band structure, with activation energy <1 eV for excitation into the conduction band.

The room temperature conductivity of $[Rh(CNCHCH_2)_4]ClO_4$ is ~2 Ω^{-1} cm^{-1} as measured on single crystals. The plot of ln σ vs. 1/T (Appendix 2) reveals that the conductivity is activated, ΔE ~0.10 eV in the linear low temperature region. This electrical behavior is consistent with a small band gap between the dz^2 and Pz-π* bands, and conduction via thermal population of Pzπ* band. Disorder may play a role in increasing the conductivity.

The transmission of polarized light, with electric vector perpendicular to $\bar{a}_o$, through single crystals of $[Rh(CNCHCH_2)_4]ClO_4$ in the $\bar{b}_o$ direction, indicates that the activation energy for hopping between chains is very high ($\geq$1.5 eV). Although crystals are far too thin for conductivity measurements with the Montgomery configuration, it is certain that these complexes are among the most anisotropic of known quasi-one-dimensional conductors.

Powder conductivities increase with decrease in ligand size. This is presumably due to greater interchain coupling when rhodium chains are close together.

Conclusions

Tetrakis(isocyanide)rhodium(I) salts crystallize in conducting, stacked modifications if ligands and anions are reasonably small (CN-R: R = methyl, vinyl or phenyl; x^-: Cl^-, BF_4^-, ClO_4^-). Partial oxidation of the rhodium chain is likely in some of the complexes, for example $[Rh(CNC_6H_5)_{3.67}](ClO_4)_{1.33}$. However, a non-integral average oxidation state does not seem to be a necessary condition for moderately high conductivity (11). Chemical analysis and refinement of the room temperature crystal structure of $[Rh(CNCHCH_2)_4]ClO_4$ indicate that this complex has one perchlorate anion per rhodium atom. If a very low level of partial oxidation exists, it may effect the magnitude of the conductivity, but would be present as a crystallographic impurity and no metallic state would exist. A minor difference in two Rh-Rh bond lengths occurs at room temperature and probably at low temperature. This inequality, along with the differences in the chemical environments of the two crystallographically inequivalent rhodium atoms, seems to be due to steric interactions (i.e., steric repulsion, between the eclipsed sets of ligands on the equivalent Rh atoms at $x \simeq 1/3$ and $x \simeq 2/3$, results in displacement from the ideal positions and lengthening of the Rh2-Rh2′ bond). Both integral oxidation state and crystallographic inequivalence of metal atoms have been observed separately in conducting, stacked d^8 metal complexes (11,23). The conditions for conductivity in these materials seem to be less restrictive than previously thought.

Non-integral oxidation has been described as a necessary condition for high conductivity in d^8 metal complexes (5). The conductivities of complexes exhibiting both integral and non-integral oxidation states have similar dependence on temperature. Magnitudes of the room temperature conductivities of the rhodium isocyanide complexes are ~100 times less than the partially oxidized platinum complexes, while the activation energies are similar. The decrease of room temperature conductivities in the sequence:

$$K_2Pt(CN)_4Br_{0.33}\cdot H_2O > Ir(CO)_3Cl \sim K_{0.6}[Ir(CO)_2Cl_2]\cdot 0.5H_2O \gtrsim$$

$$[Rh(CNCHCH_2)_4]ClO_4$$

follows the increase in interchain distances.

References

1. K. Krogmann, Angew. Chem. Int. Ed., 8, 35 (1969).
2. H. R. Zeller, Adv. Solid State Phys., 13, 31 (1973).
3. T. W. Thomas and A. E. Underhill, Chem. Soc. Rev., 1, 99 (1972).
4. H. J. Keller in Low Dimensional Cooperative Phenomena, Ed., H. J. Keller. Nato Advanced Studies Institute Series, 7B, Plenum Press, p. 315.
5. J. S. Miller and A. J. Epstein, Chapter in Progress in Inorganic Chemistry, Vol. 20. Ed. S. J. Lippard. John Wiley and Sons, Inc., New York (1976).
6. A. P. Ginsberg, J. W. Koepke, J. J. Hansen, K. W. West, F. J. DiSalvo, C. R. Sprinkle, and R. L. Cohen, J. Inorg. Chem., 15, 514 (1976).
7. J. G. Gordon II, R. Williams, C. -H. Hsu, E. Cuellar, S. Samson, K. Mann, H. B. Gray, V. Hadek, and R. Somoano, Annals of New York Academy of Sciences, 313, 580 (1978).
8. K. R. Mann, N. S. Lewis, R. M. Williams, H. B. Gray, and J. G. Gordon II, Inorg. Chem., 17, 829 (1978).
9. R. B. Somoano, A. Gupta, W. Voksen, A. Rembaum, and R. Williams, Organometallic Polymers, Academic Press (1978).
10. K. R. Mann, J. G. Gordon II, and H. B. Gray, J. Am. Chem. Soc., 97, 3553 (1975).
11. A. H. Reis, Jr., and S. W. Peterson, Annals of New York Academy of Sciences, 313, 560 (1978).

12. J. Chatt and L. M. Venanzi, J. Chem. Soc. A., 4735 (1957).

13. D. S. Matteson and R. A. Bailey, J. Am. Chem. Soc., 90, 3761 (1968).

14. D. S. Matteson and R. A. Bailey, Chemistry and Industry, 191 (1969).

15. W. P. Weber, G. W. Gokel, and I. K. Ugi, Angew. Chem. Int. Ed., 11, 530 (1972).

16. Methyl was prepared by dehydration of methyl formamide with p-toluene sylfonyl chloride in quinoline.

17. I. Ugi, U. Fetzer, U. Enholzer, H. Knupfer, and K. Offermann, Angew. Chem. Int. Ed., 4, 472 (1965).

18. Absorption corrections were performed using the absorption coefficients from: International Tables for X-Ray Crystallography Vol. I, Kynoch Press, Birmingham (1952). Atomic scattering factors, including the corrections for the real part of anomalous dispersion for Rh and Cl^- were obtained from: International Tables for X-Ray Crystallography Vol. III., Kynoch Press, Birmingham (1962). Atomic scattering factors for Rh were obtained from: D. T. Cromer and J. T. Waber, Acta. Cryst., 18, 104 (1975).

19. S. Samson, E. Goldish, and J. Dick, to be published.

20. J. Donohue, The Structure of the Elements, Wiley, New York (1974) p. 216.

21. P. Singh, C. B. Dammann, and D. J. Hodgson, Inorg. Chem., 12, 1335 (1973).

22. K. G. Caulton and F. A. Cotton, J. Am. Chem. Soc., 93, 1914 (1971).

23. J. M. Williams and A. J. Schultz, Annals of the New York Academy of Sciences, 313,509 (1978).

CHAPTER 3

Structural Phase Transition and Disorder in $(TTF)(Cl)_x$

R. Williams, C. Lowe Ma, and S. Samson*†

A. A. Noyes Laboratory of Chemical Physics
California Institute of Technology
Pasadena, California 91125

and

S. K. Khanna and R. B. Somoano†
Jet Propulsion Laboratory
California Institute of Technology
Pasadena, California 91125

*The x-ray crystallographic studies, especially the development of the low temperature x-ray goniometer, were sponsored by the National Science Foundation under Grant No. DMR-74-19029A1. Contribution No. 0000 from the Division of Chemistry and Chemical Engineering, California Institute of Technology.

†This paper represents one phase of research performed by the Jet Propulsion Laboratory, California Institute of Technology, sponsored by the National Aeronautics and Space Administration, Contract No. NAS7-100.

Abstract

$(TTF)Cl_x$, x = 0.67 and 0.70, is a quasi-one-dimensional organic conductor with a room temperature conductivity of ~ 150 Ω^{-1} cm^{-1}. At room temperature the structure is tetragonal and consists of chains of uniformly spaced, eclipsed TTF molecules surrounding channels occupied by chloride ions, which form a disordered lattice. The chloride sublattice becomes ordered and the TTF sublattice undergoes a structural phase transition from tetragonal to monoclinic symmetry at ~ 250° K. The angle β of the monoclinic crystal increases continuously as the temperature is decreased from 245° K to 19° K. The electrical conductivity shows a sharp decrease at the phase transition which is suggestive of the formation of commensurate charge density waves in the monoclinic crystal.

Introduction

The stabilization of the metallic state in quasi-one-dimensional organic metals has been a goal of researchers for many years. These materials exhibit metallic behavior down to a temperature, T_{MI} ~ 50 -200° K, where a metal-to-nonmetal (M-NM) transition takes place, resulting in nonmetallic behavior at low temperature. It is important to understand the nature of the forces that drive this transition in order that it may be controlled, and eventually suppressed, so as to stabilize the metallic state. Some of the experimentally controllable parameters which should influence the phase transition are the interchain coupling, the degree of disorder, and the nature of the molecular stacking along the chain (i.e., slipped versus eclipsed stacking).

There have been numerous studies of the M-NM phase transition in organic metals in which the cation and anion radicals stack in a slipped fashion.[1] However, very little work has been done on systems such as the halides and pseudohalides, (i.e., thiocyanate, SCN and selenocyanate SeCN) of tetrathiafulvalene (TTF)[2,3,4], in which the TTF molecules in the chain are eclipsed. In these materials the metallic state appears to be less stable (i.e., higher T_{MI}). Recent X-ray diffuse scattering studies of $(TTF)_{12}(SCN)_7$ reveal a tetragonal-to-monoclinic structural phase transition at ~ 340° K and the presence of one-dimensional incommensurate charge density waves (CDW) below this temperature.[5] In this paper, we report the results of our single-crystal X-ray study of the crystal structure of $(TTF)Cl_x$ (x = 0.67 and 0.70) at various temperatures down to 19° K. Here, the TTF molecules are eclipsed and uniformly stacked and the chloride lattice exhibits considerable structural disorder at room temperature.[6] The electrical conductivity and thermoelectric power undergo changes at 200-250° K, which are suggestive of a M-NM transition. Similar changes are observed in all of the halides and pseudohalides of TTF.

Experimental

Crystals of $(TTF)Cl_x$ were grown by co-diffusion of solutions of (TTF) $(ClO_4)_{0.7}$, and tetraethylammonium chloride in acetonitrile. The crystal structure was studied by a variety of X-ray diffraction techniques. Oscillation and Weissenberg photographs were obtained at room temperature. In addition, oscillation photographs were obtained at 120 ± 10° K by cooling with a stream of cold N_2 gas.

The room-temperature structure of $(TTF)Cl_{0.67}$ was determined and refined with the use of a three-dimensional data set that was obtained

with nickel-filtered CuK_α radiation (λ = 1.54178 Å) and a Datex automated, locally modified General Electric quarter-circle diffractometer. The crystal used was a tetragonal prism of the size 0.11 x 0.11 x 0.63 mm^3, the prism axis being $\underline{c_o}$. A total of about 800 reflections were measured up to $2\theta = 155°$, using $2\theta - \theta$ scans. These were corrected for Lorentz, polarization, and absorption (μ = 104 cm^{-1}), and merged to a set of 303 unique reflections.

For the study of structural changes at temperatures ranging from 300° K to 19° K we used a locally designed and built low-temperature diffractometer[7] consisting of a CTI model 21 closed-cycle "Cryocooler", an E & A full-circle and base goniometer, a Syntex $P\bar{1}$ interface (and software package), a graphite monochromator of our own design, and a molybdenum-target X-ray tube. The temperature can be varied in steps of 0.1° K and kept constant for long periods of time. The crystal used for this study [$(TTF)Cl_{0.67}$] was from the same batch as that used for the room-temperature work and had the dimensions 0.17 x 0.20 x 0.27 mm^3. It was mounted with the $\underline{c_o}$-axis approximately parallel to the rotation axis.

The electrical conductivities were measured by the standard four-probe technique using aquadag contacts.

Results

General Features of the Layer Lines and Stoichiometry

A number of batches of good crystals were obtained by the co-diffusion method. The two kinds of crystals studied in detail represent the extremes of the short range of stoichiometry exhibited by disordered tetragonal $(TTF)Cl_x$.

Figure 1 shows an oscillation photograph taken at room temperature of a crystal from one of the batches, which we label $(TTF)Cl_{0.70}$. The rotation axis is $\underline{c_o}$. It is seen that there are two sets of diffuse layer lines

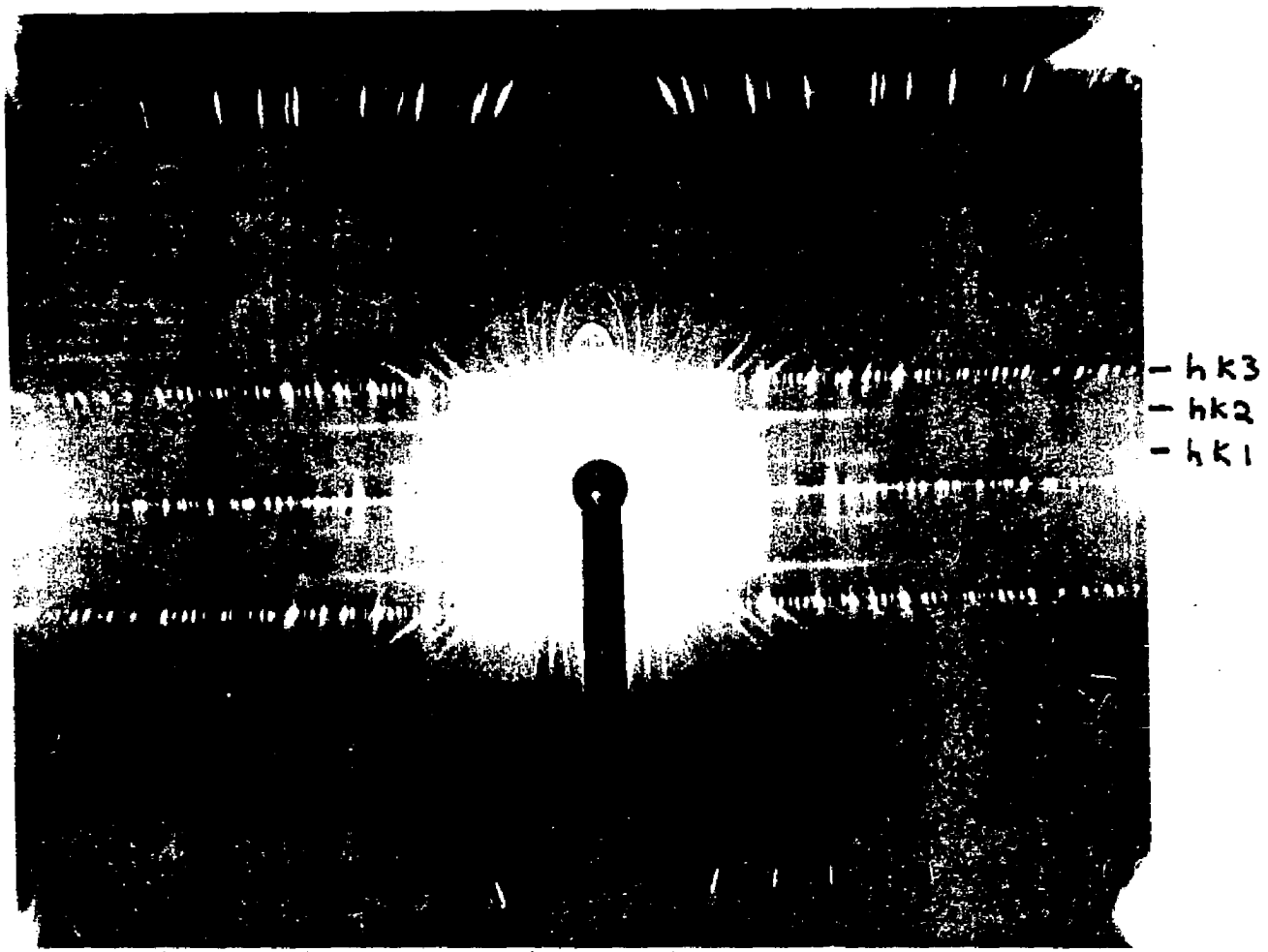

Figure 1. Oscillation photograph of $(TTF)Cl_{0.67}$.

marked hkl and hk2. Single crystals from the other batch which we label $(TTF)Cl_{0.67}$ (again, rotation axis is $\underline{c_o}$) gave rise to two similar sets of diffuse lines, which, however, differ somewhat in the spacings. In each case the hkl set corresponds to the d-spacing $d_{001} \sim 3.0 \times \underline{c_o}$ and the hk2 set to $d_{002} \sim 1.5 \times \underline{c_o}$, where $\underline{c_o}$ is the length of the cell edge that corresponds to d_{003} or the (non-diffuse) hk3 set (TTF sublattice). Each hk2 set is due solely to the chloride ions in the channels (Cl-sublattice) and the weaker hkl set results from both the Cl-sublattice and the TTF-sublattice. If the assumption is made that d_{002} is the same as the average Cl-Cl distance along z and that d_{003} represents the average TTF-TTF distance, the stoichiometry should correspond to the ratio d_{003}/d_{002}. In the absence of chemical analyses of sufficient accuracy to determine the minute differences in composition of the two batches, each label used above was assigned so as to represent the d_{003}/d_{002} ratio as determined from the corresponding oscillation photograph; see Table 1. The nominal camera radius was used for the determination of each d-spacing without applying a correction for film shrinkage. Thus, each d-spacing by itself may lack accuracy, but for the practical purpose considered here errors due to film shrinkage cancel out in the ratios. The stoichiometries 1:0.70 and 1:0.67 are consistent with the composition range previously reported[6] for the disordered tetragonal $(TTF)Cl_x$.

In $(TTF)Cl_{0.67}$ the chloride sublattice is commensurate with the TTF lattice whereas in $(TTF)Cl_{0.70}$ the two lattices are incommensurate with each other. The diffuseness of the hkl and hk2 layer lines indicates that there is a considerable degree of disorder in the chloride

Table 1. Repeat distances in the TTF and Cl Stacks

Phase	Temperature (°K)	d_{TTF} (Å)	d_{Cl} (Å)	d_{TTF}/d_{Cl}
TTF $Cl_{0.67}$	298	3.57	5.32	0.671
TTF $Cl_{0.67}$	120	3.54	5.36	0.660
TTF $Cl_{0.70}$	298	3.58	5.08	0.705
TTF $Cl_{0.70}$	120	3.57	5.36;	0.666;
			4.97	0.718

sublattices of each compound at room temperature. The diffuse nature of the spots which make up the hkl and hk2 layer lines, indicates that only very short-range order exists in the chloride sublattice.

The features of the oscillation photographs just discussed are in general similar to those that we have observed on photographs of $(TTF)Br_{0.74}$, $(TTF)_{12}(SCN)_7$, and $(TTF)_{12}(SeCN)_7$, except that in the case of $(TTF)Cl_x$, the diffuseness of the anion-sublattice reflections is considerably enhanced.

Refinement of the Room-Temperature Structure of $(TTF)Cl_{0.67}$

Weissenberg photographs of $(TTF)Cl_{0.67}$ showed that the structure is tetragonal with Laue symmetry $\underline{4}/\underline{mmm}$. All $0k\ell$ reflections were of the type $k + \ell = 2n$ and no other conditions for reflection were detectable. Thus, the probable space groups are $\underline{P4_2}/\underline{nm}$, $\underline{P\bar{4}n2}$, and $\underline{P4_2}\ \underline{mnm}$, of which the last one has all the necessary properties to incorporate the flat TTF molecules in columns parallel to the $\underline{c}$-axis and leaving channels parallel to these for the chlorides. The lengths of the edges of the smallest unit cell (TTF-lattice) are $\underline{a_o} = \underline{b_o} = 11.1931(7)$ Å and $\underline{c_o} = 3.6002(2)$ Å, as determined by a least-squares fit of 2θ values for 14 reflections measured with a diffractometer which was carefully calibrated for $2\theta_o$.

The trial structure consisted of two TTF molecules, with mmm symmetry, which are centered at (0,0,0; etc.), with $\bar{c}_o$ perpendicular to the molecular plane. The chloride ion and hydrogen atom were left out at this stage. A nearly uniform column of electron density at $x = 1/2$, $y = 0$ was observed on Fourier maps, and was ascribed to the highly disordered chloride ion. A chloride was included in the model structure; it was placed corresponding to the maximum in electron density of the column, at (1/2,0,1/4).

This trial structure was refined first isotropically and then anisotropically by full-matrix least-squares minimization of $\Sigma w(F_o^2 - F_c^2)$ and weights equal to $1/\sigma^2(F_o)^2+t)$, where t is a term accounting for errors other than counting statistics (CRYM program). The scattering factors of sulfur and chloride were corrected for the real part of anomalous dispersion; the imaginary component was ignored for this centrosymmetric space group.

Inclusion of a population factor for chloride as refinable parameter in the full matrix in some of the refinement cycles led to inconclusive results because of the high standard deviation of that parameter. Also, the chloride anisotropic temperature factor in the z direction, U_{33}, could not be refined. The Fourier section through the chloride channels ranging from z = 0 to z = 1/2 showed a variation in electron density of merely about 20% over that range, the minima being at z = 0 and z = 1/2 and the maximum at z = 1/4; see Fig. 3. Thus, the refinement was continued with 1.34 chlorides distributed over the two point sets 4d(1/2,0,1/4; etc.) and 4c(1/2,0,0; etc.) and with the inclusion of population factors P_d and P_c as refinable parameters that were constrained to $P_c = 1 - P_d$. These population parameters could be refined adequately. The anisotropic temperature factor of the chloride ions still showed high standard deviations and oscillated after partial refinement. The chloride temperature factors were held constant in the final stages of refinement, when the hydrogen atom, positioned by geometrical considerations, and an additional parameter to account for secondary extinction and counting losses, were included in the least-squares calculation. The final

agreement index obtained was R = 0.062 for all 299 reflections with $F_o > 0$ and R = 0.057 for 271 reflections with $F_o \geq 3\sigma$. The goodness-of-fit $[\Sigma w(F_o^2 - F_c^2)/n-p]^{1/2}$ for n = 299 observations and p = 30 refinable parameters (extinction included) was 4.39. This agreement is very satisfactory in view of the complications caused by the disorder of the chloride ions.

Room-Temperature Structure of $(TTF)Cl_{0.67}$

The refined atomic coordinates and the occupancies of the two point sets 4c and 4d by the 1.34 chloride ions are given in Table 2. The anisotropic temperature factors are listed in Table 3 together with the isotropic one for hydrogen.

Table 4 gives the molecular dimensions of the TTF species found in four refined structures including that of $(TTF)Cl_{0.67}$. All distances and angles (column headings a, b...etc. and α, β,... etc) as identified in the drawing at the bottom of that table are averaged over the mmm molecular symmetry observed for $(TTF)Cl_{0.67}$. Our estimated standard deviations for $(TTF)Cl_{0.67}$ are in the range of 0.009 = 0.011 Å (C-C), 0.005 - 0.006 Å (C-S) and 0.4 - 0.8 degrees (bond angles).

An interesting trend exhibited in Table 4 is the gradual elongation of the C=C bond labeled a and the shortening of the C-S bonds labeled b as the anticipated charge transfer (column e) increases. It is seen that the central C=C bond length (column a) is most sensitive to charge transfer. Some reservation seems appropriate as regards the degree of charge transfer in $(TTF)HgCl_3$ because $HgCl_3^-$ species are not clearly identifiable in

Table 2. The refined positional parameters

Kind of Atom	Occupancy	Point Set	x	y	z
C(1)	4	4f	0.04367(42)	0.04367(42)	0
C(2)	8	8i	0.24007(48)	0.15649(49)	0
S	8	8i	0.19364(12)	0.01008(11)	0
H	8	8i	0.3147(44)	0.1759(45)	0
Cl(1)	0.73(2)	4d	1/2	0	1/4
Cl(2)	0.61(2)	4c	1/2	0	0

Table 3. Refined anisotropic temperature factors for $(TTF)Cl_{0.67}$

Kind of Atom	U11	U22	U33	U12
C(1)	0.0653(10)	0.0653(10)	0.0468(32)	0.0012
C(2)	0.0781(31)	0.0987(36)	0.0736(35)	-0.0224(30)
S	0.0644(8)	0.0824(9)	0.0657(9)	0.0015(5)
Cl(1)	0.1051	0.1012	0.1069	-0.0051
Cl(2)	0.1153	0.1183	0.0678	0.0079
H	B(isotropic) = 6.00 $Å^2$			

Table 4. Dimensions of TTF cations in four refined structures

Type of Compound	Ref.	a	b	c	d	α	β	γ	δ	e
(TTF)°	10	1.349	1.757	1.726	1.314	122.7	114.5	94.3	118.6	0.
(TTF)(TCNQ)	11,24	1.369	1.743	1.736	1.323	122.6	114.7	94.9	117.7	~0.
$(TTF)Cl_{0.67}$	present paper	1.383	1.720	1.719	1.323	122.4	115.3	95.0	117.4	~0.
$(TTF)HgCl_3$	11*	1.40	1.71	1.72	1.33	122.3	115.5	94.7	117.5	~1.
		1.41	1.72	1.72	1.30	122.2	115.7	94.4	117.8	
		1.40	1.72	1.70	1.28	122.5	115.0	94.1	118.4	

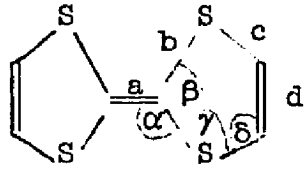

*Bond lengths and angles from Kistenmacher, private communication.

that structure. Nevertheless, the overall trend in the data is indicative of a charge transfer of nearly one electron.

Figure 2 shows a projection of the structure onto the (001) plane. The TTF cations stack in an eclipsed fashion with a uniform spacing of 3.6002 Å and form segregated columns along [00z] and [1/2,1/2,z]. The chloride ions reside in channels along [0,1/2,z] and [1/2,0,z] between the TTF chains. The electron-density map, through such a channel parallel to the channel axis as shown in Fig. 3, clearly exhibits the high disorder of the chloride ions as do the diffuse layer lines shown in Fig. 1.

Effect of Lowered Temperature on the Chloride Sublattice

1. $(TTF)Cl_{0.67}$: Oscillation photographs taken at ~120° K revealed considerable sharpening of the diffuse layer lines and the emergence of weak but sharp Bragg reflections superimposed on these. A more detailed study at various temperatures and a cooling rate of 1° K/hour with the use of our low-temperature diffractometer[7] revealed distinct effects close to 250° K. Here, the reflections with ℓ = 1, 2, and 4, associated with the chloride sublattice, increased substantially in sharpness and integrated intensity as is shown in the graph, Fig. 5a; the increase occurs over a relatively narrow temperature range (ΔT ~20° K). All of these reflections remain weak in comparison to the TTF-sublattice reflections (ℓ = 3n). Throughout this temperature range the chloride sublattice remains commensurate with the TTF sublattice. Below about 250° K the changes in the integrated intensities of the chloride-sublattice reflections (ℓ = 1, 2, and 4) are less distinct (and

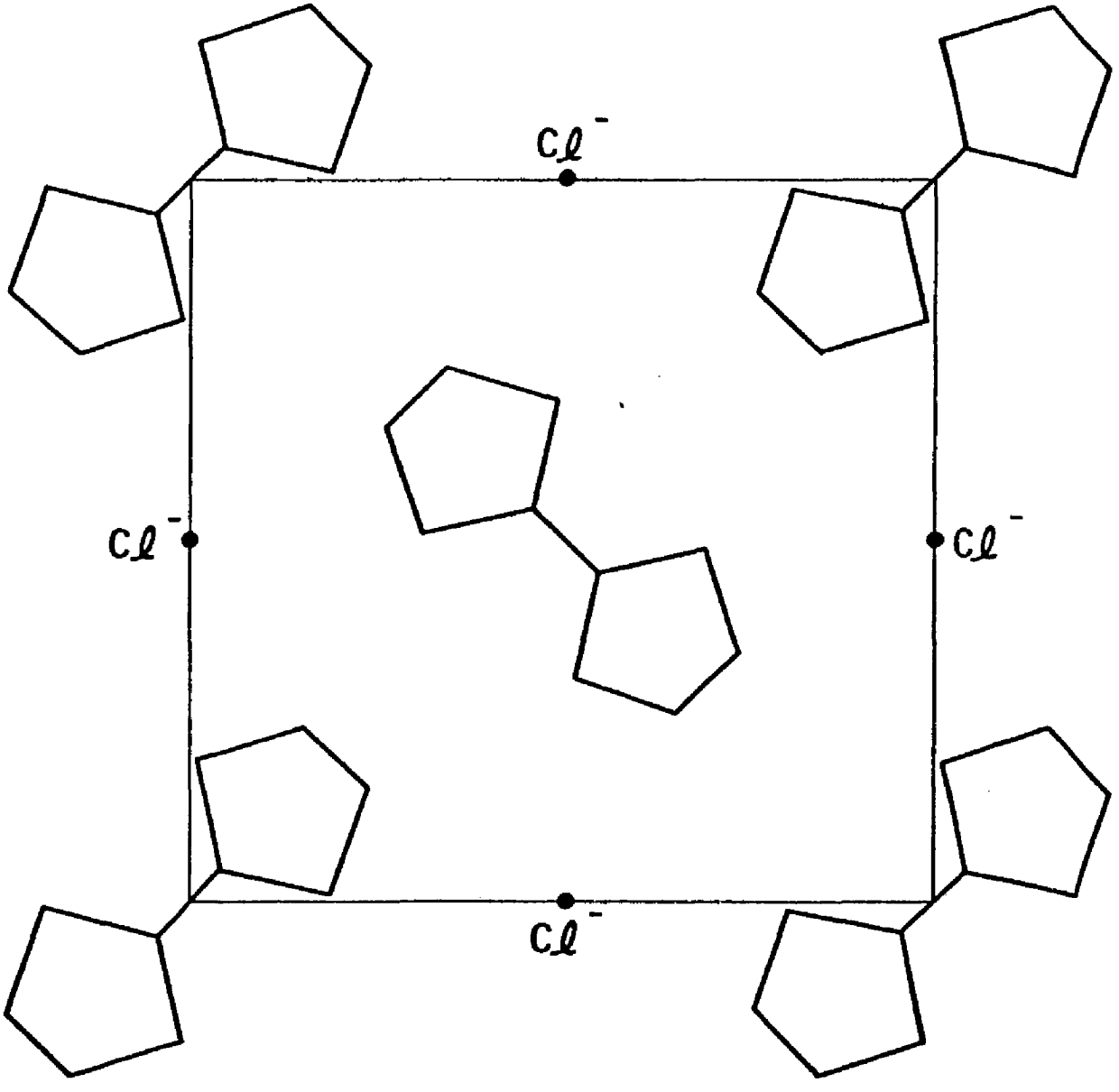

Figure 2. Projection of the $(TTF)Cl_{0.67}$ room temperature structure onto the (001) plane.

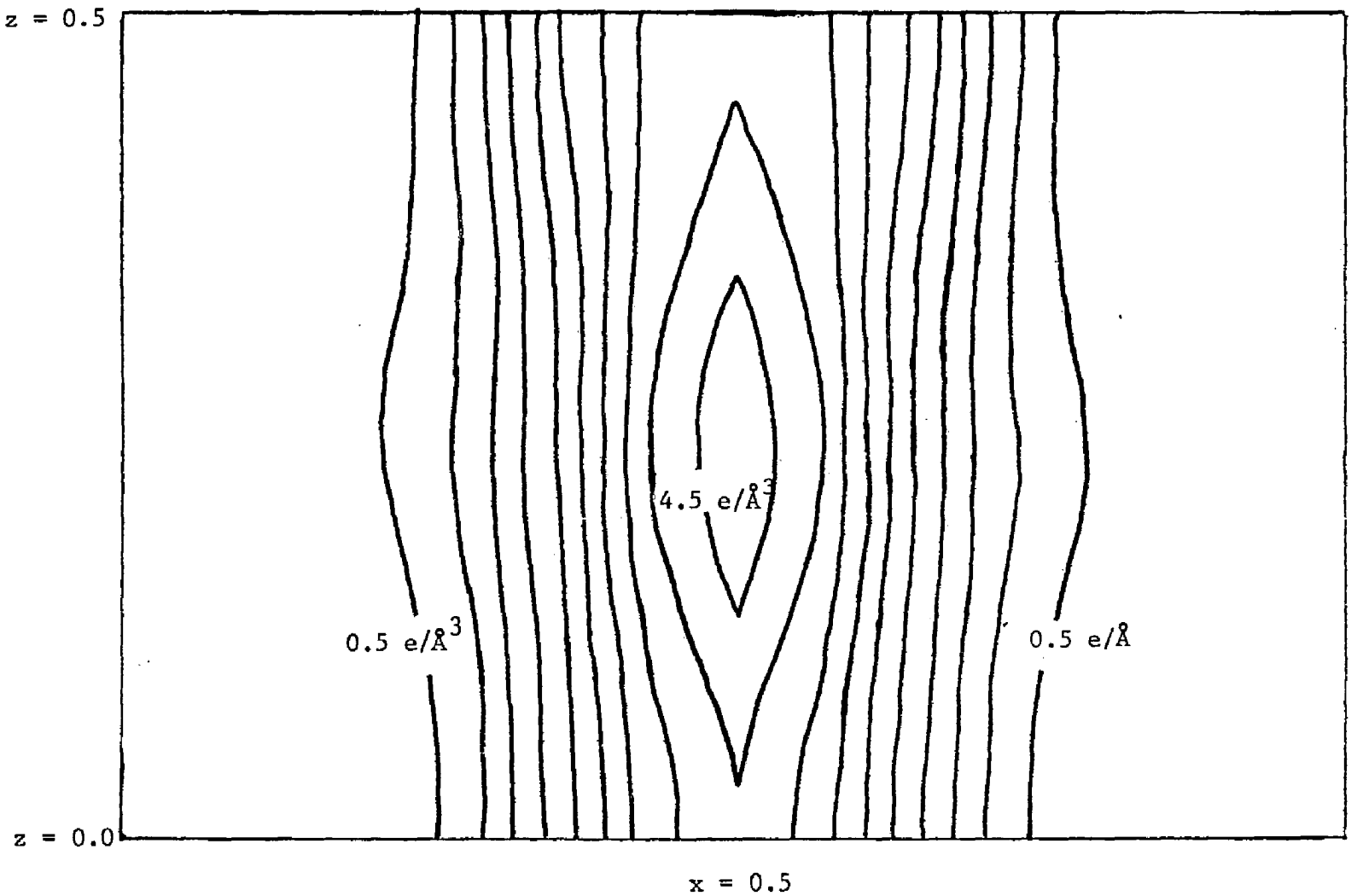

Figure 3. Electron density map of chloride ion channel in $(TTF)Cl_{0.67}$. Scale is about 0.15 Å/cm.

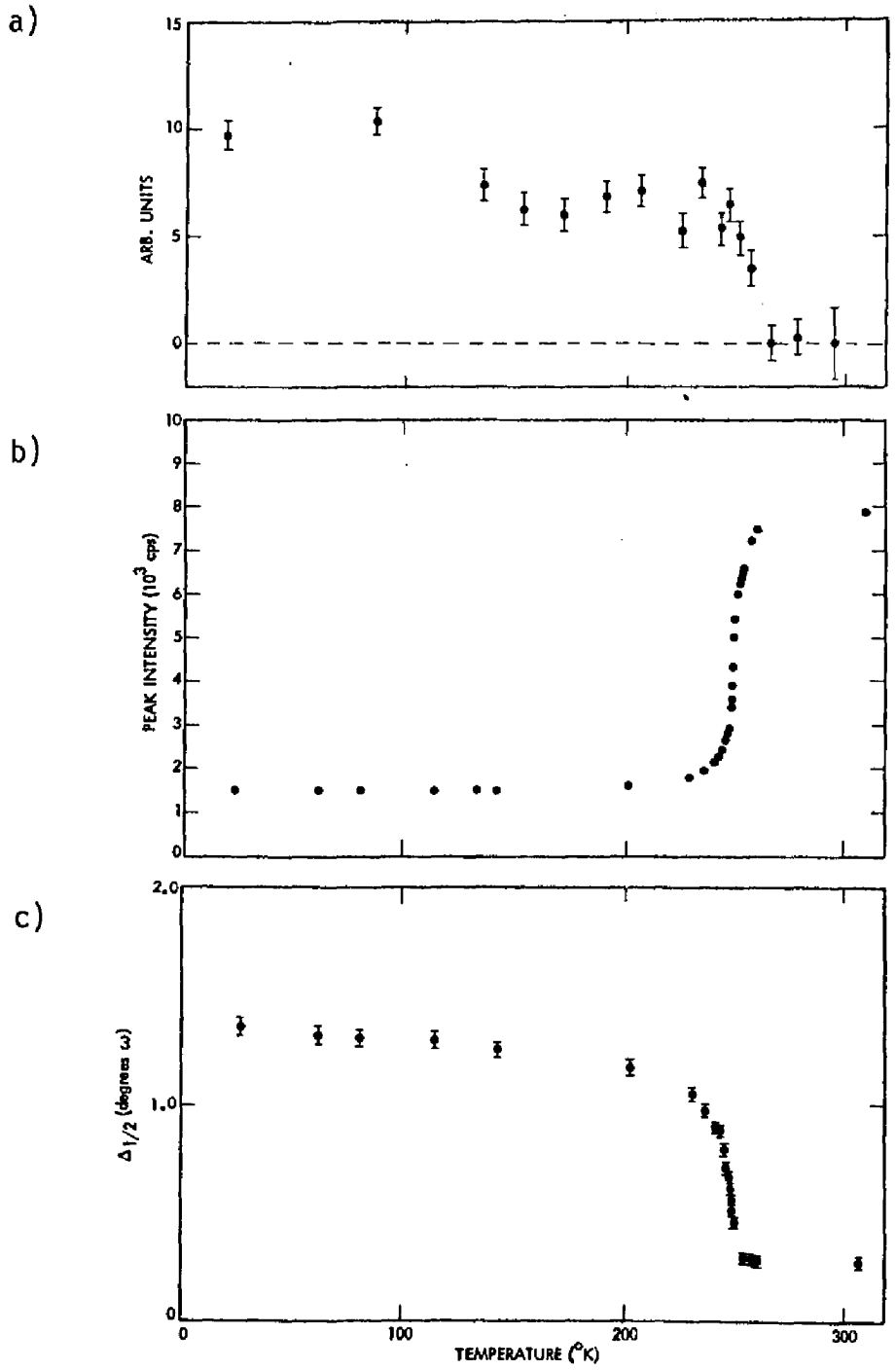

Figure 4. Temperature dependence of: a) Integrated intensity of 114 reflection; b) Peak intensity of 330 reflection; c) Full width at half-height of 330 reflection of TTF $Cl_{0.67}$. a) at 1° K/hr, b) and c) at 10° K/hr.

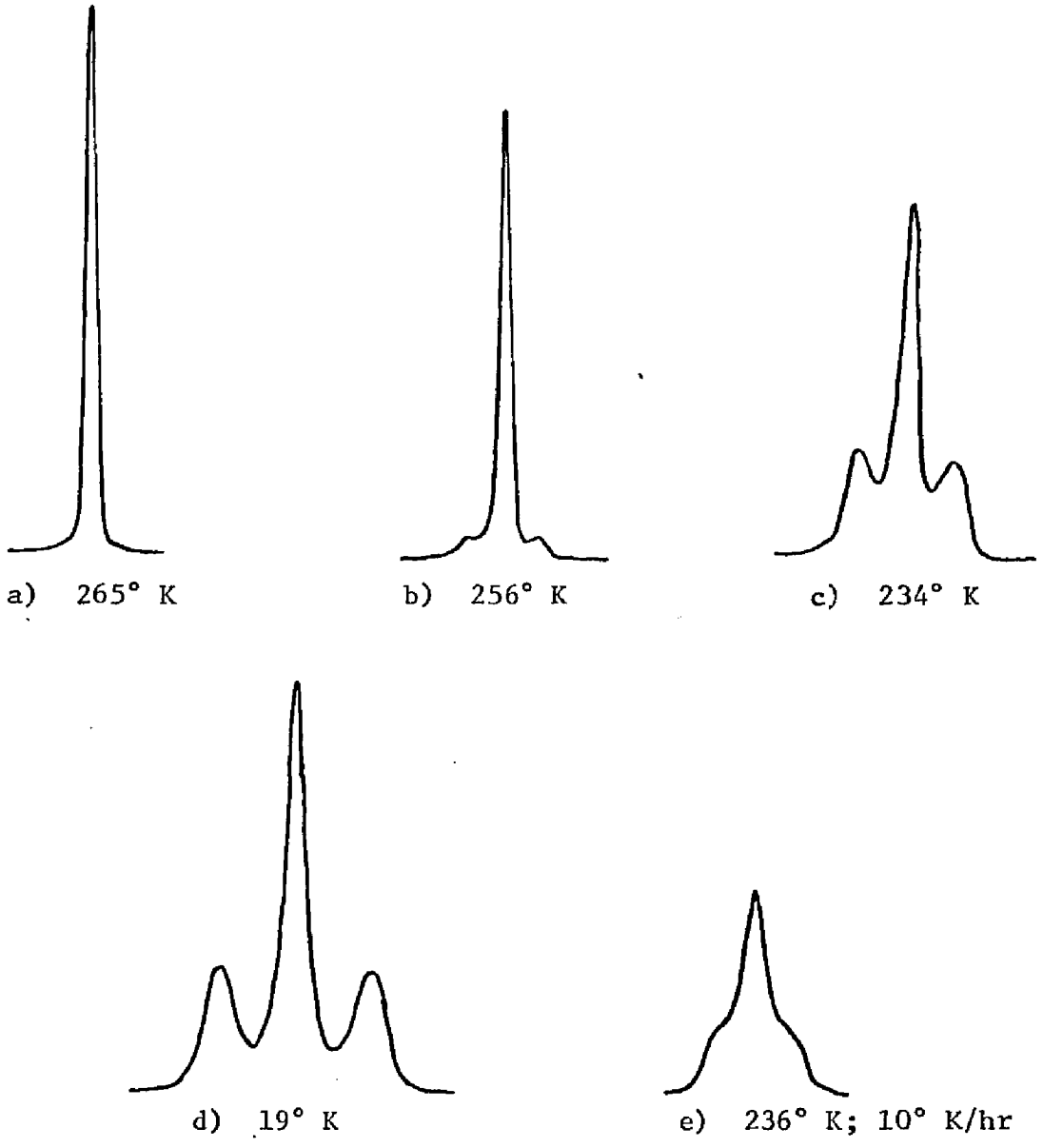

Figure 5. Peak profiles of 330 reflections (w scan) at various temperatures. Profiles a) - d) taken with cooling rate of 1° K/hour.

there is a smooth increase in the region between about 90° K and 150° K; Fig. 4a).

The relatively sharp increase in integrated intensity close to 250° K reflects ordering in the chloride sublattice, which occurs over a relatively narrow temperature range. The extremely high disorder of the chloride lattice at room temperature, together with low-temperature ordering, suggests that dynamic disorder is present at room temperature, and disappears at the phase transition.

2. $(TTF)Cl_{0.70}$: These crystals behave in a different manner on cooling. Each of the diffuse layer lines corresponding to hkl and hk2 on the room-temperature photograph splits at low temperature into a pair of closely-spaced sharper layer lines on which weak diffuse spots are superimposed. The temperature at which this splitting occurs is somewhere above 120° K. (The low-temperature diffractometer was not used for this study.) Thus, there are now two chloride sublattices, one corresponding to $(TTF)_3Cl_2$ [or $(TTF)Cl_{0.667}$] and the other to $(TTF)_7Cl_5$ [or $(TTF)Cl_{0.714}$], and each one is commensurate with the same TTF sublattice. The stoichiometries as determined from the oscillation photographs are $(TTF)Cl_{0.666}$ and $(TTF)Cl_{0.718}$ respectively. Thus, upon cooling through 250° K, the highly disordered $(TTF)Cl_{0.70}$ crystal incorporates two kinds of domains, one representing $(TTF)_3Cl_2$ and the other $(TTF)_7Cl_5$. Within each domain the chloride lattice is commensurate with the TTF lattice. A phase of stoichiometry 7/5 is also observed in the TTF-iodide system, $(TTF)_7I_5$.[2,13]

Effect of Lowered Temperature on the TTF Sublattice of $(TTF)Cl_{0.67}$

All studies of $(TTF)Cl_{0.67}$ at low temperature were carried out using the same crystal. Annealing was rapid and complete at room temperature, and there was no permanent damage to the room-temperature single crystal, even after repeated thermal cycling.

Changes in peak intensity and profile of the TTF sublattice reflections were monitored at various temperatures at cooling rates of ~ 1° K/hour, ~ 10° K/hour, and ~ 100° K/hour. In the temperature range ~ 295° K to ~ 250° K all changes were independent of cooling rate.

Figure 4b shows the temperature dependence of the peak intensity of the 330 reflections and Fig. 4c the change in full width at half maximum observed in omega scans of the same reflection. The cooling rate was 10° K/hour in both cases. Faster cooling (~ 100° K/hour) results in a greater decrease in peak intensity, and a greater increase in the width of the profile. Slower cooling (~ 1° K/hour) results in resolution of several components of the peak profile. Figure 5 shows omega-scan profiles of the same reflection at: (a) 265° K, (b) 256° K, (c) 134° K, and (d) 19° K. Figure 5e shows the effect of faster cooling (10° K/hour) on the scan profile [compare with Fig. 5c].

It is seen (Fig. 5) that peak splitting occurs as the temperature is lowered, the onset being at about 256° K (Fig. 5b). From here on the two smaller peaks in each profile increase in intensity at the expense of the larger central one. Also, the separation between the individual peaks of each profile increases as the temperature is lowered. At 153° K each component was resolved sufficiently to be measured individually with the diffractometer.

A least-squares fit of the 2θ values of the central peak of 14 profiles gave the unit-cell parameters of the tetragonal phase at 153° K; $\underline{a}_o$ = 11.126(2) Å and $\underline{c}_o$ = 3.5768(4) Å. An analysis and least-squares fit of the 2θ, ω, φ, and χ values of 13 sufficiently strong and well resolved "side peaks" revealed that they originate from a monoclinic structure with unit-cell parameters $\underline{a}_o$ = 15.742(56) Å, $\underline{b}_o$ = 15.721(38) Å, $\underline{c}_o$ = 10.744(21)Å, and β = 92.98(23) degrees. Seven of the 13 side peaks could be ascribed to one of four possible orientations of the cell of the monoclinic phase with respect to the tetragonal cell; the remaining six corresponded to a second orientation. Within experimental error, the cells of the two phases are related to each other by $a_{mono} = a_{tetr} \cdot \sqrt{2}$ and $c_{mono} = 3\ c_{tetr}$.

The four directions [110], [$\bar{1}$10], [1$\bar{1}$0], and [$\bar{1}\bar{1}$0] of the tetragonal cell are equivalent. Increasing the angle, between one of these directions and $\underline{c}_{o\,tetr}$, from 90° to β, results in a monoclinic cell. Since the four directions are equivalent, four orientations of the monoclinic cell with respect to the tetragonal cell (and crystal) can result with equal probability. Because part of the crystal retains the tetragonal structure, the result of the phase transition is a quintuple twin containing domains of the tetragonal phase and domains of the monoclinic phase having four possible orientations.

The relationship between the monoclinic $\underline{a}$,$\underline{b}$ plane and the tetragonal (001) plane is shown in Fig. 6. The monoclinic angle β increases as the temperature is lowered and reaches 93.6 degrees at 19° K. At 247° K, β is 91.8 degrees. Figure 7 shows a plot of β versus temperature.

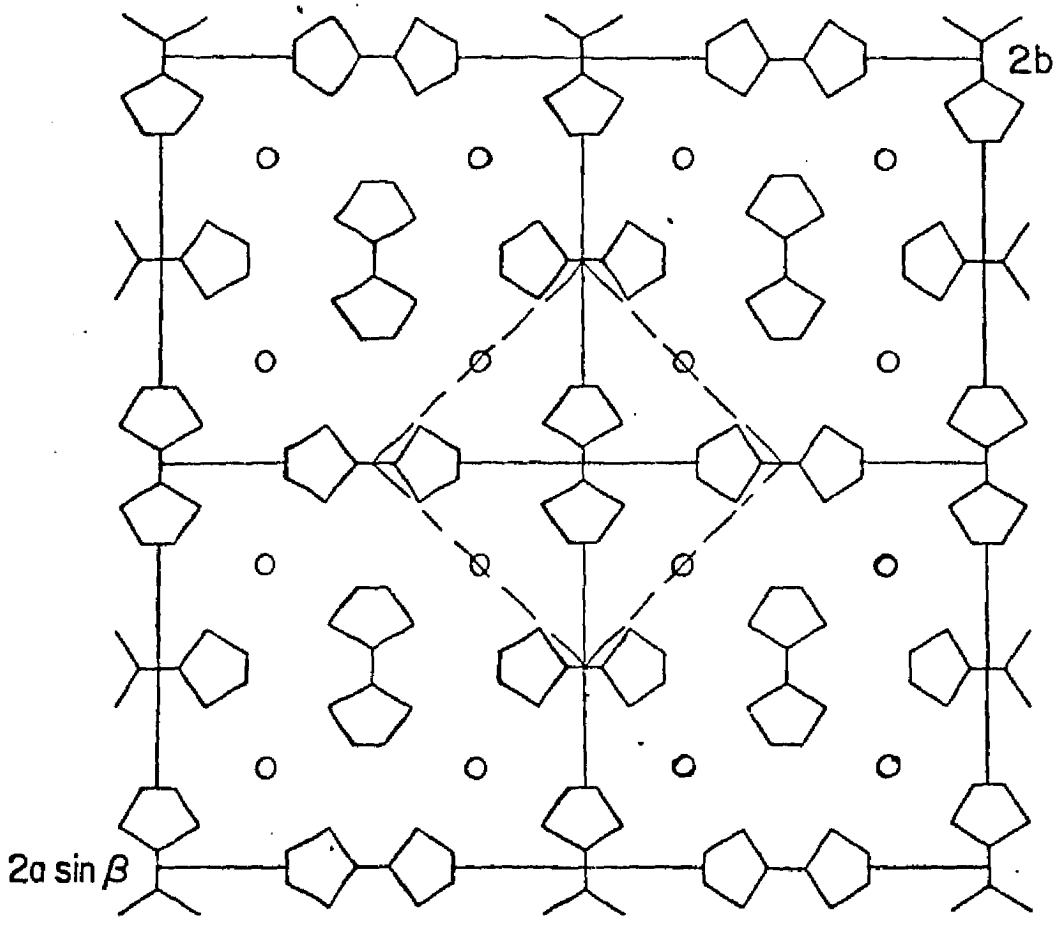

Figure 6. Relative orientations of monoclinic and tetragonal a, b planes. The dashed line shows the tetragonal cell.

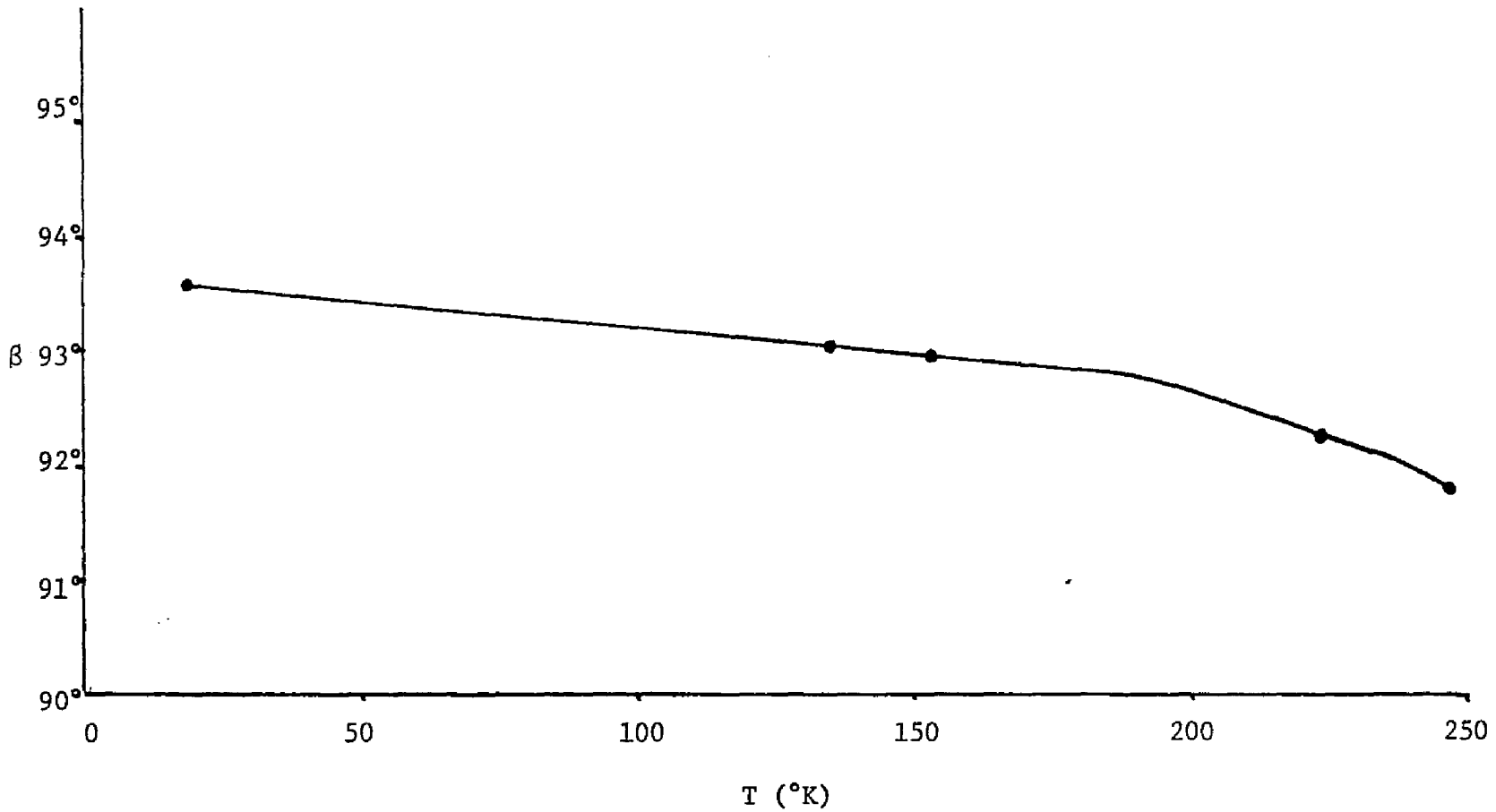

Figure 7. Monoclinic angle β vs. T for the low temperature phase of $(TTF)Cl_{0.67}$.

The arrangement of the TTF cations in the monoclinic cell cannot be determined with certainty because of the considerable overlap of reflections caused by the quintuple twinning. One interpretation of the monoclinic distortion is presented in Fig. 8, which assumes that the TTF molecules retain 2/m symmetry in space group C2/m; the eclipsed stacking is retained and the monoclinic c-axis remains perpendicular to the TTF molecular plains. This interpretation implies that the individual TTF columns are translated slightly relative to each other in the [001] direction. This slipping of parallel TTF columns is seen in the structures of several monoclinic partially oxidized TTF halides and pseudohalides.[5,6]

The location of the chloride ions in this structure cannot be determined from the present diffraction data. Nevertheless, it is tempting to attribute the tripling of the monoclinic c-axis (TTF-stacking period) to ordering of the chloride ions in each channel inasmuch as $3d_{TTF} = 2d_{Cl^-}$ (or $d_{003}/d_{002} = 0.67$ as was discussed earlier in this paper; see also Table 1). In the absence of refinable structure data (because of quintuple twinning) we cannot, of course, exclude the possibility of a very slight Peierls distortion that would tend to drive the TTF entities toward dimerization or trimerization. However, a large Peierls distortion seems unlikely because the reflections with $\ell \neq 3n$ remain weak.

The phenomenon of increasing β-angle with decreasing temperature was also observed in X-ray studies by Thomas et al.[5] of $(TTF)_5(SCN)_7$, where it is believed to reflect coupling of charge-density waves with lattice strains. We cannot rule out the possibility that the TTF stacks are undergoing a dynamic transition such as was measured in that compound and in (TTF)(TCNQ) by X-ray diffuse scattering.[1,5]

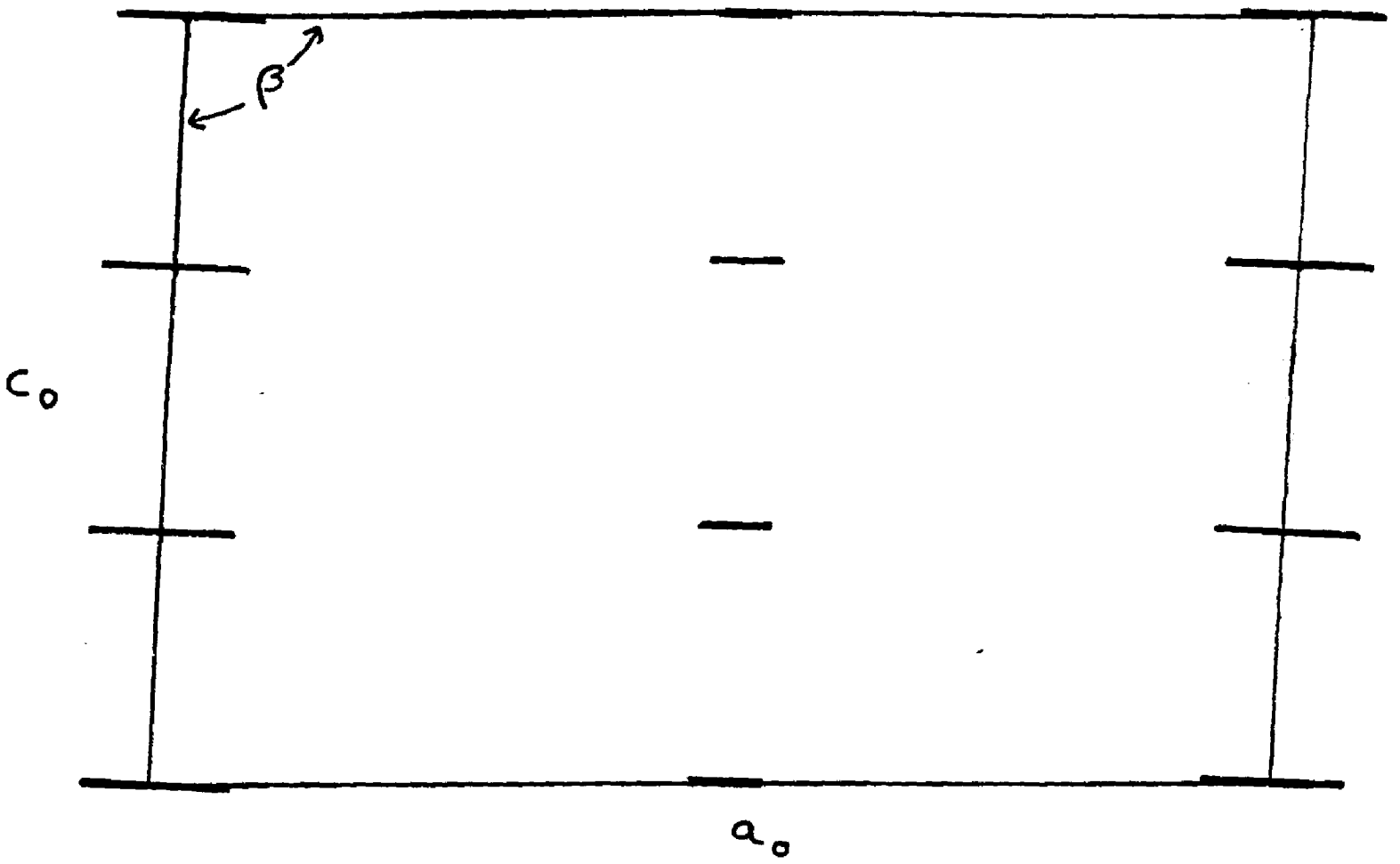

Figure 8. Interpretation of monoclinic distortion. Long and short thick lines represent side- and end-on TTF cations, respectively.

The peak broadening occurring on fast cooling of $(TTF)Cl_{0.67}$ completely obscures peak splitting when a cooling rate of ~ 100° K/hour is employed. Furthermore, while there is little peak broadening and no observable peak splitting in 2θ scans after slow cooling (~ 1° K/hour), the full width at half maximum, $W_{1/2}$, of these profiles increases dramatically with fast cooling. For example, $W_{1/2}$ corresponds to ~ 0.6° (2θ) at 300° K and ~ 3.0° (2θ) at 19° K after cooling at a rate of ~ 100° K/hour. After cooling this quickly, a very slow increase in peak intensity may occur.[14]

This peak broadening is most likely due to formation of extremely small diffracting domains within the crystal. Since there are five kinds of diffracting domains below the phase transition, it is likely that individual domains of any one kind are very small. The dependence of peak profiles on the size of diffracting domains is well understood.[15] We have not investigated this phenomenon in great detail. A calculation based on Wilson's treatment indicates that domains in $(TTF)Cl_{0.67}$ may be $\lesssim$ 300 Å in diameter after cooling to 19° K at a rate of ~ 100° K/hour.

Electrical Properties

The electrical properties of $(TTF)Cl_{0.67}$ are identical to those of $(TTF)Cl_{0.70}$ as determined by measurements on single crystals from the same batches that were used in the crystallographic work. However, the properties differ from those of the other halides of TTF.[2,3,4] The room-temperature conductivity is $\sigma \sim 150\ \Omega^{-1}cm^{-1}$, the lowest in this series of compounds. As the temperature is lowered the conductivity decreases and

drops off sharply at the phase transition (~ 250° K), and then continues to decrease less rapidly as shown in Fig. 9. The plot of log σ versus 1/T is linear only over the narrow temperature range from 125° K to 200° K and yields an activation energy, Δ, of ~ 0.13 eV. Assumption of a disordered model,[16] where $\ln \sigma \sim 1/T^{\gamma}$ and $\gamma = 1/3$ or $1/4$, did not lead to a significant improvement in the fit of the data. This was expected because the results obtained from the crystallographic work provided evidence for ordering in the chloride lattice.

The thermoelectric power (TEP) is small and positive at room temperature, and is relatively constant down to 260° K. At 250° K there occurs a sharp upturn and then the TEP continues to increase with decreasing temperature.

Thus, both the electrical conductivity and the TEP change dramatically at the phase transition. Below the transition nonmetallic behavior is observed. In view of the disorder in the chloride lattice one might expect $(TTF)Cl_x$ to behave as a disordered 1-D metal in which all the states of the conduction electrons are localized. The finite conductivity would then be due to the strong electron-phonon interaction such that electron transport takes place by phonon-assisted hopping.[18] Thus, the conductivity would be diffusive in nature and would decrease as the temperature is lowered, as was observed experimentally. However, the mere presence of disorder is not sufficient to guarantee such behavior because of the competing factors such as the disorder potential, δ, the interchain coupling, and the electronic bandwidth. For example, in an anisotropic conductor with nearest-neighbor transfer integrals, the critical value of

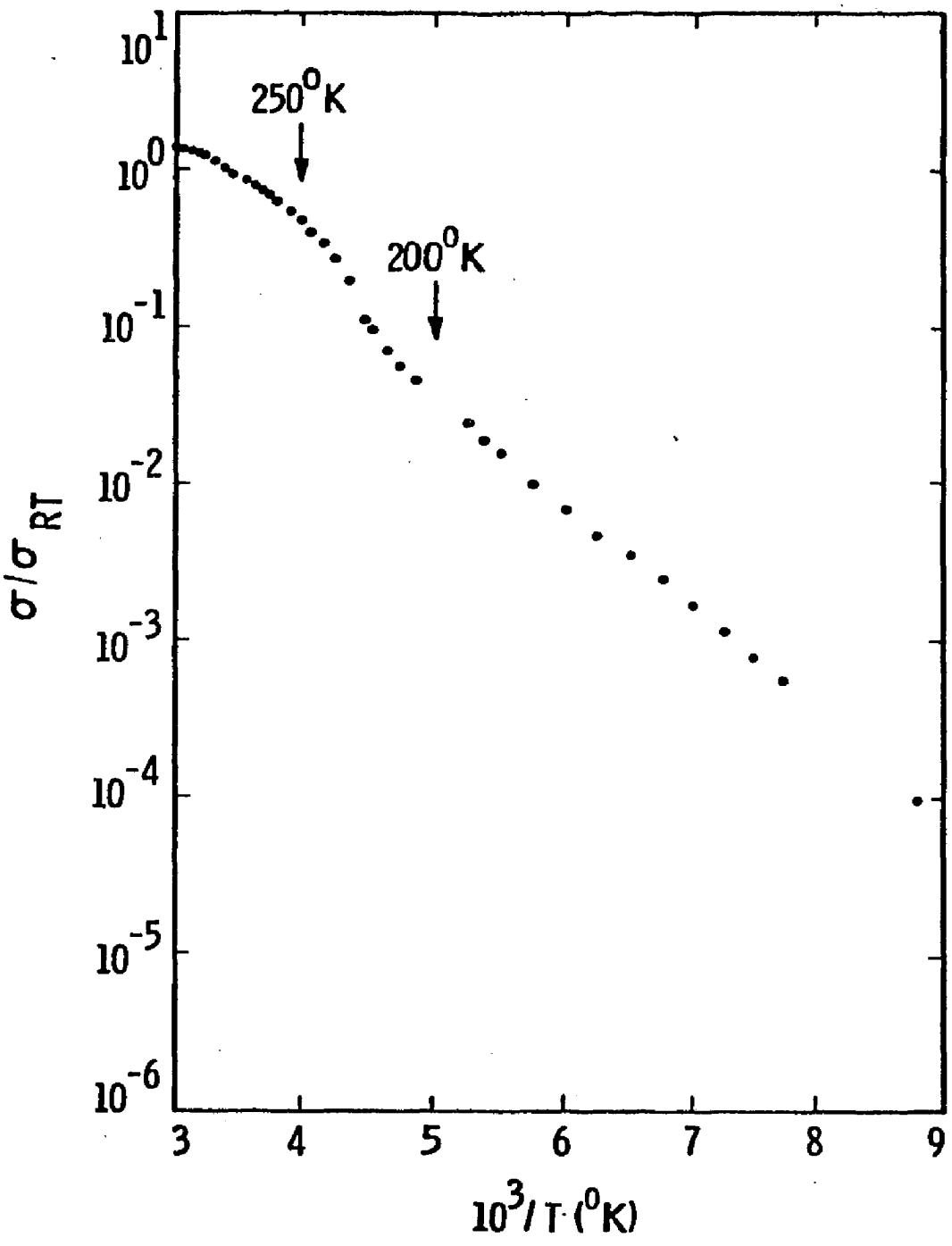

Figure 9. Temperature dependence of the conductivity of $(TTF)Cl_{0.67}$. σ_{RT} ~100 Ω^{-1} cm^{-1}.

the disorder potential is $\delta_c \sim (t_{\parallel}\, t_{\perp})^{1/2}$, where $t_{\parallel}$ is the longitudinal transfer integral (proportional to the electronic bandwidth) and $t_{\perp}$ is transverse transfer integral (interchain coupling).[19] All of the conduction-electron states will be localized only if $\delta > \delta_c$. The electronic bandwidth is expected to be large in $(TTF)Cl_x$ because of the eclipsed stacking of TTF molecules.[2,20] Similarly, the occurrence of ordering and a structural phase transition near 250° K indicates that interchain forces are not weak. Therefore, we believe that the conductivity in the high temperature state is not dominated by disorder, but reflects the presence of fluctuations, or precursors, of the phase transition.

Another example of this interaction between disorder and interchain coupling is $(\text{tetrathiatetracene})_2(\text{iodide})_3$, $(TTT)_2I_3$. This is a single-carrier, quasi-one-dimensional organic metal in which the TTT molecules stack uniformly in a slipped fashion, in contrast to the eclipsed stacking of the TTF molecules in $(TTF)_3Cl_2$.[14] The iodine chains exhibit considerable disorder. Unlike $(TTF)_3Cl_2$, the temperature dependence of the conductivity of $(TTT)_2I_3$ is metal-like, even in the presence of observable disorder. The conductivity exhibits a broad maximum near 100° K and slowly decreases as the temperature is lowered. A possible phase transition occurs at 20-25° K. X-ray diffraction studies do not reveal any significant ordering of the iodine ions, nor is there any evidence of a structural transition in the TTT lattice upon cooling to 27° K.[16] We believe that this is another example of structural disorder disrupting interchain correlations such that the phase transition is smeared and suppressed to low temperatures. Two other interesting points emerge from the comparison of $(TTF)_3Cl_2$ and

$(TTT)_2I_3$: (a) the temperature dependence of the structural disorder may vary significantly among different quasi-1D organic metals; and (b) the disorder observed at room temperature may be quite different at low temperatures.

Below the transition, the conductivity exhibits a nonmetallic temperature dependence even though the chloride sublattice is now ordered. In view of the recent work on $(TTF)_{12}(SCN)_7$,[5] which is electronically and structurally analogous to $(TTF)Cl_x$, we feel that a dynamic distortion occurs along the chains and that charge density waves are present in the monoclinic phase. However, an important difference between the monoclinic phases of the two materials should be noted. $(TTF)_{12}(SCN)_7$ exhibits structural disorder corresponding to the two possible orientations of the SCN anions in the chains,[16] while the chloride lattice is ordered in the monoclinic phase. We feel that the effect of the disorder in the SCN lattice is to favor the formation of incommensurate CDW. The influence is absent in $(TTF)_3Cl_2$ and should lead to commensurate CDW and semiconducting behavior. A similar situation is found in TaS_3 where a Peierls transition occurs along with the formation of commensurate CDW.[17] The temperature dependence of the conductivity of $(TTF)_3Cl_2$ and TaS_3 are quite similar. Obviously, $(TTF)Cl_x$ needs be studied by X-ray diffuse scattering experiments to verify or disprove our predictions.

Conclusions

The chloride sublattice in $(TTF)Cl_x$, x = 0.67 and 0.70, is disordered at room temperature. The disorder diminishes over a narrow temperature range at about 250° K. For $(TTF)Cl_{0.70}$, in which the disordered chloride

sublattice is incommensurate with the TTF sublattice at room temperature, the chloride chains order into two different configurations, resulting in the formation of the commensurate structures $(TTF)_3Cl_2$ and $(TTF)_7Cl_5$. In $(TTF)Cl_{0.67}$, the chloride sublattice is ordered and remains commensurate below the transition temperature. The TTF sublattice undergoes a static structural phase transition from tetragonal to monoclinic symmetry at ~ 250° K. This transition is incomplete in the sense that domains of both tetragonal and monoclinic symmetry are present. No evidence of a static Peierls transition is observed. The ordering of the chloride sublattice is important for the development of the structural phase transition of the TTF sublattice. Comparison of the electrical conductivity of $(TTF)Cl_x$ with other quasi-1D conductors [i.e., $(TTF)_{12}(SCN)_7$ and TaS_3] suggests that a dynamic distortion occurs along the TTF chains, resulting in the formation of commensurate CDW and semiconducting behavior. The monoclinic cell of $(TTF)Cl_{0.67}$ is similar to the room temperature cells of $(TTF)Br_{0.74-0.78}$ and $(TTF)I_{0.71}$ except that the $\underline{c_o}$-axis periods are different. We would expect to observe a high temperature tetragonal phase for the two latter materials.

Acknowledgements

We wish to thank Drs. R. Marsh, A. M. Hermann, T. Datta, and A. Rembaum for useful discussions and Professor T. J. Kistenmacher for generously providing us with his data on bond lengths and angles for $(TTF)HgCl_3$ prior to publication.

References

1. F. Denoyer, R. Comes, A. F. Garito, and A. J. Heeger, Phys. Rev. Ltr., 35, 445 (1978); C. Weyl, E. M. Engler, K. Bechgaard, G. Jenanno, and S. Etamad, Solid State Comm., 19, 925 (1976); and Galen D. Stucky, Arthur J. Schultz, and Jack M. Williams, Ann. Rev. Mater. Sci., 7, 301 (1977).
2. R. B. Somoano, A. Gupta, V. Hadek, M. Novotny, M. Jones, T. Datta, R. Deck, and A. M. Hermann, J. Chem. Phys., 63, 4970 (1973); R. B. Somoano, A. Gupta, V. Hadek, M. Novotny, M. Jones, T. Datta, R. Deck, and A. M. Hermann, Phys. Rev., B15, 595 (1977).
3. F. Wudl, D. E. Schafer, W. M. Walsh, Jr., L. W. Rupp, Jr., F. J. DiSalvo, J. V. Waszczak, M. L. Kaplan, and G. A. Thomas, J. Chem. Phys., 66, 377, (1977).
4. R. J. Warmack, T. A. Callcott, and C. R. Watson, Phys. Rev. B12, 3336 (1975).
5. G. A. Thomas, D. E. Moncton, M. Kaplan, P. Lee, T. M. Rice, and F. Wudl, Bull. Amer. Phys. Soc., 23, 381 (1978).
6. B. A. Scott, S. J. LaPlaca, J. B. Torrance, B. D. Silverman, and B. Welber, J. Amer. Chem. Soc., 99, 6631 (1977).
7. S. Samson, E. Goldish, and J. Dick, to be published.
8. International Tables for X-Ray Crystallography Vol. III. Birmingham: Kynoch Press (1962).
9. International Tables for X-Ray Crystallography Vol. I. Birmingham: Kynoch Press (1952).

References (continued)

10. W. F. Cooper, N. C. Kenney, J. W. Edmonds, A. Nagel, F. Wudl, and P. Coppens, Chem. Commun. p. 889 (1971).

11. T. J. Kistenmacher, T. E. Phillips, and D. O. Cowan, Acta Cryst., B30, 763 (1974).

12. T. J. Kistenmacher, M. Rossi, C. C. Chiang, R. P. van Duyne, T. Cape, and A. R. Siedle, J. Amer. Chem. Soc., 100, 1958 (1978) and private communication.

13. C. K. Johnson and Charles R. Watson, Jr., J. Chem. Phys., 64, 2271 (1976).

14. C. Lowe Ma, R. Williams, and S. Samson. To be published.

15. A. J. C. Wilson, X-Ray Optics. Methuen, London (1949), pp. 55-75.

16. A. N. Bloch, R. B. Weisman, and C. M. Varma, Phys. Rev. Ltr., 28, 753 (1972).

17. T. Datta, R. J. Deck, A. M. Hermann, R. B. Somoano, and Roger Williams, Bull. Amer. Phys. Soc., 23, 381 (1978).

18. A. A. Gogolin, V. I. Melnikov, and E. I. Rashba, Sov. Phys. JETP, 42, 168 (1976).

19. V. K. S. Shante and M. H. Cohen, Bull. Amer. Phys. Soc., 21, 401 (1976).

20. D. R. Salahub, R. P. Messmer, and F. Hermann, Phys. Rev., B13, 4252 (1976).

21. R. B. Somoano, S. P. S. Yen, V. Hadek, S. K. Khanna, M. Novotny, T. Datta, A. M. Hermann, and John A. Woollam, Phys. Rev., B17, 2853 (1978) and references therein.

References (continued)

22. S. K. Khanna, S. P. S. Yen, R. B. Somoano, P. M. Chaikin, C. Lowe Ma, R. Williams, and S. Samson, Phys. Rev., B19, (1979).

23. T. Sambongi, K. Tsutsumi, Y. Shiozaki, M. Yamamoto, K. Yamaya, and Y. Abe, Solid State Commun., 22, 729 (1977).

24. P. Coppens and T. N. Guru Row, Ann. New York Acad. Sci., 313, 244 (1978).

CHAPTER 4

The Structure of Low-Disorder Bis-Tetrathiatetracene Triiodide

Introduction

The tetrathiatetracene (TTT) iodide system is of great current interest because it contains two quasi-one-dimensionally conducting phases, $(TTT)_2I_3$ and (TTT)I, both of which have unusual structural and electrical properties (1,2). Furthermore, the highly conducting phase, $(TTT)_2I_3$, exists in several modifications which show a systematic variation in iodide-associated disorder and a concurrent variation in temperature dependent electrical properties (3). A room temperature x-ray diffraction study of low-disorder (l.d.) $(TTT)_2I_3$ was undertaken in order to learn more about the nature of the iodide chain (2,4).

Experimental

Long, flat, needle-like crystals of l.d. $(TTT)_2I_3$, grown by slow cooling of a nitrobenzene solution of TTT and I_2 from 95° C to room temperature, were supplied by Dr. R. B. Somoano. Crystals were six-sided prisms with [001] and [101] faces predominating and a metallic-gold luster. Crystals were initially characterized by

x-ray diffraction photography using oscillation and Weissenberg photographs. Unit cell parameters were obtained from a least-squares fit to the 2θ, ϕ, and χ values of 9 reflections manually centered on the diffractometer with the use of beam splitter and peak profiles. Crystal data are listed in Table 1. The crystals were all very small; therefore, intensity data were collected using Ni-filtered CuK$\bar{\alpha}$ radiation. A crystal measuring 0.383 x 0.043 x 0.008 mm was used for intensity data collection at room temperature on a quarter-circle G.E. diffractometer. A total of 1276 unique reflections, 915 due to the sublattice and 361 from the diffuse third layer, were measured using 2θ-θ scans and scan rates of 1°/min and 1/2°/min, and background intensities were measured at the beginning and end of each scan for periods totaling 1 min or 1 min, 20 sec. Three standard reflections, 224, 002, and 606 were measured every 40 reflections for purposes of scaling. They did not show (>1%) significant crystal decay, although oscillation photographs taken after data collection revealed that sharpness and intensity of the diffuse h3ℓ reflections of the supercell had decreased substantially. The intensities and their standard deviations were scaled (including minor decay correction), and corrected for absorption (μ = 272.9 cm^{-1}), Lorentz, and polarization effects (5). The atomic scattering factors of S and I were corrected for the real contribution to anomalous dispersion (6). 2θ-θ scans of several reflections of the subcell and third diffuse layer were recorded with a strip-chart recorder in order to compare profiles.

Table 1. Crystal Data (l.d.) TTT_2I_3

a = 18.468 (2)

b = 9.851 (1) b subcell = b/2

c = 18.299 (2)

Volume = 3329.0 $Å^3$

Space Group = Cmca (subcell)

$Pmc2_1$ (full cell)

F.W. ($C_{36}H_{16}S_8I_3$) = 1085.75

z = 4 formula units per cell

d_{calc} = 2.166 g/cm^3

μ (absorption coefficient) = 272.87 cm^{-1} CuKα rad.

Electrical measurements of TTT_2I_3 crystals were performed using standard 2 and 4 probe techniques and aquadag contacts. Conductivity vs. temperature and thermoelectric power vs. temperature are shown as plots in Appendix 2.

Photographic results

Oscillation photographs of l.d. $(TTT)_2I_3$ revealed a set of sharp diffraction lines corresponding to a spacing of 4.92 Å. Diffuse layer lines corresponding to a spacing of 9.86 Å were also seen, with spots superimposed on the third diffuse line. These diffuse spots correspond to a doubled unit cell, within the limits of the measurement. The photograph is shown in Figure 1. Weissenberg photographs of subcell layers indicated conditions for reflections, $h0\ell$: $h = 2n$, $\ell = 2n$ and $hk\ell$: $h + \ell = 2n$, consistent with Cmca symmetry. A Weissenberg photograph of the third diffuse line revealed spots with slight extension in ω and not significantly broadened in the 2θ direction. No systematic absences were seen in this Weissenberg photograph, implying that the iodide lattice and TTT lattice have different symmetry.

Structure determination and refinement

Atomic coordinates for C, S, and I atoms were obtained from previous work (7), and provided sufficient phasing to make refinement of C and S in the subcell possible. Positions of I atoms could

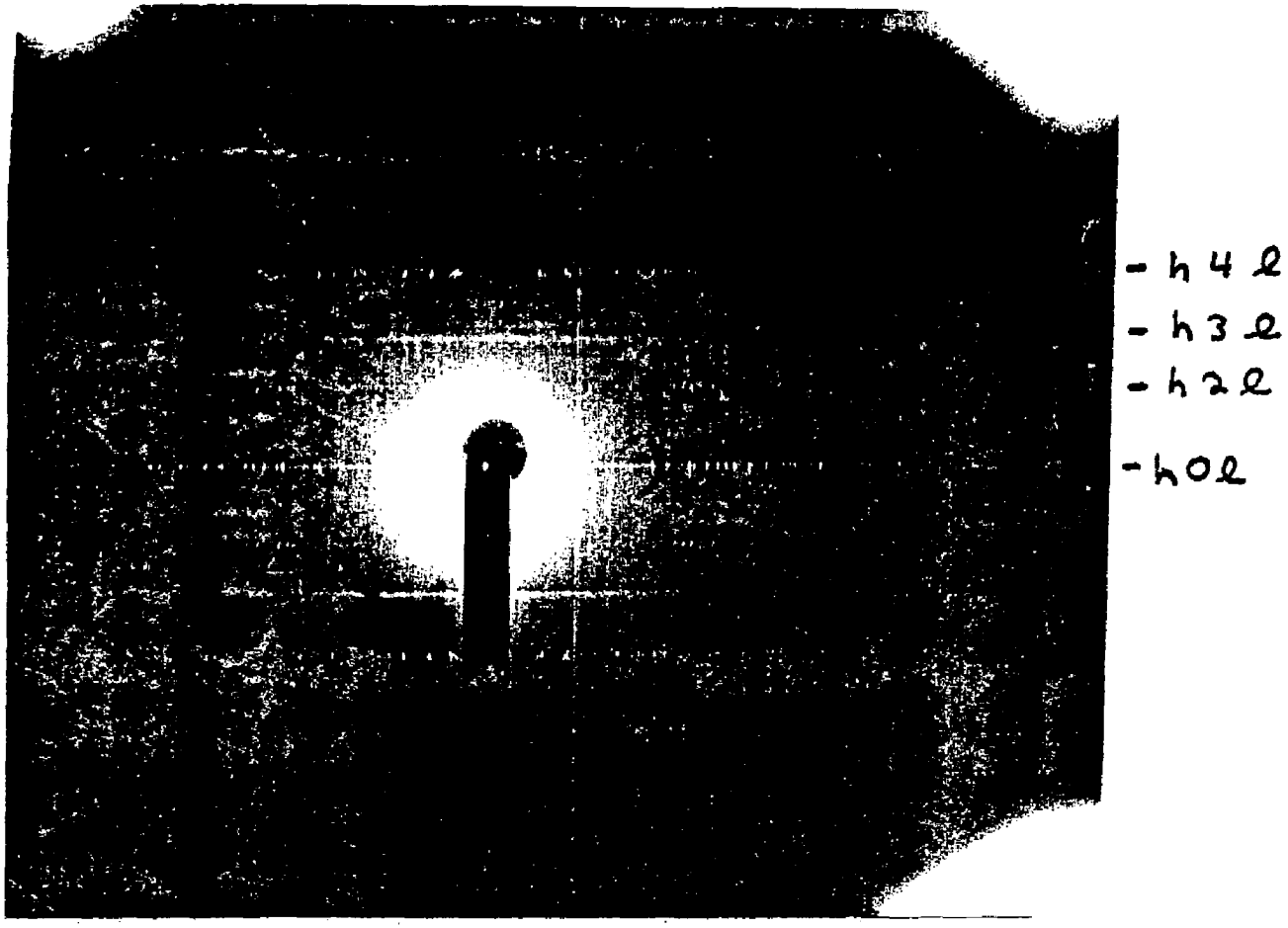

Figure 1. Oscillation photograph of (l.d.) TTT_2I_3.

not be refined. After C and S atoms were refined, I atom coordinates, populations, and anisotropic temperature factors were adjusted in order to obtain a flat difference Fourier map. H atom positions were calculated, and the final stage of refinement consisted of refining H atom coordinates and isotropic temperature factors, and I atom populations and anisotropic temperature factors. C and S atom parameters were fully refined at this level. The converged structure gave R = 0.111, wR = .037 for all 915 subcell reflections; R = 0.085, wR = .034 for 548 reflections with $F^2 > 3\sigma$. The distribution of iodine obtained from subcell data is a smoothly varying column of electron density along (¼,y,¼) with a minimum of 5.15 and a maximum of 26.2 e/Å^3. This is similar to the results obtained by Smith and Luss (4), except that they see a variation from 16 to 37 e/Å^3. Comparison of relative maxima and minima imply a greater degree of registry between the I chain and TTT lattice in (1.d.) TTT_2I_3, as is also suggested by the differences in diffuse layer line spacings observed photographically. The differences in absolute value of electron density maxima is not significant, or grid size on Fourier maps may have been different. As there is only one I-chain maximum in electron density in the asymmetric unit , interpretation is subject to question. For this reason, a structural refinement was carried out on 1276 unique data, including 915 subcell data, and 361 h3ℓ data. Since there are no systematic absences in the h3ℓ data set, the symmetry of the

full cell is lower than Cmca. Space group $Pmc2_1$ is consistent with the arrangement of the TTT molecules, and with the lack of systematic absences for h3ℓ reflections. The most important effect of adding k = 3 data is to add electron density to two of the four now independent electron density maxima along (¼,y,¼) and to subtract electron density from, and smear out, the other two maxima. The presence of weak h3ℓ, h odd, reflections requires a small displacement from x = ¼ for some of the iodine atoms. The phase of h3ℓ, h even, reflections is determined by the arbitrary selection of two of the four equivalent electron density maxima for reinforcement. The phasing of the h3ℓ, h odd, reflections cannot be determined as they are all very weak, and do not interact with other data. These reflections would have zero intensity if the iodine atoms were located precisely at x = ¼. The magnitude of the displacement can be determined from the h3ℓ, h odd, reflections, but the direction of the displacement cannot be determined. Refinement of the model was performed by adjustment of populations, temperature factors, and coordinates of iodine atoms until the difference Fourier map was nearly flat. The R factor reached 0.137 for all 1276 data, and 0.091 for 623 data with $F^2 > 36$. The weighted residuals were 0.055 and 0.050, respectively. The residual, R, for third level reflections alone was 0.297. Fourier maps of (¼,y,z) and (x,y,¼) reflections are shown in Figure 2. Note that there is significant electron density at three of the four minima; that all maxima

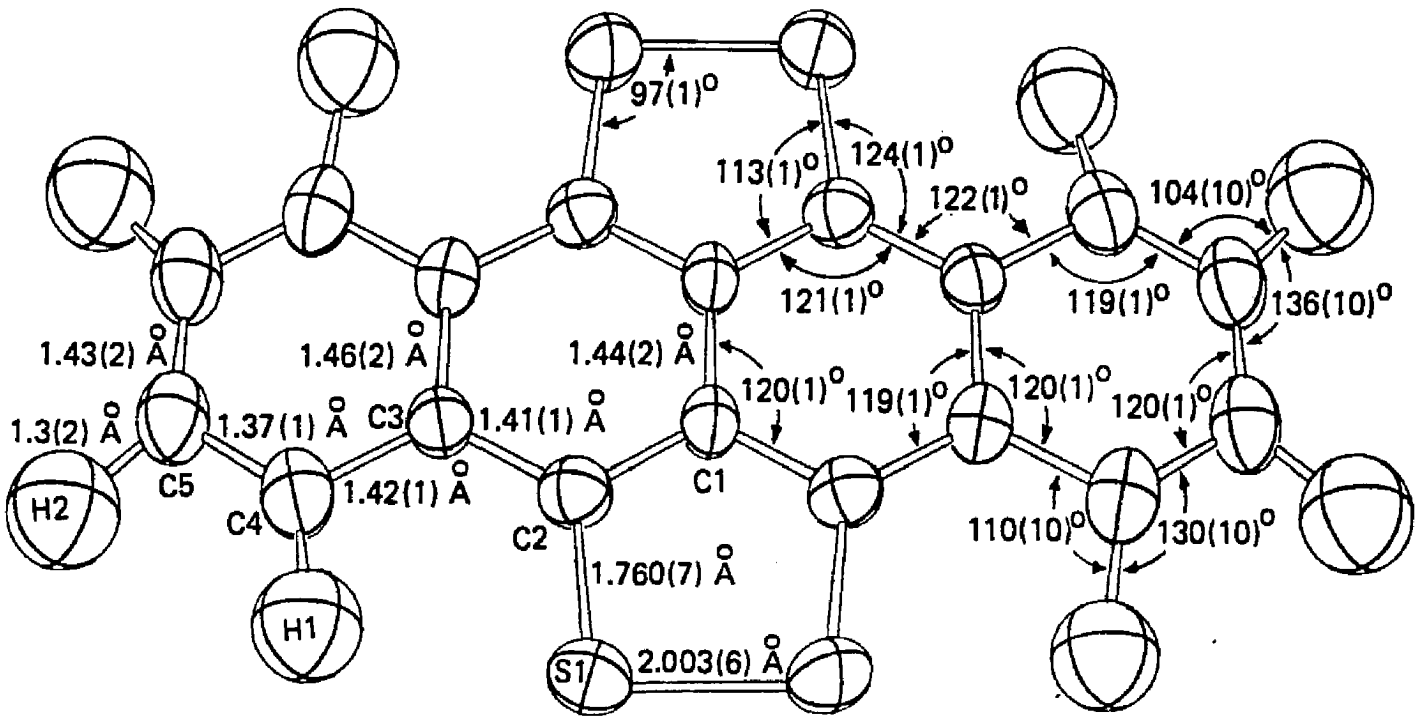

Figure 2. Bond lengths and angles in the TTT cation of (l.d.)$(TTT)_2I_3$. Estimated standard deviations are in parenthesis. Thermal ellipsoids are at the 50% probability level.

represent less than full iodide occupancy, and that the distance between the strongest maxima is 2.68 Å, just 0.02 Å longer than the I_2 bond length. Although minor diffracted intensity in diffuse lines, corresponding to one-dimensional order, could not be included in the structural refinement, this additional diffracted intensity is fairly weak. The diffraction pattern, with third level data included, is clearly inconsistent with discrete triiodide ions. The electron density map is consistent with the presence of species such as I^-, I_2, and I_3^-, which may be in dynamic equilibrium.

The atomic coordinates and temperature factors of the TTT cation were not refined in the lower symmetry space group of the complete cell. Patterson maps of the h3ℓ reflections show significant intensity only at (0,y,0); (0.5,y,0); (0.5,y,0.5); and (0,y,0.5). Thus only iodine-iodine vectors are necessary for interpretation of the Patterson map, and contributions from C and S atoms of TTT molecules are negligible.

The atomic coordinates and temperature factors of C, S, and H atoms in the subcell are given in Table 2. Figure 2 shows the molecule and its bond lengths and angles. Coordinates and temperature factors of the iodine atoms used to model the I chain structure in the subcell and full cell are given in Table 3. It should be understood that these parameters model a continuous distribution of iodide species and, individually, have little significance.

Table 2. Refined Atomic Coordinates and Temperature Factors of the TTT Cation in $(TTT)_2I_3$ (1.d.)

	x	y	z	U11	U22	U33	U12	U13	U23
C 1	96094(52)	0	0	419(55)	315(66)	373(48)	0	0	-58(57)
C 2	92395(37)	17964(176)	4441(46)	370(36)	424(59)	481(42)	11(41)	11(33)	25(47)
C 3	96052(37)	36659(178)	8951(38)	484(43)	337(45)	356(34)	-20(42)	60(34)	27(39)
C 4	92279(48)	55312(184)	13493(46)	728(57)	396(60)	420(41)	25(50)	80(41)	44(46)
C 5	96146(46)	73247(202)	17678(46)	798(58)	488(59)	416(38)	-20(50)	26(43)	-17(48)
S 1	82910(11)	15187(55)	3861(14)	362(9)	640(15)	724(14)	45(12)	39(10)	-100(15)

	x	y	z	
H 1	8473	5561	1161	B = 7.48
H 2	9135	8661	2109	B = 8.25

Atomic coordinates of C and S are multiplied by 10^5. Uij's and atomic coordinates of H atoms are multiplied by 10^4.

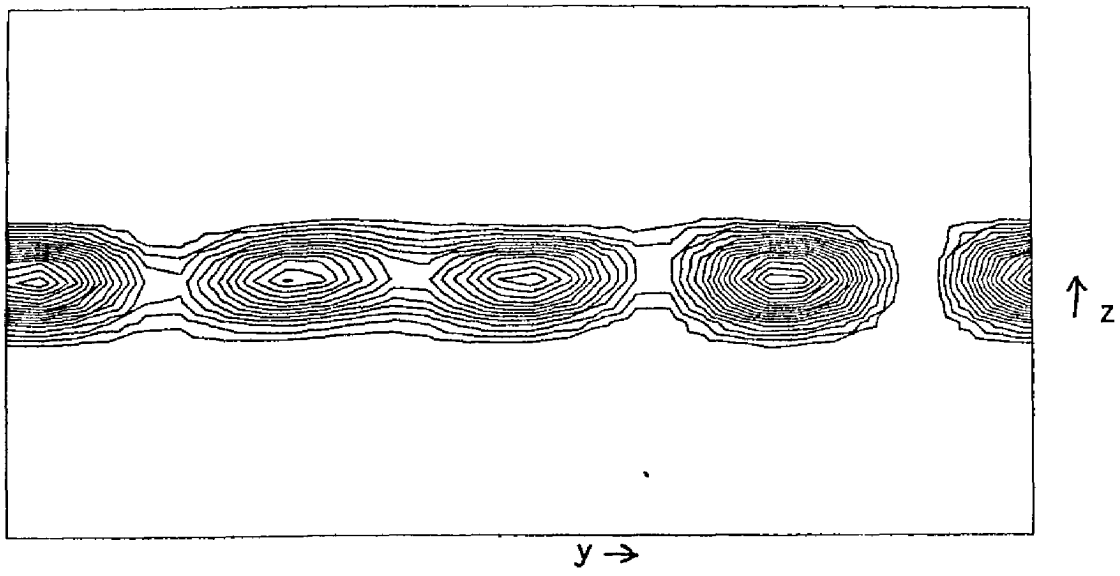

SECTION X = .250003

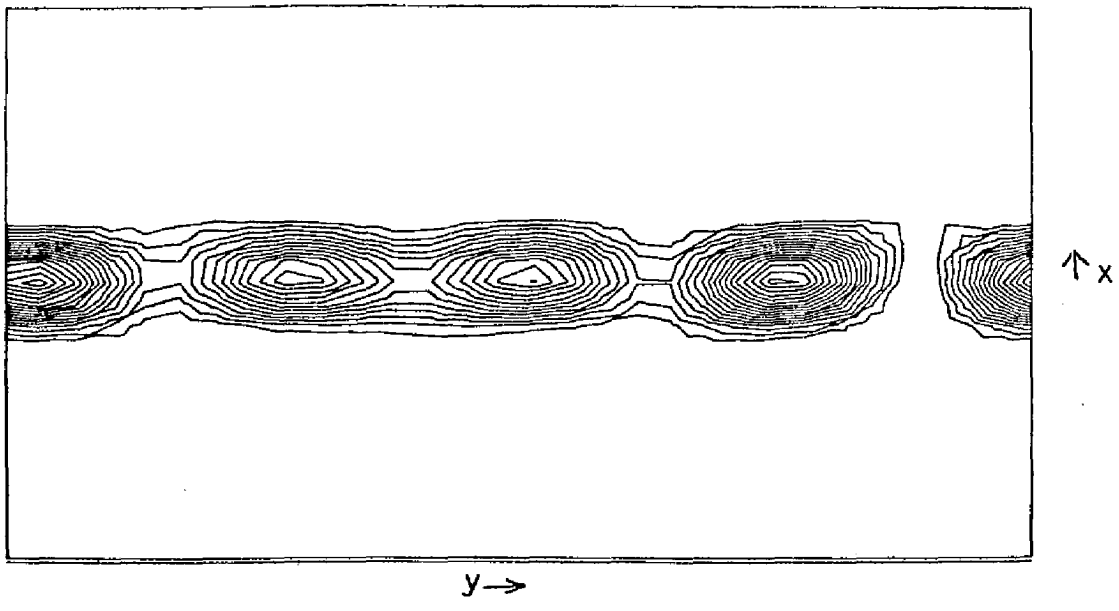

SECTION Z = .250003

Figure 3. Electron density maps through iodine chain in (1.d.) $(TTT)_2I_3$. Scale is about 0.8 Å/cm; contours at $2e/Å^3$ intervals.

Table 3. Coordinates and Temperature Factors used to Model I-Chain in TTT_2I_3

Subcell - Cmca

	x	y	z	U11	U22	U33	U12	U13	U23	Population
I 1	250	125	250	852	2306	1667	0	772	0	0.224
I 2	250	285	250	414	2624	505	0	-14	0	1.014
I 3	250	405	250	2233	435	4125	0	-683	0	0.121
Full Cell - P										
I 1	254	25	246	380	2483	560	93	171	9	0.657
I 2	253	420	248	380	12910	560	0	171	0	0.153
I 3	253	758	254	380	2483	560	93	171	9	0.693
I 4	247	278	250	380	2483	560	93	-171	92	0.351
I 5	245	499	254	380	2483	560	93	171	92	0.369
I 6	251	92	250	518	12910	679	0	171	0	0.050
I 7	248	580	250	518	12910	679	0	171	0	0.020
I 8	253	680	250	518	12910	679	0	171	0	0.060
I 9	242	194	250	518	12910	679	0	171	0	0.065
I 10	255	340	250	B=6.0						0.030
I 11	240	840	250	B=6.0						0.040
I 12	256	940	250	B=6.0						0.040

All coordinates have been multiplied by 10^3. All Uij's have been multiplied by 10^4.

Discussion

Figure 4 shows a model which adequately explains the observed electron density of the iodine chain in (l.d.) TTT_2I_3. It is likely that I_3^- is the dominant species. Two-fold disorder between the crystallographically distinct configurations shown in 4a and 4b accounts for the fractional occupancy (~.6) of two of the iodine positions (y = .28; y = .50), and the "smearing out" of electron density in the y direction. The fractional occupancy (~.8) of the other positions may be explained by additional configurations. However, the very significant electron density between maxima suggests that there is exchange of iodine atoms between sites. Intermediate configurations such as Figure 4c and 4d may be involved in transitions from 4a to 4b. These would occasionally leave the higher occupancy sites empty. Species such as I_2, I^-, I_5^-, and perhaps others would be present, although they would be much less likely than I_3^-, in agreement with the observation of I_3^- in TTT_2I_3 by Raman spectroscopy (8).

The presence of disorder in the iodide chains of TTT_2I_3 has been invoked to explain the retention of conductivity at low temperature, although the nature of the disorder and its behavior with cooling have not been understood (1-4,7). The iodide chains in (l.d.) TTT_2I_3 contain partially occupied sites which are statistically filled by several species in several possible configurations. Microscopically, these chains result in an aperiodic potential around the TTT stacks.

It is unlikely that there are important changes in the iodide chain at low temperature (3,7). This aperiodic potential may suppress a complete Peierls' transition by creating states within the gap and suppressing "locking" of charge density waves on adjacent stacks. This qualitatively explains the retention of moderate conductivity at low temperature in TTT_2I_3, although a complete explanation must await completion of low-temperature structure refinement.

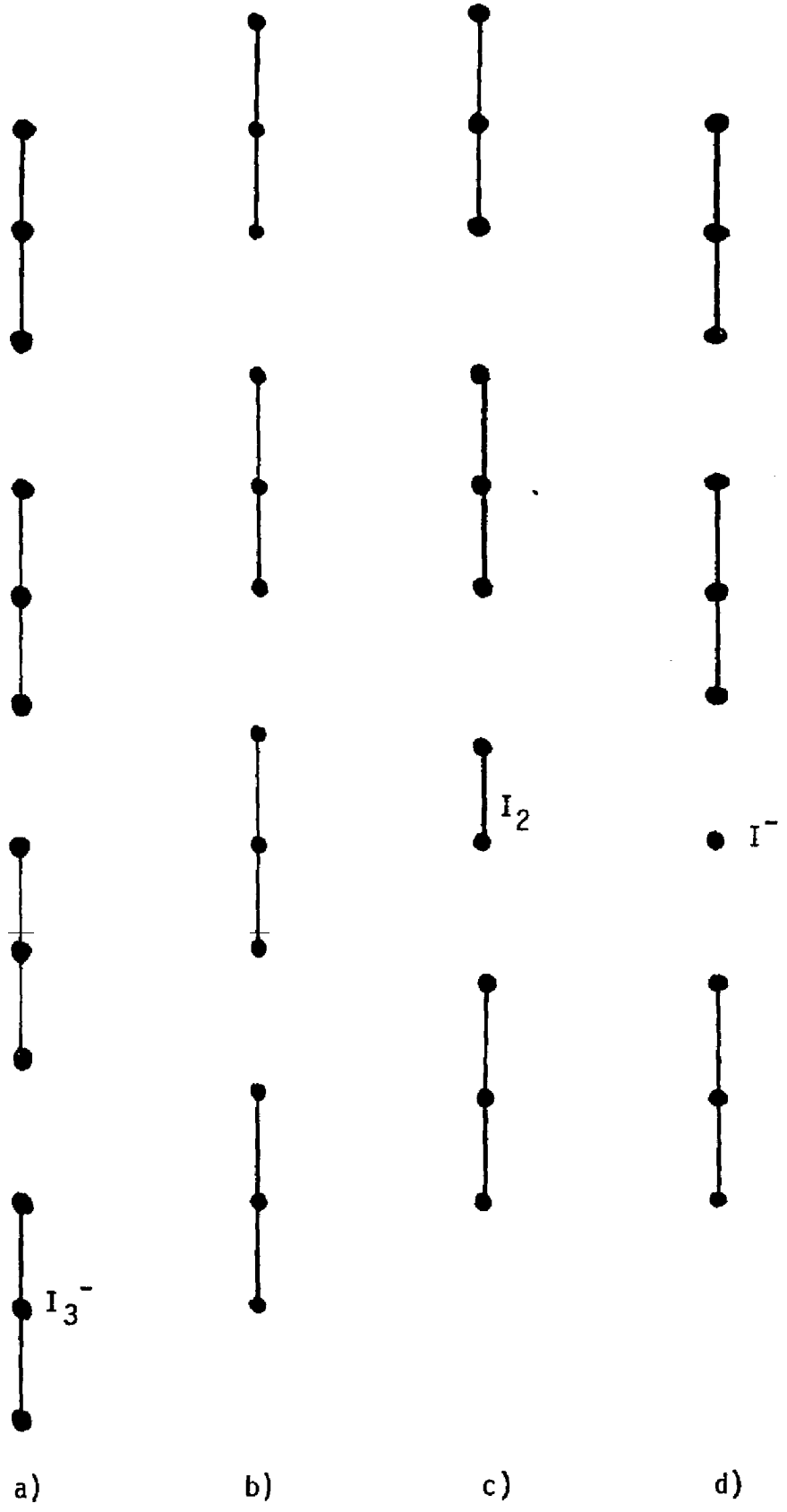

Figure 4. Possible configurations of iodine species contributing to chain in $(TTT)_2I_3$

References

1. L. C. Isett and E. A. Perez-Albuerne, Solid State Comm., 21, 433 (1977); L. C. Isett, to be published in Phys. Rev., B.
2. V. F. Kaminskii, M. L. Khidekel, R. B. Ljubovskii, I. F. Schegelov, R. P. Shibaeva, E. B. Yagubskii, A. V. Zvargkina, and G. L. Zverena, Phys. Stat. Sol. (a), 44, 77 (1977); L. I. Buravov, G. I. Zvereva, V. F. Kaminskii, L. P. Rosenberg, M. L. Khidekel, R. P. Shibaeva, I. F. Schegelov, and E. B. Yagubskii, J. Chem. Soc. Chem. Comm., 720 (1976).
3. S. K. Khanna, S. P. S. Yen, R. B. Somoano, P. M. Chaikin, C. L. Ma, R. Williams, and S. Samson, Phys. Rev., B19 (1979).
4. D. L. Smith and H. R. Luss, Acta Crystallogr., B33, 1744 (1977).
5. International Tables for X-Ray Crystallography, Vol. III, Kynoch Press, Birmingham (1962).
6. International Tables for X-Ray Crystallography, Vol I, Kynoch Press, Birmingham (1952).
7. C. L. Ma, private communication.
8. L. C. Isett and E. A. Perez-Albuerne, Annals of the New York Academy of Sciences, 313, 395 (1978).

CHAPTER 5

Tetramethyltetraselenofulvalene Bromide and Thiocyanate; Electrochemical Preparation of Conducting Organic Crystals

Tetrathiafulvalene (TTF) forms highly conducting stacked charge-transfer salts with both organic acceptors such as tetracyanoquinodimethane (TCNQ) and simpler anions such as halides and pseudohalides (1,2). Derivatives of TTF and its selenium analog, tetraselenofulvalene (TSF), also form highly conducting TCNQ complexes (3,4), but their halide and pseudohalide salts have been studied less thoroughly (5). I have prepared crystals of tetramethyltetraselenofulvalene bromide and thiocyanate $(TMTSF)Br_{0.82}$ and $(TMTSF)(SCN)_{0.50}$ in order to explore further the relation between structure and physical properties in quasi-one-dimensional conductors.

Preparation of good single crystals of organic conductors is often the most serious obstacle to study of these materials. Electrochemical crystal growth techniques have successfully exploited the conducting properties of a variety of inorganic materials (6,7) and a few organic materials (8). The crystal formed by electrolysis must be quite insoluble in the solution or melt in which the precurser is dissolved. As the conducting crystal grows, it acts as an extension of the electrode. Defects inhibit

crystal growth, because of conductivity decrease. Large crystals are, therefore, well formed single crystals. Insulating phases, which are often formed in other kinds of crystallization experiments, are avoided by this technique. Electrochemical crystal growth experiments involving oxidation of TTF, TSF, TMTSF, and HMTSF (hexamethylene-tetraselenofulvalene) in the presence of Cl^-, Br^-, I^-, SCN^-, and $SeCN^-$ were carried out at a variety of oxidation potentials and temperatures in several solvents. This investigation was not exhaustive, but some conclusions about the suitability of electrochemical crystal growth to these systems can be drawn.

Experimental

Synthesis

<u>(TMTSF)(Br)</u>$_{0.82}$: 0.01 g TMTSF was dissolved in 1.5 ml. benzonitrile containing 0.1 Molar tetraethylammonium bromide. This solution was placed in the working electrode cell (Figure 1) and oxidized, at 0.02 Volt vs. $Ag^{\circ}/AgClO_4$ (sat), with a Pt wire electrode, at 69-70° C. Well formed black crystals up to 1 mm long were recovered after eight minutes.

<u>(TMTSF)(SCN)</u>$_{0.50}$: 0.006 g TMTSF was dissolved in 1 ml benzonitrile containing 0.02 Molar tetraethylammonium thiocyanate. Oxidation, at 0.00 Volt vs. $Ag/AgCLO_4$ (sat), at a Pt wire electrode, for fifteen minutes at 56-64° C, gave good crystals up to ~1 mm long.

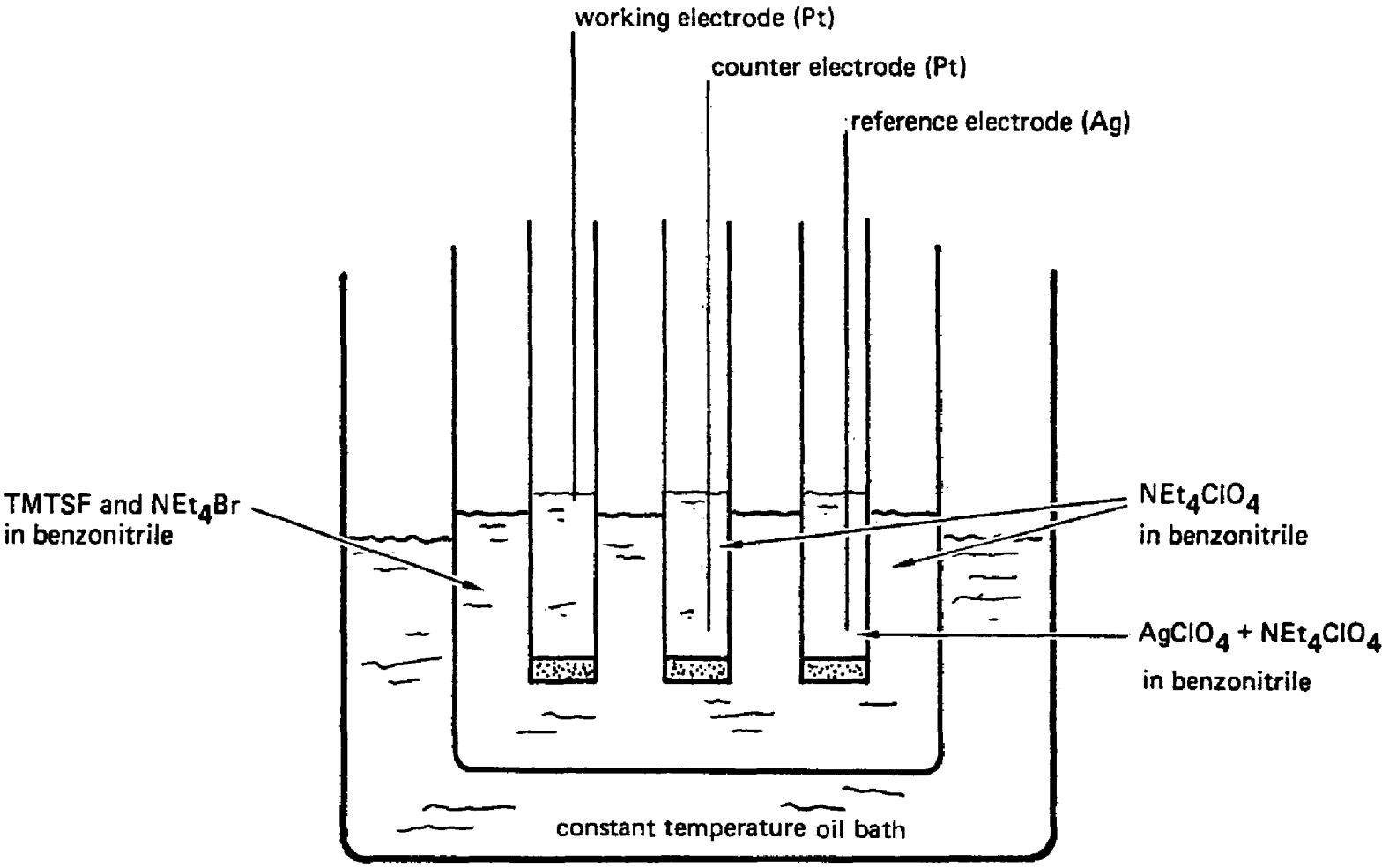

Figure 1. Electrochemical crystallization cell.

The conditions, and results, of these and other electrochemical crystallization experiments, are collected in Table 1.

The oxidizing potential was controlled using a Wenking 68 FR 0.5 potentiostat. Crystals of both of the TMTSF salts were flat needles exhibiting well formed {110} and {010} faces. Oxidation at temperatures greater than ~80° C resulted in little crystallization because of solubility of the products. Near room temperature, TMTSF is only slightly soluble in benzonitrile and oxidation gives crystals << .01 mm in thickness.

HMTSF is very insoluble in all common solvents at room temperature; a benzonitrile solution at 100° C is less than 0.02 Molar when saturated. Unfortunately, at this temperature, the oxidation product seems to be quite soluble also, even in the presence of fairly high concentrations of bromide or thiocyanate.

Oxidation of solutions containing I^- or $SeCN^-$ resulted in oxidation of the anion, and formation of no solid product. Crystals of $(TMTSF)I_x$ can be prepared by co-diffusion of $(TMTSF)ClO_4$ and NBu_4I in acetonitrile.

Electrical measurements

Conductivity and thermoelectric power were measured for both kinds of crystals at room temperature and at lower temperatures. The results are shown in Appendix 2.

Table 1. Conditions, Results of Electrochemical Crystallization Experiments

Donor, Concentration	Electrolyte, Concentration, Working Electrode Cell	Solvent	Oxidation Potential, vs. $Ag^{\circ}/AgClO_4$(sat)	Temperature	Results
TTF $1x10^{-3}$-$6x10^{-2}$M	NH_4SCN,$4x10^{-2}$M NEt_4Br,$1x10^{-1}$M NEt_4Cl,5-$20x10^{-2}$M	acetonitrile	0.0-0.5 Volt	Room Temperature	$(TTF)_{12}(SCN)_7$* good $(TTF)(Br)_{0.74}$ crystals, $(TTF)(Cl)_{0.67}$ 10x.1x.1 mm^3
TMTSF 1-$2x10^{-2}$M	NEt_4Br,$1x10^{-1}$M NEt_4SCN,$2x10^{-1}$M NBu_4I,$1x10^{-1}$M	benzonitrile	~0.0 Volt	60-80° C	$(TMTSF)(Br)_{0.82}$ good $(TMTSF)(SCN)_{0.50}$ crystals oxidation of I^-, no solid
				Room Temperature	extremely thin crystals of bromide and thiocyanate
				100-120° C	no crystals, some coating of electrode
HMTSF $7x10^{-3}$M	NEt_4Br,$1x10^{-1}$M NEt_4SCN,$2x10^{-2}$M	benzonitrile	0.0-0.2 Volt	100-120° C	no crystals, some coating of electrode
TSF $3x10^{-3}$M	NEt_4Cl,$5x10^{-2}$M KSeCN,$1.5x10^{-2}$M	acetonitrile	0.1-0.4 Volt 0.0-0.4 Volt	Room Temperature	$(TSF)Cl_x$,tiny hairlike crystals no solid produced in oxidation in presence of KSeCN

*

	%C	%H	%N
calc	33.19	1.69	3.43
found	33.01	1.94	3.39

X-ray diffraction photographs

Oscillation photographs of $(TMTSF)(Br)_{0.82}$ and $(TMTSF)(SCN)_{0.50}$ mounted with the rotation axis parallel to the C axis were taken. The C axis is ~7 Å long for both compounds, but photographs of $TMTSF(SCN)_{0.50}$ show additional weak layer lines. An oscillation photograph of $TMTSF(SCN)_{0.50}$ is shown in Figure 2. Accurate measurement of this film gave the lattice spacings listed in Table 2. The satellite reflections are due to a superperiod C' = 32.815 = 4.56 C. The presence of strong satellites of the hk0 layer indicates that the superperiod is due to a structure factor modulation rather than a C axis length modulation, since the latter would give hk0 satellites of vanishingly small intensity (9). Systematic absences ($hk\ell$, $h + k = 2n + 1$; $h0\ell$, $\ell = 2n + 1$) were determined from Weissenberg photographs prior to data collection and indicated that the space group of both compounds was Cmcm.

Data Collection

Both data sets were obtained with Ni-filtered $CuK\bar{\alpha}$ radiation ($\lambda\bar{\alpha}$ + 1.54178 Å) using 2θ-θ scans at rates of 0.5 or 1.0 degrees per minute on a locally assembled, Datex automated, General Electric quarter circle diffractometer. Background intensities were measured at both ends of the scans for a total of 60, 80, or 120 seconds. Two $TMTSF(SCN)_{0.50}$ crystals were used for data collection. An entire hemisphere of data was collected, and merged, in order to

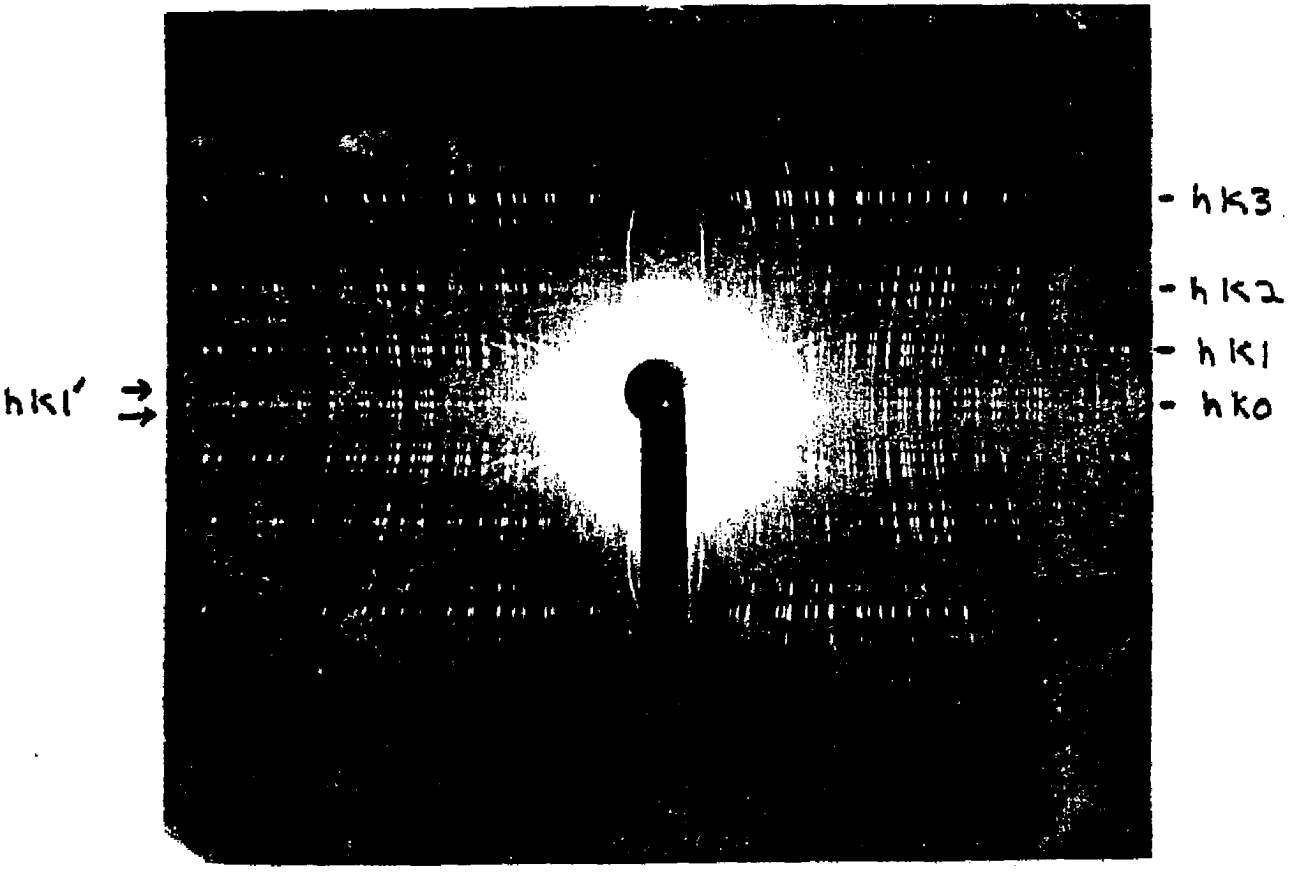

Figure 2. Oscillation photograph of $(TMTSF)(SCN)_{0.5}$.

Table 2. Layer Line Spacings of $(TMTSF)(SCN)_{0.50}$

d (Å)*	ℓ	ℓ'	$d/\ell = C_0$ (Å)	c'_0 †
32.8146	0	1'		32.8146
9.1088	1	-1'		34.2313
7.1893	1	0	7.189	
5.8934	1	+1'		32.5899
4.0242	2	-1'		33.9013
3.5983	2	0	7.197	
3.2363	2	+1'		32.2572
2.5774	3	-1'		34.4791
2.3970	3	0	7.191	
2.2268	3	+1'		31.1683
1.8000	4	0	7.200	

* Very weak $\ell = n \pm 2'$ satellite reflections were observed but could not be accurately measured.

† Calculated assuming that $d = (\ell/C_0 + \ell'/C_0')^{-1}$. $\langle C_0 \rangle = 7.1944$; $\langle C_0' \rangle = 33.063$; $C_0'_{hkl}' = 32.815$; $\langle C_0' \rangle / \langle C_0 \rangle = 4.60$.

average errors in data collection. A crystal measuring 0.070 x 0.033 x 0.533 mm^3 was used for intensity measurement of 1052 reflections due to the 9.919 x 24.124 x 7.220 $Å^3$ cell; satellite reflections could not be well resolved on the diffractometer with this crystal which required a 1 mm collimator. A smaller crystal measuring 0.073 x 0.027 x 0.193 mm^3 was used for measurement of satellite reflection intensities. Using a 0.25 mm collimator, 197 unique hk1' and hk2' satellite reflections were measured, as well as several hundred combination reflections ($hk\ell \pm \ell'$).

The $(TMTSF)(Br)_{0.82}$ crystal used for data collection measured 0.05 x 0.017 x 0.40 mm^3. All 1029 reflections of $TMTSF(Br)_{0.82}$ in one octant, having $2\theta \leq 155°$ were collected. The data from both crystals were corrected for Lorentz, polarization, absorption, and decay effects (10). The scattering factors of selenium, sulfur, and bromide were corrected for the real part of anomalous dispersion (11). Crystal data for both crystals are given in Table 3.

Structure determination and refinement - $TMTSF(Br)_{0.82}$

Symmetry, stacking, and steric considerations indicated that the TMTSF molecules were oriented perpendicularly to $\overline{C}$, lay on mirror planes at Z = 1/4 and 3/4, and that successive molecules were slipped along b by ~1.0-1.5 Å. This initial model provided adequate phasing for refinement and location of other atoms in Fourier maps. The structure was refined to R = 0.071, wR = 0.023 for 1029 data; for

Table 3. Crystal Data, $(TMTSF)Br_{0.82}$ and $(TMTSF)(SCN)_{0.50}$

$(TMTSF)(Br)_{0.82}$

a = 9.798 (2)

b = 23.837 (5)

c = 7.095 (1)

v = 1657.1 $Å^3$

Space Group = Cmcm

F.W. $(C_{10}Se_4H_{12}Br_{0.82})$ = 513.6

z = 4 formula units per cell

d_{calc} = 2.058 g/cm^3

μ (absorption coefficient) = 145.2 cm^{-1} ($CuK\overline{\alpha}$)

$(TMTSF)(SCN)_{0.50}$

a = 9.919 (3)

b = 24.124 (14)

c = 7.220 (6)

v = 1729.3 $Å^3$

Space Group = Cmcm

F.W. $(C_{10.5}Se_4H_{12}N_{0.5}S_{0.5})$ = 494.5

z = 4 formula units per cell

d_{calc} = 1.899 g/cm^3

μ (absorption coefficient) = 122.3 cm^{-1} ($CuK\overline{\alpha}$)

Space Group of modulation $Cmc2_1$

755 reflections having $F^2 > 3\sigma$, R = .061, wR = .023. During refinement, four peaks on the Fourier map of the x=0 plane indicated the incorporation of a disordered small molecule in the structure. These were refined as partially occupied carbons and nitrogens. Figure 3 shows the structure in the z = 1/4 plane. Figure 4 shows a projection showing overlap of consecutive TMTSF molecules view down z; and Table 4 shows bond angles and lengths in the molecule. Table 5 contains atom coordinates and temperature factors. Most shifts were less than $\sigma/2$, all other shifts were less than σ at refinement, except for the coordinates of Br^- ion, which has very high thermal motion in the z direction, and can be fit equally well by constraining it to the z = 1/4 plane or placing it in two-fold positions above and below this plane. Hydrogen positions refined satisfactorily but their isotropic temperature factors could not be refined. The deviation of C-H bond lengths and angles from expected values may be due to torsional motion of the methyl groups. A difference map, based on refined coordinates of non-hydrogen atoms, through the plane of the hydrogen atoms, is shown in Figure 5.

Structure determination and refinement - $TMTSF(SCN)_{0.50}$

The $TMTSF(SCN)_{0.50}$ data were phased by placing TMTSF molecules at positions equivalent to those in the refined $TMTSF(Br)_{0.82}$ structure. After several least squares refinement cycles, the thiocynates could be seen in difference Fourier maps. They lie

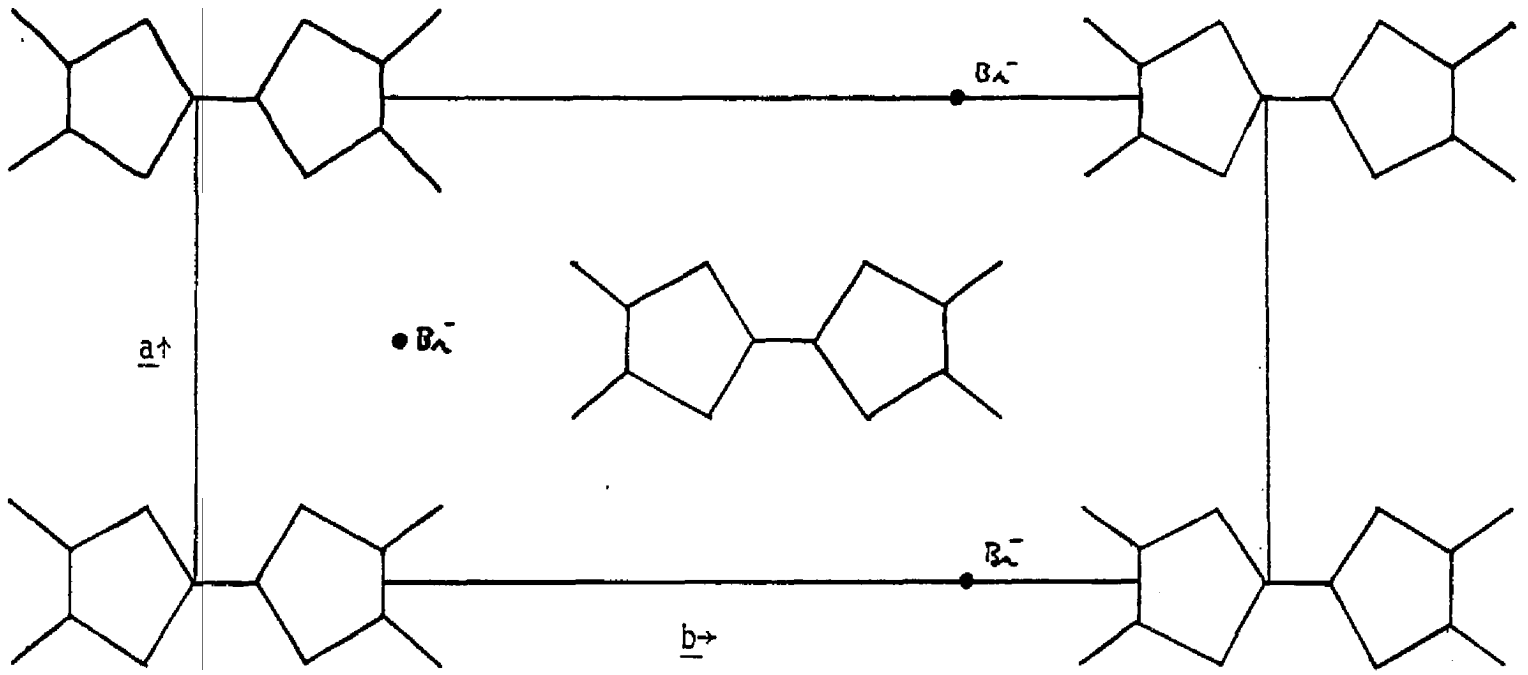

Figure 3. z = 1/4 plane of $(TMTSF)Br_{0.8}$ structure. $(TMTSF)(SCN)_{0.5}$ is isostructural.

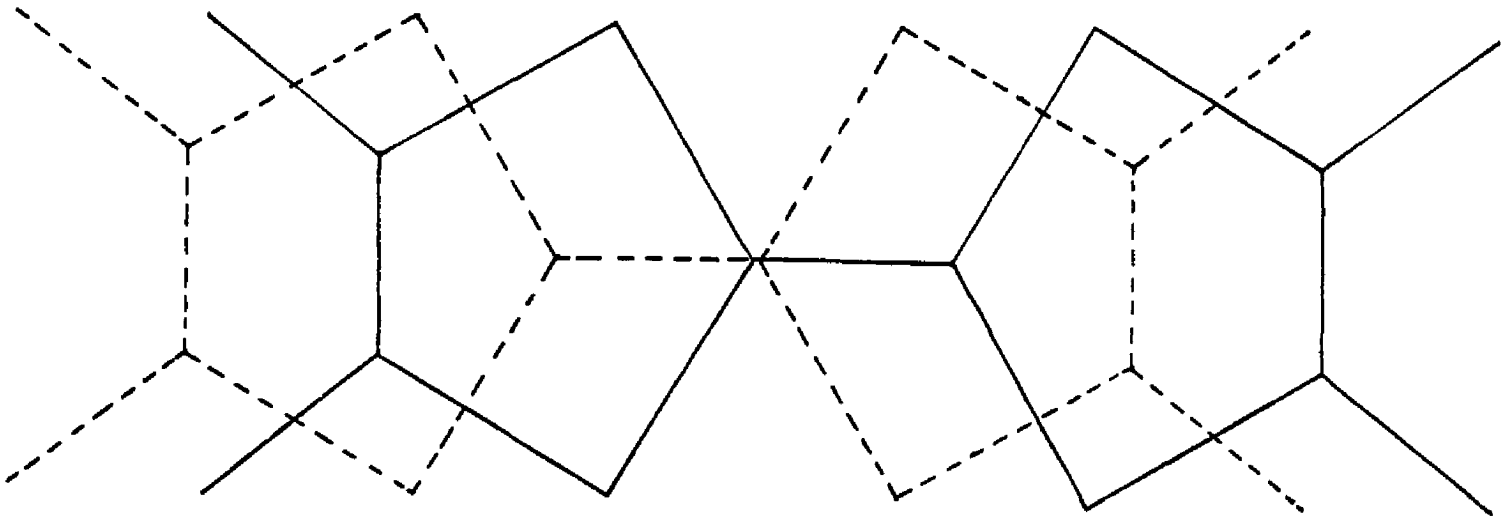

Figure 4. Overlap of consecutive TMTSF cations in $(TMTSF)Br_{0.8}$. View is down the z axis.

Table 4. Bond Lengths and Angles in $(TMTSF)Br_{0.8}$

C1 - C2	1.406	(22)
C1 - Se1	1.861	(13)
C2 - Se2	1.845	(17)
Se1 - C3	1.871	(16)
Se2 - C4	1.889	(16)
C3 - C5	1.519	(24)
C4 - C6	1.542	(24)
C3 - C3'	1.340	(36)
C4 - C4'	1.320	(36)
C5 - H1	1.24	(18)
C5 - H2	1.12	(18)
C6 - H3'	1.11	(18)
C6 - H4	1.11	(18)

<C1 - C2 - Se2	121.9	(.1)
<C2 - C1 - Se1	122.2	(.1)
<Se1 - C1 - Se1	115.6	(.2)
<Se2 - C2 - Se2	116.0	(.2)
<C1 - Se1 - C5	93.3	(1.0)
<C2 - Se2 - C4	93.2	(1.0)
<Se1 - C3 - C3'	118.9	(1.0)
<Se2 - C4 - C4'	118.7	(1.0)
<Se1 - C3 - C5	115.5	(1.0)
<Se2 - C4 - C6	114.2	(1.0)
<C3 - C5 - H1	94	(10)
<C 3 - C5 - H2	122	(10)
<C4 - C6 - H4	109	(10)

Table 5. Refined Atomic Coordinates and Temperature Factors of $(TMTSF)(Br)_{0.8}$

	x	y	z	U11	U22	U33	U12	U13	U23
Se 1	16068 (14)	9935 (5)	25000	313 (7)	359 (6)	538 (9)	-20 (6)	0	0
Se 2	15994 (13)	-4216 (5)	25000	324 (7)	359 (6)	540 (9)	36 (5)	0	0
C 1	0	5763 (56)	25000	286 (83)	248 (64)	369 (102)	0	0	0
C 2	0	-130 (73)	25000	214 (76)	391 (78)	460 (112)	0	0	0
C 3	6759 (126)	16826 (44)	25000	435 (72)	376 (55)	527 (84)	-52 (51)	0	0
C 4	6689 (131)	-11167 (45)	25000	494 (78)	376 (55)	444 (80)	9 (55)	0	0
C 5	15622 (157)	22005 (45)	25000	673 (92)	238 (49)	1076 (131)	-178 (64)	0	0
C 6	16145 (150)	-16310 (49)	25000	523 (78)	380 (56)	628 (91)	68 (60)	0	0
H 1	26450 (1000)	19750 (560)	25000	B = 6.00					
H 2	14380 (910)	24880 (370)	13610 (1000)	B = 6.00					
H 3	2535 (910)	34320 (350)	11820 (1000)	B = 6.00					
H 4	1485 (1000)	-18640 (560)	25000	B = 6.00					
Br^-	50000	17573 (20)	23600	589 (23)	755 (24)	5269 (148)	0	0	3996 (382)
<u>Solvent</u>									
C7	0	41050 (80)	17800 (290)	B = 4.50					
C8	0	45730 (140)	5240 (550)	B = 4.50					
C9	0	50670 (170)	10530 (590)	B = 4.50					
C10	0	51960 (170)	25000	B = 4.50					

All coordinates have been multiplied by 10^5; all Uij's by 10^4.

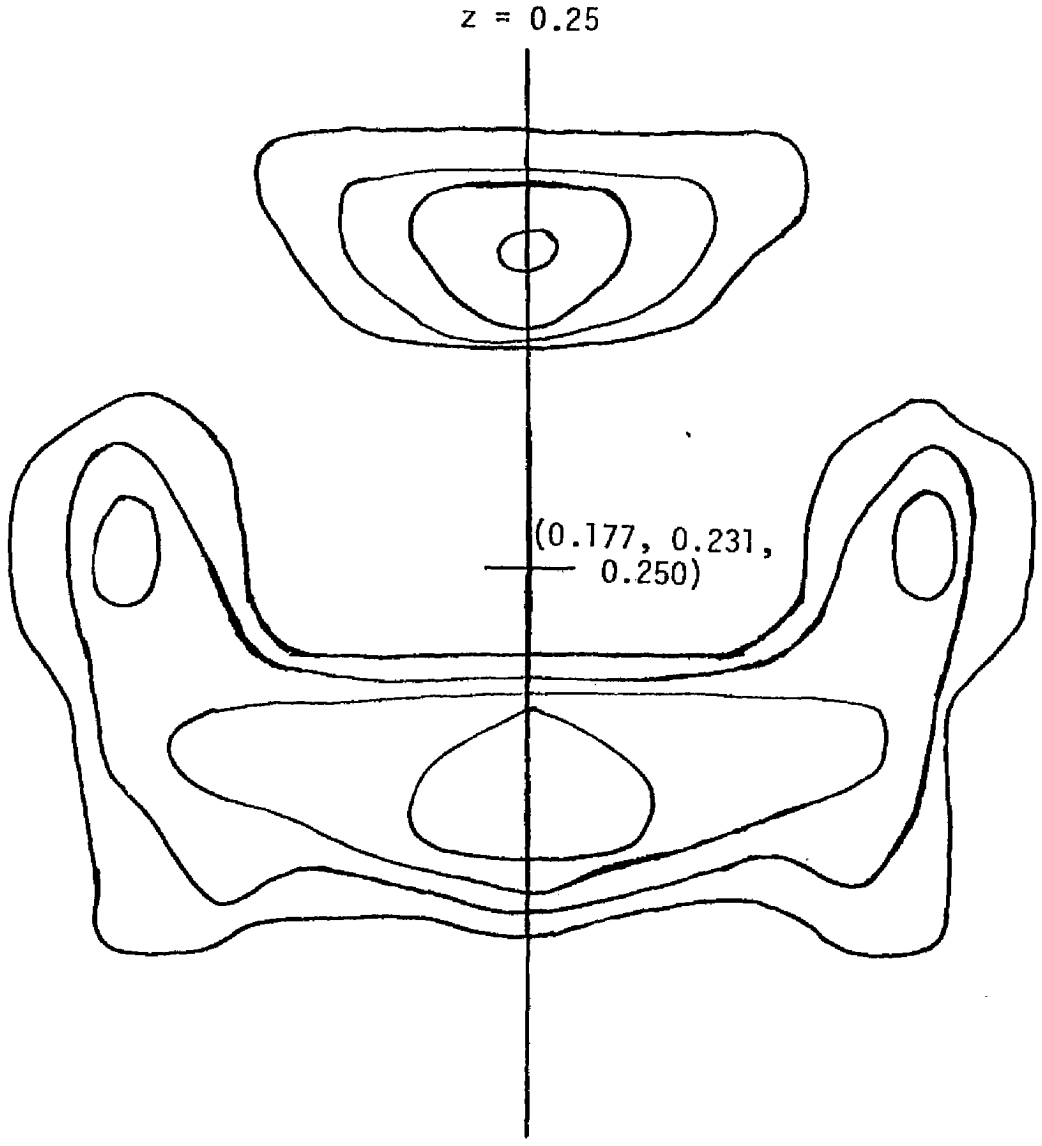

Figure 5. Difference map through hydrogens of methyl carbon (5). $F_{(calc)}$ based on refined positions of all non-hydrogen atoms. Contours are in steps of .1 e/Å^3, with outermost contour at .3 e/Å^3. Scale is 4.9 cm/Å

across mirror planes at 1/4 and 3/4, and there is two-fold disorder between sulfur and nitrogen. Electron density in the difference map also shows the presence of a disordered small molecule similar to that seen in $TMTSF(Br)_{0.82}$. Hydrogen atom positions in $TMTSF(SCN)_{0.50}$ are even less satisfactory than in the bromide. The structural refinement proceeded to R = 0.054, wR = 0.0124 for all data; R = 0.042, wR = 0.0118 for reflections with $F^2 \geq 3\sigma$. The temperature factors of the thiocyanate are fairly large, reflecting disorder and perhaps the modulation of the thiocyanate position. At the level of refinement achieved, all non-hydrogen coordinate and temperature factor shifts are less than $\sigma/4$; hydrogen coordinate shifts are less than σ and hydrogen isotropic temperature factors could not be refined.

Atom coordinates and temperature factors of the refined structure of $(TMTSF)(SCN)_{0.50}$ are given in Table 5. Bond angles and lengths of the TMTSF cation are shown on an ORTEP plot (Figure 6).

Analysis of the satellite reflections

Only the hkl' and hk2' (C' = 33.815 Å) reflections were used in the analysis of the structure modulation. The pattern of intensity, with respect to indices h and k, is about the same for the hkl' and hk2' and the combination reflections resulting from both latices. A Patterson map based on hkl' and hk2' data shows a number of peaks with interatomic vectors having x-component = 0. Only one (independent) relatively weak peak lies off of the x = 0

Table 6. Refined Atomic Coordinates and Temperature Factors for $TMTSF(SCN)_{0.50}$

	x	y	z	U11	U22	U33	U12	U13	U23
Se 1	15849(13)	9724(4)	25000	470(6)	521(6)	644(8)	-38(5)	0	0
Se 2	15855(12)	-4293(4)	25000	413(5)	519(6)	628(7)	33(4)	0	0
C 1	0	5617(55)	25000	468(73)	529(70)	434(79)	0	0	0
C 2	0	-139(57)	25000	384(58)	506(64)	509(83)	0	0	0
C 3	6744(107)	16531(40)	25000	626(62)	510(46)	631(68)	-21(45)	0	0
C 4	6595(100)	-11165(37)	25000	528(56)	470(43)	609(63)	51(41)	0	0
C 5	15512(233)	21669(63)	25000	1097(106)	651(69)	858(98)	-271(82)	0	0
C 6	15495(134)	-16238(45)	25000	556(55)	545(51)	748(76)	117(55)	0	0
H 1	2829	1794(47)	2500	B = 6.00					
H 2	1609(92)	2204(34)	1531	B = 6.00					
H 3	2205(70)	-1508(28)	1567	B = 6.00					
H 4	748(98)	-1902(46)	2500	B = 6.00					
		SCN^-							
C 7	0	32400(131)	75000	310(141)	526(150)	1159(334)	0	0	0
S/N	0	33333(88)	58084(299)	484(57)	2421(207)	1803(170)	0	0	-711(169)
		Solvent							
C 8	0	4623(19)	4607(69)	B = 10.15(1.75)					
C 9	0	4798(22)	7500	B = 10.68(2.17)					
C 10	0	4119(11)	1775(40)	B = 9.28(0.97)					
C 11	0	5111(19)	1000(88)	B = 8.91(1.94)					

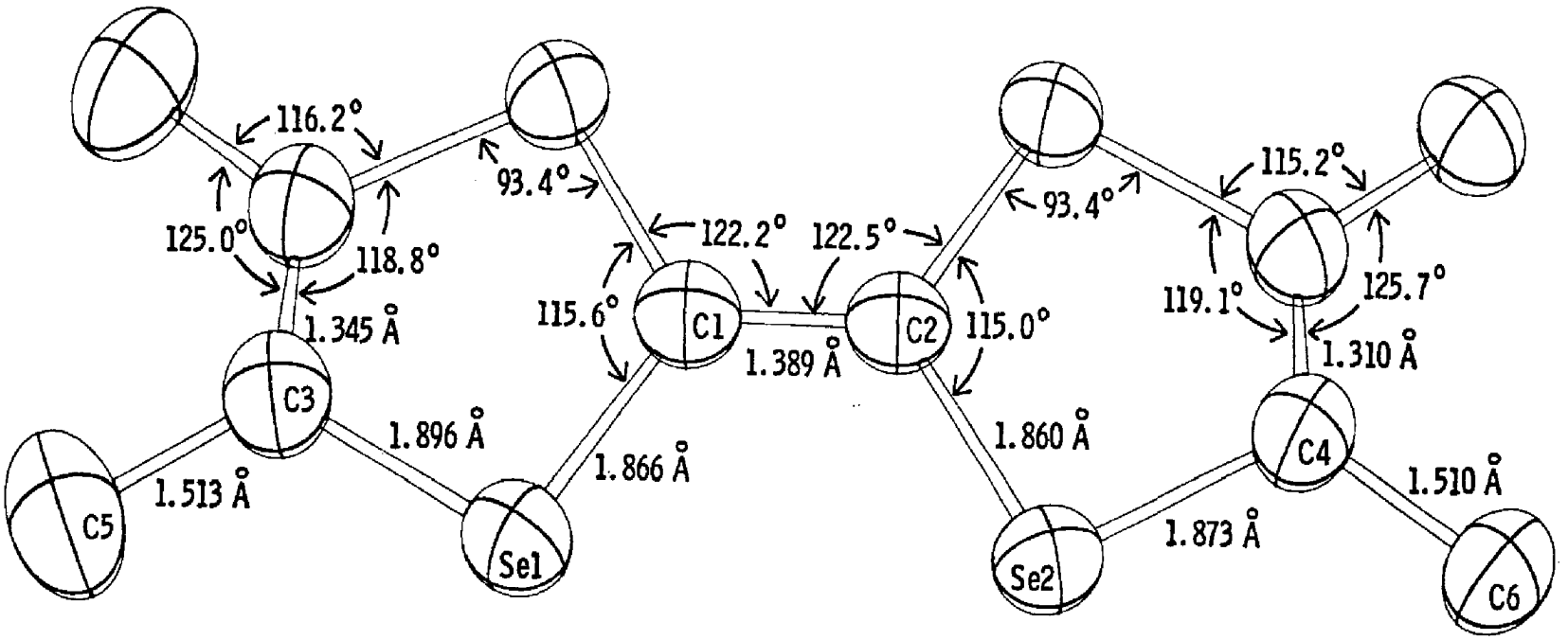

Figure 6. Bond angles and distances of the tetramethyltetraselenofulvalene cation in $(TMTSF)(SCN)_{0.5}$. Thermal ellipsoids are drawn at the 50% probability level.

plane of the Patterson. The strongest vector is (0.0, 0.025, 0.5) which was interpreted as a vector between the extreme positions of a modulated thiocyanate chain. It appears that a slight displacement in the y coordinates of the thiocyanate anions occurs with a period of 32.815 Å. This model of the modulation, in Space Group $Cmc2_1$, along with fitting of several smaller peaks, results in R = .397 for 54 reflections with $F^2 > 3\sigma$. A Fourier map based on this unrefined model is shown in Figure 7. Larger peaks (.5 e/$Å^3$) at (0.0, 0.333, 0.0), (0.0, 0.307, 0.5), and (0.0, 0.353, 0.5) are associated with the thiocyanate ions. A smaller peak (.2 e/$Å^3$) at (0.0, 0.463, 0.0) is associated with an atom in the disordered solvent molecule. Small peaks are associated with the TMTSF cations, in the region of the C=C bonds and methyl groups, but these cannot be identified with particular atoms. The atomic coordinates and temperature factors used to model the satellite data are given in Table 7.

Discussion

The TMTSF cations in $(TMTSF)(Br)_{0.82}$ and $(TMTSF)(SCN)_{0.50}$ are slip-stacked and have their molecular planes perpendicular to $\bar{c}_0$, as shown in Figure 8a. This method of stacking is quite different than the stacking of TTF cations in TTF halides (8b) and (TTF)(TCNQ) (8c). The stacking is rather similar to that observed in tetra-

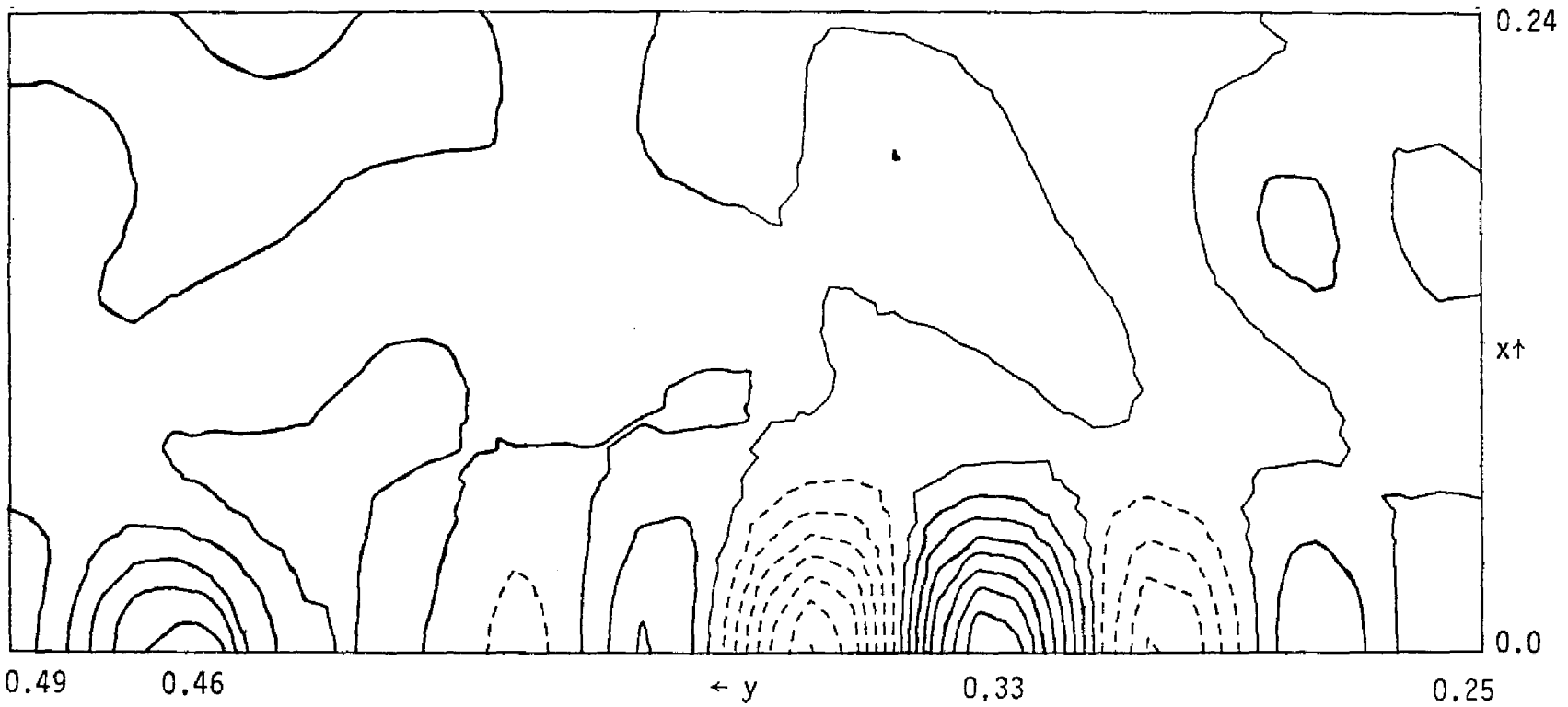

Figure 7. Electron density map of satellite reflection data (z=0). Contour intervals are at ~.05 e/Å^3. Scale is ~3.44 cm/Å. Dotted contours represent positive electron density at z = 0.5; solid contours at z = 0.0. Strong peaks at and near y = 0.33 are due to the thiocyanate ion; peak at y = 0.46 is an atom in the solvent molecule.

Table 7. Atomic Coordinates and Temperature Factors used to model $(TMTSF)(SCN)_{0.5}$ Structure Modulation

	x	y	z	U11	U22	U33	Population
S 1	0	3333	0	498	443	321948	1.9
S 2	0	3066	5000	498	443	321948	0.9
S 3	0	3528	5000	498	443	321948	1.5
C 1	0	4628	0	498	443	321948	2.0
C 2	0	1580	5000	498	443	321948	1.4
C 3	0	150	5000	498	443	321948	1.5
C 4	1850	1600	5000	498	443	321948	0.7

$U_{ij} = 0$ for $i \neq j$.

All parameters have been multiplied by 10^4.

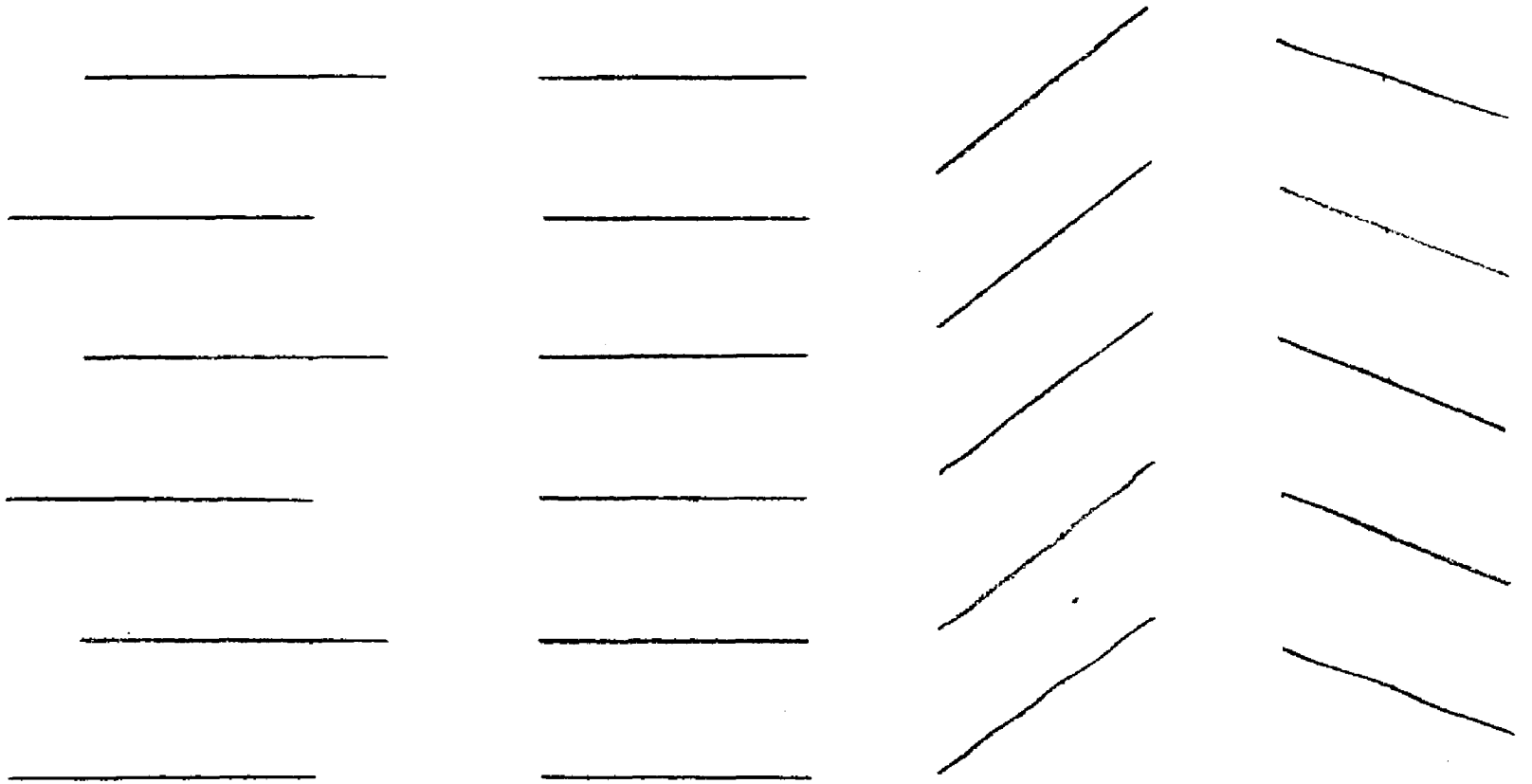

a) $(TMTSF)Br_{0.8}$ and $(TMTSF)(SCN)_{0.5}$.

b) $(TTF)Cl_{0.67}$

c) (TTF)(TCNQ)

Figure 8. Stacking in some organic conductors.

methyltetrathiafulvalene bromide, $(TMTTF)(Br)_{0.5}$; where only a slight tilt away from perpendicularity to the stacking axis is observed (5).

Interchain coupling should be quite low in $(TMTSF)(Br)_{0.82}$ and $(TMTSF)(SCN)_{0.50}$. There are no short contacts between stacks, and van der Waals contacts (3.77 Å in the bromide) only occur between methyl groups (see Figure 3). TMTSF salts, including those with TCNQ, generally have longer interchain contacts than are observed for TTF and HMTSF, for example (4).

High disorder exists in both $(TMTSF)(Br)_{0.82}$ and $(TMTSF)(SCN)_{0.50}$. In the former, the bromide ion exhibits very high thermal parameters in the z direction. In the latter, the orientation of the thiocyanates is two-fold disordered. In both compounds, anion sites are not fully occupied, and a partially occupied small molecule (solvent) site exists in the x=0 plane.

The period of the modulation of the $(TMTSF)(SCN)_{0.50}$ structure is similar to the periods of incommensurate charge density waves observed in $K_2Pt(CN)_4Br_{0.30} \cdot xH_2O$, (TTF)(TCNQ), (TSeF)(TCNQ), (HMTSF)(TCNQ), and (HMTTF)(TCNQ) (12). It is not unreasonable to interpret the modulation of the SCN^- chain as a response to a charge density wave on the cation column.

While the electronic transport properties of $(TMTSF)(Br)_{0.82}$ and $(TMTSF)(SCN)_{0.50}$ are still being investigated, several predictions may be made on the basis of the structural properties. Exchange

of anions between sites cannot occur, so that some disorder will be retained at low temperature. Thiocyanate orientational disorder will also be retained, while the high thermal motion of the bromide ions should decrease. Disorder in $(TMTSF)(SCN)_{0.50}$ may be expected to result in retention of moderate conductivity to lower temperatures than in the bromide.

The 32.8 Å superperiod in $(TMTSF)(SCN)_{0.50}$ may be tentatively identified as a distortion resulting from an incommensurate charge density wave. If this is true, then $2k_F = .215\ c^*$, which implies that the average charge on each TMTSF is +0.43. This is reasonable in view of the uncertainty in the stoichiometry of this material, and the possibility of back-charge transfer ($SCN^- + TMTSF^+ \rightarrow SCN^0 + TMTSF^0$).

References

1. M. J. Cohen, L. B. Coleman, A. F. Garita, and A. J. Heeger, Phys. Rev., B10, 1298 (1974).
2. R. B. Somoano, A. Gupta, V. Hadek, M. Novotny, M. Jones, T. Datta, R. Deck, and A. M. Hermann, J. Chem. Phys., 63, 4970 (1973); R. B. Somoano, A. Gupta, V. Hadek, M. Novotny, M. Jones, T. Datta, R. Deck, and A. M. Hermann, Phys. Rev., B15, 595 (1977).
3. P. Delhaes, S. Flandrois, J. Amiell, G. Keryer, E. Toreilles, J. M. Fabre, L. Giral, C. S. Jacobsen, K. Bechgaard, Annals of the New York Academy of Sciences, 313, 467 (1978); K. Bechgaard, D. O. Cowan, and A. N. Bloch, J. Chem. Soc. Chem. Commun., 671 (1975); A. N. Bloch, D. O. Cowan, R. E. Pyle and R. H. Banks, Phys. Rev. Lett., 34, 1561 (1975).
4. T. J. Kistenmacher, Annals of the New York Academy of Sciences, 313, 333 (1978); K. Bechgaard, D. O. Cowan, and A. N. Bloch, Mol. Cryst. and Liq. Cryst., 32, 227 (1976).
5. P. J. L. Galigne, B. Liautaro, S. Peytavin, G. Brun, J. M. Fabre, E. Torreilles, and L. Giral, Acta. Cryst., B34, 620 (1978).
6. J. S. Miller, Science, 194, 189 (1976).
7. J. M. Williams and A. J. Schultz, Annals of the New York Academy of Sciences, 313, 509 (1978).

8. R. C. Wheland and J. L. Gillson, J. Am. Chem. Soc., 98, 3916 3926 (1976).

9. A. J. C. Wilson, X-ray Optics, Methuen, London (1949).

10. International Tables for X-Ray Crystallography, Vol. I, Kynoch Press, Birmingham, England (1952).

11. International Tables for X-ray Crystallography, Vol. III, Kynoch Press, Birmingham, England (1962) p. 202.

12. S. Megtert, J. P. Pouget, and R. Comes, Annals of the New York Academy of Sciences, 313, 234 (1978).

APPENDIX 1

Structure Factors Tables

The following tables contain the observed and calculated structure factors for refined and partly refined structures reported in this thesis. The heading above each group gives the indices for that group of reflections, with one index indicated by a letter. That index varies and is given in the first column. F_{obs} is given in the second column, F_{calc} in the third, and the standard deviation in the fourth. A negative sign on F_{obs} means that the observed intensity, $I \sim F^2_{obs}$, was negative.

A. $[Rh(CNCHCH_2)_4]ClO_4$ - Structure factors, room temperature data obtained with Ni-filtered CuKα radiation. Space group Immm.

	0 K 0		
2	2992	3018	16
4	3069	2963	33
6	1479	1253	11
8	2509	2591	20
10	1529	1422	11
12	1534	1517	11
14	989	1024	8
16	876	826	8
18	494	520	6
20	453	461	6
22	310	330	7
24	199	215	8
26	129	127	9
28	65	96	11
	0 K 1		
1	1710	2542	13
3	1716	1695	11
5	2009	1520	16
7	1223	1251	9
9	1625	1515	12
11	1446	1383	11
13	1212	1122	9
15	903	910	8
17	736	627	7
19	426	490	6
21	395	385	6
23	214	267	8
25	164	165	8
27	89	108	10
	0 K 2		
0	2977	3388	17
2	1593	1432	12
4	4008	3995	25
6	1315	1291	10
8	1761	1770	14
10	1320	1192	10
12	1154	1101	9
14	872	825	7
16	817	793	7
18	498	472	6
20	373	388	6
22	274	285	7
24	165	203	9

26	139	126	6
28	84	91	8
	0 K 3		
1	1657	1520	12
3	1303	1246	9
5	2131	2009	15
7	2173	2187	15
9	1502	1509	11
11	914	896	7
13	951	864	8
15	806	825	7
17	613	524	6
19	288	365	7
21	320	305	7
23	205	237	8
25	163	157	8
27	86	102	10
	0 K 4		
0	2345	2363	16
2	1029	1082	8
4	1828	1843	13
6	2024	1965	16
8	1661	1590	12
10	1131	1112	8
12	1026	1110	8
14	798	787	7
16	559	566	6
18	302	331	7
20	287	323	7
22	253	259	7
24	178	188	8
26	117	115	8
	0 K 5		
1	1594	1723	12
3	1403	1447	10
5	1355	1312	10
7	1285	1244	9
9	1234	1366	10
11	1167	1201	9
13	836	800	7
15	503	503	6
17	349	362	7
19	287	322	7
21	295	278	7

23	193	205	8
25	130	131	8
27	55	84	11
	0 K 6		
0	1717	1606	13
2	1300	1323	9
4	1153	1054	9
6	930	991	8
8	1166	1115	9
10	1096	1101	9
12	803	787	7
14	487	498	6
16	353	427	7
18	312	323	7
20	271	277	7
22	207	204	7
24	123	140	9
26	82	89	8
	0 K 7		
1	1091	1163	9
3	979	994	7
5	866	896	7
7	941	914	8
9	843	835	7
11	649	604	6
13	487	467	6
15	394	429	7
17	363	350	7
19	282	263	7
21	180	196	9
23	135	136	8
25	88	91	8
	0 K 8		
0	1066	1079	9
2	973	952	8
4	886	879	7
6	835	853	7
8	700	649	7
10	524	460	6
12	392	428	7
14	408	440	6
16	366	367	7
18	271	245	7
20	181	181	8

22	147	127	7
24	46	91	15
	0 K 9		
1	749	727	7
3	725	716	7
5	674	667	7
7	541	493	6
9	380	352	7
11	347	380	7
13	369	395	7
15	333	301	7
17	234	218	7
19	169	169	8
21	114	121	9
23	56	90	12
	0 K 10		
0	536	563	6
2	538	533	6
4	466	467	6
6	368	359	7
8	277	312	8
10	329	362	7
12	344	326	7
14	285	236	7
16	188	201	8
18	156	156	8
20	109	109	9
22	53	86	11
	0 K 11		
1	445	465	6
3	396	408	6
5	314	343	7
7	314	336	7
9	316	334	7
11	277	263	7
13	195	200	9
15	151	175	10
17	144	127	8
19	91	90	9
	0 K 12		
0	345	271	7
2	313	256	7

4	285	244	7
6	281	259	7
8	275	248	7
10	216	206	8
12	189	174	8
14	147	142	8
16	107	97	9
18	51	80	12
	0 K 13		
1	202	183	8
3	226	191	7
5	230	202	7
7	223	194	7
9	172	168	8
11	157	144	8
13	130	110	8
15	80	78	9
	0 K 14		
0	163	150	8
2	142	152	9
4	171	157	7
6	156	149	8
8	142	131	8
10	105	112	9
12	56	87	13
	0 K 15		
1	105	68	9
3	99	89	9
5	96	87	9
7	79	82	9
9	56	75	11
	1 K 0		
1	459	448	4
3	75	135	8
5	482	470	4
7	279	280	5
9	211	219	5
11	62	1	15
13	53	7	19
15	-29	42	32
17	112	67	14
19	69	49	21

21	41	2	29
23	49	7	24

1 K 1

0	434	433	4
2	1347	1292	10
4	647	656	5
6	926	627	7
8	120	64	8
10	303	335	5
12	161	172	8
14	100	140	13
16	124	97	12
18	81	70	19
20	23	45	39
22	-42	6	28
24	35	12	27

1 K 2

1	228	211	4
3	1054	1069	8
5	694	677	6
7	263	265	5
9	-14	46	33
11	93	102	11
13	18	68	35
15	36	42	29
17	143	114	11
19	47	65	28
21	-71	7	20
23	75	4	17

1 K 3

0	656	617	5
2	744	777	6
4	503	417	5
6	238	215	5
8	193	188	6
10	49	98	19
12	94	99	13
14	56	70	22
16	97	107	16
18	85	53	18
20	-31	39	34
22	46	5	25
24	-74	24	16

1 K 4

1	181	190	7
3	203	198	6
5	222	210	5
7	176	129	6
9	39	13	22
11	77	60	15
13	28	61	33
15	49	25	26
17	54	51	26
19	-38	37	30
21	38	15	29
23	41	15	25

1 K 5

0	347	335	5
2	358	159	5
4	-15	60	34
6	39	131	22
8	76	49	14
10	97	54	13
12	93	94	15
14	-70	61	20
16	55	6	25
18	51	7	25
20	-49	28	25
22	11	10	43

1 K 6

1	29	23	27
3	102	50	11
5	38	3	24
7	52	19	20
9	23	18	34
11	88	61	16
13	-20	10	41
15	78	12	20
17	18	32	43
19	69	38	20
21	65	17	19

1 K 7

0	16	9	37
2	56	82	19
4	50	50	22
6	65	105	19

8	-31	31	32
10	42	65	28
12	38	8	31
14	-39	15	32
16	-18	46	42
18	-46	37	27
20	-50	21	23

1 K 8

1	44	30	26
3	-59	1	21
5	-25	12	35
7	-66	6	20
9	28	39	37
11	-16	49	46
13	-44	11	29
15	49	54	26
17	86	44	17
19	50	25	23

1 K 9

0	50	34	25
2	80	56	18
4	33	61	33
6	51	63	26
8	-57	30	24
10	74	12	20
12	-7	37	51
14	80	45	18
16	59	33	21
18	-31	25	30

1 K 10

1	88	77	17
3	92	76	17
5	89	45	17
7	45	7	29
9	-45	14	28
11	42	36	28
13	59	25	22
15	38	19	28
17	25	25	31

1 K 11

0	48	11	28
2	67	3	21

4	13	15	46
6	-18	2	41
8	-42	7	28
10	46	22	25
12	72	10	17
14	-34	13	28

1 K 12

1	27	21	34
3	64	21	21
5	-59	26	21
7	46	32	25
9	-10	27	44
11	39	17	26

1 K 13

0	28	3	32
2	-56	11	21
4	-31	17	30
6	-54	29	20
8	82	22	14

2 K 0

0	575	579	5
2	440	422	5
4	2355	2094	16
6	84	207	12
8	528	467	5
10	-50	2	19
12	110	142	11
14	89	30	15
16	-38	73	30
18	136	112	13
20	46	25	27
22	-26	10	35
24	-44	2	23

2 K 1

1	458	454	4
3	915	773	7
5	161	166	7
7	196	220	6
9	224	178	5
11	108	55	11
13	39	21	26
15	45	15	26

17	25	69	37
19	140	72	12
21	17	12	42
23	47	0	24

2 K 2

0	2159	2128	15
2	781	727	6
4	556	460	5
6	381	362	4
8	162	156	7
10	143	188	8
12	92	83	13
14	97	80	14
16	-34	32	33
18	134	134	13
20	-30	16	34
22	-54	9	23
24	31	13	26

2 K 3

1	334	291	5
3	278	159	5
5	353	382	5
7	479	419	5
9	41	45	22
11	-59	68	19
13	56	46	21
15	71	96	21
17	52	58	26
19	49	42	26
21	-64	7	21
23	-19	13	37

2 K 4

0	608	629	5
2	100	77	11
4	-35	23	22
6	405	379	5
8	93	51	12
10	26	7	30
12	54	57	22
14	102	111	15
16	52	23	26
18	-61	43	23
20	-17	7	42
22	-34	17	30

2 K 5

1	202	138	6
3	-38	43	23
5	58	34	16
7	-22	94	32
9	94	84	13
11	159	204	10
13	-56	58	24
15	72	43	20
17	-5	5	54
19	53	29	24
21	47	17	25

2 K 6

0	159	182	8
2	40	112	24
4	63	57	18
6	81	70	15
8	5	88	45
10	151	148	10
12	27	3	37
14	70	27	21
16	50	6	27
18	-49	45	26
20	59	23	21

2 K 7

1	29	80	30
3	40	82	26
5	83	52	16
7	59	79	22
9	81	54	18
11	-55	11	26
13	60	11	25
15	34	34	33
17	83	50	17
19	-31	33	32

2 K 8

0	93	136	15
2	45	17	27
4	-31	5	33
6	71	81	20
8	66	4	21
10	54	75	27

12	71	32	22
14	-57	46	24
16	81	49	18
18	54	38	22

2 K 9

1	-58	55	24
3	-45	97	28
5	46	97	28
7	91	3	17
9	70	57	21
11	-28	3	36
13	52	54	25
15	86	40	17
17	40	31	26

2 K 10

0	79	36	20
2	71	93	22
4	100	51	16
6	56	10	25
8	56	4	24
10	33	40	33
12	78	37	18
14	-47	13	25
16	56	22	20

2 K 11

1	-32	13	33
3	-71	1	20
5	42	16	28
7	80	6	17
9	44	32	27
11	44	15	26
13	-34	6	28

2 K 12

0	21	14	38
2	12	18	44
4	-28	15	34
6	-34	33	30
8	-51	37	23
10	-30	18	30

1	-54	2	22
3	59	12	19
5	-53	24	21
7	-26	25	31

3 K 0

1	3349	3692	26
3	2006	1758	16
5	1151	1143	9
7	1+44	1389	11
9	1375	1424	10
11	1266	1185	10
13	980	978	8
15	864	764	7
17	509	535	6
19	444	419	6
21	283	334	7
23	208	231	8
25	133	141	8
27	80	94	9

3 K 1

0	2855	2664	17
2	2807	2635	18
4	1573	1457	11
6	1549	1409	11
8	1245	1194	10
10	1333	1291	10
12	942	916	8
14	927	943	8
16	589	585	7
18	487	493	6
20	347	346	6
22	248	279	7
24	153	173	9
26	96	114	9

3 K 2

1	1419	1385	10
3	1745	1641	12
5	1627	1650	12
7	1441	1347	11
9	1093	1140	8
11	1014	894	8
13	808	771	7
15	795	682	7
17	505	494	6

19	388	359	6
21	257	283	7
23	191	209	8
25	123	136	9
27	80	91	8

3 K 3

0	1230	1243	9
2	1424	1436	10
4	1521	1550	11
6	1691	1659	11
8	1333	1354	10
10	1014	996	8
12	735	703	7
14	759	781	7
16	532	513	6
18	353	387	7
20	257	270	7
22	224	236	6
24	162	163	8
26	95	108	9

3 K 4

1	1234	1257	10
3	1232	1198	10
5	1405	1409	10
7	1469	1418	11
9	1115	1148	9
11	904	885	8
13	724	734	7
15	604	545	6
17	312	351	7
19	263	275	7
21	228	246	8
23	185	192	7
25	115	126	8

3 K 5

0	1341	1427	15
2	1227	1297	10
4	1021	1049	8
6	1095	1042	9
8	1064	1101	8
10	990	1008	8
12	770	782	7
14	554	580	6
16	326	347	7

18	250	294	8
20	249	252	7
22	192	208	7
24	139	141	8
26	58	50	10

3 K 6

1	1119	1124	9
3	945	955	8
5	843	858	7
7	888	870	8
9	892	502	8
11	787	772	7
13	521	529	6
15	359	368	7
17	280	303	7
19	250	258	8
21	192	204	8
23	141	146	8
25	96	95	7

3 K 7

0	973	948	8
2	902	994	8
4	792	781	7
6	740	729	7
8	741	723	7
10	636	623	7
12	458	442	7
14	345	378	7
16	317	335	7
18	254	262	7
20	198	191	8
22	120	139	9
24	79	96	9

3 K 8

1	808	780	7
3	741	718	7
5	694	675	7
7	637	618	7
9	496	465	6
11	369	346	7
13	342	363	7
15	348	348	7
17	257	251	7
19	182	176	8

21	134	131	8	9	213	200	7	3	166	123	7	16	-58	0	24	10	-35	15	33
23	81	93	8	11	178	161	7	5	89	3	12	18	73	52	19	12	53	6	25
				13	140	134	8	7	49	106	20	20	65	18	19	14	38	21	30
	3 K	9		15	97	102	9	9	149	93	9					16	-45	33	26
				17	51	74	11	11	61	2	21		4 K	5					
0	646	604	7					13	58	24	24						4 K	9	
2	588	645	7		3 K	13		15	12	28	49	1	99	94	14				
4	585	560	7					17	70	57	21	3	66	16	19	1	-36	54	34
6	473	492	7	0	172	157	9	19	60	35	23	5	78	47	17	3	-23	41	41
8	379	344	7	2	194	159	8	21	44	0	26	7	69	85	20	5	-28	20	37
10	282	297	7	4	190	168	8					9	43	26	29	7	-40	14	30
12	324	338	7	6	187	169	7		4 K	2		11	27	21	38	9	-75	10	19
14	305	303	7	8	167	156	8					13	30	5	37	11	-53	8	24
16	242	216	7	10	145	131	8	0	104	123	11	15	-6	11	52	13	64	23	20
18	167	163	8	12	114	108	8	2	152	217	8	17	-77	21	19	15	37	31	26
20	112	124	9	14	87	81	7	4	34	18	25	19	49	21	24				
22	71	88	9					6	245	251	6						4 K	10	
					3 K	14		8	58	15	19		4 K	6					
	3 K	10						10	112	77	12					0	47	10	27
				1	128	122	8	12	41	11	28	0	119	157	13	2	-13	39	45
1	467	459	7	3	124	127	9	14	112	74	14	2	74	4	18	4	42	14	28
3	434	428	7	5	134	127	8	16	20	2	43	4	21	0	40	6	25	28	37
5	356	357	7	7	112	117	8	18	105	77	14	6	-38	82	31	8	68	10	20
7	285	298	7	9	97	102	8	20	-27	15	34	8	-8	4	51	10	57	5	22
9	274	288	7	11	80	85	7	22	57	11	20	10	-47	5	29	12	-46	18	25
11	283	296	7									12	-69	12	23				
13	246	237	8		3 K	15			4 K	3		14	42	17	29		4 K	11	
15	195	181	8									16	40	2	29				
17	144	153	8	0	71	81	10	1	95	119	13	18	-7	22	48	1	-59	5	22
19	112	113	8	2	83	61	8	3	174	163	8	20	-17	16	37	3	-27	12	35
				4	66	81	9	5	134	187	9					5	6	16	49
	3 K	11						7	108	40	12		4 K	7		7	66	7	19
					4 K	0		9	-34	30	30					9	-64	5	19
0	367	373	7					11	106	81	14	1	44	21	29	11	68	16	17
2	343	362	7	0	876	932	7	13	61	29	23	3	38	60	31				
4	292	304	7	2	60	89	15	15	78	11	19	5	47	43	28		4 K	12	
6	247	273	8	4	101	137	11	17	-42	55	29	7	-91	8	18				
8	259	275	7	6	61	153	17	19	54	50	23	9	34	5	35	0	32	3	30
10	247	250	7	8	402	351	5	21	-27	19	32	11	50	32	28	2	16	12	39
12	202	193	9	10	-38	4	27					13	63	12	22	4	-41	14	26
14	175	159	7	12	99	93	15		4 K	4		15	-7	8	50	6	-34	15	27
16	135	130	8	14	48	46	27					17	-57	27	22				
18	89	91	9	16	-29	17	36	0	344	378	5						5 K	0	
				18	98	68	16	2	45	29	24		4 K	8					
	3 K	12		20	-44	8	27	4	-41	88	25					1	365	352	5
				22	-26	5	33	6	59	66	21	0	-55	67	26	3	95	92	13
1	287	230	7					8	72	58	19	2	56	41	25	5	296	302	6
3	251	219	7		4 K	1		10	112	97	14	4	-28	25	38	7	260	201	7
5	233	217	8					12	49	34	27	6	-53	4	27	9	-88	76	16
7	236	221	7	1	85	13	12	14	-24	1	40	8	76	8	21	11	60	0	23

13	68	14	22
15	63	18	23
17	55	36	25
19	12	50	44
21	39	18	26

5 K 1

0	147	212	9
2	-35	94	27
4	108	123	12
6	241	178	7
8	-74	42	19
10	113	70	13
12	87	53	18
14	-51	54	28
16	81	51	18
18	75	44	18
20	76	41	17

5 K 2

1	126	133	11
3	279	298	6
5	355	308	6
7	-43	68	27
9	61	1	22
11	57	13	24
13	42	17	31
15	75	51	20
17	77	77	19
19	-53	47	23
21	-45	11	23

5 K 3

0	274	247	7
2	145	151	10
4	302	277	6
6	176	227	9
8	148	133	11
10	71	18	21
12	-22	42	41
14	-25	27	40
16	71	84	20
18	-41	32	28
20	-68	18	18

5 K 4

1	127	120	13
3	48	16	26
5	145	104	12
7	122	107	13
9	84	41	19
11	-86	53	19
13	57	72	26
15	94	38	16
17	7	15	49
19	14	11	41

5 K 5

0	92	12	17
2	75	58	20
4	56	17	25
6	-30	9	36
8	64	33	23
10	-37	94	35
12	95	105	17
14	60	3	23
16	-49	12	26
18	-53	1	23

5 K 6

1	69	26	22
3	56	17	25
5	60	23	25
7	61	13	24
9	77	76	21
11	71	82	22
13	-39	0	31
15	35	19	32
17	20	16	38

5 K 7

0	74	22	21
2	-35	0	35
4	77	28	21
6	52	19	28
8	56	47	26
10	77	22	20
12	-53	22	25
14	38	6	30
16	-50	38	24

5 K 8

1	64	20	24
3	63	42	24
5	-32	64	37
7	41	45	31
9	-65	24	22
11	32	46	34
13	11	12	46
15	23	47	35

5 K 9

0	-37	33	32
2	-51	31	27
4	29	70	37
6	33	38	33
8	39	25	30
10	73	27	18
12	-33	25	31

5 K 10

1	10	46	48
3	44	47	28
5	55	21	23
7	52	8	24
9	-42	6	26
11	56	30	20

5 K 11

0	42	24	27
2	31	15	16
4	57	3	21
6	47	1	23
8	-34	21	27

6 K 0

0	1714	1726	13
2	1325	1191	10
4	1084	1043	9
6	683	650	7
8	835	792	8
10	643	660	7
12	676	647	7
14	493	490	6
16	406	410	6
18	288	284	7
20	226	230	7
22	147	166	7

24	74	113	9

6 K 1

1	1228	1221	9
3	1013	960	8
5	823	773	7
7	731	731	7
9	742	685	7
11	585	604	10
13	578	529	6
15	425	436	6
17	352	326	6
19	231	246	7
21	179	191	7
23	98	136	9

6 K 2

0	1019	1071	12
2	829	797	10
4	932	931	11
6	754	772	10
8	818	748	10
10	552	537	9
12	559	522	7
14	437	418	6
16	369	358	7
18	251	246	7
20	186	199	7
22	150	149	7

6 K 3

1	695	691	10
3	745	770	10
5	824	837	10
7	769	778	10
9	677	633	7
11	512	504	7
13	491	423	6
15	356	348	7
17	254	258	8
19	175	194	8
21	162	158	7
23	105	122	7

6 K 4

0	738	741	7
2	671	677	7
4	786	757	7
6	709	722	7
8	729	709	7
10	552	568	7
12	498	469	6
14	366	349	7
16	244	272	8
18	182	189	8
20	152	164	8
22	111	125	8

6 K 5

1	675	699	7
3	626	626	7
5	616	614	7
7	610	645	7
9	611	599	7
11	498	492	6
13	385	380	7
15	259	272	7
17	191	196	6
19	146	165	8
21	126	143	8

6 K 6

0	646	668	7
2	584	591	7
4	535	538	7
6	517	521	7
8	530	511	7
10	475	461	6
12	379	383	7
14	271	273	7
16	192	209	8
18	156	170	8
20	137	144	7

6 K 7

1	550	541	7
3	493	499	7
5	461	451	7
7	437	417	7
9	390	386	7
11	314	325	7
13	264	256	7
15	209	214	8

17	178	181	7
19	136	139	7

6 K 8

0	467	467	7
2	454	440	7
4	432	405	6
6	384	354	7
8	307	306	7
10	278	253	7
12	222	221	8
14	208	210	7
16	152	132	8
18	121	132	7

6 K 9

1	371	364	7
3	345	339	7
5	315	298	7
7	258	249	7
9	224	205	8
11	197	190	8
13	177	190	8
15	171	163	6
17	113	119	7

6 K 10

0	278	291	7
2	266	274	7
4	229	245	8
6	207	209	8
8	188	190	8
10	178	171	7
12	152	164	8
14	119	135	8

6 K 11

1	215	211	7
3	197	196	7
5	158	176	8
7	159	162	8
9	150	155	8
11	140	139	7
13	104	110	7

6 K 12

0	160	146	7
2	154	143	7
4	144	139	8
6	137	136	7
8	125	131	7
10	52	115	8

6 K 13

1	101	100	8
3	106	103	7
5	87	105	8

7 K 0

1	160	124	12
3	-49	20	29
5	-37	12	34
7	79	80	21
9	80	76	19
11	46	24	28
13	70	5	20
15	-37	19	30
17	50	20	23

7 K 1

0	32	10	40
2	110	120	16
4	58	61	18
6	24	72	42
8	32	16	37
10	-36	47	33
12	-47	24	28
14	7	4	50
16	55	30	22

7 K 2

1	87	74	21
3	-50	35	31
5	-59	28	27
7	67	28	24
9	-42	25	31
11	49	33	27
13	-77	26	19
15	-59	16	22

7 K 3

0	68	58	26
2	21	8	46
4	86	73	20
6	-60	18	26
8	61	53	25
10	61	35	24
12	58	41	24
14	24	6	37
16	-32	17	30

7 K 4

1	71	38	25
3	-37	36	36
5	14	50	49
7	39	30	32
9	61	33	24
11	50	13	26
13	68	13	20
15	-42	2	26

7 K 5

0	56	64	28
2	67	38	24
4	64	36	25
6	19	43	44
8	69	30	22
10	36	13	33
12	20	20	40
14	53	10	22

7 K 6

1	61	35	25
3	82	1	20
5	25	32	40
7	53	21	34
9	51	14	26
11	-39	15	30
13	39	5	28

7 K 7

0	-39	4	32
2	67	1	22
4	45	14	29
6	81	6	19
8	34	11	32
10	53	4	23

7 K 8

1	36	18	31
3	57	13	23
5	-51	4	25
7	-94	10	15
9	74	13	17

7 K 9

0	-26	24	34
2	13	18	43
4	47	4	24

8 K 0

0	92	48	18
2	46	82	31
4	86	93	19
6	73	78	21
8	96	86	17
10	20	3	40
12	-46	19	27

8 K 1

1	65	62	26
3	77	33	21
5	40	13	32
7	36	37	33
9	26	22	37
11	-48	5	27
13	-20	2	38

8 K 2

0	101	70	19
2	-11	47	52
4	39	67	34
6	96	98	18
8	-28	10	38
10	16	14	43
12	-40	1	29

8 K 3

1	91	54	20
3	-8	58	55
5	116	120	15
7	105	83	16
9	-95	35	17
11	9	24	49

8 K 4

0	91	67	19
2	-46	8	31
4	-93	27	19
6	59	61	25
8	-69	44	22
10	40	48	30

8 K 5

1	-10	9	52
3	-60	14	26
5	20	8	43
7	51	15	27
9	-57	41	24

8 K 6

0	39	7	32
2	65	3	23
4	96	12	16
6	73	3	20
8	-62	19	22

8 K 7

1	-37	12	31
3	49	14	26
5	54	13	23

9 K 0

1	532	532	7
3	459	454	7
5	360	362	7
7	320	315	7
9	282	297	7
11	264	278	7
13	213	250	7
15	175	209	8

9 K 1

0	429	485	7

2	463	476	7	11	226	235	8					10	224	235	7	4	194	210	7
4	356	370	7	13	195	205	8	1	276	285	8	12	173	185	8	6	186	192	7
6	332	341	7	15	152	170	8	3	301	300	7					8	162	174	7
8	296	294	7					5	292	310	7		9 K	6		10	140	157	7
10	279	282	7		9 K	3		7	289	304	7								
12	228	244	7					9	249	273	7	1	242	268	7		9 K	8	
14	188	222	8	0	290	301	8	11	211	222	8	3	228	251	8				
16	135	172	8	2	334	321	7	13	175	172	8	5	229	243	7	1	181	200	7
				4	293	315	8					7	223	236	7	3	180	185	7
	9 K	2		6	312	329	7		9 K	5		9	184	214	8	5	156	161	7
				8	285	289	7					11	150	182	8	7	130	141	8
1	376	386	7	10	245	250	8	0	273	282	7								
3	359	353	7	12	202	199	8	2	267	284	7		9 K	7			9 K	9	
5	319	334	7	14	150	166	9	4	256	276	7								
7	313	315	7					6	274	283	7	0	227	238	7	0	145	165	6
9	279	274	7		9 K	4		8	255	271	7	2	232	230	6	2	139	156	7

B. $[Rh(CNCHCH_2)_4]ClO_4$ - Structure factors 22° K data obtained with graphite-monochromatized MoKᾱ radiation. Space group Immm.

	0 K 0		
2	3230	3426	25
4	3078	2669	23
6	1179	1161	17
8	2256	2363	20
10	1438	1309	18
12	1230	1578	21
14	889	895	27
16	762	773	33
18	525	559	47
20	481	485	49
22	390	308	59
24	168	230	117
	0 K 1		
1	3054	2567	23
3	1797	1610	15
5	2224	1793	19
7	1268	1448	17
9	1620	1376	18
11	1339	1511	20
13	1239	1106	21
15	848	803	30
17	729	604	39
19	359	516	67
21	524	371	46
23	245	260	90
	0 K 2		
0	2972	2415	22
2	1676	1547	15
4	3578	3403	27
6	1326	1442	17
8	1641	1637	18
10	1339	1161	19
12	979	1148	23
14	826	771	29
16	706	681	40
18	426	512	58
20	355	423	70
22	400	231	60
24	-144	214	132
	0 K 3		
1	1662	1514	17

3	1396	1231	17
5	1781	2080	18
7	2051	2066	20
9	1324	1464	19
11	891	934	23
13	923	836	26
15	727	706	34
17	575	531	48
19	232	443	95
21	440	320	54
23	290	235	81
	0 K 4		
0	1755	1552	18
2	1071	1224	17
4	1583	1436	17
6	1772	1982	19
8	1295	1278	19
10	1094	1084	21
12	880	972	26
14	754	738	32
16	412	480	61
18	359	393	68
20	233	326	92
22	317	236	74
24	417	178	56
	0 K 5		
1	1430	1664	18
3	1317	1256	18
5	1096	1336	18
7	1089	1019	19
9	991	1177	23
11	982	1013	26
13	715	677	34
15	488	458	52
17	325	374	77
19	400	334	64
21	291	242	77
23	177	184	116
	0 K 6		
0	1213	1364	19
2	1152	1409	19
4	846	867	23
6	867	979	23
8	987	895	24

10	933	938	27
12	466	617	54
14	444	533	51
16	-102	389	153
18	314	310	72
20	58	242	183
22	140	178	133
24	126	129	143
	0 K 7		
1	836	999	25
3	823	881	25
5	709	849	29
7	823	757	27
9	541	712	43
11	442	563	52
13	310	478	72
15	436	354	53
17	358	265	58
19	212	231	102
21	-226	164	99
23	-235	119	99
	0 K 8		
0	717	813	31
2	744	787	30
4	681	692	32
6	680	642	34
8	528	509	43
10	360	416	63
12	332	340	67
14	423	316	55
16	340	273	67
18	286	222	77
20	233	151	97
22	334	106	73
24	58	82	249
	0 K 9		
1	549	610	40
3	591	596	39
5	429	584	51
7	503	465	45
9	261	354	81
11	159	305	113
13	264	300	80
15	-135	250	130

17	-205	173	105
19	274	122	81
21	-252	98	136
23	-212	75	159
	0 K 10		
0	487	439	47
2	418	391	54
4	267	401	80
6	199	304	95
8	333	280	63
10	261	266	85
12	452	248	53
14	246	180	88
16	152	130	121
18	-358	109	71
20	-139	91	201
22	-446	64	104
24	227	45	160
	0 K 11		
1	303	298	70
3	56	275	182
5	178	243	110
7	255	226	79
9	218	226	93
11	199	175	100
13	307	132	73
15	122	110	139
17	312	99	75
19	338	72	114
21	346	51	110
23	145	39	203
	0 K 12		
0	212	212	99
2	330	193	69
4	475	201	48
6	189	188	102
8	280	188	79
10	-86	145	156
12	132	119	131
14	-230	99	99
16	187	75	162
18	-230	52	159
20	467	43	91
22	341	35	139

	0 K 13		
1	80	144	208
3	96	144	206
5	63	141	232
7	237	129	133
9	125	109	193
11	245	91	132
13	281	75	130
15	-204	54	163
17	-253	44	151
19	204	38	166
	0 K 14		
0	242	99	129
2	-156	101	172
4	326	97	105
6	284	90	119
8	245	78	136
10	256	67	128
12	147	55	197
14	287	43	132
16	385	37	109
18	-246	29	156
	1 K 0		
1	259	437	31
3	-187	213	35
5	590	734	23
7	231	174	44
9	204	256	54
11	-147	203	75
13	180	4	76
15	173	190	89
17	182	109	98
19	-277	64	77
21	-95	63	150
23	191	77	104
	1 K 1		
0	245	104	25
2	1229	654	12
4	665	323	18
6	605	694	23
8	178	111	56
10	73	203	107

12	245	198	53
14	116	32	109
16	135	245	115
18	99	92	143
20	-73	96	152
22	402	81	52
24	-295	76	78

1 K 2

1	236	275	31
3	600	993	17
5	492	503	24
7	65	377	98
9	-156	16	65
11	-105	148	89
13	129	51	98
15	-151	189	105
17	199	153	94
19	-264	79	90
21	-168	76	103
23	-163	74	112

1 K 3

0	695	911	18
2	399	586	28
4	352	372	33
6	293	200	34
8	-49	350	107
10	-195	8	57
12	-144	108	91
14	-26	32	182
16	141	166	113
18	-166	67	119
20	-282	67	72
22	254	67	80
24	138	63	127

1 K 4

1	169	165	51
3	190	121	50
5	-17	129	132
7	187	42	53
9	111	40	91
11	-152	9	85
13	175	83	87
15	93	92	136
17	-88	127	149
19	-252	59	86
21	149	76	116
23	341	59	67

1 K 5

0	273	233	37
2	200	76	51
4	150	55	60
6	-133	24	63
8	163	144	70
10	-244	67	57
12	86	99	138
14	99	31	130
16	250	84	87
18	191	43	104
20	-210	50	96
22	-173	52	115
24	-328	45	74

1 K 6

1	153	143	69
3	102	115	92
5	-107	137	94
7	-182	167	74
9	178	29	79
11	274	15	63
13	-130	54	120
15	124	17	134
17	92	58	154
19	-215	28	89
21	170	47	111
23	-117	35	138

1 K 7

0	251	62	52
2	120	44	90
4	99	33	104
6	-71	86	129
8	232	29	70
10	-246	15	75
12	103	0	140
14	148	8	118
16	160	43	104
18	167	39	107
20	-102	35	144
22	304	31	77
24	-178	27	171

1 K 8

1	178	109	81
3	-169	77	88
5	125	83	109
7	-66	31	149
9	147	31	105
11	110	47	139
13	-137	4	127
15	-271	34	76
17	-353	34	63
19	29	14	198
21	242	20	92
23	216	20	154

1 K 9

0	-269	147	68
2	-126	91	122
4	182	90	93
6	225	68	85
8	182	90	97
10	289	73	71
12	197	14	93
14	108	9	127
16	266	4	77
18	304	9	70
20	278	16	78
22	228	16	142
24	504	13	90

1 K 10

1	44	67	184
3	-61	47	164
5	167	69	108
7	168	54	100
9	-281	43	75
11	233	6	81
13	-179	16	102
15	102	5	141
17	-96	8	148
19	311	13	74
21	123	7	207
23	278	9	144

1 K 11

0	84	78	141
2	-231	53	82
4	150	61	115
6	91	35	170
8	129	23	119
10	116	11	128
12	-358	21	74
14	158	5	115
16	-195	0	105
18	126	1	204
20	306	0	130
22	-343	7	127
24	388	7	111

1 K 12

1	-150	67	111
3	164	61	106
5	179	59	103
7	-363	41	62
9	102	39	139
11	112	26	133
13	181	18	105
15	-266	9	87
17	323	9	109
19	133	2	205
21	276	4	145

1 K 13

0	-130	60	178
2	-114	53	181
4	-268	48	118
6	300	36	105
8	-310	31	112
10	-366	22	99
12	152	18	174
14	-193	13	165
16	246	8	143
18	187	0	178
20	160	0	195

1 K 14

1	234	42	132
3	-132	39	182
5	-196	34	151
7	183	29	157
9	-506	23	87
11	-107	18	207
13	144	13	189
15	252	7	145
17	262	4	143

2 K 0

0	702	524	16
2	500	371	22
4	1966	2019	16
6	-231	178	44
8	337	382	36
10	225	204	51
12	234	140	56
14	-124	173	112
16	-60	79	168
18	189	127	107
20	276	51	71
22	87	88	145
24	-322	63	77

2 K 1

1	482	344	24
3	764	830	18
5	-218	14	44
7	205	165	50
9	27	107	141
11	-242	19	55
13	-43	71	148
15	198	167	85
17	-80	148	159
19	250	51	79
21	80	78	151
23	81	76	153

2 K 2

0	1823	1804	17
2	644	734	19
4	520	450	21
6	379	359	28
8	-110	43	84
10	-157	230	76
12	-161	40	85
14	237	170	73
16	-200	142	93
18	-222	126	98
20	320	58	61
22	184	80	102
24	259	61	85

2 K 3

1	197	380	44
3	-5	160	140
5	207	83	49
7	315	340	39
9	6	121	163
11	-170	59	71
13	-61	82	145
15	-384	155	56
17	229	123	86
19	120	50	122
21	375	62	57
23	-331	61	70

2 K 4

0	456	426	23
2	64	120	88
4	76	104	90
6	301	280	39
8	76	133	110
10	110	10	100
12	-232	111	66
14	299	107	71
16	254	93	86
18	-210	64	95
20	72	55	156
22	161	63	113
24	166	52	115

2 K 5

1	211	173	52
3	86	31	87
5	57	141	116
7	146	102	78
9	-73	111	124
11	228	165	66
13	-63	77	148
15	278	33	79
17	170	72	109
19	191	38	93
21	211	53	93
23	-349	44	71

2 K 6

0	152	114	65
2	-122	153	85
4	83	103	100
6	-95	170	105
8	-123	95	103
10	194	28	82
12	-205	2	89
14	210	1	96
16	-178	52	108
18	-257	29	80
20	-343	36	66
22	-159	40	120
24	210	34	153

2 K 7

1	84	40	114
3	-59	9	131
5	-296	52	56
7	182	29	91
9	-87	46	145
11	-244	27	79
13	-157	18	107
15	-256	19	84
17	204	36	88
19	135	33	124
21	-211	36	98
23	-268	25	137

2 K 8

0	246	128	69
2	100	108	120
4	-231	49	74
6	-186	37	86
8	-218	15	93
10	131	40	129
12	170	19	98
14	60	6	167
16	-146	35	117
18	-136	34	122
20	-178	17	110
22	221	17	138
24	242	19	145

2 K 9

1	-70	84	143
3	88	65	140
5	95	62	134
7	-115	65	136
9	-243	108	87
11	269	60	68
13	-197	5	103
15	171	30	105
17	-246	13	85
19	-104	4	147
21	-107	14	210
23	-203	17	162

2 K 10

0	-101	60	134
2	-42	37	169
4	56	55	137
6	69	58	158
8	229	76	77
10	80	21	153
12	203	6	89
14	-175	1	109
16	323	11	70
18	210	5	99
20	-81	15	230
22	-555	11	90
24	44	7	271

2 K 11

1	185	43	89
3	-177	46	96
5	165	60	100
7	-72	37	154
9	94	13	134
11	214	6	91
13	120	25	127
15	217	6	94
17	441	7	81
19	-154	5	186
21	-433	0	111
23	490	5	87

2 K 12

0	-157	66	105
2	-152	56	110
4	180	63	99
6	-214	39	87
8	-139	34	120
10	201	30	93
12	139	26	120
14	307	5	71
16	398	4	100
18	303	7	128
20	168	0	206
22	134	6	214

2 K 13

1	-283	56	113
3	-172	50	158
5	52	38	231
7	177	29	151
9	-483	27	82
11	-409	17	95
13	-552	11	81
15	332	13	120
17	260	8	138
19	176	2	177

2 K 14

0	-471	42	87
2	-207	40	146
4	128	33	184
6	-124	27	184
8	251	23	123
10	398	17	95
12	83	15	224
14	-127	12	214
16	373	4	108
18	-224	0	171

3 K 0

1	3524	3590	27
3	1729	1756	17
5	1057	1175	17
7	1330	1261	18
9	1200	1369	20
11	1113	1190	23
13	930	984	27
15	805	655	36
17	452	518	59
19	469	436	55
21	347	321	66
23	76	219	173

3 K 1

0	2751	2685	22
2	2488	2425	21
4	1326	1330	17
6	1346	1401	18
8	887	1045	30
10	1128	1230	21
12	825	930	29
14	771	831	37
16	573	515	48
18	395	467	66
20	407	353	57
22	67	261	171
24	-43	179	200

3 K 2

1	1281	1166	17
3	1542	1456	18
5	1448	1622	18
7	1308	1335	19
9	999	1133	20
11	940	877	25
13	691	769	38
15	762	580	37
17	439	467	60
19	408	352	61
21	315	287	72
23	325	205	73

3 K 3

0	1086	941	17
2	1245	1360	17
4	1307	1359	18
6	1367	1680	20
8	1118	1170	22
10	901	570	24
12	689	705	33
14	642	671	43
16	470	464	57
18	248	408	92
20	490	307	49
22	309	227	77
24	153	163	130

3 K 4

1	1097	1137	19
3	1055	1086	18
5	1200	1336	20
7	1099	1268	22
9	890	1036	25
11	762	808	33

13	613	644	44
15	481	464	55
17	228	344	95
19	227	306	92
21	-288	229	84
23	257	175	89

3 K 5

0	1134	1290	20
2	981	1176	21
4	843	623	22
6	851	993	25
8	881	847	26
10	753	844	33
12	637	635	40
14	455	492	57
16	263	332	83
18	269	292	80
20	220	236	98
22	323	177	64

3 K 6

1	869	1057	24
3	810	894	27
5	705	819	29
7	588	736	38
9	737	716	33
11	545	650	45
13	440	477	59
15	419	349	57
17	-79	266	162
19	-65	236	174
21	203	172	105

3 K 7

0	743	636	30
2	640	605	33
4	664	670	36
6	592	588	42
8	610	554	43
10	555	543	47
12	413	392	60
14	221	316	96
16	282	261	77
18	-207	220	102
20	-154	162	130

3 K 8

1	585	622	43
3	606	558	42
5	482	534	55
7	485	500	53
9	404	382	61
11	373	279	61
13	261	271	65
15	344	268	68
17	120	199	140
19	-334	145	76

3 K 9

0	281	533	88
2	439	480	57
4	509	495	50
6	218	417	104
8	266	303	84
10	150	246	123
12	1050	274	31
14	-95	234	150
16	202	158	106
18	277	120	84
20	283	98	130

3 K 10

1	412	333	58
3	113	317	145
5	233	286	91
7	283	230	77
9	334	232	63
11	318	225	73
13	-173	163	119
15	-62	118	177
17	76	112	167
19	290	86	89
21	-194	59	178

3 K 11

0	87	253	162
2	-112	221	134
4	155	217	115
6	-156	188	115
8	215	197	93
10	-85	162	159
12	189	123	108
14	-283	107	87
16	341	96	71
18	285	61	86
20	267	46	145

3 K 12

1	301	166	72
3	233	160	89
5	365	163	63
7	285	156	80
9	143	136	124
11	-180	109	116
13	-58	96	184
15	349	66	74
17	-263	44	101
19	-85	43	180
21	415	38	114

3 K 13

0	282	117	77
2	395	115	57
4	-34	118	200
6	47	111	187
8	163	100	119
10	119	84	148
12	-283	68	90
14	-197	46	117
16	-313	42	90
18	320	40	91

3 K 14

1	212	82	100
3	97	82	157
5	231	78	99
7	-302	71	87
9	105	60	160
11	-349	49	84
13	311	40	67
15	229	36	108
17	-215	28	124

4 K 0

0	761	1018	20
2	201	173	51
4	162	262	66
6	135	104	79
8	304	311	49
10	223	118	69
12	135	30	109
14	86	182	143
16	-298	90	72
18	-281	89	71
20	217	31	90
22	285	63	80
24	271	52	85

4 K 1

1	62	12	105
3	284	242	41
5	-93	101	97
7	116	18	93
9	-203	3	73
11	253	72	66
13	-200	90	90
15	308	162	64
17	-207	104	90
19	237	61	82
21	297	52	77
23	61	59	171

4 K 2

0	200	250	57
2	-90	272	97
4	-122	1	85
6	162	345	75
8	-154	106	85
10	149	170	97
12	204	11	81
14	217	129	86
16	297	93	69
18	-207	90	89
20	121	48	129
22	298	62	74
24	226	50	97

4 K 3

1	-80	225	102
3	-161	146	74
5	125	155	87
7	159	85	82
9	-240	87	69
11	-105	35	126
13	-229	36	86
15	182	76	98
17	94	52	136
19	-146	58	122
21	-262	57	83
23	-344	51	71

4 K 4

0	273	303	49
2	168	30	68
4	-36	87	140
6	-120	50	93
8	116	125	110
10	-133	78	113
12	-259	0	77
14	-25	40	193
16	133	80	114
18	205	63	91
20	123	50	129
22	-167	50	116

4 K 5

1	178	71	74
3	141	11	87
5	-163	17	84
7	-161	19	93
9	192	17	88
11	-128	31	118
13	-234	50	84
15	-154	58	104
17	238	65	78
19	-187	37	106
21	308	45	71

4 K 6

0	-138	65	99
2	-276	38	61
4	-134	1	100
6	-151	69	98
8	-96	60	134
10	298	38	66
12	252	33	78
14	171	22	99
16	114	40	127
18	269	32	86
20	-311	32	76

4 K 7

1	-121	36	124
3	125	3	121
5	99	52	136
7	151	60	118
9	-255	13	80
11	-286	0	72
13	-306	11	67
15	-282	29	77
17	30	39	191
19	-247	21	91

4 K 8

0	233	51	83
2	136	61	123
4	175	49	103
6	244	55	84
8	197	37	89
10	-207	30	87
12	-81	5	140
14	306	25	68
16	251	23	82
18	-77	14	166

4 K 9

1	-175	72	109
3	94	54	175
5	-184	64	107
7	-216	51	92
9	135	31	112
11	66	2	156
13	-159	4	112
15	211	2	97
17	-306	9	78

4 K 10

0	-339	72	66
2	-306	58	70
4	-273	52	82
6	-180	23	97
8	-141	9	112
10	52	9	175
12	288	21	71
14	-252	2	86
16	117	12	139

4 K 11

1	164	52	99
3	112	38	127
5	204	23	92
7	-385	11	61
9	-102	24	137
11	257	11	78
13	-175	0	115

4 K 12

0	236	56	83
2	-325	46	69
4	128	40	127
6	-276	28	78
8	-166	27	111
10	-216	11	99

4 K 13

1	-470	36	89
3	250	34	130
5	-160	30	174
7	147	24	179

5 K 0

1	314	380	43
3	194	71	66
5	334	306	46
7	90	171	116
9	-51	49	144
11	-298	26	61
13	-107	10	132
15	-298	94	72
17	-253	90	82
19	238	68	86
21	-177	54	114
23	296	52	77

5 K 1

0	-185	141	66
2	-161	40	76
4	-205	133	67
6	206	141	71
8	-189	47	76
10	-206	14	78
12	255	69	70
14	-159	45	109
16	125	130	117
18	-38	67	181
20	-243	61	90
22	269	48	81

5 K 2

1	121	119	92
3	-52	351	138
5	210	288	73
7	199	88	73
9	135	22	105
11	-216	24	81
13	151	51	114
15	-248	128	76
17	148	101	110
19	54	54	174
21	-213	44	99

5 K 3

0	180	295	78
2	222	136	67
4	206	265	75
6	-63	128	137
8	196	125	78
10	318	18	57
12	142	43	110
14	-186	74	99
16	164	109	110
18	-65	46	159
20	181	37	104
22	214	40	99

5 K 4

1	42	136	151
3	170	45	87
5	121	52	113
7	185	84	81
9	219	65	77
11	80	67	142
13	36	88	184
15	-224	76	84
17	162	52	110
19	-163	26	116
21	-203	36	105

5 K 5

0	165	12	89
2	215	92	74
4	326	29	55
6	100	32	120
8	-63	69	148
10	-41	83	169
12	165	87	95
14	145	31	113
16	100	34	145
18	66	25	167
20	-291	32	77

5 K 6

1	-290	58	64
3	-112	37	117
5	134	53	110
7	-140	35	106
9	-186	52	88
11	-240	42	73
13	-173	10	101
15	259	4	81
17	239	28	88
19	-156	26	117

5 K 7

0	-299	63	67
2	-145	33	111
4	154	4	108
6	-56	20	159
8	134	35	115
10	52	12	163
12	-138	17	118
14	-352	5	66
16	224	28	90
18	-153	29	123

5 K 8

1	140	35	113
3	18	17	190
5	186	1	93
7	127	5	116
9	-147	36	109
11	-165	60	108
13	100	6	140
15	-90	29	151
17	133	28	129

5 K 9

0	-264	56	71
2	-234	35	77
4	188	26	90
6	-133	27	117
8	-101	74	133
10	63	58	163
12	-257	0	84
14	146	18	119
16	245	8	89

5 K 10

1	286	9	66
3	333	13	59
5	275	41	73
7	-265	56	79
9	180	27	101
11	-200	7	98
13	-247	3	86

5 K 11

0	114	20	133
2	243	16	82
4	-190	40	102
6	-41	33	182
8	142	16	118
10	118	5	138
12	-405	15	63

5 K 12

1	-28	39	195
3	139	38	122
5	-103	32	146
7	-102	18	144

6 K 0

0	1534	1652	22
2	1124	1071	23
4	898	888	26
6	571	517	36
8	688	706	34
10	495	582	45
12	529	638	43
14	432	411	51
16	418	338	53

18	397	254	58
20	227	216	93

6 K 1

1	1085	1091	23
3	883	774	26
5	684	644	31
7	661	613	34
9	641	581	38
11	525	563	43
13	456	476	50
15	499	346	44
17	314	285	68
19	197	235	103
21	220	179	103

6 K 2

0	853	667	26
2	776	635	28
4	757	803	30
6	614	692	36
8	732	669	32
10	566	483	40
12	496	484	46
14	410	345	52
16	392	297	54
18	245	237	85
20	238	197	77

6 K 3

1	695	551	30
3	703	635	31
5	706	776	33
7	662	736	37
9	635	577	38
11	458	468	49
13	479	371	47
15	277	286	74
17	202	234	98
19	384	198	76

6 K 4

0	594	624	35
2	657	599	34
4	668	612	35
6	643	645	38
8	633	577	38
10	468	463	48
12	501	380	44
14	337	287	64
16	263	220	75
18	154	186	117
20	162	157	119

6 K 5

1	634	601	35
3	526	518	42
5	499	504	44
7	577	510	40
9	471	454	48
11	489	396	48
13	277	301	77
15	225	215	87
17	181	167	105
19	368	151	64

6 K 6

0	448	547	48
2	512	526	42
4	380	418	58
6	477	405	48
8	408	366	54
10	433	361	51
12	412	293	52
14	166	219	109
16	223	166	92
18	260	146	83
20	249	118	128

6 K 7

1	448	442	50
3	426	384	51
5	427	332	53
7	319	306	66
9	428	277	49
11	381	236	57
13	14	189	207
15	-199	165	104
17	-131	140	131
19	462	112	78

6 K 8

0	331	344	67
2	347	334	64
4	363	300	60
6	386	272	57
8	364	222	58
10	365	182	59
12	182	166	102
14	189	158	103
16	271	129	84
18	359	99	88
20	-147	73	174

6 K 9

1	296	272	74
3	251	258	82
5	230	228	92
7	220	183	89
9	234	155	86
11	336	147	63
13	266	138	83
15	215	110	135
17	258	86	117
19	124	65	190

6 K 10

0	306	193	73
2	229	179	90
4	230	166	92
6	159	142	107
8	302	136	67
10	186	122	103
12	322	108	73
14	-270	89	119
16	-400	72	94
18	0	52	289
20	445	39	85

6 K 11

1	195	121	100
3	-236	116	92
5	204	115	105
7	-293	111	80

6 K 12

0	-107	90	151
2	240	87	90
4	330	92	109

7 K 0

1	298	104	59
3	215	98	77
5	280	32	64
7	-282	53	66
9	144	34	97
11	229	29	74
13	113	63	132
15	-244	101	86
17	265	56	82
19	232	26	92

7 K 1

0	-301	48	61
2	265	71	66
4	222	96	80
6	-125	27	109
8	-221	47	78
10	-179	21	92
12	-160	72	101
14	-115	74	135
16	-88	82	152
18	-136	33	132

7 K 2

1	190	70	85
3	-247	53	70
5	212	69	80
7	159	87	98
9	200	80	83
11	-130	59	109
13	-171	41	103
15	-164	61	113
17	236	48	88
19	283	34	77

7 K 3

0	-144	2	104
2	207	24	83
4	219	74	80
6	63	50	144
8	88	85	139
10	123	44	114
12	-329	18	65
14	-203	13	96
16	-312	46	76
18	223	35	91

7 K 4

1	-30	62	171
3	183	44	89
5	-221	72	81
7	58	45	151
9	191	54	89
11	214	6	85
13	320	3	67
15	215	32	96
17	283	44	80

7 K 5

0	-174	33	90
2	103	5	123
4	166	61	94
6	-149	25	103
8	250	15	74
10	-331	20	59
12	130	9	118
14	274	24	78
16	-143	44	127

7 K 6

1	-159	13	97
3	100	15	121
5	296	11	59
7	-236	23	76
9	-160	33	103
11	169	20	103
13	233	24	89
15	283	33	80

7 K 7

0	-289	27	69
2	99	14	135
4	-205	1	91
6	237	26	80
8	338	32	62
10	286	6	75
12	195	23	103
14	122	26	143

7 K 8			
1	-114	2	134
3	-171	11	105
5	252	34	82
7	149	39	118
9	-191	4	103
11	-242	14	92
13	-346	13	73
7 K 9			
0	256	35	80
2	-309	33	72
4	-45	36	179
6	-195	24	100
8	231	0	86
10	-257	9	89
7 K 10			
1	-172	39	109
3	-268	27	80
5	175	10	111
7	-114	6	142
8 K 0			
0	-99	78	121
2	217	115	76
4	151	88	97
6	-84	56	133
8	-255	59	70
10	244	33	74
12	53	5	169
14	346	47	66
16	-195	47	109
8 K 1			
1	-364	73	52
3	-147	68	99
5	-232	15	73
7	-265	9	68
9	246	16	75
11	210	15	86
13	63	27	173
15	345	58	64
8 K 2			
0	-66	105	136
2	100	47	120
4	-103	104	121
6	187	107	87
8	-193	14	89
10	176	21	100
12	-209	3	93
14	163	60	117
16	126	58	141
8 K 3			
1	118	82	114
3	82	57	136
5	382	109	50
7	230	53	75
9	232	22	81
11	-179	8	98
13	161	38	118
15	-396	58	62
8 K 4			
0	-114	73	122
2	192	38	89
4	-156	21	105
6	-221	40	86
8	222	46	84
10	383	46	57
12	-146	43	112
14	-202	46	102
8 K 5			
1	144	14	105
3	23	16	182
5	-148	8	109
7	65	13	155
9	251	50	77
11	156	49	111
13	335	31	72
8 K 6			
0	188	3	94
2	195	15	89
4	91	4	135
6	106	4	129
8	168	32	106
10	-271	37	74
12	-99	13	145
8 K 7			
1	-179	13	104
3	81	1	155
5	130	14	125
7	191	20	102
9	103	16	149
11	-369	7	69
8 K 8			
0	-249	11	88
2	349	2	60
4	-246	14	88
6	93	9	153
8	339	11	70
8 K 9			
1	-258	3	90
3	-149	0	125
9 K 0			
1	565	438	42
3	440	331	51
5	307	233	67
7	357	210	63
9	391	223	56
11	191	235	107
13	365	208	64
15	604	149	62
17	213	118	156
19	-80	96	223
21	280	74	124
9 K 1			
0	545	395	46
2	496	366	50
4	366	246	65
6	458	238	51
8	304	212	75
10	311	225	77
12	415	206	63
14	-266	167	98
16	211	123	142
18	-158	106	171
20	100	84	211
9 K 2			
1	400	279	58
3	425	238	53
5	450	250	52
7	349	259	72
9	400	225	60
11	344	199	71
13	278	163	89
15	264	121	122
17	228	104	141
19	-268	89	137
9 K 3			
0	459	218	53
2	376	230	64
4	254	239	89
6	354	282	69
8	366	250	65
10	257	211	93
12	279	163	89
14	372	122	94
16	-233	95	140
18	408	86	90
20	-201	72	165
9 K 4			
1	339	219	69
3	340	228	72
5	421	238	57
7	337	241	75
9	398	207	65
11	356	168	72
13	382	124	67
15	269	92	117
17	203	78	154
19	327	71	111
9 K 5			
0	259	218	93
2	343	217	72
4	262	194	89
6	243	199	100
8	415	185	65
10	382	160	69
12	-165	128	135
14	429	56	86
16	-405	73	93
18	-326	66	110
9 K 6			
1	277	205	88
3	423	179	59
5	299	159	83
7	300	151	84
9	252	130	99
11	0	118	288
13	393	55	90
15	-281	74	124
17	-182	63	173
9 K 7			
0	-216	177	100
2	344	165	73
4	195	138	112
6	295	120	87
8	-221	100	109
10	54	52	228
12	318	83	112
14	179	71	165
16	-306	63	122
9 K 8			
1	223	140	110
3	-58	125	194
5	-232	103	133
7	201	86	142
9	-122	75	189
11	176	70	157
13	267	65	128
15	329	60	113
9 K 9			
0	-119	111	187
2	432	104	80
4	-54	88	236
6	218	72	138
8	419	65	87
10	-239	59	138
12	222	59	146

9 K 10

1	134	71	174
3	416	58	92
7	232	54	132
9	379	52	96
11	323	50	114

9 K 11

0	-218	44	147
2	159	43	167
4	-264	45	127
6	-385	46	100
8	323	46	106

10 K 0

0	241	79	87
2	-75	0	160
4	316	39	65
6	-227	31	92
8	-52	12	214
10	183	7	142
12	-297	19	114
14	-166	49	158
16	-328	36	105
18	-411	15	102

10 K 1

1	161	17	108
3	-119	28	137
5	-248	35	87
7	365	15	85
9	-415	14	84
11	252	21	121
13	286	33	114
15	240	39	132
17	-339	22	110

10 K 2

0	234	16	93
2	182	27	101
4	-343	14	73
6	-339	28	91
8	-203	32	134
10	322	39	100
12	-291	19	112
14	-79	23	218
16	404	19	91

10 K 3

1	282	15	81
3	203	16	103
5	260	21	115
7	339	31	90
9	194	38	142
11	-55	16	229
13	-158	2	165
15	344	9	105
17	241	16	137

10 K 4

0	137	15	159
2	156	4	150
4	175	30	149
6	-342	31	98
8	-476	24	81
10	191	8	144
12	327	7	107
14	206	3	143
16	-58	16	235

10 K 5

0	-153	9	167
2	-539	15	72
4	-475	23	85
6	214	5	141
8	262	14	119
10	289	17	116
12	335	1	104
14	336	18	108

10 K 6

0	-369	18	108
2	-81	14	224

10 K 7

1	-144	19	170
3	-258	10	121
5	-176	4	153
7	238	17	126
9	-220	10	141
11	317	6	107
13	-59	18	247

10 K 8

0	-146	10	169
2	381	2	89
4	280	11	123
6	-300	18	116
8	269	6	127
10	240	10	135

10 K 9

1	149	10	173
3	-205	13	146
5	140	11	172
7	-192	0	164

10 K 10

1	53	42	227
3	-274	21	116
5	187	11	144
7	-95	16	202
9	-223	1	134
11	-150	8	172
13	-82	13	226

11 K 1

0	200	27	142
2	-92	23	190
4	132	22	169
6	-402	0	90
8	-376	3	99
10	-283	4	122
12	305	9	111

11 K 2

1	-187	7	151
3	-76	26	211
5	314	43	102
7	415	25	88
9	187	7	150
11	230	2	138
13	-352	14	110

11 K 3

0	-368	32	96
2	-304	7	109
4	440	38	83
6	124	36	181
8	-160	19	172
10	237	6	133
12	-203	11	158

11 K 4

1	199	18	149
3	-489	5	80
5	264	18	126
7	-411	17	91
9	-216	19	151
11	-212	18	148

11 K 5

0	329	1	104
2	139	2	180
4	323	1	106
6	-295	4	120
8	286	18	119
10	-144	23	189

11 K 6

1	-302	2	123
3	-58	1	244
5	-452	5	94
7	-186	13	157

11 K 7

0	-164	0	174
2	165	2	175
4	420	10	93

12 K 0

0	259	121	100
2	-147	103	143
4	258	81	101
6	515	59	83

12 K 1

1	467	105	63
3	324	81	80
5	356	65	106

12 K 2

0	322	89	85
2	235	73	109
4	352	62	77

12 K 3

1	545	69	71

C. $(TTF)Cl_{0.67}$ - Structure factors, room temperature $P4_2/mnm$ phase. Ni-filtered CuK$\bar{\alpha}$ radiation.

H 0 0

2	515	372
4	1334	1256
6	880	887
8	25	1
10	282	273
12	24	19
14	8	3

H 0 1

1	1606	1551
3	40	35
5	1135	1108
7	54	59
9	115	102
11	136	132
13	48	49

H 0 2

0	1441	1437
2	44	44
4	498	512
6	422	415
8	59	52
10	151	141
12	14	2

H 0 3

1	421	453
3	49	12
5	403	384
7	34	17
9	38	35

H 0 4

0	296	333
2	30	50
4	131	138
6	131	108

H 1 0

1	671	745
2	642	610
3	710	629
4	40	25
5	737	693
6	237	232
7	304	308
8	170	178
9	19	38
10	105	103
11	86	77
12	42	38
13	101	104
14	29	34

H 1 1

1	709	690
2	272	281
3	-8	5
4	506	490
5	143	147
6	319	312
7	165	170
8	227	228
9	145	143
10	176	163
11	44	38
12	50	47
13	39	42

H 1 2

1	462	484
2	229	221
3	152	158
4	22	6
5	482	475
6	138	132
7	124	117
8	113	106
9	28	7
10	71	63
11	65	62
12	24	24

H 1 3

1	126	132
2	65	70
3	39	14
4	153	150
5	68	57
6	129	116
7	80	61
8	103	91
9	61	54
10	58	59

H 1 4

1	103	90
2	41	42
3	33	51
4	21	7
5	148	98
6	49	33

H 2 0

2	528	596
3	111	105
4	31	10
5	347	331
6	31	18
7	126	122
8	508	482
9	96	101
10	121	127
11	44	42
12	131	122
13	29	31
14	43	39

H 2 1

2	219	201
3	763	756
4	92	88
5	138	128
6	249	229
7	515	499
8	70	74
9	156	154
10	71	72
11	26	21
12	34	31
13	137	134

H 2 2

2	482	476
3	46	25
4	140	137
5	173	163
6	78	77
7	87	79
8	362	341
9	65	62
10	55	51
11	30	27
12	89	88

H 2 3

2	67	63
3	277	263
4	24	26
5	52	49
6	104	85
7	207	186
8	42	32
9	65	63
10	30	27

H 2 4

1	78	87
3	29	2
4	42	13
5	52	39
6	32	5

H 3 0

3	1446	1339
4	84	64
5	76	74
6	139	123
7	556	572
8	87	91
9	249	262
10	24	36
11	23	0
12	15	1
13	144	149

H 3 1

3	88	82
4	464	449
5	151	146
6	36	31
7	12	14
8	497	495
9	76	74
10	66	62
11	24	0
12	122	120
13	27	24

H 3 2

3	625	586
4	29	14
5	43	44
6	79	68
7	303	293
8	55	51
9	136	131
10	24	21
11	17	11
12	17	1

H 3 3

2	281	263
3	25	21
4	163	141
5	52	43
6	32	16
7	15	2
8	191	190
9	29	26
10	21	20

H 3 4

3	136	147
4	25	5
5	16	1
6	-16	20

H 4 0

4	152	156
5	93	100
6	488	498
7	37	31
8	231	221
9	136	143
10	185	182

11	26	19	3
12	42	40	1
13	55	53	1

H 4 1

4	121	93	1
5	466	463	3
6	30	17	5
7	102	93	2
8	59	61	3
9	35	40	5
10	78	82	1
11	80	79	1
12	18	15	2
13	64	66	1

H 4 2

4	17	14	5
5	58	52	2
6	233	224	2
7	24	19	4
8	172	171	1
9	93	86	1
10	97	93	1
11	8	12	4
12	30	34	1

H 4 3

4	39	27	4
5	177	168	2
6	36	11	3
7	40	39	3
8	30	20	1
9	23	16	2

H 4 4

4	35	22	4
5	-8	5	7

H 5 0

4	93	100	2
5	701	675	5
6	110	112	1
7	12	7	6
8	65	65	1
9	101	90	1
10	36	34	2
11	125	118	1
12	24	15	1
13	32	36	1

H 5 1

5	92	88	1
6	435	431	3
7	171	169	2
8	47	43	4
9	53	51	3
10	206	198	2
11	25	22	3
12	8	5	4

H 5 2

5	472	465	3
6	82	73	1
7	36	36	3
8	48	40	2
9	76	76	1

H 5 3

5	30	19	3
6	161	162	2
7	72	67	1
8	20	16	2
9	23	17	2

H 6 0

6	251	260	2
7	253	259	2
8	36	29	2
9	16	15	4
10	182	183	2
11	81	81	1
12	13	4	2

H 6 1

6	243	242	2
7	77	74	3
8	90	94	2
9	86	87	1
10	38	43	2
11	81	81	1
12	49	49	1

H 6 2

6	119	121	2
7	164	161	2
8	45	43	2
9	15	11	4

H 6 3

6	99	98	1
7	20	26	2
8	38	40	1

H 7 0

7	265	267	2
8	27	22	3
9	63	62	1
10	55	53	1
11	16	9	2
12	48	45	1

H 7 1

7	130	135	1
8	163	162	1
9	21	3	3
10	35	36	1
11	63	63	1

H 7 2

7	137	137	1
8	23	17	3
9	30	23	1
10	37	33	1

H 7 3

7	54	56	1
8	58	62	1

10	99	101	1
11	50	51	1

H 8 0

8	179	174	2
9	39	38	2
10	20	15	1
11	15	10	2

H 8 1

8	38	38	2
9	85	83	1
10	-2	2	7
11	17	9	1

H 8 2

8	120	123	1
9	25	23	1

H 9 0

9	26	29	1
10	45	45	1

H 9 1

9	52	53	1
10	60	57	1

H 9 2

9	8	7	6

H 10 0

10	117	109	1

D. (1.d.)$(TTT)_2I_3$ - Structure factors Cmca subcell. Ni-filtered CuK$\bar{\alpha}$ radiation.

	H 0 0		
2	1109	867	8
4	1849	1670	19
6	1346	1147	14
8	317	390	7
10	2187	2183	22
12	1868	1976	20
14	1607	1631	18
16	549	433	11
18	264	242	12
20	180	138	12
22	262	254	8
	H 0 2		
0	261	422	9
6	2840	2836	28
8	2600	2648	27
10	1059	966	12
12	351	215	8
14	413	335	9
16	815	775	11
18	947	915	12
20	886	845	10
22	346	331	7
	H 0 4		
0	2396	2349	25
2	2882	2713	28
4	1694	1558	18
6	858	762	10
8	1194	1109	13
10	1341	1297	14
12	1543	1538	16
14	1227	1201	14
16	692	670	10
18	234	217	11
20	191	158	11
22	282	276	8
	H 0 6		
0	1358	1218	15
2	1966	1917	20
4	1710	1621	17
6	1623	1593	12
8	1518	1500	16
10	1058	1063	12
12	924	865	11
14	711	665	10
16	644	609	10
18	534	494	8
20	447	432	8
22	291	292	7
	H 0 8		
0	1057	931	12
2	1460	1394	16
4	1418	1373	15
6	1736	1660	18
8	1426	1377	15
10	853	793	11
12	673	626	10
14	500	480	10
16	623	576	10
18	614	582	9
20	436	447	8
	H 0 10		
0	1949	1902	21
2	1750	1708	18
4	560	424	9
6	864	790	11
8	506	396	10
10	796	746	11
12	1522	1535	17
14	554	502	11
16	590	566	9
18	149	153	16
20	70	7	21
	H 0 12		
0	407	271	10
2	419	286	9
4	1666	1601	18
6	1102	1095	13
8	1272	1206	15
10	831	795	12
12	374	359	13
14	563	523	9
16	289	302	10
18	552	522	8
	H 0 14		
0	1408	1335	15
2	1008	950	12
4	588	560	10
6	192	98	16
8	318	279	12
10	678	642	10
12	867	772	11
14	699	657	9
16	292	277	8
18	97	90	11
	H 0 16		
0	331	295	12
2	389	359	10
4	667	625	10
6	857	800	11
8	671	629	10
10	361	355	8
12	195	181	11
14	127	131	13
16	245	253	6
	H 0 18		
0	579	593	10
2	462	447	10
4	355	333	8
6	374	354	8
8	256	227	9
10	309	314	8
12	359	360	6
14	268	266	6
	H 0 20		
0	382	372	7
2	329	296	7
4	254	279	8
6	267	287	8
8	222	218	8
10	248	259	7
12	213	236	6
	H 0 22		
0	251	175	7
2	411	426	6
4	197	195	7
6	198	183	6
	H 1 0		
1	23	0	20
3	46	0	25
5	41	0	21
7	28	0	24
9	33	0	22
11	27	0	26
13	-62	0	18
15	42	0	25
17	-26	0	30
19	65	0	24
21	18	0	38
	H 1 1		
1	274	326	7
3	937	1095	10
5	608	689	7
7	265	275	7
9	568	617	8
11	415	455	8
13	87	72	23
15	383	384	10
17	294	310	11
19	-63	36	26
21	221	201	8
	H 1 2		
1	283	346	10
3	654	733	8
5	288	332	6
7	100	95	13
9	415	479	7
11	259	282	9
13	125	108	17
15	254	257	12
17	182	176	15
19	36	23	37
21	161	148	11
	H 1 3		
1	1255	1450	14
3	357	417	7
5	63	150	18
7	176	173	9
9	695	788	9
11	278	319	9
13	-34	68	29
15	225	260	13
17	152	117	15
19	87	80	21
21	201	167	9
	H 1 4		
1	1761	1574	18
3	320	415	7
5	432	454	7
7	158	130	10
9	1046	1122	12
11	278	319	9
13	26	50	49
15	457	490	9
17	198	193	15
19	-19	68	46
21	279	267	8
	H 1 5		
1	947	1070	11
3	112	73	15
5	144	167	11
7	200	208	9
9	372	374	8
11	100	74	19
13	29	65	48
15	253	258	13
17	-33	27	27
19	76	71	24
21	26	9	38
	H 1 6		
1	733	802	9
3	1121	1301	12
5	179	251	10
7	78	40	20
9	757	836	9
11	644	650	9
13	408	426	9
15	330	329	11
17	377	358	8
19	109	85	18
21	354	311	7

H 1 7

1	108	143	17
3	404	446	8
5	302	326	8
7	250	245	9
9	34	18	38
11	242	293	12
13	391	399	10
15	65	76	33
17	106	79	20
19	98	72	20
21	111	80	14

H 1 8

1	170	165	12
3	1063	1189	12
5	147	184	15
7	146	144	14
9	509	548	9
11	686	714	10
13	330	341	11
15	211	209	14
17	313	309	10
19	-32	29	33
21	312	265	7

H 1 9

1	203	211	11
3	384	429	9
5	51	37	36
7	67	71	30
9	298	310	11
11	358	322	11
13	123	129	23
15	62	68	37
17	59	83	33
19	56	6	29
21	160	139	8

H 1 10

1	361	392	8
3	378	387	9
5	335	374	10
7	92	106	28
9	344	393	11
11	209	206	17
13	80	34	31
15	257	268	13
17	158	182	12
19	60	44	25

H 1 11

1	160	153	13
3	379	382	9
5	386	372	10
7	125	146	24
9	246	286	16
11	39	125	57
13	83	9	32
15	333	261	10
17	214	187	11
19	32	14	32

H 1 12

1	-35	9	22
3	162	205	16
5	-26	58	28
7	95	47	27
9	127	102	25
11	151	146	22
13	67	1	37
15	-26	53	44
17	26	53	40
19	-26	11	27

H 1 13

1	201	195	13
3	341	347	10
5	104	116	25
7	-21	33	35
9	361	323	12
11	319	263	12
13	-51	74	36
15	77	87	24
17	91	132	19

H 1 14

1	43	11	42
3	142	156	19
5	-58	56	20
7	-42	6	26
9	119	56	22
11	116	140	26
13	99	145	22
15	54	41	27
17	47	32	23

H 1 15

1	83	110	29
3	355	341	10
5	-36	34	27
7	54	80	27
9	103	126	23
11	251	264	10
13	258	213	10
15	37	15	30
17	161	122	7

H 1 16

1	88	85	26
3	349	301	10
5	-72	49	17
7	101	44	24
9	162	136	14
11	266	235	9
13	253	215	8
15	56	13	19

H 1 17

1	142	142	17
3	187	207	15
5	-35	24	20
7	90	85	21
9	38	16	35
11	230	163	8
13	67	56	18
15	53	19	17

H 1 18

1	376	359	8
3	108	68	17
5	102	115	18
7	91	20	18
9	315	259	8
11	103	53	15
13	18	5	34

H 1 19

1	197	180	10
3	46	63	32
5	79	65	20
7	89	87	17
9	94	79	16
11	75	10	14

H 1 20

1	185	137	10
3	147	118	12
5	104	91	15
7	0	26	72
9	187	156	7
11	36	61	21

H 1 21

1	61	4	20
3	95	54	14
5	-57	32	24
7	-34	25	32
9	-38	26	24

H 1 22

1	-56	16	22
3	141	114	8
5	52	37	17

H 1 23

1	-20	10	32

H 2 0

0	1141	1189	12
4	561	519	7
6	147	21	11
8	220	163	9
10	563	541	9
12	555	530	9
14	489	447	9
16	164	157	17
18	31	35	40
20	-55	1	23

H 2 1

0	167	206	9
4	499	510	7
6	261	286	8
8	394	413	7
10	187	139	12
12	215	223	12
14	87	121	28
16	-113	35	10
18	167	135	12
20	213	171	9

H 2 2

0	388	312	7
4	961	1006	8
6	592	579	8
8	684	646	9
10	475	444	8
12	134	207	19
14	371	348	10
16	181	166	14
18	324	293	6
20	324	287	8

H 2 3

0	1013	1053	11
4	439	518	7
6	135	185	12
8	319	354	8
10	110	65	19
12	886	909	11
14	184	141	14
16	104	133	23
18	180	159	12
20	280	238	8

H 2 4

0	933	934	11
2	765	740	10
4	133	13	14
6	614	532	8
8	230	159	10
10	301	270	9
12	746	746	10
14	141	119	18
16	294	254	11
18	127	99	17
20	-26	11	33

H 2 5

0	619	730	9
2	420	503	9
4	674	654	9
6	955	975	11
8	694	686	9
10	100	27	21
12	600	613	10
14	255	244	11
16	82	67	25
18	409	353	8
20	409	362	7

H 2 6

0	462	419	9
2	486	417	9
4	424	405	9
6	609	599	9
8	403	377	9
10	330	297	10
12	289	268	12
14	178	154	17
16	208	188	12
18	215	209	11
20	136	130	13

H 2 7

0	1463	1559	16
2	310	301	10
4	55	86	36
6	523	556	9
8	521	567	9
10	395	375	10
12	601	581	10
14	561	505	10
16	53	19	33
18	221	192	11
20	277	261	8

H 2 8

0	332	401	10
2	909	928	11
4	385	341	10
6	281	224	8
8	628	601	10
10	173	106	17
12	271	263	13
14	183	170	17
16	274	268	10
18	75	77	25
20	150	156	9

H 2 9

0	969	1039	12
2	188	155	13
4	373	353	10
6	459	451	11
8	681	684	11
10	113	109	26
12	300	302	12
14	230	214	12
16	85	98	26
18	227	181	10
20	281	249	7

H 2 10

0	673	613	10
2	377	356	9
4	341	303	11
6	235	221	15
8	159	172	23
10	357	350	13
12	312	295	13
14	289	240	11
16	55	106	38
18	58	82	18

H 2 11

0	431	379	9
2	262	286	12
4	-33	9	27
6	174	128	17
8	-44	77	26
10	177	110	19
12	267	226	15
14	222	185	14
16	73	60	26
18	-49	52	21

H 2 12

0	188	191	16
2	185	177	15
4	400	382	11
6	440	408	11
8	353	349	12
10	220	161	15
12	78	51	30
14	144	116	16
16	172	141	11
18	177	175	7

H 2 13

2	-28	98	31
4	60	102	40
6	153	175	19
8	50	52	44
10	152	172	21
12	107	72	21
14	77	43	24
16	17	17	42

H 2 14

2	111	33	22
4	259	243	9
6	162	176	18
8	108	33	23
10	320	320	10
12	240	218	10
14	240	223	9
16	47	35	22

H 2 15

2	129	156	20
4	134	118	20
6	218	196	12
8	272	256	10
10	85	67	22
12	57	30	28
14	84	68	17
16	53	94	10

H 2 16

2	197	184	15
4	249	255	13
6	225	230	10
8	294	256	9
10	120	113	15
12	24	29	38
14	82	54	13

H 2 17

0	326	292	8
2	222	207	11
4	101	39	19
6	158	116	13
8	136	87	13
10	121	96	13
12	255	218	7
14	109	102	9

H 2 18

0	118	154	17
2	228	210	9
4	172	169	12
6	81	2	19
8	143	132	12
10	129	146	12
12	75	66	13

H 2 19

0	149	99	12
2	141	95	12
4	209	214	9
6	182	135	9
8	194	175	8
10	58	70	17

H 2 20

0	-75	30	22
2	183	177	9
4	-11	28	49
6	202	181	7
8	107	114	10

H 2 21

0	188	174	8
2	120	113	10
4	79	36	13
6	44	22	18

H 2 22

0	78	74	10
2	80	56	11

H 3 0

1	43	0	19
3	-57	0	16
5	77	0	15
7	-35	0	33
9	-66	0	22
11	79	0	16
13	-66	0	19
15	66	0	26
17	-57	0	26
19	-35	0	27

H 3 1

1	346	362	8
3	985	1088	11
5	93	109	21
7	74	15	25
9	566	573	9
11	737	728	10
13	485	464	9
15	227	190	10
17	372	321	8
19	75	66	21

H 3 2

1	141	149	16
3	121	117	17
5	339	362	9
7	177	164	14
9	161	158	16
11	99	153	26
13	273	259	11
15	232	202	11
17	80	38	21
19	72	27	20

H 3 3

1	313	290	11
3	593	621	10
5	288	316	10
7	147	141	15
9	492	481	9
11	400	377	10

13	140	139	18
15	262	235	10
17	266	228	9
19	68	25	21

H 3 4

1	49	2	45
3	268	290	13
5	102	75	23
7	57	23	32
9	122	129	21
11	138	160	18
13	97	11	24
15	71	68	27
17	131	102	15
19	-27	5	29

H 3 5

1	116	142	31
3	265	261	15
5	119	165	24
7	76	62	29
9	220	204	14
11	156	135	17
13	-44	14	26
15	181	147	12
17	134	109	15
19	83	19	17

H 3 6

1	218	249	17
3	136	170	26
5	-32	75	27
7	50	42	41
9	183	186	18
11	154	136	18
13	30	23	50
15	50	77	35
17	81	85	22
19	52	46	25

H 3 7

1	25	16	61
3	60	61	42
5	93	43	33
7	-26	23	34
9	-64	45	22
11	-33	8	33
13	52	39	36
15	23	40	50
17	-54	21	24
19	40	3	25

H 3 8

1	81	85	33
3	189	171	17
5	158	157	25
7	123	127	27
9	96	26	29
11	118	106	24
13	-96	51	21
15	95	61	23
17	111	69	18

H 3 9

1	334	358	12
3	242	182	15
5	142	136	25
7	-36	10	29
9	363	346	13
11	177	115	20
13	87	43	27
15	203	164	13
17	102	52	16

H 3 10

1	297	329	13
3	213	205	16
5	85	57	32
7	138	105	26
9	-38	106	30
11	134	106	22
13	-14	20	54
15	67	26	28
17	72	72	18

H 3 11

1	684	687	11
3	239	174	14
5	162	154	21
7	143	94	21
9	520	467	11
11	145	119	20
13	52	50	35
15	332	263	8
17	100	59	11

H 3 12

1	183	222	17
3	110	166	27
5	101	45	25
7	98	114	30
9	51	60	37
11	119	54	19
13	47	39	32
15	-32	14	30

H 3 13

1	429	406	10
3	320	254	11
5	192	159	15
7	-56	1	33
9	469	388	8
11	216	158	11
13	-71	33	22
15	229	201	7

H 3 14

1	162	121	17
3	154	146	19
5	122	75	17
7	118	103	18
9	45	6	34
11	47	77	31
13	76	11	16

H 3 15

1	125	92	17
3	297	260	9
5	206	150	11
7	62	64	27
9	210	197	10
11	136	130	13
13	60	34	17

H 3 16

1	139	155	15
3	-48	28	34
5	54	41	28
7	73	25	21
9	106	91	15
11	61	37	19

H 3 17

1	95	53	17
3	103	126	18
5	73	71	21
7	76	30	17
9	154	94	8
11	101	85	10

H 3 18

1	56	1	24
3	116	82	13
5	34	24	30
7	-52	16	26
9	30	34	24

H 3 19

1	31	24	29
3	31	19	29
5	61	27	17
7	20	5	28

H 3 20

1	43	21	19
3	-80	9	15

H 4 0

0	420	393	10
2	328	314	12
4	193	185	14
6	388	353	10
8	256	258	12
10	-29	45	34
12	346	255	8
14	240	166	10
16	-54	17	23

H 4 1

0	61	11	34
2	70	47	31
4	126	8	18
6	130	140	20
8	101	23	21
10	-25	30	36
12	71	4	25
14	62	47	27
16	-42	22	26

H 4 2

0	456	454	10
2	149	119	21
4	160	117	17
6	372	326	10
8	298	264	11
10	89	75	24
12	262	220	10
14	220	185	10
16	57	3	24

H 4 3

0	174	158	18
2	111	143	37
4	165	118	19
6	206	127	14
8	124	121	22
10	46	54	40
12	228	209	11
14	28	34	41
16	-21	11	35

H 4 4

0	134	102	23
2	261	254	22
4	149	193	25
6	133	114	21
8	89	55	28
10	26	56	47
12	318	269	9
14	33	8	38
16	94	56	17

H 4 5

0	571	530	11
2	82	14	46
4	245	269	19

6	27	23	57
8	321	323	11
10	19	35	53
12	452	350	8
14	-75	53	22
16	-7	16	44
H 4 6			
0	354	388	15
2	317	347	15
4	192	196	23
6	109	23	28
8	125	103	22
10	207	202	13
12	235	213	10
14	180	153	12
16	133	120	14
H 4 7			
0	565	570	14
2	-41	0	26
4	185	121	20
6	156	114	25
8	311	248	11
10	73	112	32
12	307	261	10
14	-24	80	39
16	70	42	20
H 4 8			
0	240	215	17
2	-70	59	19
4	83	81	36
6	148	82	24
8	166	113	18
10	97	47	26
12	147	112	16
14	91	73	23
H 4 9			
0	213	159	17
2	151	122	22
4	145	81	19
6	257	269	13
8	114	110	26
10	-45	43	40

12	174	114	15
14	134	109	14
H 4 10			
0	220	212	15
2	205	127	15
4	139	109	17
6	246	200	12
8	146	144	19
10	63	24	32
12	212	161	10
14	125	83	12
H 4 11			
0	91	147	26
2	76	95	27
4	72	35	28
6	160	102	15
8	139	68	15
10	-55	41	33
12	120	100	13
14	57	72	17
H 4 12			
0	288	253	10
2	123	109	18
4	106	52	20
6	249	198	10
8	188	123	11
10	28	43	39
12	173	141	9
H 4 13			
0	131	104	16
2	66	30	27
4	-41	43	36
6	57	12	27
8	61	78	25
10	56	6	22
12	46	28	19
H 4 14			
0	193	148	11
2	114	82	15
4	119	77	15

6	176	133	10
8	145	108	11
10	-62	0	21
H 4 15			
0	162	136	12
2	108	93	15
4	56	26	24
6	73	35	18
8	108	82	12
H 4 16			
0	275	283	7
2	74	111	18
4	74	62	17
6	100	49	12
8	88	107	11
H 4 17			
0	216	188	7
2	-77	27	19
4	84	62	13
H 5 0			
1	-82	0	29
3	-29	0	44
5	80	0	29
9	-51	0	35
11	-54	0	27
13	55	0	20
H 5 1			
1	216	204	12
3	20	65	64
5	38	30	39
7	47	75	35
9	109	122	18
11	-44	49	30
13	-52	21	21
H 5 2			
1	403	380	8
3	80	1	35
5	28	45	43

7	-34	82	48
9	268	226	9
11	87	28	19
13	49	1	27
H 5 3			
1	177	168	15
3	68	51	58
5	89	11	25
7	64	27	29
9	41	84	39
11	55	36	28
13	43	3	30
H 5 4			
1	176	149	18
3	300	237	15
5	150	116	20
7	114	42	19
9	271	210	10
11	196	135	11
13	75	40	20
H 5 5			
1	-113	6	21
3	15	52	71
5	-89	6	25
7	59	19	34
9	37	21	41
11	-46	36	28
H 5 6			
1	124	105	35
3	-27	257	49
5	219	181	15
7	119	93	24
9	269	214	11
11	201	131	12
H 5 7			
1	91	28	32
3	55	20	37
5	43	51	43
7	27	25	56
9	63	32	35

11	50	0	31
H 5 8			
1	175	123	16
3	307	248	10
5	103	45	21
7	-34	9	41
9	220	173	12
11	225	193	8
H 5 9			
1	37	62	43
3	58	47	32
5	87	104	22
7	90	45	20
9	41	50	31
H 5 10			
1	-63	20	27
3	260	209	9
5	74	14	22
7	30	18	36
9	102	68	13
H 5 11			
1	29	6	39
3	-24	26	42
5	107	73	14
7	33	34	31
H 5 12			
1	54	47	24
3	20	22	38
5	81	94	17
7	-63	45	21
H 5 13			
1	45	36	23
3	59	58	19
5	55	39	17
H 6 0			
0	167	159	54

2	117	28	87
H 6 1			
2	66	113	109
H 6 2			
0	309	289	38
H 6 4			
0	259	181	23

E. (1.d.)$(TTT)_2I_3$ - Structure factors $Pmc2_1$, full cell. Ni-filtered CuK$\bar{\alpha}$ radiation.

	H 0 0		
2	2212	1785	16
4	3690	3222	37
6	2665	2369	29
8	634	944	15
10	4365	4412	44
12	3727	4021	40
14	3208	3339	35
16	1097	1053	22
18	567	611	23
20	361	260	24
22	523	598	16
	H 0 2		
0	521	1066	18
6	5666	5410	57
8	5187	5169	53
10	2112	2077	24
12	701	641	17
14	825	855	18
16	1627	1669	22
18	1891	1965	24
20	1769	1774	21
22	691	741	15
	H 0 4		
0	4761	4466	51
2	5750	5091	56
4	3380	3165	36
6	1712	1659	20
8	2383	2394	26
10	2676	2708	29
12	3080	3164	33
14	2448	2548	28
16	1381	1458	20
18	467	542	23
20	381	446	22
22	564	625	16
	H 0 6		
0	2710	2645	30
2	3922	3879	41
4	3413	3367	35
6	3239	3301	24
8	3030	3134	32
10	2191	2267	25
12	1844	1861	23
14	1420	1461	21
16	1286	1331	20
18	1066	1072	17
20	892	937	16
22	581	643	15
	H 0 8		
0	2109	2116	24
2	2914	2977	32
4	2830	2945	31
6	3465	3488	37
8	2845	2885	31
10	1702	1749	22
12	1344	1422	20
14	998	1022	20
16	1243	1266	20
18	1225	1234	18
20	671	925	16
	H 0 10		
0	3889	3949	41
2	3493	3566	37
4	1118	1164	18
6	1725	1732	23
8	1010	1023	20
10	1589	1629	23
12	3037	3121	35
14	1107	1127	22
16	1178	1165	19
18	297	361	32
20	139	126	42
	H 0 12		
0	813	803	20
2	836	857	18
4	3325	3306	36
6	2199	2359	26
8	2538	2527	30
10	1659	1668	25
12	747	707	26
14	1123	1093	19
16	578	649	21
18	1102	1064	16
	H 0 14		
0	2809	2786	31
2	2012	2034	24
4	1174	1247	20
6	384	416	33
8	635	657	23
10	1353	1375	21
12	1730	1562	22
14	1396	1352	18
16	564	581	17
18	193	183	22
	H 0 16		
0	661	697	25
2	777	829	21
4	1331	1325	20
6	1710	1653	22
8	1340	1296	21
10	722	755	17
12	390	407	23
14	253	285	26
16	490	514	13
	H 0 18		
0	1157	1199	20
2	922	931	20
4	710	719	17
6	746	719	17
8	511	500	18
10	618	635	16
12	716	718	13
14	535	526	12
	H 0 20		
0	763	737	15
2	656	605	15
4	508	550	17
6	533	566	16
8	444	437	16
10	495	502	14
12	425	464	13
	H 0 22		
0	502	378	14
2	821	779	13
4	394	379	15
6	376	362	13
	H 2 0		
1	47	1	41
3	92	3	50
5	82	4	43
6	46	25	56
7	56	4	49
8	-99	26	36
9	65	3	45
10	-106	27	35
11	53	1	53
12	98	27	39
13	-124	0	36
14	119	28	38
15	84	2	50
16	46	27	65
17	-53	3	60
19	130	4	48
21	35	4	77
	H 2 1		
1	546	636	15
3	1871	2171	21
5	1214	1358	15
6	90	101	35
7	528	617	14
8	-64	81	46
9	1134	1261	16
10	-33	64	63
11	828	939	16
12	115	48	34
13	174	106	46
14	80	35	49
15	764	766	20
16	-83	26	49
17	586	618	23
19	-126	41	52
21	441	401	17
	H 2 2		
1	566	683	20
3	1306	1457	16
5	576	659	13
6	49	64	49
7	201	231	26
8	14	57	76
9	828	976	14
10	70	50	45
11	518	597	19
12	77	44	47
13	250	189	34
14	-27	39	82
15	507	487	25
16	-111	35	40
17	364	355	30
19	73	8	74
21	321	301	22
	H 2 3		
1	2504	2832	28
3	713	904	14
5	127	370	37
6	69	98	38
7	351	444	19
8	44	80	57
9	1387	1513	18
10	10	63	83
11	555	570	16
12	23	48	76
13	-68	241	57
14	80	36	52
15	449	560	27
16	-74	27	50
17	304	293	31
19	173	205	42
21	401	322	19
	H 2 4		
1	3515	3804	37
3	639	886	15
5	863	1020	14
6	46	112	47
7	315	311	20
8	22	58	72
9	2088	2210	24
10	81	84	45
11	555	573	19
12	38	71	71
13	52	127	98
14	106	59	41
15	913	1032	19
16	-82	50	50
17	395	438	30
19	-39	152	92

21	556	498	17

H 2 5

1	1890	2087	22
3	223	203	30
5	288	246	21
6	-75	93	35
7	400	319	19
8	95	77	34
9	742	877	16
10	-112	62	40
11	201	44	39
12	-100	48	45
13	58	206	96
14	-109	37	45
15	466	415	26
16	-70	28	55
17	-66	50	55
19	151	95	49
21	53	68	77

H 2 6

1	1463	1598	19
3	2236	2541	25
5	357	481	21
6	125	148	24
7	157	53	40
8	-90	130	37
9	1510	1723	19
10	-149	112	31
11	1286	1451	19
12	103	94	45
13	815	817	19
14	-89	77	51
15	658	606	22
16	-133	63	36
17	754	669	17
19	218	141	37
21	707	665	15

H 2 7

1	217	256	33
3	806	828	17
5	603	741	17
6	79	87	35
7	500	394	18
8	-20	73	73
9	68	91	76
10	-156	60	31
11	484	702	24
12	-105	46	49
13	780	712	20
14	24	37	89
15	139	255	67
16	-73	29	52
17	212	84	41
19	196	111	40
21	222	217	28

H 2 8

1	340	359	24
3	2121	2376	25
5	294	432	31
6	43	170	51
7	291	242	28
8	-142	150	26
9	1016	1020	18
10	-43	129	70
11	1370	1361	20
12	10	109	104
13	660	744	22
14	73	90	59
15	422	487	29
17	624	671	20
19	-64	102	66
21	624	493	14

H 2 9

1	405	447	22
3	767	901	18
5	102	153	71
6	-103	79	31
7	133	56	60
8	156	68	25
9	595	538	22
10	-23	56	84
11	714	526	22
12	-58	46	69
13	246	355	46
14	113	37	42
15	124	213	74
17	117	242	66
19	113	74	59
21	320	236	16

H 2 10

1	720	753	17
3	755	752	18
5	668	695	20
6	58	177	49
7	184	263	57
8	95	157	39
9	686	853	23
10	51	136	69
11	417	454	34
12	-104	115	52
13	161	20	62
14	-158	95	34
15	512	488	26
17	395	315	24
19	120	33	50

H 2 11

1	320	305	27
3	756	728	19
5	774	685	20
6	21	70	76
7	250	374	48
8	-44	61	67
9	491	643	32
10	-11	52	98
11	78	319	113
12	-86	43	56
13	166	91	64
14	112	35	40
15	665	475	20
17	427	316	22
19	64	46	53

H 2 12

1	-70	29	45
3	324	417	32
4	14	186	81
5	-53	147	56
6	-29	172	74
7	189	48	55
8	-44	154	70
9	253	154	51
10	77	134	57
11	302	236	43
12	-88	114	55
13	135	60	74
15	-52	139	68
17	52	157	79
19	-53	59	54

H 2 13

1	402	391	27
3	680	720	21
4	27	66	74
5	208	295	50
6	34	60	76
7	-43	55	71
8	77	53	53
9	720	569	24
10	101	46	45
11	637	465	24
12	-37	39	81
13	-103	193	72
15	154	256	49
17	181	300	38

H 2 14

1	86	24	65
3	285	332	39
4	-111	170	42
5	-115	70	41
6	67	158	56
7	-84	23	51
8	157	142	29
9	237	76	45
10	-86	124	52
11	232	240	52
13	199	305	44
15	108	41	54
17	93	98	46

H 2 15

1	167	208	59
3	708	650	21
4	18	55	87
5	-73	74	55
6	106	51	40
7	188	99	54
8	-94	45	47
9	205	297	47
11	502	557	21
13	515	368	20
15	74	37	61
17	321	196	15

H 2 16

1	176	167	52
3	696	552	21
4	-144	148	33
5	-143	93	35
6	-89	138	40
7	201	70	47
8	-59	125	59
9	324	306	28
11	530	484	19
13	506	354	17
15	113	7	39

H 2 17

1	284	267	35
3	373	416	29
4	-133	45	36
5	-71	73	41
7	180	143	42
9	77	53	70
11	459	279	17
13	134	134	37
15	105	7	34

H 2 18

1	751	704	16
3	217	158	35
5	205	225	37
7	183	62	37
9	630	521	16
11	206	88	30
13	36	37	67

H 2 19

1	394	349	21
3	92	122	64
5	158	108	41
7	178	181	34
9	187	136	32
11	150	40	29

H 2 20

1	369	260	20

3	294	230	24
5	208	179	31
7	0	58	144
9	374	316	15
11	72	130	41

H 2 21

1	123	14	41
3	190	101	28
5	-113	54	49
7	-68	56	65
9	-75	64	48

H 2 22

1	-111	30	45
3	282	220	17
5	105	83	34

H 2 23

1	-40	20	64

H 3 0

0	237	342	30
1	122	28	101
2	293	335	26
3	183	82	37
4	326	316	22
5	218	124	31
6	300	288	26
7	198	153	37
8	297	257	28
9	142	169	53
10	326	225	28
11	191	173	46
12	206	194	51
14	220	164	51
15	184	155	56
16	237	136	44
17	0	138	143
18	188	111	51
19	53	120	98

H 3 1

0	498	756	18
1	218	30	70
2	504	739	18
3	206	86	32
4	549	693	17
5	51	132	63
6	566	628	17
7	236	166	31
8	557	553	18
9	233	187	35
10	534	477	21
12	437	403	25
13	219	195	46
14	443	333	28
15	119	186	78
16	308	269	39
17	165	171	56
18	260	214	41

H 3 2

0	266	338	30
1	237	28	58
2	298	331	29
3	158	60	43
4	270	312	28
5	158	122	43
6	340	286	22
7	178	150	42
8	264	256	32
9	67	166	74
10	303	224	31
11	116	170	69
12	235	193	44
14	237	164	47
15	18	153	139
16	181	136	55
18	87	111	85
19	191	118	45

H 3 3

0	521	716	20
1	166	28	70
2	513	701	22
3	141	62	51
4	546	659	17
5	165	127	42
6	560	599	18
7	157	160	47
8	519	530	20
9	120	181	62
10	485	456	24
11	104	190	77
12	404	387	30
14	416	321	30
16	259	260	47
17	146	167	63
18	275	206	39
19	101	149	72

H 3 4

0	299	325	34
2	296	319	38
3	197	75	42
4	302	303	27
5	175	114	43
6	298	279	28
7	11	142	124
8	231	251	39
9	82	158	80
10	238	221	40
11	231	162	42
12	210	191	52
13	176	157	60
14	232	162	49
16	221	135	48
17	106	131	77
19	124	114	64

H 3 5

0	495	645	26
1	140	26	68
2	525	633	26
3	62	76	97
4	500	598	21
5	142	117	55
6	555	547	19
7	194	149	42
8	509	486	21
9	145	169	58
10	476	422	25
11	0	178	160
12	448	358	30
13	145	178	71
14	339	298	37
15	154	171	53
16	255	242	47
17	113	158	77
18	195	192	53

H 3 6

0	265	307	41
1	192	23	52
2	214	302	53
3	85	67	94
4	293	287	36
5	83	104	83
6	304	267	32
7	166	130	52
8	236	241	43
10	298	214	36
12	258	186	44
13	247	146	45
14	162	158	66
15	209	136	50
16	188	133	56

H 3 7

0	507	559	22
1	256	23	39
2	479	549	26
3	72	67	105
4	517	571	25
5	170	105	57
6	429	480	29
8	436	429	29
9	62	153	107
10	391	375	33
11	141	162	73
12	416	320	32
13	82	163	99
14	301	267	44
16	233	217	52
17	58	145	106
18	247	173	43

H 3 8

0	329	283	32
1	137	20	65
2	257	279	42
3	175	59	60
4	253	267	50
5	171	91	62
6	103	249	90
7	191	115	55
8	243	227	47
9	78	129	101
10	199	202	60
11	192	134	61
12	101	177	99
13	116	122	95
14	264	152	43
15	260	124	42
16	114	126	50
17	72	111	97
18	41	106	115

H 3 9

0	384	468	29
1	215	20	45
2	461	461	27
3	35	58	127
4	450	439	30
6	425	406	34
7	193	117	63
8	345	366	44
10	341	321	43
12	303	275	50
13	127	145	84
14	218	230	61
16	148	189	75

H 3 10

0	192	255	53
1	132	17	70
2	272	252	40
3	199	50	54
4	276	242	43
5	175	78	69
6	162	227	79
8	246	208	59
10	100	187	105
11	46	117	136
13	258	116	49
14	127	142	86
15	54	109	123
17	278	99	38

H 3 11

0	360	380	34
1	-139	17	72
2	327	375	39
3	147	49	69

4	349	358	39
5	89	78	99
6	394	333	39
7	267	100	48
8	218	301	74
9	347	115	44
10	283	266	59
12	301	229	49
13	152	125	80
14	166	193	77
16	179	158	62

H 3 12

0	151	224	70
1	208	14	51
2	143	222	75
3	17	42	144
4	156	214	71
5	189	65	63
7	158	83	78
8	147	185	86
9	234	94	58
10	201	167	67
11	162	99	77
12	96	148	104
14	263	128	44
15	67	94	103

H 3 13

0	224	300	56
2	379	296	33
3	145	40	72
4	343	283	38
5	108	64	93
6	290	265	48
7	183	83	66
8	199	240	61
9	196	96	62
10	243	213	53
12	284	184	45
15	150	102	56

H 3 14

1	117	11	84
3	36	34	133
4	205	183	56
9	67	78	107
10	136	145	75
12	122	129	77
14	164	113	51

H 3 15

0	320	230	40
2	261	227	47
4	299	218	40
8	247	186	45
9	40	79	119
11	0	84	153
13	170	86	47

H 3 16

0	159	159	62
1	178	9	56
3	87	27	89
4	167	152	59
6	149	144	67
7	154	54	60
8	211	134	47
10	0	122	148
11	199	66	40

H 3 17

0	180	171	58
1	110	8	76
2	252	169	43
3	141	25	63
4	219	162	48
5	133	40	66
6	257	152	40
7	19	52	128
8	139	140	63
9	160	61	51
10	97	125	72

H 3 18

1	173	7	51
4	23	123	122
5	121	33	63
6	175	117	49
7	121	42	60

H 3 19

0	145	124	59
1	95	6	72
2	121	122	64
4	147	118	52
6	148	111	49

H 4 0

0	2278	2558	25
4	1120	1218	15
6	294	270	22
8	439	485	18
10	1123	1221	18
12	1108	1122	18
14	975	1017	19
16	327	378	34
18	62	114	80
20	-110	86	46

H 4 1

0	333	338	18
4	995	1106	15
6	521	677	16
8	786	918	15
10	373	361	24
12	429	387	24
14	173	301	56
16	-225	128	20
18	334	298	25
20	425	379	19

H 4 2

0	775	819	14
4	1956	2157	15
6	1181	1339	16
8	1366	1430	18
10	949	1006	17
12	267	349	37
14	741	763	21
16	362	399	29
18	647	632	17
20	647	609	16

H 4 3

0	2021	2284	23
4	876	936	15
6	270	306	25
8	637	624	17
10	219	232	38
12	1767	1891	23
14	369	365	29
16	209	307	46
18	360	283	24
20	559	464	16

H 4 4

0	1863	2012	22
2	1527	1620	21
4	266	289	28
6	1225	1186	17
8	460	459	21
10	602	651	19
12	1490	1569	21
14	283	318	37
16	586	559	22
18	255	268	34
20	-52	71	66

H 4 5

0	1235	1365	19
2	838	920	19
4	1346	1412	18
6	1905	2080	22
8	1385	1462	19
10	200	126	43
12	1198	1141	19
14	509	463	23
16	164	189	50
18	817	776	16
20	816	731	15

H 4 6

0	962	961	18
2	971	968	18
4	846	920	19
6	1216	1280	18
8	804	844	18
10	659	668	21
12	576	623	24
14	357	355	34
16	415	439	24
18	429	436	22
20	271	290	26

H 4 7

0	2919	3140	32
2	619	767	20
4	110	89	73
6	1044	1061	18
8	1040	1037	19
10	788	837	21
12	1199	1221	21
14	1121	1091	20
16	106	24	66
18	441	364	22
20	552	474	17

H 4 8

0	663	730	20
2	1814	1846	27
4	769	773	21
6	560	546	17
8	1253	1257	21
10	346	288	34
12	542	558	26
14	366	351	35
16	546	546	21
18	150	202	50
20	379	335	19

H 4 9

0	1933	1959	24
2	376	355	27
4	744	789	20
6	915	1014	22
8	1360	1423	22
10	225	156	52
12	598	560	25
14	459	378	24
16	170	232	53
18	453	405	21
20	561	530	14

H 4 10

0	1342	1250	20
2	752	759	19
4	680	653	22
6	469	459	31
8	318	393	46
10	712	718	27

12	623	617	27
14	577	511	22
16	110	242	76
18	196	170	36

H 4 11

0	861	829	19
2	523	612	24
4	-67	81	54
6	347	219	34
8	-88	106	53
10	353	267	38
12	533	498	30
14	444	410	28
16	147	146	52
18	-98	72	43

H 4 12

0	377	372	32
2	369	382	31
4	799	768	22
6	878	822	23
8	705	698	24
10	440	350	30
12	157	133	60
14	287	236	32
16	344	291	23
18	353	361	15

H 4 13

2	-57	175	62
4	120	224	80
6	305	380	39
8	100	97	89
10	305	371	42
12	214	177	43
14	155	97	48
16	34	6	84

H 4 14

2	222	173	45
4	516	461	19
6	323	351	37
8	216	151	47
10	639	639	20
12	479	432	21
14	479	434	18
16	54	97	45

H 4 15

2	259	316	41
4	269	241	40
6	435	394	25
8	544	523	20
10	170	126	44
12	114	53	56
14	168	125	35
16	187	198	21

H 4 16

2	394	350	30
4	458	474	26
6	450	429	21
8	587	498	18
10	240	207	31
12	49	77	77
14	165	123	27

H 4 17

0	654	564	17
2	443	436	22
4	201	64	38
6	316	266	27
8	272	160	27
10	241	161	26
12	509	427	15
14	219	230	19

H 4 18

0	235	264	34
2	455	377	19
4	344	292	24
6	162	83	39
8	286	229	24
10	259	250	23
12	150	137	27

H 4 19

0	298	201	24
2	283	217	24
4	418	392	19
6	364	290	19
8	388	316	16
10	116	125	35

H 4 20

0	-151	80	45
2	366	300	19
4	-22	81	99
6	404	303	15
8	214	195	20

H 4 21

0	375	319	16
2	241	209	21
4	158	90	27
6	89	66	36

H 4 22

0	157	112	21
2	161	154	22

H 6 0

1	86	4	38
3	-114	13	33
5	155	20	31
7	-71	26	67
9	-133	28	44
11	157	25	33
13	-132	28	39
15	133	25	51
17	-114	22	53
19	-71	19	55

H 6 1

1	692	729	16
3	1965	2172	23
5	187	301	42
7	148	98	51
9	1129	1175	19
11	1471	1450	21
13	969	881	19
15	454	426	21
17	742	638	16
19	150	128	42

H 6 2

1	282	279	32
3	242	200	34
5	677	720	18
7	353	329	28
9	323	304	32
11	198	309	53
13	546	519	23
15	463	423	21
17	159	85	43
19	144	66	40

H 6 3

1	625	583	22
3	1184	1276	20
5	576	672	20
7	293	293	31
9	981	963	19
11	798	729	20
13	281	263	36
15	523	520	20
17	532	481	18
19	137	44	42

H 6 4

1	98	32	90
3	536	569	27
5	204	174	47
7	115	79	65
9	244	261	43
11	276	338	37
13	194	36	47
15	143	149	53
17	263	198	29
19	-55	28	57

H 6 5

1	231	297	63
3	530	517	31
5	237	351	48
7	152	141	58
9	440	442	28
11	311	289	34
13	-88	21	52
15	362	284	24
17	267	212	31
19	167	20	35

H 6 6

1	436	450	35
3	272	365	52
5	-65	161	55
7	100	85	82
9	365	387	36
11	308	282	37
13	61	67	101
15	100	160	70
17	161	166	44
19	104	104	51

H 6 7

1	49	28	122
3	120	129	84
5	187	71	66
7	-53	76	69
9	-128	108	45
11	-67	51	67
13	104	52	73
15	46	72	99
17	-108	37	49
19	30	35	50

H 6 8

1	162	162	66
3	376	362	35
5	316	314	50
7	245	255	55
9	193	72	58
11	236	207	49
13	-191	107	43
15	191	142	46
17	221	151	36

H 6 9

1	667	720	24
3	482	403	30
5	283	252	51
7	-73	27	58
9	725	683	26
11	353	219	41
13	174	107	54
15	405	352	26

17	235	149	32

H 6 10

1	593	651	27
3	426	418	33
5	169	136	64
7	275	239	52
9	-76	206	60
11	268	213	45
13	-28	41	109
15	134	37	56
17	145	154	37

H 6 11

1	1366	1313	22
3	476	389	26
5	323	318	42
7	285	148	43
9	1038	999	23
11	265	266	39
13	105	84	71
15	663	503	16
17	200	139	22

H 6 12

1	366	379	35
3	221	285	53
5	202	72	51
7	196	200	61
9	102	110	75
11	238	103	38
13	94	73	64
15	-64	23	61

H 6 13

1	857	764	20
3	635	546	22
5	383	357	30
7	-112	37	65
9	937	750	17
11	432	310	22
13	-143	81	45
15	457	418	14

H 6 14

1	324	235	34
3	308	284	38
5	244	139	35
7	237	194	36
9	90	7	67
11	94	146	62
13	152	23	33

H 6 15

1	250	186	35
3	593	520	19
5	412	301	22
7	125	153	54
9	420	395	21
11	272	282	26
13	120	54	34

H 6 16

1	277	272	30
3	-97	73	68
5	107	76	56
7	147	46	42
9	213	180	31
11	122	76	37

H 6 17

1	190	105	35
3	205	259	36
5	147	140	42
7	153	53	35
9	307	177	17
11	202	168	20

H 6 18

1	112	18	48
3	233	154	26
5	69	50	61
7	-105	28	52
9	61	75	48

H 6 19

1	63	35	59
3	63	37	58
5	122	51	34
7	41	15	55

H 6 20

1	86	43	39
3	-161	14	31

H 8 4

0	839	783	20
2	655	553	25
4	386	435	29
6	775	819	20
8	512	577	24
10	-59	64	69
12	691	575	17
14	479	389	20
16	-108	6	46

H 8 1

0	122	9	69
2	140	94	62
4	251	11	37
6	260	302	40
8	203	44	43
10	-49	53	72
12	141	13	49
14	124	113	55
16	-85	51	52

H 8 2

0	910	987	20
2	297	343	41
4	319	187	35
6	744	647	21
8	595	492	22
10	178	195	49
12	524	479	20
14	439	429	20
16	114	11	49

H 8 3

0	348	407	36
2	223	307	74
4	330	219	39
6	416	303	29
8	248	221	45
10	93	106	80
12	456	404	22
14	56	107	82
16	-43	4	71

H 8 4

0	267	168	47
2	521	463	45
4	298	415	50
6	266	326	42
8	178	230	57
10	52	196	95
12	635	498	18
14	66	12	76
16	187	80	35

H 8 5

0	1139	1051	23
2	164	56	52
4	489	511	38
6	54	117	114
8	641	630	22
10	38	87	107
12	903	687	17
14	-150	72	45
16	-14	39	86

H 8 6

0	708	695	31
2	633	691	30
4	384	322	47
6	218	40	57
8	250	231	45
10	404	358	26
12	470	408	21
14	359	254	25
16	266	229	26

H 8 7

0	1128	1108	28
2	-82	34	52
4	370	258	41
6	312	267	50
8	622	512	23
10	146	234	65
12	612	508	20
14	-48	173	78

16	140	78	39

H 8 8

0	479	453	34
2	-140	138	38
4	165	132	72
6	296	173	48
8	352	204	37
10	193	105	52
12	294	241	32
14	183	156	47

H 8 9

0	425	346	35
2	302	266	44
4	291	156	39
6	513	526	27
8	229	215	52
10	-91	100	80
12	348	232	30
14	268	234	28

H 8 10

0	439	406	31
2	410	274	30
4	276	233	35
6	491	437	24
8	291	289	37
10	126	38	63
12	423	323	21
14	250	173	24

H 8 11

0	182	268	53
2	152	177	55
4	144	86	57
6	320	225	30
8	277	135	30
10	-109	66	66
12	241	193	27
14	114	139	35

H 8 12

0	575	510	21
2	247	245	37

4	213	127	40
6	497	399	21
8	376	252	23
10	56	87	78
12	346	302	18
H 8 13			
0	261	204	32
2	133	41	54
4	-82	69	73
6	114	11	55
8	123	136	50
10	113	11	44
12	93	72	38
H 8 14			
0	385	304	23
2	228	177	30
4	238	154	30
6	352	285	20
8	290	220	22
10	-123	10	41
H 8 15			
0	324	245	24
2	216	131	30
4	112	47	47
6	146	55	35
8	217	138	23
H 8 16			
0	549	494	15
2	149	169	37

4	148	108	34
6	199	133	25
8	175	194	23
H 8 17			
0	431	325	15
2	-153	34	38
4	169	131	26
H 10 0			
1	-165	0	58
3	-58	0	89
5	160	0	59
9	-101	1	70
11	-108	1	55
13	109	1	40
H 10 1			
1	435	372	23
3	40	118	129
5	77	49	79
7	93	125	71
9	217	216	36
11	-88	90	60
13	-104	43	42
H 10 2			
1	805	703	17
3	159	59	70
5	57	103	86
7	-69	144	97
9	535	458	18
11	174	73	38

13	98	15	54
H 10 3			
1	353	291	31
3	136	83	117
5	176	19	50
7	129	41	58
9	82	156	77
11	109	67	56
13	85	5	59
H 10 4			
1	352	316	37
3	599	496	30
5	300	268	41
7	228	108	38
9	542	444	20
11	392	276	22
13	151	69	41
H 10 5			
1	-227	5	42
3	29	104	142
5	-178	16	50
7	118	35	68
9	75	41	83
11	-93	63	56
H 10 6			
1	248	205	71
3	-55	558	97
5	438	391	30
7	237	220	49

9	538	438	22
11	401	279	24
H 10 7			
1	183	52	64
3	111	48	74
5	86	76	87
7	54	34	112
9	126	66	71
11	101	15	62
H 10 8			
1	350	252	32
3	614	523	21
5	205	139	43
7	-68	25	63
9	440	356	24
11	449	385	17
H 10 9			
1	75	120	86
3	116	70	64
5	175	166	45
7	181	57	40
9	83	91	62
H 10 10			
1	-126	57	55
3	520	406	19
5	148	19	44
7	61	13	72
9	203	159	26

H 10 11			
1	58	19	78
3	-48	51	85
5	214	134	29
7	66	61	62
H 10 12			
1	108	82	49
3	41	25	76
5	163	175	34
7	-126	81	42
H 10 13			
1	91	56	46
3	118	108	39
5	110	84	35
H 12 0			
0	333	394	108
2	234	92	174
H 12 1			
2	133	209	218
H 12 2			
0	617	526	76
H 12 4			
0	516	337	46

F. $(TMTSF)Br_{0.8}$ - Structure factors, Ni-filtered CuK$\bar{\alpha}$ radiation.

Space group Cmcm.

0 K 0

2	2374	2290	24
4	1300	1119	10
6	550	640	6
8	1168	1164	9
10	310	474	7
12	273	351	7
14	2828	2734	19
16	1666	1603	13
18	940	934	9
20	1192	1166	10
22	1071	1132	9
24	256	263	10
26	101	110	17
28	329	341	6
30	252	302	5

1 K 0

1	1994	2161	14
3	652	581	5
5	1318	1396	10
7	709	569	6
9	427	535	6
11	675	762	6
13	793	714	7
15	1127	1074	9
17	339	320	7
19	995	1006	9
21	647	552	7
23	192	153	11
25	94	73	18
27	77	52	19
29	189	173	6

2 K 0

0	464	215	5
2	684	824	6
4	-30	85	24
6	1572	1519	11
8	322	336	5
10	109	209	13
12	969	939	8
14	446	409	6
16	1093	1030	9
18	167	121	12
20	751	680	8
22	311	231	8
24	-39	53	37
26	53	57	24
28	33	58	27

3 K 0

1	4382	4052	32
3	421	271	5
5	645	656	5
7	1171	1236	9
9	390	298	6
11	135	233	10
13	1577	1584	12
15	2522	2377	19
17	556	522	7
19	861	806	8
21	1166	1107	9
23	665	717	7
25	132	122	14
27	143	146	10
29	264	289	5

4 K 0

0	1111	1322	8
2	904	1074	7
4	263	407	5
6	1506	1418	11
8	207	195	7
10	35	137	28
12	924	916	8
14	997	892	9
16	1130	1138	10
18	178	203	12
20	875	794	8
22	430	345	9
24	76	78	21
26	46	58	23
28	98	92	10

5 K 0

1	361	489	5
3	843	823	7
5	605	628	6
7	333	316	6
9	381	356	6
11	433	486	6
13	267	200	9
15	314	251	9
17	423	404	8
19	426	414	7
21	441	353	7
23	83	49	20
25	64	36	21
27	40	12	18

6 K 0

0	3485	3519	24
2	1537	1482	11
4	248	237	7
6	648	635	7
8	608	657	7
10	119	212	16
12	398	364	8
14	1550	1487	12
16	1090	1004	9
18	330	316	9
20	945	866	8
22	855	852	8
24	135	133	11
26	44	79	16

7 K 0

1	1131	1235	9
3	722	781	7
5	707	740	7
7	620	570	7
9	284	252	9
11	454	499	7
13	613	538	11
15	748	679	9
17	362	350	8
19	644	620	8
21	721	644	7
23	225	195	7

8 K 0

0	71	57	30
2	186	192	11
4	207	208	10
6	344	357	7
8	157	180	13
10	99	6	20
12	196	208	14
14	255	194	10
16	363	373	8
18	39	29	33
20	134	128	11
22	-64	58	16

9 K 0

1	1608	1589	12
3	-66	96	28
5	454	401	8
7	391	419	9
9	71	88	27
11	104	118	19
13	750	731	8
15	1112	1086	9
17	257	228	7
19	401	385	5

10 K 0

0	869	876	8
2	532	568	7
4	201	217	11
6	563	570	7
8	53	18	30
10	51	12	29
12	377	379	8
14	636	574	6
16	528	532	6

11 K 0

1	39	49	34
3	119	154	15
5	60	99	26
7	42	1	31
9	66	95	21
11	25	50	32
13	-40	28	19

12 K 0

0	1096	1027	9
2	498	451	6
4	117	127	11
6	209	194	7

0 K 1

0	-69	0	13
2	1368	1372	10
4	1889	1761	13
6	2271	2168	16
8	3369	3030	25
10	1405	1318	11
12	1528	1515	12
14	1742	1628	13
16	194	228	10
18	347	365	7
20	622	672	7
22	915	883	9
24	692	676	8
26	648	686	7
28	811	655	7

1 K 1

1	36	35	19
3	320	351	5
5	200	305	7
7	2584	2387	19
9	1153	1202	9
11	119	92	11
13	546	498	6
15	927	913	8
17	50	99	29
19	77	8	22
21	547	527	7
23	439	418	7
25	57	9	28
27	415	417	6
29	399	441	5

2 K 1

0	-32	0	22
2	180	137	6
4	755	735	6
6	1755	1792	12
8	2486	2289	18
10	465	376	6
12	490	430	6
14	536	578	6
16	490	452	7
18	244	297	9
20	282	237	8
22	533	485	7
24	56	66	27
26	238	235	7
28	227	229	6

3 K 1

1	1068	1109	8
3	165	102	6
5	1815	1903	13
7	3066	2960	21
9	2275	2223	16
11	756	793	7
13	1902	1791	14
15	786	781	8
17	91	133	20
19	433	464	8
21	700	676	7
23	882	852	11
25	153	160	11
27	773	808	7
29	385	431	4

4 K 1

0	10	0	36
2	-24	17	27
4	185	167	6
6	1780	1799	13
8	2214	2213	16
10	102	54	13
12	556	543	7
14	924	916	8
16	464	458	8
18	144	199	16
20	352	309	8
22	562	513	8
24	122	123	14
26	334	329	6
28	344	374	4

5 K 1

1	216	202	6
3	476	479	5
5	91	82	13
7	1403	1459	11
9	553	513	6
11	301	257	7
13	91	24	20
15	355	348	9
17	74	51	24
19	72	94	28
21	389	372	7
23	263	242	8
25	43	17	26
27	147	170	6

6 K 1

0	55	0	21
2	795	816	7
4	496	517	6
6	1693	1668	13
8	2154	2160	16
10	544	529	7
12	1149	1091	10
14	936	848	8
16	116	159	22
18	151	183	17
20	483	466	7
22	764	724	7
24	365	370	6
26	491	529	4

7 K 1

0	10	0	36
2	-24	17	27
4	185	167	6
6	1780	1799	13
8	2214	2213	16
10	102	54	13
12	556	543	7
14	924	916	8
16	464	458	8
18	144	199	16
20	352	309	8
22	562	513	8
24	122	123	14
26	334	329	6
28	344	374	4

8 K 1

0	-79	0	22
2	84	84	21
4	98	119	19
6	331	331	7
8	417	417	7
10	131	60	17
12	25	10	50
14	197	213	13
16	139	146	17
18	97	133	17
20	65	34	18
22	74	82	12

9 K 1

1	382	400	9
3	-30	26	46
5	803	784	8
7	1176	1116	10
9	957	939	9
11	172	192	15
13	823	803	8
15	396	378	7
17	22	43	39
19	164	178	8

10 K 1

0	62	0	26
2	123	95	17
4	113	59	18
6	825	825	8
8	975	956	9
10	95	81	21
12	360	355	8
14	476	478	6
16	163	188	8

11 K 1

1	43	52	32
3	119	108	13
5	76	78	21
7	124	171	13
9	101	68	14
11	59	24	19
13	-12	65	33

12 K 1

0	-42	0	25
2	224	233	7
6	523	480	5

0 K 2

0	5371	5302	40
2	1949	1943	14
4	1012	1021	8
6	1092	999	8
8	762	681	7
10	403	344	6
12	546	481	6
14	2316	2191	17
16	1469	1475	11
18	736	754	8
20	1160	1094	9
22	921	874	8
24	182	193	12
26	66	89	22
28	278	264	5

1 K 2

1	2410	2423	18
3	368	440	5
5	783	778	7
7	402	456	5
9	217	196	7
11	396	389	6
13	680	736	7
15	1126	1058	9
17	188	134	11
19	891	844	8
21	551	544	7
23	228	250	10
25	90	53	19
27	53	69	20
29	160	176	6

2 K 2

0	870	793	7
2	820	863	6
4	36	1	22
6	881	909	7
8	-22	13	34
10	190	121	8
12	633	655	7
14	559	588	7
16	938	834	8
18	96	55	19
20	601	559	7
22	314	330	9
24	103	87	16
26	-22	43	37
28	73	88	13

3 K 2

1	2865	3085	21
3	-31	47	24
5	874	935	7
7	1102	1063	9
9	90	50	14
11	54	9	24
13	1444	1322	11
15	2087	1999	15
17	620	595	7
19	761	754	8
21	1051	949	9
23	507	521	7
25	70	92	20
27	121	105	9

4 K 2

0	1795	1739	13
2	942	1012	7
4	329	305	5
6	902	947	7
8	-14	51	41
10	107	76	14
12	662	678	7
14	987	973	9
16	1020	944	9
18	225	222	11
20	729	672	7
22	392	408	8
24	110	104	15
26	37	45	24

5 K 2

1	774	762	7
3	591	594	6
5	342	317	6
7	209	260	8
9	133	145	13
11	282	254	8
13	221	244	11
15	348	303	8
17	293	253	11
19	357	334	9
21	361	352	8
23	136	125	13
25	61	23	16

6 K 2

0	2563	2726	19
2	1264	1308	10

4	222	237	8
6	768	759	7
8	427	422	7
10	139	159	15
12	460	408	7
14	1263	1198	10
16	962	934	9
18	249	241	11
20	864	806	8
22	723	686	9
24	101	94	10

7 K 2

1	1310	1295	11
3	546	604	7
5	493	501	7
7	478	491	7
9	129	105	15
11	340	324	8
13	540	528	9
15	723	656	9
17	276	240	10
19	569	532	7
21	615	604	7
23	220	231	6

8 K 2

0	310	292	8
2	217	164	10
4	186	176	11
6	178	190	12
8	82	60	24
10	-57	22	35
12	131	128	18
14	275	262	10
16	313	304	8
18	27	2	35
20	81	95	16
22	37	1	16

9 K 2

1	1267	1298	10
3	57	29	32
5	460	459	8
7	391	378	8
9	19	9	49
11	37	38	27

13	670	627	8
15	945	940	9
17	255	249	6
19	352	356	5

10 K 2

0	957	917	9
2	502	504	8
4	199	190	12
6	434	434	8
8	61	75	28
10	-40	2	31
12	307	306	7
14	583	566	6
16	504	459	5

11 K 2

1	120	111	15
3	61	109	25
5	63	35	20
7	16	2	43
9	25	47	32
11	-20	7	29

12 K 2

0	874	849	7
2	437	406	5

0 K 3

0	-85	0	19
2	849	785	7
4	674	609	6
6	1920	1836	14
8	2696	2460	19
10	861	769	7
12	1091	994	9
14	1236	1232	10
16	331	283	8
18	160	73	13
20	488	496	8
22	789	728	8
24	504	466	7
26	501	501	6
28	593	691	5

1 K 3

1	204	248	6
3	52	32	18
5	672	640	6
7	1436	1425	11
9	972	1011	8
11	-49	29	27
15	556	553	7
17	110	16	17
19	175	166	12
21	403	376	7
23	345	385	8
25	76	13	17
27	349	376	5

2 K 3

0	45	0	19
2	112	107	10
4	68	23	16
6	1218	1209	9
8	1425	1464	11
10	59	8	24
12	486	521	7
14	534	476	7
16	205	253	11
18	73	31	26
20	273	212	9
22	372	374	7
24	92	110	17
26	191	222	7
28	130	186	7

3 K 3

1	498	530	5
3	169	203	8
5	1093	1169	9
7	2501	2540	19
9	1671	1589	13
11	676	625	7
13	1276	1228	10
15	768	726	8
17	124	40	17
19	219	210	12
21	603	586	7
23	679	627	7
25	150	143	9
27	547	608	5

4 K 3

0	52	0	20
2	145	178	9
4	256	270	7
6	1280	1304	10
8	1470	1525	11
10	179	176	11
12	561	591	7
14	785	736	8
16	255	282	10
18	60	7	30
20	325	264	9
22	406	398	7
24	142	147	10
26	252	289	5

5 K 3

1	49	53	24
3	199	215	9
5	207	173	9
7	824	879	8
9	450	490	7
11	129	155	16
13	214	175	11
15	201	171	12
17	-59	17	35
19	-66	39	30
21	300	266	7
23	195	234	8
25	-34	5	20

6 K 3

0	-60	0	26
2	508	517	7
4	112	117	16
6	1338	1382	11
8	1815	1789	14
10	306	282	9
12	837	755	8
14	684	652	8
16	237	183	10
18	79	24	25
20	351	353	7
22	639	597	6
24	241	252	5

7 K 3

1	149	150	14
3	202	209	10
5	459	453	7
7	1351	1369	11
9	691	714	7
11	320	324	10
13	488	462	9
15	354	335	9
17	36	33	39
19	131	115	13
21	397	380	5

8 K 3

0	55	0	33
2	-35	12	43
4	98	85	22
6	260	223	11
8	220	261	12
10	187	146	14
12	-16	82	58
14	220	187	11
16	14	79	51
18	76	24	15
20	55	35	14

9 K 3

1	236	224	11
3	113	76	19
5	532	538	8
7	1004	986	9
9	732	704	8
11	172	167	13
13	579	582	7
15	332	343	6
17	43	11	19

10 K 3

0	35	0	38
2	115	122	17
4	170	150	12
6	650	639	8
8	722	723	8
10	128	125	12
12	327	332	6
14	441	391	5

11 K 3

1	-27	7	32
3	33	58	29
5	-26	14	31
7	45	83	21
9	60	78	15

0 K 4

0	3139	3273	22
2	1548	1430	12
4	554	523	7
6	882	818	8
8	345	323	8
10	179	82	12
12	611	534	7
14	1509	1463	12
16	1046	1046	9
18	493	510	7
20	934	846	8
22	615	563	7
24	115	139	12
26	44	34	18

1 K 4

1	1529	1607	11
3	155	113	10
5	485	454	6
7	318	306	8
9	71	70	24
11	79	7	22
13	462	490	8
15	836	768	8
17	-33	22	39
19	595	544	7
21	374	394	7
23	191	213	9
25	42	9	22

2 K 4

0	735	828	7
2	495	493	6
4	132	123	11
6	478	466	6
8	104	99	17
10	43	56	35
12	267	251	10
14	497	489	7
16	555	538	7
18	28	42	45
20	340	345	8
22	247	283	8
24	46	61	23
26	-49	6	16

3 K 4

1	1813	1939	13
3	201	233	9
5	697	741	7
7	704	683	7
9	-41	2	36
11	220	211	11
13	1061	960	9
15	1380	1361	11
17	516	484	8
19	604	572	7
21	762	680	7
23	311	333	6
25	75	28	12

4 K 4

0	1328	1363	10
2	602	629	7
4	297	288	7
6	508	536	7
8	180	129	11
10	-62	55	40
12	323	316	9
14	780	751	8
16	721	626	8
18	178	153	13
20	428	438	7
22	290	325	7
24	60	76	15

5 K 4

1	584	615	7
3	281	252	8
5	181	158	11
7	169	178	13
9	-72	54	25
11	-49	4	34
13	147	153	17
15	282	239	10
17	161	125	13
19	211	199	9
21	240	261	7
23	125	117	8

6 K 4

0	1701	1736	13
2	970	991	8
4	126	120	15
6	613	608	7
8	199	226	12
10	87	35	23
12	429	390	8
14	846	809	8
16	670	677	7
18	113	159	16
20	653	618	6
22	452	463	5

7 K 4

1	968	972	9
3	288	329	9
5	318	307	9
7	338	339	8
9	94	34	21
11	114	106	19
13	364	364	8
15	522	477	7
17	146	137	11
19	356	355	5

8 K 4

0	289	302	9
2	99	68	20
4	156	162	14
6	86	82	22
8	-40	1	38
10	81	63	22
12	-21	19	45
14	212	222	9
16	205	203	7
18	-69	2	13

9 K 4

1	868	883	8
3	49	40	31
5	366	366	7
7	280	265	8
9	56	10	25
11	79	39	18
13	484	462	6
15	679	668	6

10 K 4

0	696	705	8
2	324	333	7
4	145	161	11
6	272	278	7
8	74	79	17
10	-64	77	16

11 K 4

1	68	105	15
3	46	46	17

0 K 5

0	-56	0	38
2	438	419	7
4	386	284	8
6	1335	1255	11
8	1703	1584	13
10	563	489	8
12	648	619	7
14	839	821	8
16	261	257	9
18	-63	50	30
20	318	327	7
22	487	494	6
24	259	297	5

1 K 5

1	168	175	10
3	71	33	24
5	403	383	8
7	792	701	8
9	603	558	8
11	49	6	35
13	438	373	7
15	322	243	10
17	56	18	30
19	127	99	14
21	221	216	8
23	231	241	6

2 K 5

0	-30	0	37
2	139	111	13
4	-47	61	31
6	665	628	8
8	767	744	8
10	69	13	31
12	361	335	8
14	321	241	9
16	50	82	39
18	49	20	38
20	153	113	11
22	223	221	7
24	42	62	18

3 K 5

1	251	259	9
3	106	164	18
5	741	743	8
7	1671	1675	13
9	1070	1011	9
11	376	379	8
13	802	799	8
15	500	527	8
17	56	66	29
19	133	122	13
21	385	402	6
23	364	402	5

4 K 5

0	-20	0	46
2	139	141	14
4	160	194	13
6	750	734	7
8	883	833	8
10	122	125	18
12	414	385	9
14	468	415	8
16	140	119	15
18	36	1	34
20	163	149	9
22	233	239	5

5 K 5

1	74	69	23
3	145	127	14
5	114	104	17
7	441	441	8
9	262	275	10
11	114	88	22
13	143	101	17
15	61	36	29
17	-74	13	22
19	63	25	19
21	151	155	7

6 K 5

0	17	0	52
2	296	301	9
4	-29	36	45
6	903	932	9
8	1194	1183	10
10	210	183	12
12	493	480	8
14	445	440	7
16	150	159	11
18	-10	19	42
20	215	237	5

7 K 5

1	110	116	18
3	143	138	15
5	293	285	8
7	802	797	8
9	417	434	8
11	216	202	10
13	310	287	8
15	182	158	9
17	-54	6	20

8 K 5

0	34	0	37
2	32	20	39
4	66	76	25
6	125	105	15
8	111	119	16
10	76	97	21
12	-58	55	23
14	105	103	11

9 K 5

1	133	122	12
3	36	52	32
5	366	351	6
7	658	672	7
9	462	462	6
11	110	106	11

10 K 5

0	42	0	22
2	58	85	18
4	105	107	12

0 K 6

0	1760	1739	13
2	819	842	8
4	309	224	10
6	487	401	8
8	186	127	14
10	103	52	23
12	313	294	9
14	878	807	8
16	601	546	7
18	303	314	7
20	479	508	6
22	284	315	5

1 K 6

1	825	832	8
3	84	13	25
5	297	315	10
7	194	213	15
9	75	4	30
11	72	17	28
13	339	294	6
15	464	456	7
17	59	24	25
19	297	297	7
21	201	222	6

2 K 6

0	398	433	7
2	265	232	9
4	79	131	25
6	318	299	8
8	63	96	35
10	-72	24	32
12	172	134	15
14	303	304	9
16	312	331	8
18	-26	60	36
20	187	182	7

3 K 6

1	1089	1068	9
3	123	194	18
5	410	375	9
7	362	319	9
9	-47	20	40
11	89	111	27
13	579	538	8
15	793	746	8
17	254	262	8
19	316	334	6
21	322	399	5

4 K 6

0	682	729	8
2	339	319	9
4	142	216	18
6	337	334	10
8	114	105	22
10	-52	28	40
12	202	173	15
14	464	455	8
16	358	377	7
18	80	58	16
20	209	240	5

5 K 6

1	315	332	10
3	130	106	19
5	147	126	16
7	148	134	17
9	81	6	27
11	-43	2	40
13	66	91	29
15	131	149	14
17	58	82	13

6 K 6

0	952	975	9
2	553	596	8
4	31	29	45
6	310	312	9
8	120	104	19
10	66	19	29
12	205	217	11
14	466	444	9
16	314	361	6

7 K 6

1	535	543	8
3	185	168	12
5	187	201	12
7	195	215	12
9	45	1	32
11	80	54	20
13	197	213	8

8 K 6

0	139	167	13
2	31	16	36
4	85	125	19
6	52	67	26
8	-71	13	20
10	25	35	31

9 K 6

1	534	508	6
3	-44	36	23

0 K 7

0	-67	0	37
2	207	230	13
4	188	91	18
6	696	593	9
8	846	753	9
10	271	247	11
12	336	317	8
14	403	413	7
16	86	124	17
18	30	14	26

1 K 7

1	40	69	43
3	64	9	35
5	191	226	18
7	459	364	10
9	322	297	11
11	75	19	26
13	210	183	11
15	137	121	13
17	28	4	30

2 K 7

0	46	0	38
2	71	31	30
4	53	68	38
6	364	353	10
8	442	391	10
10	14	18	60
12	177	172	13
14	116	123	16
16	84	48	15
18	-32	1	23

3 K 7

1	125	132	19
3	-20	118	55
5	422	345	8
7	841	820	9
9	530	451	9
11	213	203	12
13	408	421	7
15	199	263	9
17	-38	29	21

4 K 7

0	-53	0	34
2	71	47	28
4	77	130	27
6	414	402	9
8	466	431	8
10	63	78	31
12	196	198	10
14	207	213	8
16	69	69	13

5 K 7

1	-43	27	36
3	-67	47	27
5	110	75	18

7	246	242	10
9	141	151	15
11	-46	35	31
13	73	44	17

6 K 7

0	-41	0	33
2	158	173	12
4	49	16	29
6	460	460	7
8	541	590	7
10	109	87	14

7 K 7

1	14	52	45
3	80	63	18
5	128	162	12
7	380	423	6

0 K 8

0	808	773	9
2	364	374	8
4	133	119	22
6	206	183	20
8	96	50	45
10	124	36	40
12	148	118	24

1 K 8

1	425	403	8
3	-88	25	31
5	118	140	44
7	205	96	25
9	-110	9	35
11	-45	0	42
13	100	147	13

2 K 8

0	170	197	15
2	113	116	19
4	100	50	21
6	129	132	20
8	-83	49	25
10	-52	0	29
12	41	71	27

3 K 8

1	477	457	8
3	66	75	27
5	201	181	12
7	203	137	11
9	-36	16	37
11	-15	35	41

4 K 8

0	322	336	8
2	147	154	14
4	-33	57	40
6	118	150	18
8	45	51	33

5 K 8

1	149	169	14
3	-107	66	19
5	-42	51	37

G. $(TMTSF)(SCN)_{0.5}$ - Structure factors, Ni-filtered CuK$\bar{\alpha}$ radiation. Space group Cmcm.

0 K 0

2	2729	2290	19
4	1271	1066	10
6	989	1377	8
8	954	812	8
10	147	128	16
12	409	586	9
14	1575	1833	15
16	1618	1601	12
18	537	571	8
20	1157	1195	9
22	844	851	8
24	335	316	9
26	109	75	11
28	-21	36	30
30	141	155	5

1 K 0

1	2260	3317	16
3	361	168	5
5	982	628	8
7	857	682	8
9	113	19	17
11	172	18	14
13	674	647	8
17	161	157	11
19	699	698	7
21	533	540	7
23	302	322	6
25	37	39	26
27	44	27	21
29	74	69	11

2 K 0

0	264	1482	6
2	442	612	5
4	49	173	26
6	1202	758	9
8	293	393	8
10	78	44	25
12	497	346	8
14	547	610	9
16	757	743	7
18	119	141	16
20	422	397	7
22	349	391	6
24	92	97	14
26	39	52	23
28	-33	8	22
30	41	43	11

3 K 0

1	4343	3391	30
3	87	285	16
5	912	1174	8
7	1306	1425	10
9	210	75	11
11	118	292	20
13	1097	1091	11
15	1823	1768	13
17	755	779	7
19	679	719	7
21	880	956	8
23	530	549	6
25	53	4	19
27	71	57	13
29	89	89	7

4 K 0

0	1515	2492	12
2	810	979	7
4	344	433	7
6	1221	982	10
8	316	420	9
10	61	39	33
12	504	428	9
14	1001	1033	9
16	907	928	8
18	121	153	16
20	577	576	6
22	437	463	6
24	115	128	11
26	73	60	14
28	-18	15	25

5 K 0

1	322	838	8
3	554	410	7
5	268	149	10
7	335	271	9
9	-10	25	64
11	134	62	12
13	171	150	11
15	239	227	10
17	186	197	12
19	182	147	9
21	268	284	7
23	149	167	9
25	29	22	26
27	26	13	20

6 K 0

0	3076	2597	22
2	1577	1513	11
4	132	72	19
6	791	960	7
8	507	465	6
10	32	8	34
12	363	428	7
14	957	900	8
16	890	862	8
18	88	97	18
20	695	736	6
22	625	633	6
24	197	190	6
26	80	61	8

7 K 0

1	1224	1515	9
3	550	479	6
5	499	422	6
7	644	598	7
9	-25	75	42
11	200	131	10
13	498	469	7
15	643	665	6
17	239	229	8
19	401	396	6
21	540	543	5
23	290	290	5
25	37	20	13

8 K 0

0	92	256	22
2	33	36	36
4	146	160	12
6	163	63	11
8	11	24	54
10	-27	23	42
12	65	27	21
14	162	169	10
16	178	169	9
18	35	46	27
20	27	5	27
22	50	6	14

9 K 0

1	1314	1144	10
3	107	122	18
5	417	438	6
7	372	387	6
9	77	73	19
11	19	68	40
13	440	453	6
15	687	675	6
17	259	255	6
19	262	263	5
21	298	319	4

10 K 0

0	862	993	7
2	466	483	6
4	165	190	9
6	418	362	6
8	186	175	8
10	36	28	27
12	238	200	7
14	481	481	5
16	385	378	4
18	85	84	7

11 K 0

1	69	8	17
3	55	56	19
5	-21	42	34
7	-45	14	22
9	-50	5	19
11	-112	21	8
13	29	42	20

12 K 0

0	687	596	6
2	368	347	5
4	72	36	12
6	170	173	5
8	89	98	8

0 K 1

2	1024	852	8
4	1279	790	10
6	2245	2262	17
8	3480	3514	26
10	1085	1011	9
12	1123	1099	10
14	1698	1694	13
16	642	657	6
18	54	22	27
20	316	316	8
22	555	581	6
24	445	440	6
26	309	311	5
28	616	603	5
30	352	351	4

1 K 1

1	307	543	5
3	189	41	8
5	484	712	6
7	2039	1618	15
9	1362	1318	11
11	68	14	29
13	791	825	8
17	56	30	25
19	48	70	30
21	238	247	9
23	310	325	6
25	69	60	17
27	309	303	5
29	314	259	4

2 K 1

2	64	238	20
4	290	154	7
6	1436	1222	11
8	2125	1788	16
10	74	95	27
12	669	733	8
14	529	542	9
16	347	294	7
18	-22	29	43
20	90	102	20
22	256	256	7
24	104	127	13

26	152	160	8
28	181	174	6

3 K 1

1	702	567	7
3	27	124	35
5	1439	1290	11
7	3265	3398	24
9	2107	2126	15
11	699	730	8
13	1476	1419	12
15	1085	1115	9
17	211	196	10
19	112	79	17
21	421	434	6
23	524	526	6
25	14	31	38
27	505	479	5
29	363	363	4

4 K 1

2	254	341	8
4	171	399	12
6	1639	1520	13
8	2011	1694	15
10	271	277	11
12	696	738	6
14	933	931	8
16	410	392	7
18	57	0	28
20	136	157	12
22	323	320	6
24	169	169	8
26	225	228	6
28	295	287	4

5 K 1

1	-24	107	45
3	314	193	8
5	95	130	22
7	878	725	9
9	562	537	9
11	150	121	11
13	178	212	11
15	187	155	12
17	80	60	23
19	-71	12	20

21	125	131	12
23	143	150	9
25	38	29	22
27	99	100	7

6 K 1

2	489	460	8
4	250	128	11
6	1520	1554	12
8	2015	2099	15
10	404	386	6
12	818	780	7
14	834	803	8
16	368	390	8
18	9	23	48
20	212	200	7
22	425	434	5
24	254	225	5
26	248	247	4

7 K 1

1	198	245	9
3	267	216	7
5	489	539	6
7	1582	1495	12
9	891	890	8
11	355	352	7
13	584	594	7
15	445	407	6
17	68	89	20
19	43	54	25
21	265	253	6
23	259	273	5
25	78	63	7

8 K 1

2	40	2	33
4	-6	131	57
6	127	83	15
8	146	83	15
10	174	186	12
12	-4	7	53
14	157	157	10
16	66	86	20
18	-15	2	36
20	47	3	19
22	-31	4	18

8	692	687	8
10	229	126	12
12	477	508	9
14	1651	1623	14
16	1373	1364	11
18	460	489	7
20	1029	1052	8
22	768	750	7
24	286	282	6
26	81	66	13
28	70	31	11

1 K 2

1	2789	2736	21
3	118	14	14
5	491	580	7
7	454	562	7
9	94	38	23
11	54	3	36
13	573	578	9
15	985	987	8
17	170	135	11
19	623	610	7
21	476	479	6
23	288	283	6
25	62	36	17
27	32	24	23
29	66	62	9

2 K 2

0	1261	1170	10
2	545	597	6
4	154	132	12
6	543	661	7
8	312	334	9
10	87	9	27
12	337	298	11
14	514	553	6
16	658	634	7
18	115	128	16
20	357	345	7
22	349	345	6
24	98	87	12
26	74	47	14
28	38	7	17

3 K 2

1	2726	2861	19
3	365	343	7
5	1070	1050	9
7	1259	1181	10
9	103	89	21
11	168	218	17
13	988	977	8
15	1573	1540	12
17	578	678	9
19	605	624	7
21	848	845	8
23	490	483	6
25	43	2	21
27	39	51	19

4 K 2

0	2163	2109	16
2	823	878	8
4	433	399	8
6	723	816	8
8	322	356	10
10	94	16	25
12	388	364	7
14	885	906	8
16	815	812	7
18	101	127	19
20	523	511	6
22	412	407	6
24	118	113	10
26	59	52	14
28	17	13	20

5 K 2

1	764	707	8
3	323	367	9
5	118	137	19
7	163	243	17
9	81	22	18
11	85	43	19
13	155	142	13
15	217	197	11
17	158	167	14
19	160	128	10
21	253	252	7
23	141	149	8
25	40	19	19
27	30	12	14

9 K 1

3	12	12	45
5	579	531	6
7	982	975	8
9	734	719	6
11	87	77	16
13	567	537	6
15	437	437	5
17	98	103	11
19	46	34	17
21	135	147	4

10 K 1

2	117	99	12
4	154	173	10
6	665	634	6
8	793	737	7
10	181	179	8
12	330	325	6
14	428	409	5
16	182	189	6
18	-31	21	15

11 K 1

1	-22	12	32
3	56	26	20
5	33	33	28
7	36	46	25
9	40	14	22
11	81	57	11
13	62	43	11

12 K 1

2	91	76	10
4	82	70	10
6	313	332	4
8	360	406	4

0 K 2

0	5174	5443	38
2	2294	2101	17
4	814	827	8
6	1484	1227	12

6 K 2

0	2170	2248	16
2	1320	1333	10
4	89	84	16
6	850	826	7
8	426	407	7
10	69	0	24
12	352	370	8
14	834	795	8
16	773	753	7
18	68	83	17
20	662	654	7
22	580	560	6
24	154	168	6

7 K 2

1	1366	1330	11
3	401	417	6
5	367	376	7
7	490	511	7
9	55	76	29
11	160	115	13
13	428	412	6
15	594	583	6
17	217	203	8
19	369	350	5
21	494	483	5
23	256	256	4

8 K 2

0	236	221	9
2	-15	31	49
4	149	142	13
6	32	55	39
8	22	20	44
10	-35	19	31
12	-30	24	33
14	149	151	10
16	156	150	9
18	-19	41	35
20	50	3	16
22	-31	7	16

9 K 2

1	1002	1009	8
3	136	106	11
5	395	389	6
7	370	336	6
9	69	69	20
11	5	60	50
13	398	401	6
15	620	598	6
17	228	227	6
19	225	232	4

10 K 2

0	904	874	7
2	432	427	6
4	163	170	9
6	325	318	6
8	148	155	9
10	-54	26	22
12	188	177	7
14	429	427	5
16	333	335	4

11 K 2

1	52	9	20
3	79	49	14
5	36	38	25
7	15	13	35
9	40	4	19
11	19	19	26
13	37	38	13

12 K 2

0	525	529	5
2	289	309	5
4	44	32	14
6	145	153	5

0 K 3

2	532	646	8
4	380	499	9
6	1865	1822	14
8	2548	2445	19
10	755	797	9
12	847	839	7
14	1259	1284	10
16	512	512	7
18	81	21	22
20	222	243	8
22	445	462	6
24	358	337	5
26	249	240	5
28	480	474	4

1 K 3

1	454	319	7
3	-9	63	55
5	698	583	8
7	1102	1184	10
9	1044	952	10
11	-52	11	45
13	669	642	7
15	555	557	7
17	-48	33	32
19	58	49	28
21	197	196	8
23	254	252	6
25	43	48	21
27	239	237	5

2 K 3

2	280	221	8
4	223	129	10
6	938	933	9
8	1229	1200	11
10	146	112	20
12	525	523	6
14	451	428	7
16	250	233	9
18	-50	16	32
20	65	78	21
22	209	203	8
24	101	93	11
26	129	126	8
28	130	134	5

3 K 3

1	285	370	9
3	197	177	11
5	934	1042	9
7	2493	2473	19
9	1552	1563	13
11	524	495	6
13	1121	1107	9
15	849	847	8
17	176	163	12
19	55	54	24
21	328	343	6
23	407	407	5
25	4	27	42
27	380	374	4

4 K 3

2	273	224	11
4	351	262	9
6	1145	1149	9
8	1398	1406	11
10	290	239	7
12	589	589	7
14	723	706	8
16	292	301	9
18	-40	8	30
20	132	119	11
22	250	248	6
24	143	129	8
26	176	177	5

5 K 3

1	141	90	10
3	152	155	10
5	185	133	9
7	518	534	6
9	414	393	7
11	72	74	24
13	180	163	12
15	100	121	21
17	45	46	28
19	39	8	29
21	105	106	12
23	120	119	9
25	38	21	16

6 K 3

2	322	349	7
4	78	85	20
6	1195	1205	10
8	1594	1593	13
10	286	314	8
12	625	609	7
14	632	616	7
16	298	301	7
18	-7	22	48
20	154	156	8
22	341	342	5
24	176	175	5

7 K 3

1	206	165	10
3	164	172	12
5	447	412	7
7	1151	1152	10
9	693	691	7
11	264	272	7
13	466	464	6
15	329	308	6
17	72	73	17
19	13	43	39
21	211	200	5
23	208	214	4

8 K 3

2	42	4	33
4	120	103	13
6	117	66	13
8	84	64	17
10	149	145	11
12	-57	7	23
14	-65	124	20
16	68	68	17
18	-25	2	27
20	9	3	30

9 K 3

1	94	102	16
3	24	8	37
5	403	415	6
7	780	759	7
9	569	561	6
11	95	59	13
13	435	423	6
15	338	341	5
17	65	84	12

10 K 3

2	81	74	15
4	167	137	8
6	509	498	6
8	593	573	6
10	139	142	9

12	256	256	5	6	458	435	10	9	-52	17	32
14	313	322	4	8	214	211	9	11	80	21	24
				10	51	13	30	13	74	104	22
	11 K	3		12	186	198	13	15	135	131	13
				14	367	390	8	17	113	106	13
1	-37	9	23	16	433	417	7	19	90	87	14
3	-47	21	19	18	118	95	13	21	186	177	7
5	53	28	16	20	234	231	7	23	94	105	9
7	60	36	14	22	229	237	6				
9	20	12	24	24	27	61	27		6 K	4	
				26	39	32	15				
	0 K	4						0	1511	1501	12
					3 K	4		2	889	912	8
0	3087	3189	32					4	100	67	18
2	1525	1428	13	1	1763	1821	14	6	543	546	7
4	544	464	10	3	253	299	12	8	277	277	9
6	890	844	10	5	715	719	7	10	54	9	25
8	396	435	12	7	727	741	7	12	262	250	8
10	102	86	18	9	63	78	26	14	568	546	6
12	380	342	7	11	145	120	14	16	243	508	14
14	1114	1108	9	13	705	681	8	18	72	55	16
16	909	889	8	15	1057	1037	9	20	460	457	5
18	333	325	6	17	470	459	6	22	389	391	4
20	726	725	7	19	428	416	6				
22	512	515	6	21	597	583	6		7 K	4	
24	207	197	6	23	327	331	5				
26	38	44	17	25	-27	1	22	1	915	907	8
								3	300	286	8
	1 K	4			4 K	4		5	254	259	7
								7	356	337	6
1	1516	1570	12	0	1350	1351	15	9	42	62	29
3	122	97	19	2	592	609	6	11	58	80	24
5	401	410	10	4	263	278	8	13	294	282	6
7	376	354	11	6	532	518	6	15	407	394	6
9	-50	41	30	8	177	231	12	17	161	139	8
11	23	2	45	10	34	2	39	19	256	244	5
13	396	398	8	12	249	239	10	21	327	340	4
15	651	653	7	14	613	619	8				
17	114	85	18	16	560	552	6		8 K	4	
19	426	417	6	18	74	77	19				
21	331	332	6	20	358	352	6	0	142	146	11
23	196	194	7	22	282	278	6	2	16	19	42
25	38	28	20	24	83	78	10	4	83	101	18
27	43	17	12					6	58	38	22
					5 K	4		8	-37	12	30
	2 K	4						10	-21	13	37
				1	442	459	6	12	51	16	22
0	651	706	8	3	248	251	8	14	103	108	13
2	407	440	9	5	64	95	25	16	107	107	10
4	65	78	33	7	184	168	11	18	-16	29	27

				3	-26	59	41
	9 K	4		5	325	352	7
				7	713	681	7
1	693	690	7	9	548	549	8
3	80	70	16	11	-8	10	62
5	270	272	6	13	360	382	9
7	228	225	7	15	324	325	7
9	64	51	19	17	12	24	46
11	56	42	20	19	52	30	22
13	288	280	5	21	117	122	10
15	405	417	5	23	161	154	7
				25	42	31	13
	10 K	4					
					2 K	5	
0	607	598	6				
2	301	294	6	2	87	127	18
4	109	120	11	4	82	78	19
6	228	219	6	6	537	547	7
8	100	107	11	8	690	665	7
10	-4	19	40	10	26	74	48
12	120	124	6	12	291	302	10
				14	268	263	7
	11 K	4		16	152	143	11
				18	-74	9	18
1	38	10	18	20	-13	46	38
3	57	36	12	22	130	124	8
5	43	27	14	24	25	53	22
	-9 K	5			3 K	5	
5	272	257	8	1	247	203	8
				3	119	116	15
	0 K	5		5	651	636	7
				7	1390	1424	11
2	416	368	7	9	941	908	8
4	330	264	9	11	271	275	10
6	1100	1089	9	13	696	672	7
8	1412	1375	11	15	497	507	6
10	526	478	7	17	103	105	14
12	510	493	8	19	36	32	26
14	765	759	8	21	209	209	6
16	285	308	7	23	240	246	5
18	-42	10	27				
20	153	148	9		4 K	5	
22	274	285	6				
24	209	204	5	2	95	126	19
				4	135	154	15
	1 K	5		6	681	681	7
				8	843	818	8
1	120	168	14	10	122	152	19

12	365	360	7
14	416	425	7
16	195	184	9
18	-35	9	27
20	83	71	14
22	159	150	6

5 K 5

1	33	56	38
3	84	95	21
5	71	84	26
7	338	312	8
9	212	230	9
11	41	37	32
13	72	96	21
15	44	70	27
17	40	27	24
19	-6	5	43
21	57	67	13

6 K 5

2	102	204	14
4	73	47	19
6	724	726	7
8	957	949	8
10	196	195	9
12	382	367	6
14	381	369	6
16	167	181	9
18	38	17	22
20	95	98	8

7 K 5

1	98	93	15
3	121	107	12
5	241	247	8
7	718	696	7
9	418	418	6
11	172	163	9
13	285	280	6
15	186	182	7
17	34	46	21
19	-10	28	25

8 K 5

2	57	5	21

4	63	67	19
6	52	42	22
8	46	37	23
10	79	89	16
12	38	5	24
14	76	80	12
16	46	44	13

9 K 5

1	72	57	17
3	47	0	22
5	263	257	6
7	466	463	5
9	344	343	5
11	46	35	17
13	232	263	4

10 K 5

2	65	41	13
4	88	88	10
6	300	308	5

0 K 6

0	1590	1579	12
2	755	747	8
4	274	223	12
6	450	443	9
8	234	218	12
10	-23	33	44
12	186	184	10
14	596	585	9
16	476	465	6
18	181	181	8
20	395	395	5
22	258	279	6

1 K 6

1	741	761	8
3	75	73	27
5	241	214	11
7	222	183	17
9	39	25	36
11	22	2	44
13	209	211	9
15	348	343	6
17	24	37	33

19	228	230	6
21	170	181	6

2 K 6

0	308	361	9
2	234	226	10
4	27	44	45
6	243	223	11
8	90	106	20
10	71	4	23
12	108	106	16
14	201	209	9
16	235	227	7
18	65	59	18
20	130	121	8
22	118	129	6

3 K 6

1	921	933	8
3	96	161	22
5	356	374	8
7	386	382	7
9	31	44	38
11	-41	65	33
13	380	367	6
15	569	556	6
17	253	251	7
19	222	216	6
21	301	315	4

4 K 6

0	670	688	6
2	343	318	6
4	148	144	11
6	293	272	7
8	123	121	14
10	78	2	19
12	116	130	15
14	342	336	6
16	302	298	6
18	21	35	30
20	179	187	5

5 K 6

1	228	248	8
3	138	134	12

5	32	45	34
7	84	89	18
9	48	12	26
11	46	12	26
13	76	53	17
15	54	65	21
17	44	52	19
19	49	50	12

6 K 6

0	812	799	7
2	476	492	6
4	-44	27	28
6	278	289	7
8	157	151	10
10	32	9	31
12	137	135	11
14	291	291	6
16	270	267	5

7 K 6

1	488	488	6
3	177	163	8
5	166	135	8
7	179	182	9
9	-11	37	43
11	83	45	14
13	154	151	7
15	201	207	4

8 K 6

0	4	75	48
2	-48	5	22
4	83	59	14
6	34	21	26
8	-38	4	23
10	54	7	15
12	-8	9	30

9 K 6

0	356	370	5
3	33	35	22
5	132	149	7
7	108	121	7

0 K 7

2	179	164	12
4	152	120	15
6	508	458	7
8	666	639	7
10	241	228	8
12	235	226	8
14	343	356	6
16	126	145	10
18	-6	1	35

1 K 7

1	73	79	20
3	42	27	31
5	169	161	12
7	334	310	8
9	272	257	8
11	58	12	23
13	190	177	8
15	141	151	10
17	25	12	27
19	49	16	12

2 K 7

2	86	48	17
4	48	27	28
6	261	258	8
8	316	315	8
10	-19	30	44
12	155	147	10
14	139	127	10
16	49	70	19
18	-16	6	26

3 K 7

1	79	92	19
3	70	45	21
5	296	303	7
7	683	669	7
9	440	426	6
11	144	131	11
13	319	323	6
15	220	244	6
17	49	54	14

4 K 7

2	-7	58	50
4	46	83	28
6	336	325	7
8	400	382	6
10	83	72	19
12	179	173	9
14	196	207	7
16	79	91	10

5 K 7

1	22	26	36
3	60	47	20
5	45	34	24
7	145	147	11
9	107	110	14
11	49	16	22
13	33	42	23
15	16	29	24

6 K 7

2	112	99	13
4	14	21	41
6	338	344	6
8	448	451	6
10	95	93	11
12	163	172	6

7 K 7

1	26	45	29
3	52	54	20
5	121	117	9
7	330	333	5
9	179	199	6

8 K 7

0	686	666	10
2	343	318	8
4	109	89	19
6	195	182	11
8	-53	90	28
10	-70	7	18
12	89	78	12
14	230	246	5

1 K 8

1	333	333	6
3	47	35	28
5	96	88	19
7	61	75	27
9	-30	12	34
11	-20	3	33
13	99	88	9

2 K 8

0	138	142	12
2	42	87	31
4	-58	20	25
6	97	92	17
8	23	43	40
10	-35	0	28
12	70	46	13

3 K 8

1	380	382	6
3	81	64	18
5	158	155	11
7	152	159	11
9	-27	19	33
11	42	31	20

4 K 8

0	294	279	6
2	132	128	11
4	103	61	12
6	102	115	13
8	-42	50	25
10	-40	0	19

5 K 8

1	89	111	14
3	44	61	22
5	-42	15	22
7	-20	38	30

6 K 8

0	306	342	5
2	181	215	6

0 K 9

2	-85	60	74
4	-144	44	49

1 K 9

1	-96	30	52
3	-61	11	82

H. $(TMTSF)(SCN)_{0.5}$ - Structure factors, Ni-filtered CuKα radiation, satellite reflections, Space group $Pmc2_1$.

0 K 1′

2	124	260
4	91	79
6	155	284
8	203	550
10	-22	230
12	64	170
14	533	443
16	537	450
18	203	74
20	519	304
22	405	342
24	161	38
26	-68	184
28	-50	124

1 K 1′

1	61	271
3	29	36
5	149	294
7	129	172
9	57	112
11	14	101
13	169	332
15	351	260
17	81	346
19	290	317
21	256	206
23	168	243
25	30	212
27	-47	62

2 K 1′

0	40	0
2	-38	95
4	-6	153
6	194	267
8	34	398
10	-26	172
12	128	183
14	134	365
16	259	409
18	71	92
20	185	264
22	174	322
24	57	51

26	42	163	29	25	-30	157	31	5	28	39	47
								7	69	52	29
								9	-26	27	45
								11	43	64	36
								13	107	117	21
								15	227	80	10
								17	91	128	17

3 K 1′

1	137	128	7	0	-39	0	42				
3	58	32	13	2	105	57	13				
5	119	147	9	4	-26	30	33				
7	244	179	6	6	129	106	13				
9	43	73	23	8	75	219	21				
11	32	184	31	10	66	127	22				
13	287	309	9	12	58	93	30				
15	562	207	9	14	271	247	11				
17	267	332	11	16	311	274	11				
19	256	292	14	18	22	50	50				
21	436	171	9	20	316	189	10				
23	263	232	11	22	310	216	9				
25	39	191	31	24	67	25	19				
27	58	48	20								

4 K 1′

0	-25	0	25	3	74	7	20				
2	45	76	18	5	91	67	18				
4	60	78	15	7	95	76	19				
6	193	175	7	9	35	43	38				
8	21	305	33	11	-31	92	44				
10	29	154	30	13	132	175	18				
12	122	137	14	15	185	122	16				
14	285	312	9	17	85	189	26				
16	312	350	10	19	179	174	13				
18	-24	73	48	21	255	107	10				
20	273	234	11								
22	218	277	12								
24	37	39	34								
26	52	144	21								

5 K 1′

1	45	138	20	8	28	118	44				
3	46	9	20	10	54	76	31				
5	-16	146	36	12	-59	74	31				
7	50	89	21	14	-2	153	68				
9	39	72	28	16	104	185	18				
11	60	100	24	18	-46	45	30				
13	35	227	35	20	28	121	31				
15	89	181	22								
17	77	241	25								
19	67	233	29								
21	137	154	16	1	81	39	26				
23	42	175	33	3	-24	4	46				

6 K 1′

0	-331	0	15	10	-47	83	22				
2	-82	5	29	12	68	56	17				
4	38	40	36	14	146	3	11				
6	107	74	25	16	100	46	16				
8	28	118	44								
10	54	76	31								
12	-59	74	31								
14	-2	153	68	1	30	116	18				
16	104	185	18	3	18	192	27				
18	-46	45	30	5	45	69	19				
20	28	121	31	7	-19	45	34				
22				9	59	107	18				
24				11	-36	6	27				
26				13	-37	5	29				
28				15	99	24	16				

7 K 1′

1	48	66	27								
3	74	7	20								
5	91	67	18								
7	95	76	19								
9	35	43	38								
11	-31	92	44								
13	132	175	18								
15	185	122	16								
17	85	189	26								
19	179	174	13								
21	255	107	10								

8 K 1′

0	-39	0	42								
2	105	57	13								
4	-26	30	33								
6	129	106	13								
8	75	219	21								
10	66	127	22								
12	58	93	30								
14	271	247	11								
16	311	274	11								
18	22	50	50								
20	316	189	10								
22	310	216	9								
24	67	25	19								

9 K 1′

1	105	57	13								
3	-26	30	33								
5	129	106	13								
7	75	219	21								
9	66	127	22								
11	58	93	30								
13	271	247	11								
15	311	274	11								
17	22	50	50								
19	316	189	10								
21	310	216	9								
23	67	25	19								

10 K 1′

0	69	0	27								
2	21	16	47								
4	71	13	25								
6	45	42	37								
8	61	87	27								
10	-36	56	36								
12	72	41	22								
14	140	108	13								

11 K 1′

1	49	33	28								
3	-27	1	37								
5	28	33	35								
7	-36	24	31								
9	26	20	35								

0 K 2′

0	71	386	10								
2	-36	69	22								
4	40	91	23								
6	-26	231	30								
8	63	45	18								
10	-47	83	22								
12	68	56	17								
14	146	3	11								
16	100	46	16								

1 K 2′

1	30	116	18								
3	18	192	27								
5	45	69	19								
7	-19	45	34								
9	59	107	18								
11	-36	6	27								
13	-37	5	29								
15	99	24	16								

2 K 2′

0	-44	305	16
2	-34	53	20
4	49	68	16
6	46	186	19
8	38	38	23
10	-48	66	22
12	44	43	24
14	-51	3	27
16	60	37	25

3 K 2′

1	42	56	18
3	-21	162	27
5	39	58	21
7	87	45	12
9	10	56	41
11	-11	4	42
13	91	11	17
15	82	25	23

4 K 2′

0	-13	212	33
2	21	43	29
4	37	54	22
6	40	138	24
8	35	30	26
10	-56	53	21
12	-4	37	54

5 K 2′

1	-13	58	36
3	33	101	26
5	46	38	22
7	25	28	32
9	65	63	19
11	-28	2	37

6 K 2′

0	55	140	23
2	-14	33	40
4	31	40	30
6	55	97	24
8	28	22	38

11 K 2′

1	67	15	30	5	88	10	21	9	45	17	33
3	-62	27	30	7	28	8	47				

APPENDIX 2

Electrical properties of crystals. Conductivities were measured using the standard 4 probe technique. Silver paint contacts were used with $[Rh(CNCHCH_2)_4]ClO_4$; aquadag contacts were used with all other crystals.

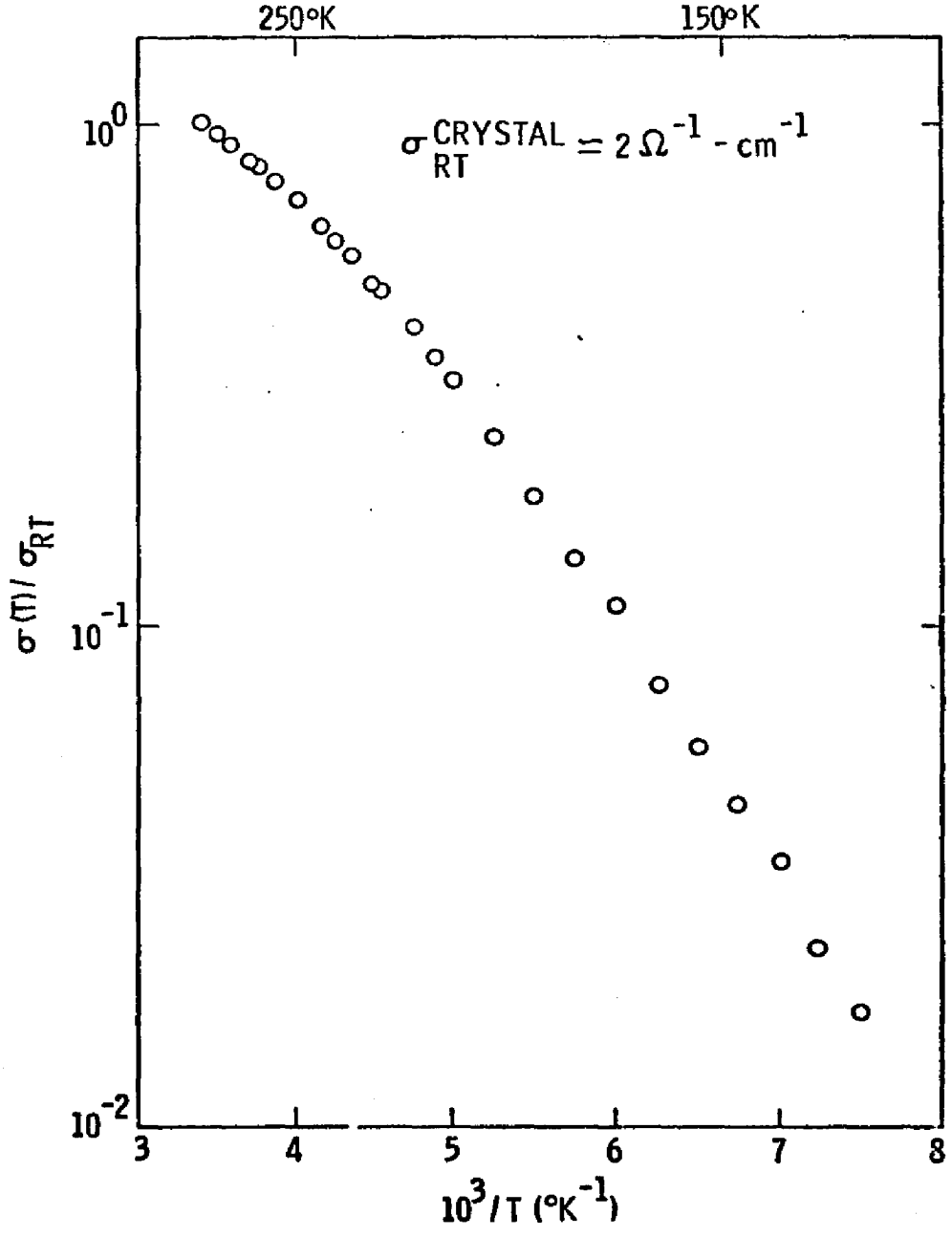

A. Conductivity of $[Rh(CNCHCH_2)_4]ClO_4$

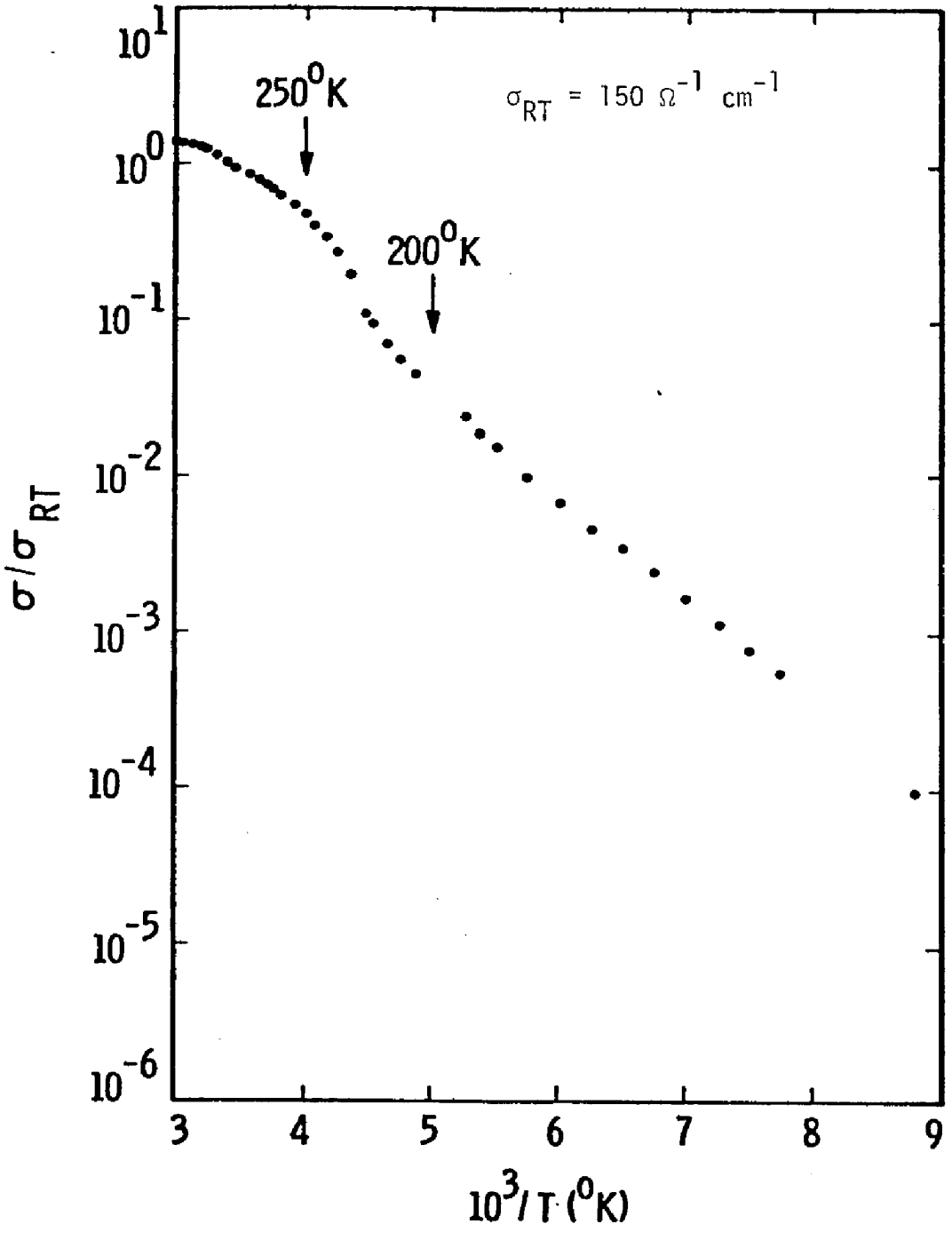

B. Conductivity of $(TTF)Cl_{0.67}$.

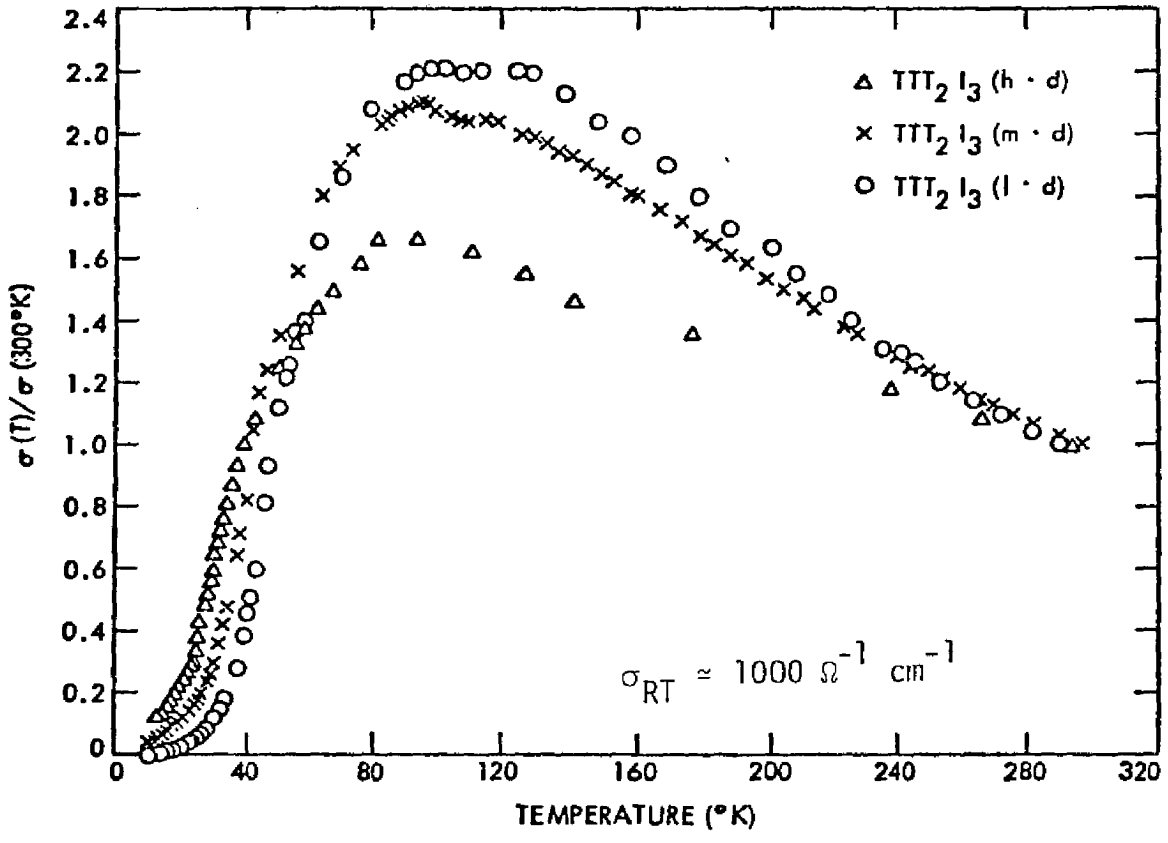

C. Conductivity of high, medium, and low disorder $(TTT)_2I_3$ crystals.

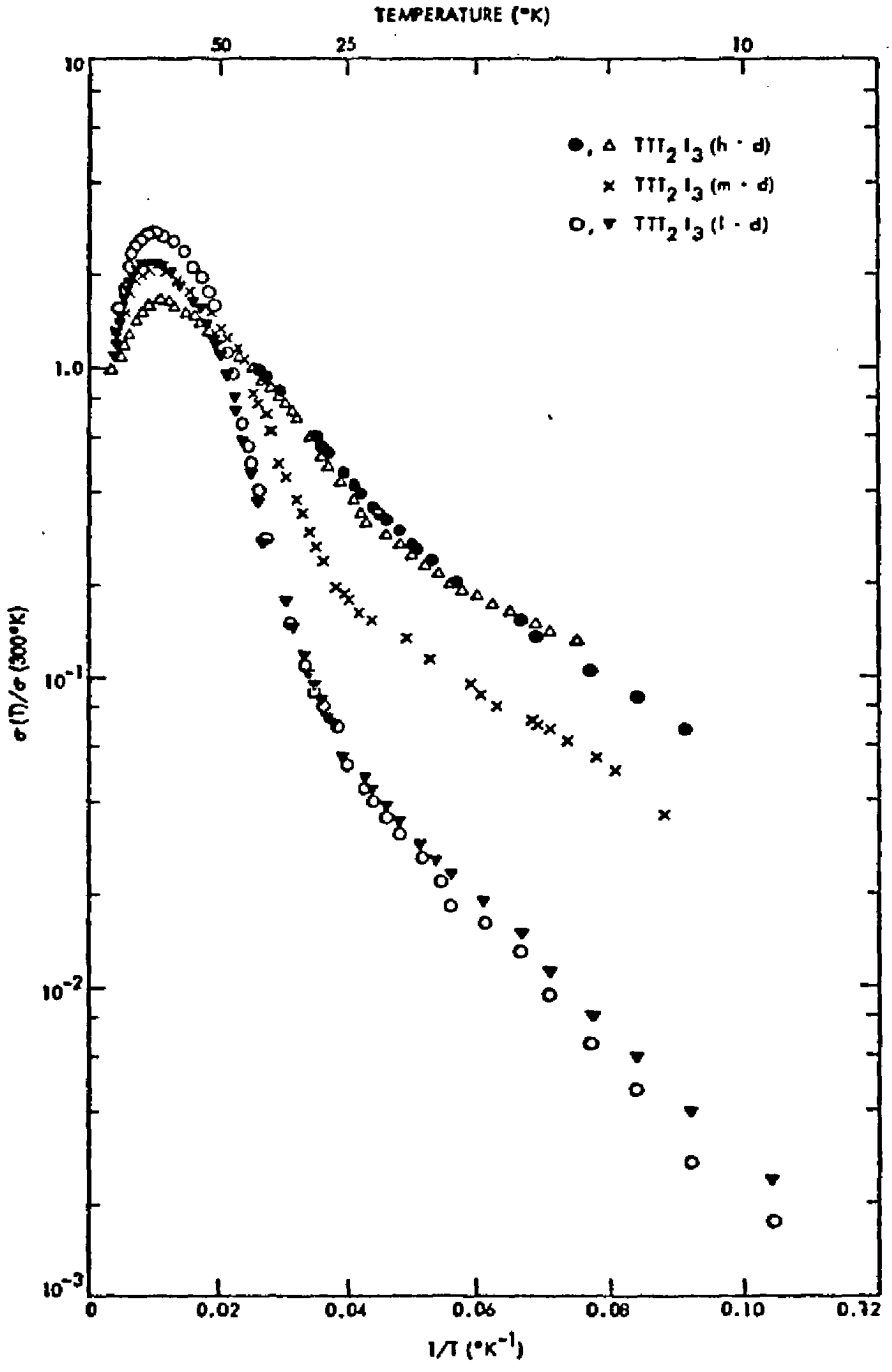

D. Conductivity of high, medium, and low disorder $(TTT)_2I_3$ crystals. This 1/T plot emphasizes low temperature region.

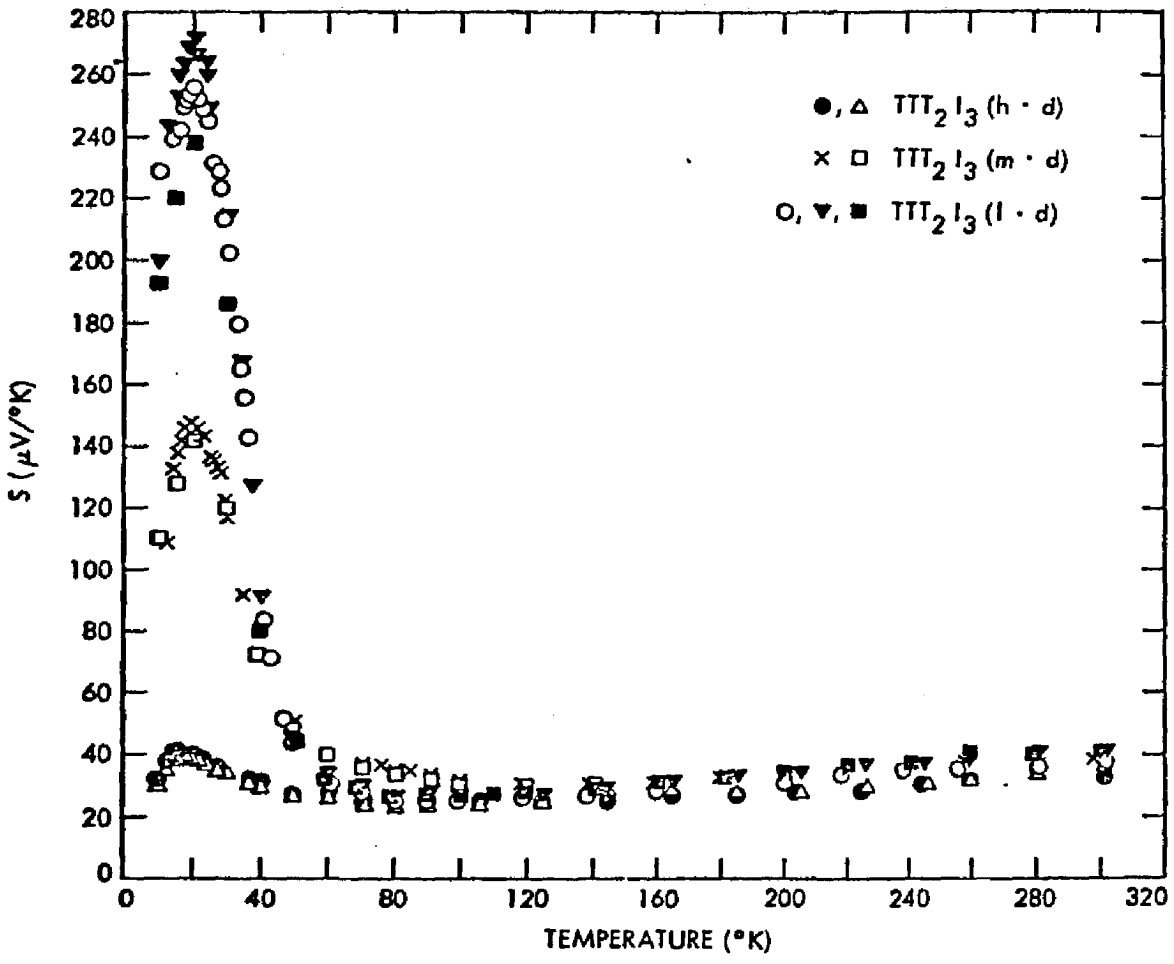

E. Thermoelectric power of high, medium, and low disorder TTT_2I_3 crystals. The peak at ~20° K may represent a phase transition.

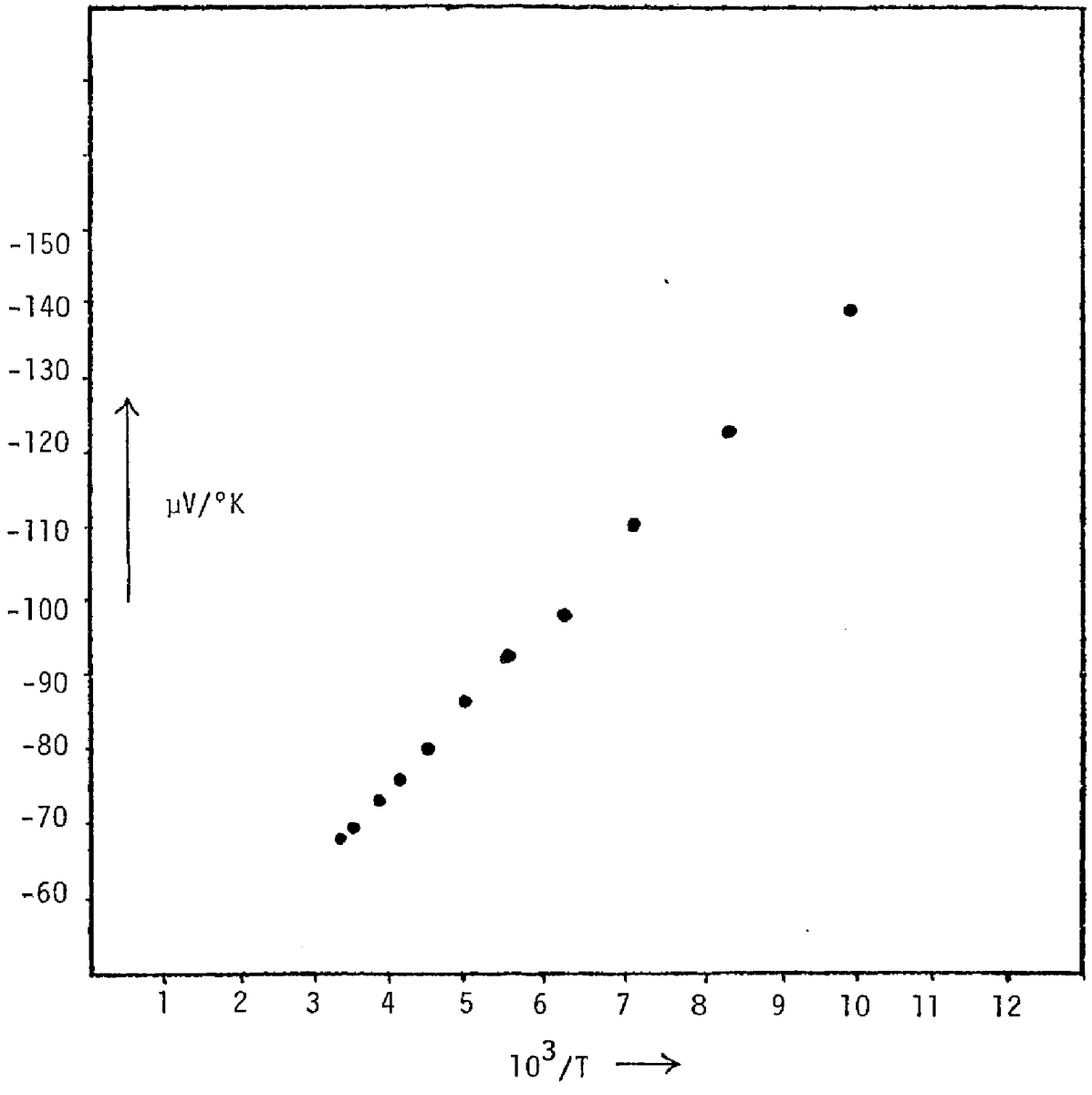

F. Thermoelectric power of $(TMTSF)Br_{0.8}$.

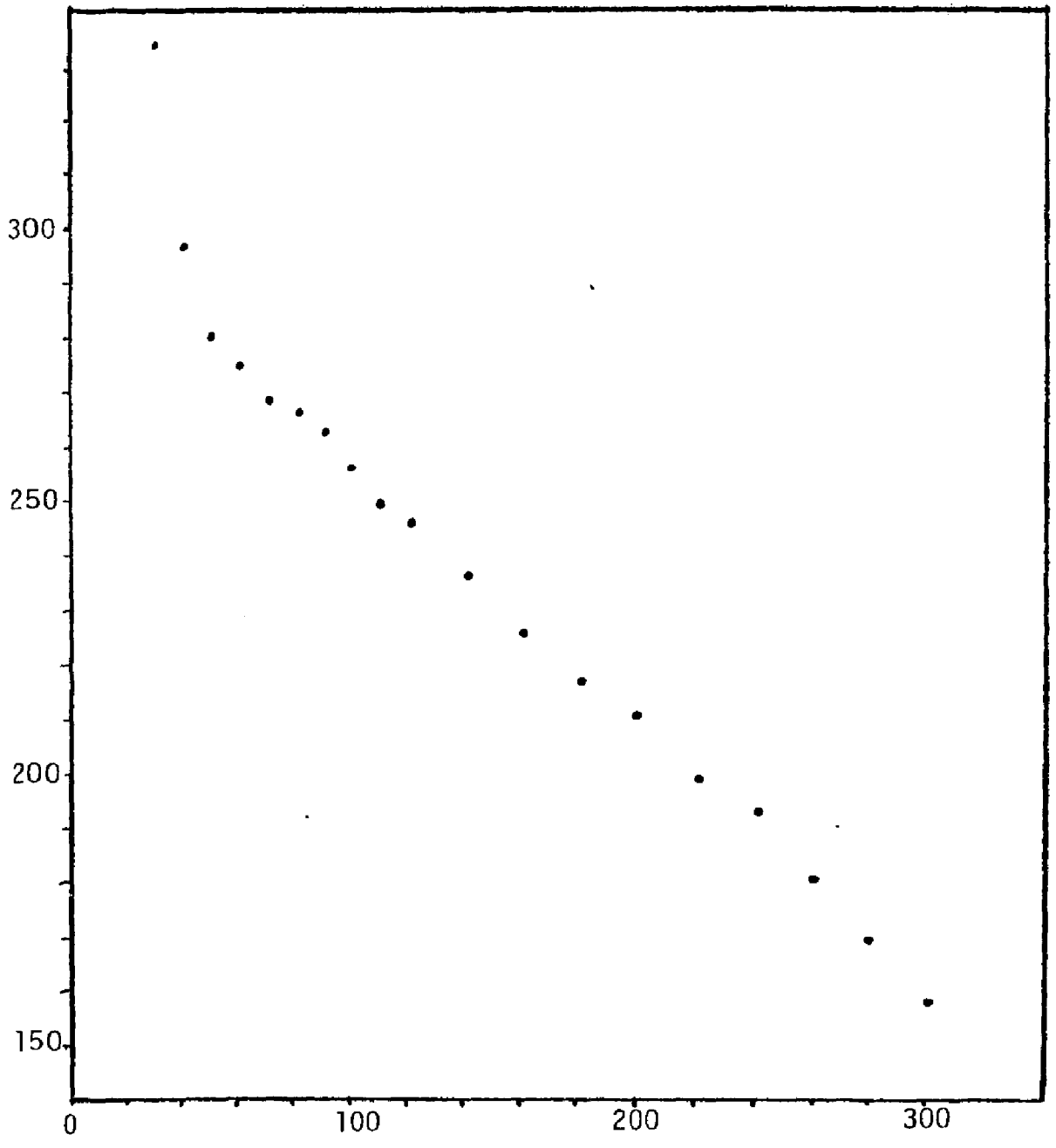

G. Thermoelectric power of $(TMTSF)(SCN)_{0.5}$.

APPENDIX 3

Notes on Structure Refinement

All structure refinement was carried out using CRYM system programs and the Institute's IBM 370/3032 computer. Least-squares refinement proceeds by minimization of the quantity $\Sigma w(F_{obs}^2-F_{cacl}^2)$. The weighted residual, wR, is $\Sigma w^2(F_{obs}^2-F_{calc}^2)^2/\Sigma w^2|F_{obs}|^4$. The residual, R, is $\Sigma\big||F_{obs}|-|F_{calc}|\big|/\Sigma|F_{obs}$. The real goodness of fit is $[\Sigma w(F_{obs}^2-F_{calc}^2)^2/n-p]^{1/2}$. Weights are determined from counting statistics:

$$w = 1/(\sigma^2 F_{obs}^2+t)$$

where t is a term which accounts for errors other than counting statistics.

In the refinement of structures with considerable disorder, refinement of some parameters is difficult or impossible. There are three important cases.

1) Atoms are located close to, but not on, symmetry elements such as mirror planes or rotation axes. Terms in matrices blow up if refinement places the atom very close to the symmetry elements.

2) The fitting function is incorrect. If thermal motion is high, approximation with thermal ellipsoids may be far from correct.

Compare, for example, the electron density map and ORTEP of carbon 6 in the room temperature structure of $[Rh(CNCHCH_2)_4]ClO_4$.

3) The fitting function is not unique. Fitting very "smeared out" electron density such as that observed for halide chains in $(TTT)_2I_3$ and $(TTF)Cl_{0.67}$ or the disordered perchlorates in $[Rh(CNCHCH_2)_4]ClO_4$, can be done in many ways which are equally valid.

In all cases, the observed electron density is far more informative than the parameters used to fit it. Some parameters were not refined by least squares. A fit which provided a flat difference map, low residuals, and convergence of refinable parameters was considered satisfactory.

The kinds of structure disorder and distortion which give rise to diffuse spots in the diffraction patterns of $(TTF)Cl_{0.67}$ and $(TTT)_2I_3$, and satellite reflections in the diffraction pattern of $(TMTSF)(SCN)_{0.5}$, are fairly well understood.

Disorder which appears as "mistakes" with respect to an ideal lattice gives rise to broadening of diffraction peaks (1,2,3). This phenomenon arises for the same reason that peak broadening in powder diffraction occurs. Diffraction peaks are infinitely sharp only for infinite lattices. As the number of repeating units in a diffracting domain (a single particle in powder diffraction or a mosaic block in single crystal diffraction) decreases, the resulting diffraction spots will increase in width. According to Wilson's treatment, the probability of mistakes (α) will determine the

average size of the diffracting domains and the intensity (I) as a function of a normalized coordinate (w) in reciprocal space will be given by:

$$I(w) \sim \frac{\alpha}{\alpha^2+\pi^2 w^2}$$

This expression was used to determine the size of diffracting domains in $(TTF)Cl_{0.67}$ after fast cooling. It also might be used to determine the range of order of the chloride sublattice in $(TTF)Cl_{0.67}$ at room temperature, and the iodide lattice in $(TTT)_2I_3$. This was not done quantitatively for the following reasons.

a) Accurate profiles must be obtained using a very small or narrow aperture for the x-ray beam.

b) Chloride sublattice reflections were extremely weak and very diffuse at room temperature.

c) The diffuse third layer reflections were only ~50% wider than sublattice reflections in (l.d.)$(TTT)_2I_3$, and w scans could not be obtained on the quarter-circle diffractometer.

Qualitatively, the range of order of chlorides in $(TTF)Cl_{0.67}$ might be $\lesssim$100 Å. The range of order of iodide ions in (l.d.)$(TTT)_2I_3$ is hard to estimate, as part of the diffracted intensity indicates only one-dimensional order, while the spots on the diffuse third layer indicate quite long three-dimensional order ($\gtrsim$1000 Å).

Modulation of structures results in superperiods and leads to the observation of satellite reflections on diffraction patterns.

Early treatments of this effect distinguished between modulation of unit cell parameters and structure factor amplitude (4). In the first case, for modulation in, say, the x direction of the crystal, satellites with index h = 0 will have very small intensity. If the structure factor amplitude is modulated, these satellites will have significant intensity. Later treatments describe satellite intensity for specific kinds of structure modulation (5). A number of structures have been solved in which refinement of satellite, or study of its significance, played an important role (6,7).

The modulation of the $(TMTSF)(SCN)_{0.5}$ structure clearly involved structure factor amplitude modulation rather than unit cell parameter modulation. Patterson maps showed that most of the modulation was associated with the x = 0 plane. Further details of the model are given in Chapter 5. In general, satellites of order greater than one are not observed or are very weak. No attempt was made to fit the great decrease in intensity on going from first- to second-order satellites, which could be observed for $(TMTSF)(SCN)_{0.5}$.

The space groups used to fit the full cell data of $(l.d.)(TTT)_2I_3$ and the satellite data of $(TMTSF)(SCN)_{0.5}$ were picked to be consistent with the basic structures of the crystals. Symmetry elements which the superperiod necessarily destroyed were removed, and lower symmetry space groups were then picked which contained the remaining symmetry of the structure. Likewise, the space group of the low temperature monoclinic phase of $(TTF)Cl_{0.67}$ has the most symmetry that

can remain after the distortion of the tetragonal cell. A good treatment of derivative crystal structures exists (8).

References

1. A. J. C. Wilson, X-Ray Optics, Chapter V, London, Methuen (1949).
2. B. T. M. Willis, Proc. Roy. Soc., A248, 183 (1958).
3. K. Dornberger-Schiff, Acta Cryst., 9, 593 (1956).
4. A. J. C. Wilson, X-Ray Optics, Chapter VIII, London, Methuen (1949).
5. H. Böhm, Zeitschrift fur Kristallographie, 143, 56-66 (1976); H. Bölm, Acta Cryst., A31, 622 (1975).
6. H. Kobayashi, Acta Cryst., B30, 1010 (1974).
7. P. B. Jamieson, D. deFontaine, and S. C. Abrahams, J. Appl. Cryst., 2, 24 (1969).
8. M. J. Buerger, J. Chem. Phys., 15, 1 (1947).